



National Library
of Canada

Acquisitions and
Bibliographic Services Branch

395 Wellington Street
Ottawa, Ontario
K1A 0N4

Bibliothèque nationale
du Canada

Direction des acquisitions et
des services bibliographiques

395, rue Wellington
Ottawa (Ontario)
K1A 0N4

Your file *Votre référence*

Our file *Notre référence*

NOTICE

The quality of this microform is heavily dependent upon the quality of the original thesis submitted for microfilming. Every effort has been made to ensure the highest quality of reproduction possible.

If pages are missing, contact the university which granted the degree.

Some pages may have indistinct print especially if the original pages were typed with a poor typewriter ribbon or if the university sent us an inferior photocopy.

Reproduction in full or in part of this microform is governed by the Canadian Copyright Act, R.S.C. 1970, c. C-30, and subsequent amendments.

AVIS

La qualité de cette microforme dépend grandement de la qualité de la thèse soumise au microfilmage. Nous avons tout fait pour assurer une qualité supérieure de reproduction.

S'il manque des pages, veuillez communiquer avec l'université qui a conféré le grade.

La qualité d'impression de certaines pages peut laisser à désirer, surtout si les pages originales ont été dactylographiées à l'aide d'un ruban usé ou si l'université nous a fait parvenir une photocopie de qualité inférieure.

La reproduction, même partielle, de cette microforme est soumise à la Loi canadienne sur le droit d'auteur, SRC 1970, c. C-30, et ses amendements subséquents.

UNIVERSITY OF ALBERTA

Landslides and Geotechnical Properties of Volcanic
Tuff on Mount Cayley, British Columbia

BY

Zhongyou Lu



A thesis submitted to the Faculty of Graduate Studies and
Research in partial fulfillment of the requirements for the
degree of Doctor of Philosophy

DEPARTMENT OF GEOLOGY

EDMONTON, ALBERTA

SPRING, 1993



National Library
of Canada

Acquisitions and
Bibliographic Services Branch

395 Wellington Street
Ottawa, Ontario
K1A 0N4

Bibliothèque nationale
du Canada

Direction des acquisitions et
des services bibliographiques

395, rue Wellington
Ottawa (Ontario)
K1A 0N4

Your file *Votre référence*

Our file *Notre référence*

The author has granted an irrevocable non-exclusive licence allowing the National Library of Canada to reproduce, loan, distribute or sell copies of his/her thesis by any means and in any form or format, making this thesis available to interested persons.

L'auteur a accordé une licence irrévocable et non exclusive permettant à la Bibliothèque nationale du Canada de reproduire, prêter, distribuer ou vendre des copies de sa thèse de quelque manière et sous quelque forme que ce soit pour mettre des exemplaires de cette thèse à la disposition des personnes intéressées.

The author retains ownership of the copyright in his/her thesis. Neither the thesis nor substantial extracts from it may be printed or otherwise reproduced without his/her permission.

L'auteur conserve la propriété du droit d'auteur qui protège sa thèse. Ni la thèse ni des extraits substantiels de celle-ci ne doivent être imprimés ou autrement reproduits sans son autorisation.

ISBN 0-315-81976-6

Canada

UNIVERSITY OF ALBERTA

RELEASE FORM

NAME OF AUTHOR Zhongyou Lu

TITLE OF THESIS Landslides and Geotechnical Properties
of Volcanic Tuff on Mount Cayley,
British Columbia

DEGREE Doctor of Philosophy

YEAR THIS DEGREE GRANTED Spring 1993

Permission is hereby granted to the UNIVERSITY OF ALBERTA LIBRARY to reproduce single copies of this thesis and to lend or sell such copies for private, scholarly or scientific research purposes only.

The author reserves all other publication and other rights in association with the copyright in the thesis, and except as hereinbefore provided neither the thesis nor any substantial portion thereof may be printed or otherwise reproduced in any material form whatever without the author's prior written permission.

[Handwritten signature]
.....

Box 11530-40 143..
Edmonton, Alberta
Canada T6J 0R6

Mark
.....1993

National Library
of Canada

Canadian Theses Service

Bibliothèque nationale
du Canada

Service des thèses canadiennes

NOTICE

THE QUALITY OF THIS MICROFICHE
IS HEAVILY DEPENDENT UPON THE
QUALITY OF THE THESIS SUBMITTED
FOR MICROFILMING.

UNFORTUNATELY THE COLOURED
ILLUSTRATIONS OF THIS THESIS
CAN ONLY YIELD DIFFERENT TONES
OF GREY.

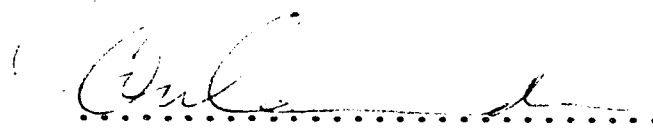
AVIS

LA QUALITE DE CETTE MICROFICHE
DEPEND GRANDEMENT DE LA QUALITE DE LA
THESE SOUMISE AU MICROFILMAGE.

MALHEUREUSEMENT, LES DIFFERENTES
ILLUSTRATIONS EN COULEURS DE CETTE
THESE NE PEUVENT DONNER QUE DES
TEINTES DE GRIS.

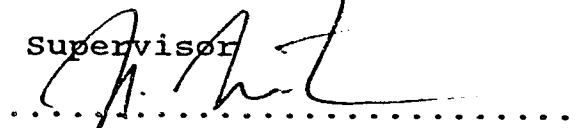
THE UNIVERSITY OF ALBERTA
FACULTY OF GRADUATE STUDIES AND RESEARCH

The undersigned certify that they have read, and recommended to the Faculty of Graduate Studies and Research for acceptance, a thesis entitled Landslides and Geotechnical Properties of Volcanic Tuff on Mount Cayley, British Columbia submitted by Zhongyou Lu in partial fulfillment of the requirements for the degree of Doctor of Philosophy.


.....

Dr. D.M. Cruden

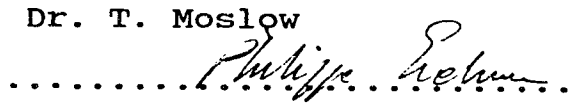
Supervisor


.....

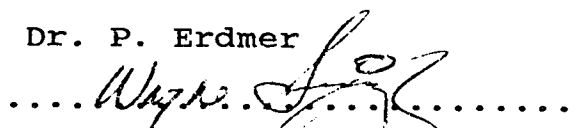
Dr. N.R. Morgenstern


.....

Dr. T. Moslow


.....

Dr. P. Erdmer


.....

Prof. K.J. Savigny

External Examiner

5 March 1993.....

ABSTRACT

A major rock slide and debris flow occurred on Mount Cayley, in June, 1984. 3.2 million cubic metres of volcanics travelled 2.0 km down Avalanche Creek at velocities up to 35 m/s to dam the confluence of Avalanche and Turbid Creeks. The breaking of the landslide dam caused an extremely fast debris flow. The velocity of the debris flow and associated wind gusts, up to 34 m/s, caused superelevations, hurled rocks and wood through the air, uprooted trees and spattered mud 16 m up trees.

The 1963 rock slide began at the head of Dusty Creek, and terminated at the new confluence of Dusty and Turbid Creeks. About 5×10^6 m³ of columnar-jointed dacite and poorly consolidated pyroclastic rocks slid 2.4 km downstream. The deposits of the 1963 rock slide have distinct layers which can be traced back to bedrock units in the depleted zone.

Volcanic tuff constitutes the basal rupture zones of the 1963 and the 1984 rock slides. The tuff has a low dry density, 13.6 KN/m³, high porosity, 36%, and very low slake durability, 25%. Two yield points are recognized from stress-strain, volume change-strain and pore pressure-strain curves of uniaxial and triaxial tests. The yield points define the starts of crushing and shearing, the destruction of the natural structure and the development of microfracturing of the tuff. The tuff shows a rapid drop of the strength after passing peak. The peak friction angle of dry tuff is 35°, saturated tuff has peak values of $\phi' = 29^\circ$, $c' = 216$ kPa and residual values of $\phi_r = 17^\circ$, $c_r = 65$ kPa.

Two major modes, Tuff Type and Dacite Type, of slope movement are recognized. Tuff Type landslides involve Units 4 and 5 of the volcanic rocks, they transport deposits with a special grain size distribution with D50 value less than 5 mm. Dacite Type landslides involve Units 2 and 3 of the volcanic rocks, they transport deposits with D50 value larger than 10 mm.

The Turbid Creek fan has been built by eight prehistoric episodes of slope movement from Mount Cayley. A new episode of slope movement started in 1963 and is going on at present. Three unstable slopes are recognized on Mount Cayley. Their sizes, movement paths, velocities and impacts on the environment are discussed.

ACKNOWLEDGEMENTS

The author wishes to express his gratitude to his supervisor Dr. D.M. Cruden for his interest and intense enthusiasm in the subject, and his guidance and support for this research. His ideas, time and valuable discussions throughout the course of this research in making it a success are very much appreciated.

Special thanks are presented to Dr. N.R. Morgenstern for his guidance and discussions of this research.

Special thanks are also presented to Dr. T. Moslow for his discussions of this research.

Thanks to Dr. S.G. Evans of Geological Survey of Canada for his valuable support in the field study.

Thanks are given to Mr. Steve Gamble of the Department of Civil Engineering for his co-operation in laboratory testings.

Thanks are also given to Mr. David Bechtel and Mr. Bruno Kasper, the author's assistants, for their hard working in the field.

Also thanks to Ms. Ruto O. Jaugelis for her valuable photos and excellent descriptions of the 1984 debris flow which she witnessed.

Field work has been supported by the Geological Survey of Canada through a grant in aid to Dr. D.M. Cruden and by the Natural Sciences and Engineering Research Council of Canada through an operating grant to Dr. D.M. Cruden

Table of Contents

Chapter	Page
ABSTRACT	iv
Acknowledgements	vi
1 INTRODUCTION	1
1.1 OBJECTIVES	1
1.2 GEOLOGIC SETTING	3
2 THE ROCK SLIDE AND DEBRIS FLOW FROM MOUNT CAYLEY IN JUNE, 1984	8
2.1 INTRODUCTION	8
2.2 EVENT DOCUMENTATION	8
Airphoto interpretation	10
Eyewitness accounts	14
2.3 THE ROCK SLIDE	19
Stratigraphy	19
Geotechnical properties of the tuff	20
Slope movement mechanism	22
Ice blocks	26
Run up	28
2.4 THE LANDSLIDE DAM	28
Rock slide deposits	28
Filling of the reservoir	32
Transformation of the landslide dam into debris flow ..	35
The velocity of the debris flow	36
2.5 THE DEBRIS FLOW	37
Debris flow deposits	37

Superelevation of debris flow	40
Mud spatters on trees	41
Uprooted trees	41
Airborne wood splinters	43
Deposits on both sides of Dusty Creek	45
2.6 CONCLUSIONS	47
3 THE KINEMATICS OF THE 1963 ROCK SLIDE ON MOUNT CAYLEY	49
3.1 INTRODUCTION	49
3.2 THE AIR PHOTO INTERPRETATION	50
Rock slide recognition	50
Rock fragment flow recognition	54
Landslide dam recognition	57
3.3 THE ROCK SLIDE	58
Geologic setting	58
Slope movement mechanics	64
3.4 ROCK FRAGMENT FLOW	67
General movement path	67
Movement trajectory of blocks	67
Velocity estimate	68
3.5 THE LANDSLIDE DAM	70
Major characteristics of 1963 landslide deposits	70
Block 1	70
Block 2	77
Block 3	81
3.6 INFLUENCE OF 1963 ROCK SLIDE ON ENVIRONMENT	90
3.7 DISCUSSION	93

3.8 CONCLUSIONS	94
4 GEOTECHNICAL PROPERTIES OF VOLCANIC TUFF AND SLOPE MOVEMENT ON MOUNT CAYLEY	96
4.1 INTRODUCTION	96
4.2 BASIC PROPERTIES OF VOLCANIC TUFF	99
Homogeneity and isotropy	99
Dry bulk density	103
Porosity	103
Slake durability	105
Point load strength	107
Direct shear test	108
Tilting table test	109
4.3 GEOTECHNICAL PROPERTIES DETERMINED FROM UNIAXIAL AND TRIAXIAL TESTS	109
Introduction	109
Two yield points and collapse	110
Critical stresses in collapse	116
Uniaxial strength	116
Behaviour of tuff under triaxial stresses	117
Strength determination	130
Pore pressure behaviour	140
4.4 COMPARISON WITH OTHER ROCKS AND SOILS	145
Comparison with Chasm tuff	145
Comparison with Canary Islands volcanic rocks	156
Comparison with volcanic tuffs in Italy	158
Comparison with loess	158

Comparison with residual soils	159
4.5 GEOTECHNICAL PROPERTIES AND LANDSLIDES FROM MOUNT CAYLEY	160
Introduction	160
Tuffs and rock slides	161
Tuffs and debris flows	162
4.6 CONCLUSIONS	163
5 COMPARISON OF THE 1984 AND THE 1963 EVENTS	166
5.1 INTRODUCTION	166
5.2 COMPARISON OF DEPLETION ZONE AND MAIN TRACK	168
5.3 COMPARISON OF TRAVEL DISTANCE, ANGLE AND VELOCITY	170
5.4 COMPARISON OF DEPOSITS	172
Geometry	172
Structure	173
Grainsize distribution	175
Plasticity	175
Water involvement	177
5.5 COMPARISON OF DAM	177
5.6 COMPARISON OF IMPACT ON THE ENVIRONMENT	181
5.7 CONCLUSIONS	188
6 HISTORY OF SLOPE MOVEMENT FROM MOUNT CAYLEY	190
6.1 INTRODUCTION	190
6.2 HISTORY ESTABLISHED FROM GEOLOGICAL MAPPING	191
Section 51.	191
Section 71	196
Section 54	199

Section 55	201
Section 56	201
Section 57	201
Seven typical deposition units	202
6.3 TWO MAJOR MODES OF SLOPE MOVEMENT	206
Two major types of grain size distribution	206
Two modes of slope movement	213
6.4 INTERPRETATION OF RADIOCARBON DATES	217
6.5 A NEW EPISODE OF SLOPE MOVEMENT	223
Evidence from air photos	223
Clue from annual ring counting	224
Information from records of logging road bridge	224
6.6 HAZARDOUS SLOPES ON MOUNT CAYLEY	225
Introduction	225
Hazardous slope 200 m downstream from 1984 head scarp	225
Hazardous slope near Peak 2251	233
Hazardous slope near the peak of Mount Cayley	239
6.7 SUMMARY AND DISCUSSION	239
7 CONCLUSIONS AND SUGGESTIONS	247
7.1 CONCLUSIONS	247
7.2 SUGGESTIONS FOR FUTURE RESEARCH.....	253
BIBLIOGRAPHY	255

List of Tables

Table	Page
2.1 Atterberg limits of the fines in 1984 deposits	33
3.1 Average values of Schmidt Hammer rebounds	62
3.2 Travel distance and junction angles	69
3.3 Main characteristics of deposits in Block 1	78
3.4 Main characteristics of deposits in Block 2	79
3.5 Main characteristics of deposits in Block 3	82
3.6 Comparison of pre-1963, 1963 and 1984 deposits	89
4.1 Summary of laboratory work	100
4.2 V_p values of tuff block and specimens	102
4.3 Brittleness index	126
4.4 Critical stresses at yield points	139
4.5 Comparison of geotechnical properties of Mount Cayley tuff and Chasm tuff	155
5.1 D50 values	176
5.2 Comparison of the deposits of the 1963 and the 1984 events	178
5.3 Comparison of the 1963 and the 1984 dams	182
5.4 Summary of the comparison of the two events	183
6.1 D50 values of prehistoric slope movement deposits	209
6.2 Comparison of D50 values	210
6.3 Main element comparison between the 1984 rock slide and hazardous slope 1	232

List of Figures

Figure	Page
1.1 Location map	2
1.2 Map of the study area	4
2.1 An overview of the 1984 rock slide and debris flow	9
2.2 (a) Air photo showing the 1984 rock slide (b) An overlay of the air photo showing the landform changes	11
2.3 Air photo of the study area on August 8, 1973	12
2.4 Geology of the study area after the 1984 rock slide and debris flow	15
2.5 The rock sequence in the left lateral margin of the rock slide	16
2.6 Longitudinal profile of the 1984 rock slide and debris flow	17
2.7 Debris flow moving over the logging road (photo by Jaugelis)	18
2.8 Projection on a Wulff net of the mean poles to bedding in the tuff and to the joint sets	24
2.9. The geometries of the depletion zones of the 1984 rock slide	25
2.10 Ice covering over Avalanche Creek at site 1	27
2.11 Cross-section at bends C-C' and E-E	29
2.12. Distribution of 1984 rock slide and debris flow deposits	31
2.13 Cumulative grain-size curves of rock slide deposits,	

and subsurface and surface debris flow deposits	34
2.14. Section G-G'	39
2.15. Mud spatters on the north (upstream) side of trees (site 32, Fig. 2.12)	42
2.16 Uprooted trees up to 1.5 m across (site 33, Fig. 2.12)	44
2.17 Airborne wood splinters (site 42, Fig. 2.12)	46
3.1 (a) Air photo showing the 1963 rock slide (b) An overlay on the air photo showing the landform changes	51
3.2 (a) Air photo taken on Aug. 2, 1947. (b) An overlay showing the location of the depleted zone	52
3.3 (a) Air photo giving the details of the landform changes on Aug. 8, 1973. (b) An overlay showing the drainage change caused by 1963 rock slide	53
3.4 Isopleth map of the depletion, main track and accumulation	55
3.5 Cross-sections of the depletion zone	56
3.6 Rock Units 1-5 showing Members 1-9 (M ₁)-(M ₉)	60
3.7 A view from the south-southeast of the rupture surface developed along a tuff layer in Member 1	61
3.8 Contoured structural diagram of poles to joints in dacite and tuff on Schmidt net	63
3.9 Lateral scarps and joints from the SSW	65
3.10 Slope stability analysis on a Wulff net	66
3.11 The accumulation zone of the 1963 rock slide	71
3.12 The boundary between block 1, and block 3	72

3.13	The boundary between block 2, and block 3	73
3.14	Three blocks viewed from a helicopter	74
3.15	Three blocks, viewed from ground	75
3.16	Block 1	76
3.17	Three layers in block 2	80
3.18	Block 3	84
3.19	Stratigraphy of blocks and their correlation	85
3.20	Three layers on the other side of block 3	86
3.21	Cumulative grain size curves of rock slide deposits	87
4.1	Grain size distribution of tuff	98
4.2	Locations of the specimens on the block sample before drilling	101
4.3	A microscopic view of the composition of Mount Cayley tuff	104
4.4	The microstructure of Mount Cayley tuff	106
4.5	Stress-strain curve of dry tuff under uniaxial compression (T 2.2).....	111
4.6	Stress-strain curve of T 2.5	112
4.7	Stress-strain curve of T 2.6	113
4.8	Stress-strain curve of T 2.8	114
4.9	Stress-strain and volume change curves of saturated tuff under triaxial compression (consolidated and drained test on T 4.9)	118
4.10	Stress-strain and volume change curves of T 4.8	119
4.11	Stress-strain and volume change curves of T 4.10 ...	120

4.12	Stress-strain and volume change curves of T 4.11	...121
4.13	Stress-strain and volume change curves of T 4.6122
4.14	Stress-strain and volume change curves of T 4.2123
4.15	Stress-strain and volume change curves of T 4.3124
4.16	Mohr circles and envelope at peak strength131
4.17	Mohr circles and envelope at residual strength132
4.18	p-q diagram at peak strength133
4.19	p-q diagram at residual strength134
4.20	p_c - q_c diagram of critical stresses at the first yield points136
4.21	p_c - q_c diagram of critical stresses at the second yield points137
4.22	Stress-strain and pore pressure curves of saturated tuff under triaxial compression (consolidated and undrained test on T 4.5)141
4.23	Stress-strain and pore pressure curves of T 4.1	...142
4.24	Location map of Chasm Slides146
4.25	A microscopic view of the composition of Chasm tuff148
4.26	The microstructure of Chasm tuff150
4.27	Stress-strain curve of dry Chasm tuff under uniaxial compression152
4.28	Stress-strain curve of saturated Chasm tuff under triaxial compression154
5.1	The depletion zones of the 1963 and the 1984 events167

5.2	The 1984 debris flow deposits	174
6.1	A map of slope movement deposits in downstream Turbid Creek valley and its fan	192
6.2	(a) Air photo showing four levees between Turbid and Terminal Creeks. (b) An overlay of the air photo ...	193
6.3	Section 51	194
6.4	Section 71	197
6.5	Section 54	200
6.6	Section 41	204
6.7	Grain size distribution curves	208
6.8	Slope movement and drainage development	216
6.9	Radiocarbon dates on the time scale	220
6.10	Location of three major hazardous slopes	226
6.11	Hazardous slope 1	228
6.12	The front of hazardous slope 1	229
6.13	Tension cracks on hazardous slope 1	230
6.14	Hazardous slope 2	234
6.15	Air photo and its overlay showing hazardous slope 2	235
6.16	A profile of hazardous slope 2 and its overlay ...	236
6.17	Cracking on hazardous slope 2 shown on photo and overlay	237
6.18	Hazardous slope 3	241
6.19	Air photo and overlay showing hazardous slope 3 ...	242
6.20	A tension crack near the peak of Mount Cayley	243

1. INTRODUCTION

1.1 OBJECTIVES

This thesis examines the landslides on Mount Cayley, British Columbia (Fig. 1.1), the geotechnical properties of volcanic tuff and their relationship between landslides and the tuff. The major objectives of the dissertation are to determine:

1. the kinematics of two major events, the 1984 rock slide and its successive debris flow and the 1963 rock slide,
2. the velocities of these landslides based on the field phenomena created by these events,
3. the geotechnical properties of Mount Cayley tuff and their role in landslide development on Mount Cayley,
4. the major modes of landslide on Mount Cayley based on the lithology of landslide deposits, and
5. the history of slope movement on Mount Cayley and the hazardous slopes.

To achieve these objectives, I carried out a detailed field investigation in June-September 1989 and a new laboratory testing programme from May, 1990 to December, 1991.

This thesis is written in paper format. Chapter 1 states the objectives and the geologic setting. Chapter 2 documents the 1984 event and forms a paper which appeared in the Canadian Geotechnical Journal (Cruden and Lu 1992). Chapter 3 describes the kinematics of the 1963 rock slide, especially the lithology of the deposits. Chapter 4 presents the results of testing the Mount Cayley tuff and a comparison with the Chasm tuff, other volcanic tuffs in Spain and

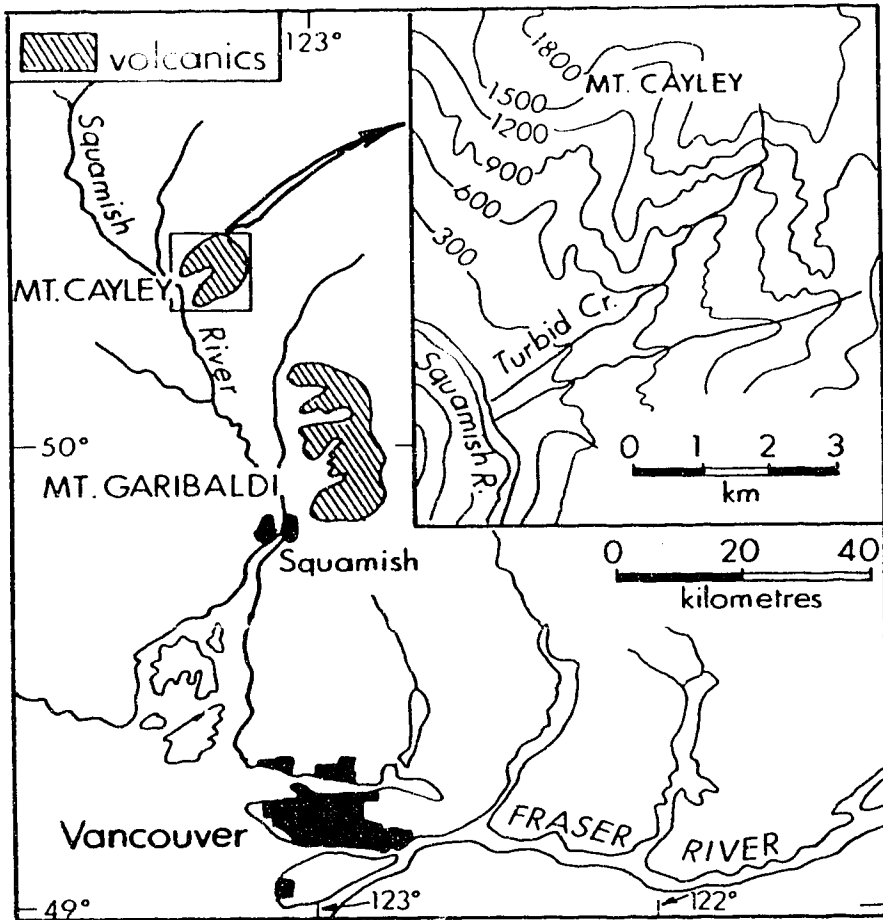


Figure 1.1 Location map

Italy, loess and residual soils. Chapter 5 compares the 1963 rock slide with the 1984 event. Chapter 6 discusses the history of slope movement on Mount Cayley and establishes two modes of slope movement on Mount Cayley from the study of lithology of prehistoric landslide deposits in the study area. A part of Chapter 6 forms a discussion which appeared in the Canadian Journal of Earth Sciences (Lu 1992). Finally, Chapter 7 gives the main conclusions and suggestions for future research.

1.2 GEOLOGIC SETTING

Mount Cayley is one of 12 Quaternary volcanoes forming the Mount Garibaldi Volcanic Belt, which extends about 120 km from Mount Garibaldi at the head of Howe Sound to Meager Mountain near the head of Lillooet River (Clague and Souther 1982). The age of volcanic activity in this belt ranges from Pliocene to Holocene, the most recent major eruption having occurred at Meager Mountain about 2400 years ago (Nasmith et al. 1967; Read 1979). According to Green et al. (1988), the ages of the volcanic rocks on Mount Cayley are approximately determined to be 0.31 to 3.8 Ma.

The present edifice of the Mount Cayley volcanic complex rises to a group of three precipitous pyramidal peaks; Mount Cayley with an elevation of almost 2400 m and the slightly lower but equally rugged summits of Wizard Peak and Pyroclastic Peak (Fig. 1.2). The complex rests on a highly irregular basement surface of plutonic and metamorphic rocks belonging to the Mesozoic to early Tertiary Coast Plutonic Complex. The topography prior to eruption was similar to that of the present Coast Mountains. Thus, the basal

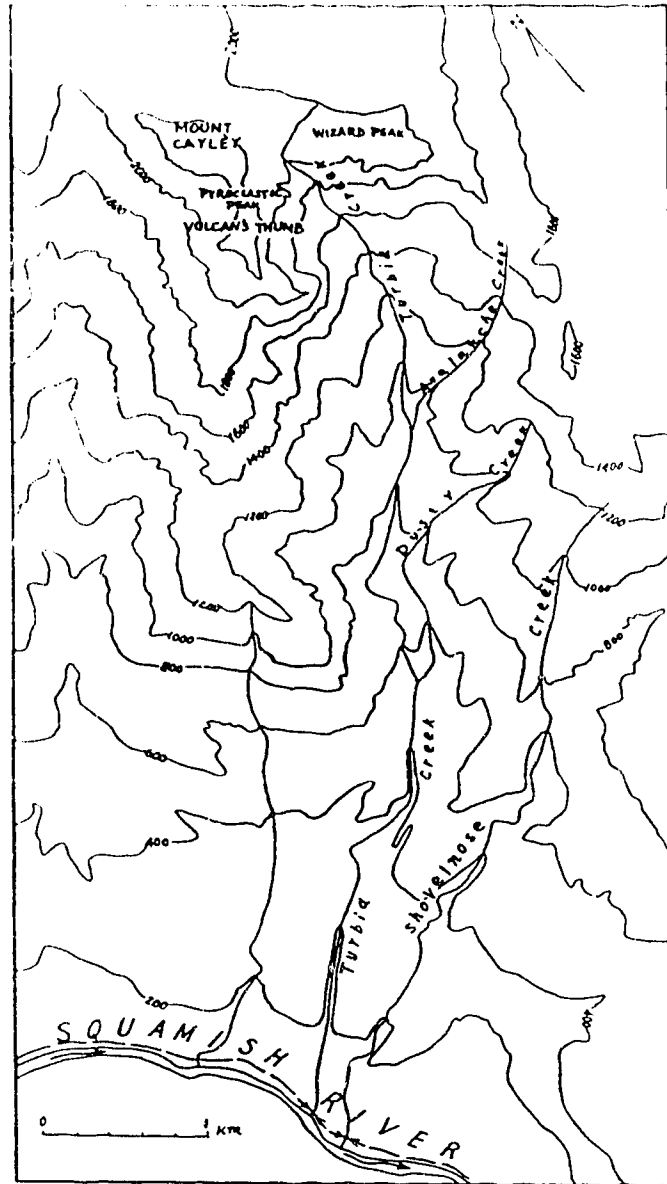


Figure 1.2 Map of the study area

members of the Mount Cayley pile rest on a variety of materials, ranging from glacially scoured basement rocks to buried colluvium up to 25 m thick (Clague and Souther 1982).

The Mount Cayley complex formed during at least three distinct eruptive periods: the Mount Cayley, Vulcan's Thumb, and Shovelnose stages. The earliest, or Mount Cayley, stage produced a composite pile of dacite flows, tuffs, and breccia. During the subsequent Vulcan's Thumb stage of activity, an extensive tephra cone was superimposed on the southwestern flank of the Mount Cayley edifice. Vulcan's Thumb, the largest in a cluster of slender pinnacles, represents a remnant of vent breccia deposited in the upper part of this volcano. The base of the Vulcan's Thumb succession rests on a steep westerly dipping surface that truncates older deposits of the Mount Cayley stage and laps onto the basement surface. A majority of the Vulcan's Thumb rocks are extensively weathered. The third, or Shovelnose, stage of activity produced two domes and related flows of hypersthene, biotite dacite in the valley of Shovelnose Creek (Fig. 1.2) (Green et al. 1988).

According to Clague and Souther (1982), the bedrock in the study area consists of six units (Fig. 3.5).

Unit 1 consists of basement rock, granodiorite, quartz diorite, and gneiss.

Unit 2 is the rocks of the Mount Cayley stage which are mainly porphyritic hornblende dacite flows and rhyodacite pyroclastics. The basal unit is a complex of overlapping flows, dykes, and pyroclastic deposits, all of which have undergone moderate to

intense hydrothermal alteration. In the Dusty Creek valley (Fig. 1.2), this unit consists of up to 150 m of columnar-jointed dacite flows, which overlie a basement surface. A layer of pale green, bedded lapilli tuff, 2-3 m thick, is present locally between these flows and the basement surface.

Unit 3 overlies the basal unit of the Mount Cayley stage. This unit is a complex of coarse breccia, flows and domes. In the source areas of Dusty and Avalanche Creeks (Fig. 1.2), this unit comprises up to 250 m of pyroclastic rocks and subordinate discontinuous flows, all of rhyodacitic composition. The pyroclastics range from loosely aggregated tuff breccia containing angular blocks about 1 m across to laminated green and white lapilli tuff. Although the internal structure of this unit is complicated by lateral variations in the thickness of pyroclastic wedges, most beds dip steeply off the mountain towards the southwest. The related flows and intrusions are characterized by very irregular, sinuous to radiating, small columns, which were formed by joints.

Unit 4 consists of porphyritic biotite rhyodacite flows. In Dusty Creek, a single massive rhyodacite flow, which dips and thickens towards the southeast from 50 to 200 m, disconformably overlies the Mount Cayley sequence. The base of this flow is aphyric to vitreous, and its central part is complexly jointed; a blocky breccia caps the flow.

Unit 5 consists of porphyritic dacite tuff breccia and tuff. In the source area of Dusty Creek, these pyroclastic rocks consist of up to 150 m of steeply southwest dipping tuff breccia containing

angular blocks up to about 3 m across.

Unit 6 is the rocks of the youngest, or Shovelnose, stage consisting mainly of porphyritic dacite flows, domes, and cupolas.

The joint measurements and the detail of the rocks mapped from the 1989 field investigation are given in Chapters 2 and 3.

2 THE ROCK SLIDE AND DEBRIS FLOW FROM MOUNT CAYLEY

BRITISH COLUMBIA IN JUNE, 1984

2.1 INTRODUCTION

To the six major historic rock slides that have been documented in Quaternary volcanic centres in the Coast Mountains of British Columbia (Evans 1984, 1986, 1987), we add this detailed report of the rock slide and debris flow which occurred on Mount Cayley, B.C. in June, 1984. This is the first of these events that has surviving eyewitnesses. It is also the first report describing the conversion of a landslide dam into a debris flow.

The debris flow completely removed the bridge and its approaches that carried the logging road up the Squamish Valley across the mouth of Turbid Creek (Figs. 1.2 and 2.1). It blocked the Squamish River during surges, engulfed 0.5 km of the logging road in mud from the Creek and introduced huge quantities of sediments to the Squamish River, leading to significant channel changes (Jordan 1987; Hickin and Sichingabula 1988; Cruden and Lu 1989).

To understand this event, a field investigation and a laboratory testing programme were carried out (Lu 1988). The stages of the event rock slide, landslide dam and debris flow are presented in this Chapter. We first consider its documentation.

2.2 EVENT DOCUMENTATION

Three stages of the 1984 event can be inferred, a rock slide, a landslide dam and a debris flow, but only the debris flow was seen. The two earlier stages in the movement are interpreted from



Figure 2.1 An overview of the 1984 rock slide and debris flow looking NEE at site 15 (Fig. 2.12). Note that A and T represent Avalanche and Turbid Creeks, and W points out the depletion zone of the 1984 rock slide.

air photos and field mapping.

Air Photo Interpretation

A scarp at the head of Avalanche Creek at elevation of 1600 m and new deposits in the valleys of Avalanche and Turbid Creeks are clearly shown on the air photo taken in 1986 (Fig. 2.2). Comparing the air photo with the air photos taken in 1982 and 1973 (Fig. 2.3), significant changes can be recognized (Fig. 2.2).

1. A rock mass on the northwest slope of Avalanche Creek disappeared in the 1986 air photo (J in Fig. 2.2-b).

2. A large portion of the southeast slope was swept away (K in Fig. 2.2-b) exposing a distinct white-grey tuff layer between Members 6 and 7, and the yellow hard tuff of Member 6 (L in Fig. 2.2-b). Groundwater seepages are present along the top of the tuff layer (G in Figs. 2.2-b and 2.5).

3. A high forest trimline on both sides of Avalanche Creek on the 1986 air photos, indicates the level the rock slide debris reached during movement (N in Fig. 2.2-b).

4. A small ridge between Avalanche and Turbid Creeks was locally overtopped and eroded by the rock slide debris (O in Fig. 2.2-b).

5. Landslide dam remnants show on the 1986 air photos from the confluence to 500 m downstream (P-P in Fig. 2.2-b).

6. The valley of Turbid Creek downstream from the dam remnant was blanketed by debris flow deposits (Q in Fig. 2.2-b).

7. The stream channel of Turbid Creek straightened (W in Fig. 2.2-b). Turbid Creek shifted its main channel back to its position

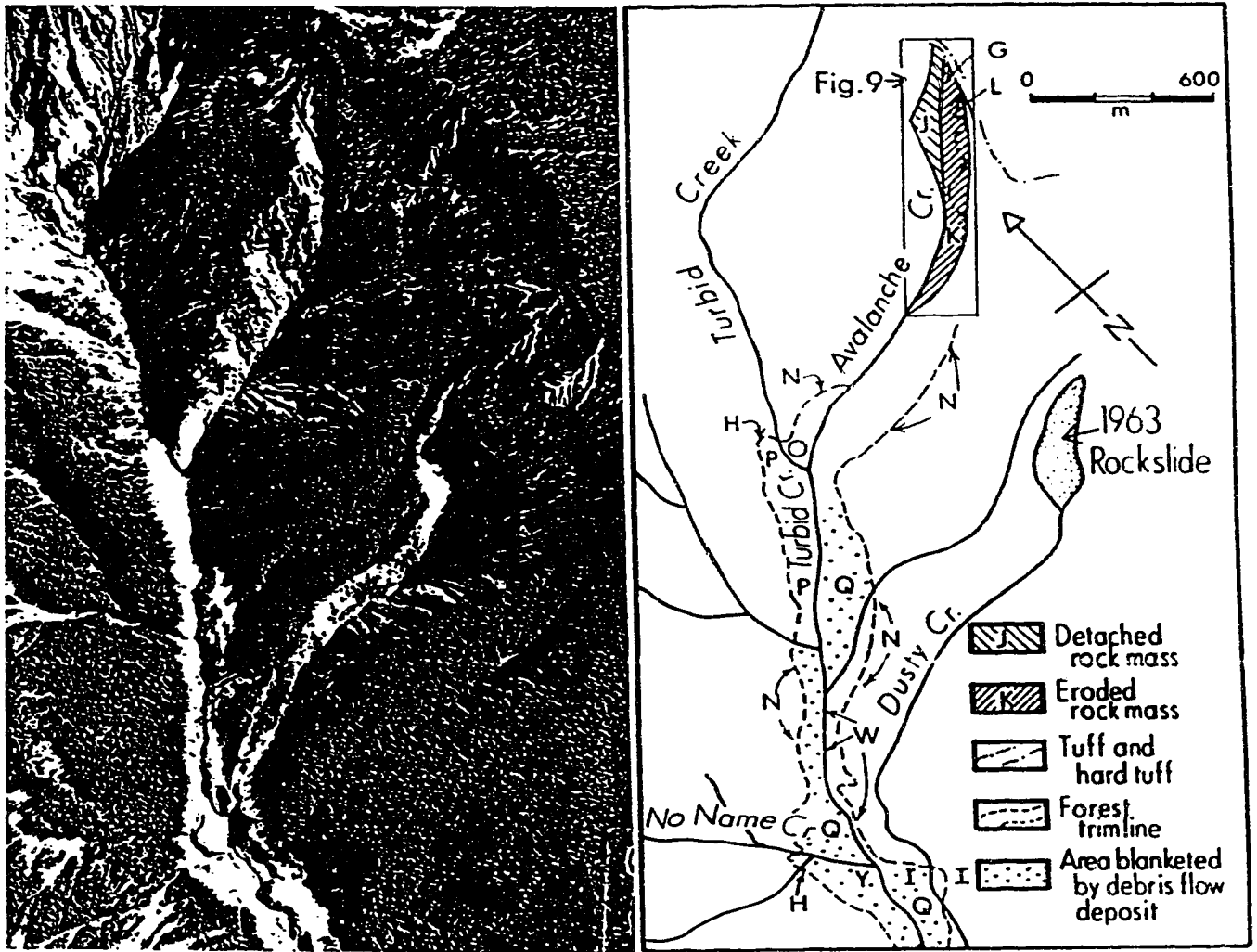


Figure 2.2 (a) Air photo showing the 1984 rock slide on July 30, 1986 (Province of British Columbia photos BC86061-097). (b) An overlay of the air photo showing the landform changes in Turbid Creek caused by the 1984 rock slide and debris flow.



Figure 2.3 Air photo of the study area on August 8, 1973
(Province of British Columbia photos BC7520-259).

before the 1963 rock slide (Clague and Souther 1982) near the confluence of Turbid and No Name Creeks (Y in Fig. 2.2-b).

8. The rock slide ran up the northwest slope of Turbid Creek immediately below the confluence of Turbid and Avalanche Creeks (H in Fig. 2.2-b).

9. Another superelevation site on the west slope of Turbid Creek can be easily recognized on the 1986 air photos (H, south of No Name Creek in Fig. 2.2-b).

10. High forest trimlines in the Turbid Creek valley indicate the power of the debris flow (N in Fig. 2.2-b).

11. The debris flow overtopped the terraces formed by the 1963 rock slide deposits, passed Dusty Creek and left its deposits on both sides of Dusty Creek (I-I in Fig. 2.2-b).

The debris flow passed the present mouth of Dusty Creek and continued its movement till it entered the Squamish River. The debris flow was confined to the Turbid Creek channel downstream.

Interpretation of these photographs indicated that the 1984 event began as a rock slide at the head of Avalanche Creek. A rock mass detached from northwest slope of Avalanche Creek and impacted the southeast wall of the valley, knocked down a large portion of the wall, broke up and eroded ice from Avalanche Creek. The rock slide was confined to the valley of Avalanche Creek till it overtopped the small ridge between Avalanche and Turbid Creeks, damming the two creeks with rock slide debris. The rock slide had travelled 2.0 km downstream on a slope of 20° (Fig. 2.6). The rupture of this dam created a debris flow. The dam remnant, the

thick deposits at the confluence, and the debris flow deposits downstream in Turbid Creek were mapped in the summers of 1986 and 1989. Yellow hard tuff, breccia, purple lapilli and breccia seen in the deposits can be traced to the Avalanche Creek scarp (Figs. 2.4 and 2.5).

With Avalanche and Turbid Creeks dammed, water accumulated behind the dam from ice in the debris and the water flowing down the two creeks after two days of rain (Jordan 1987). When the debris dam was breached, the flow carried ice and debris downstream rapidly on a slope of 5° (Fig. 2.6).

Eyewitness Accounts

Nobody saw the rock slide in Avalanche Creek, but at least eight people (R.O. Jaugelis, C. Deminger and J. Thompson among them) witnessed the debris flow at the mouth of Turbid Creek.

Water Survey of Canada technician, Ruta O. Jaugelis wrote "The magnitude of the event was awe-inspiring, in terms of the noise rumbling from the distance and the volume of mud and debris coming down in successive waves, large enough to flow above the road level as the picture shows.the picture was taken at not quite the peak of a typical wave (Fig. 2.7). The momentum was enough that the flow crossed the Squamish River and travelled up the right bank against the rock face, then back down into the river. Enough mud and debris was carried down in successive waves to back up the Squamish River upstream for a distance." (personal communication, 1987).

The Squamish Times (July 10, 1984) reported, "About 4:30 on

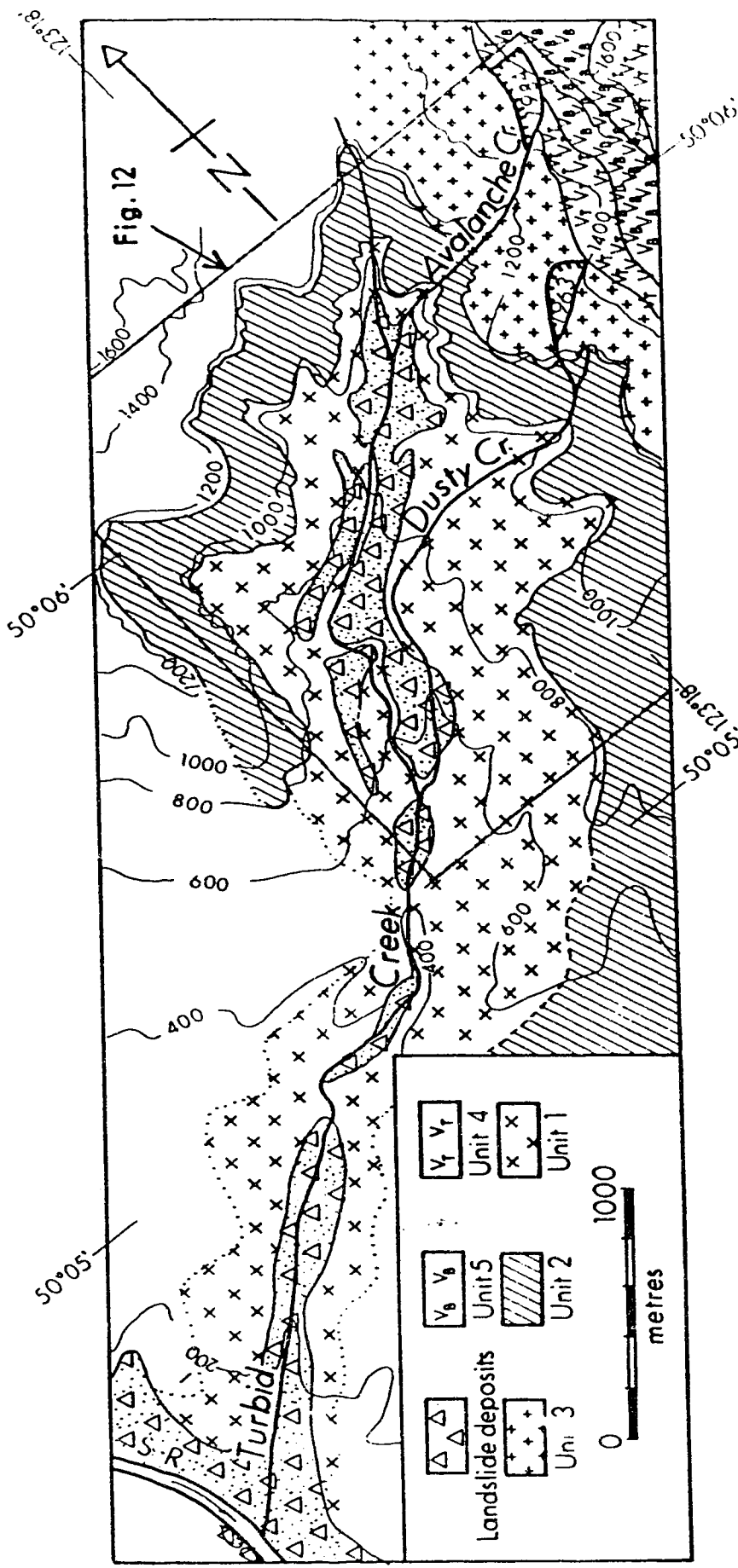


Figure 2.4 Geology of the study area after the 1984 rock slide

and debris flow. S.B. represents the Squamish River.
 and debris flow. S.R. represents the Squamish River.

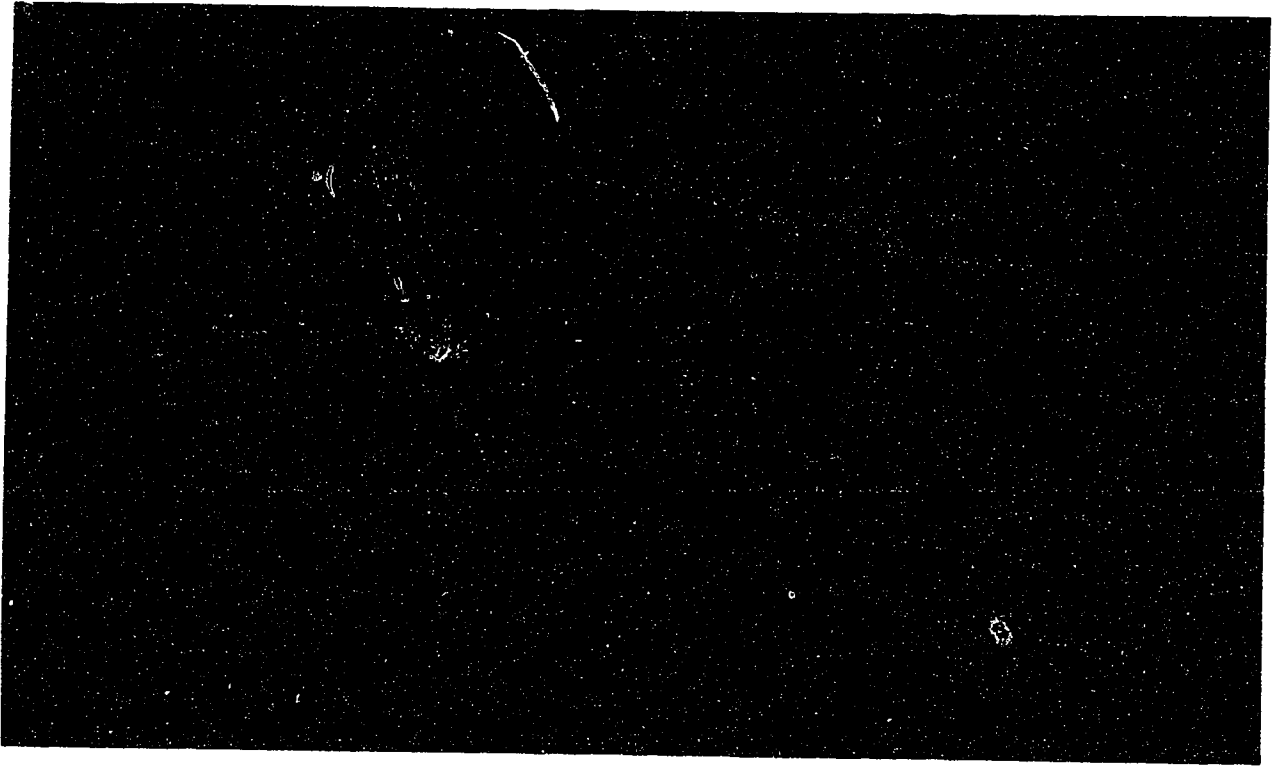


Figure 2.5 The rock sequence in the left lateral margin of the rock slide looking NNE at site 1 (Fig. 2.12). The height of trees, 16-18 m, gives scale. (4)-(5) and (M_6)-(M_9) are units 4 and 5, and members 6 to 9 respectively. W is a part of the depletion zone. F shows ground fracture. G is the groundwater seepage and S is the sampling location.

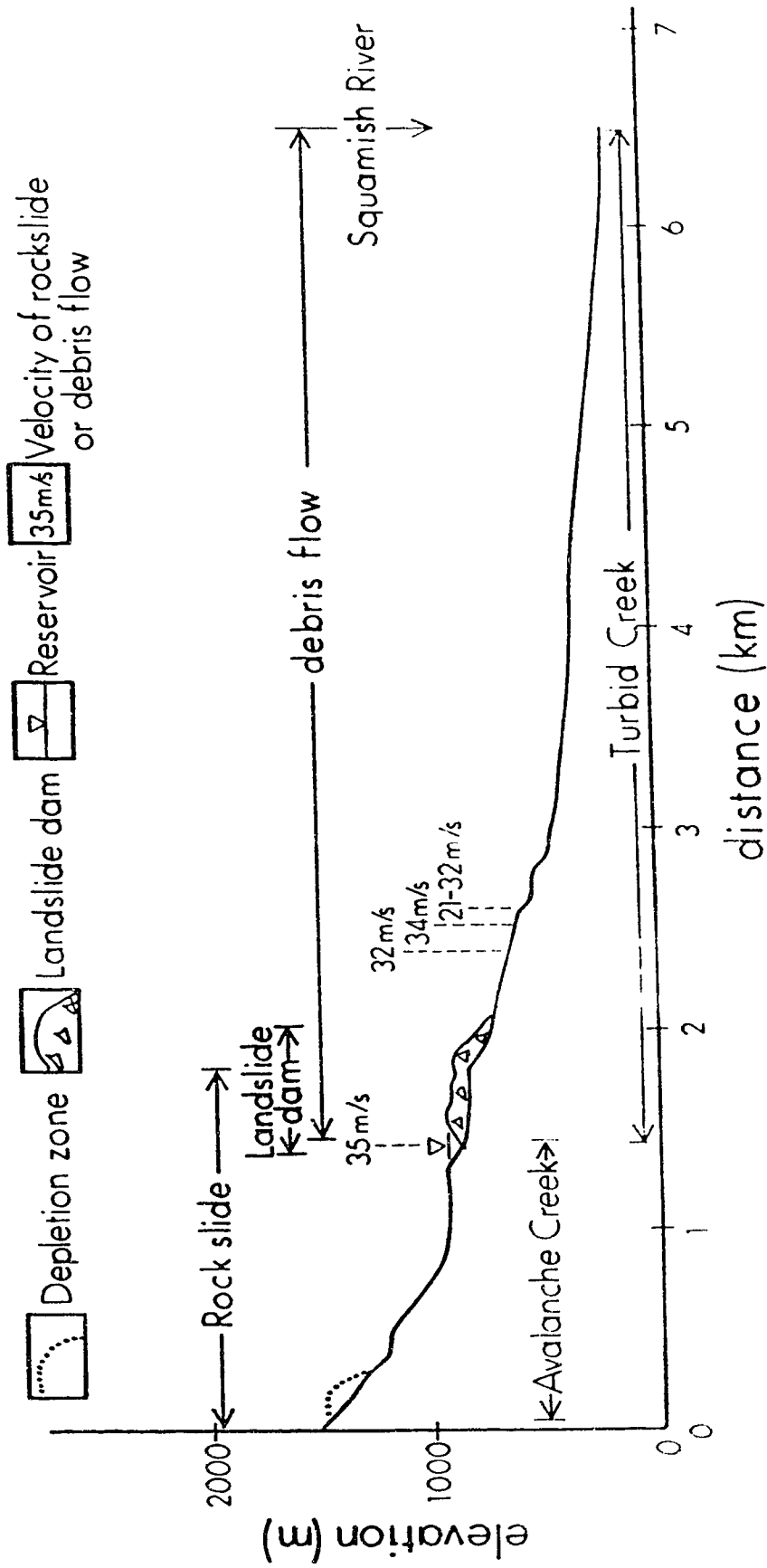


Figure 2.6 Longitudinal profile of the 1984 rock slide and debris flow. The dotted line shows the slope before the rock slide.



Figure 2.7 Debris flow moving over the logging road (photo by Jaugelis). S.R. represents the Squamish River.

Thursday afternoon, after a few days of heavy rain, a wall of mud and debris came down the bed of Mud Creek, taking out the bridge which was at least 30 feet above the stream bed.The mud came down in waves, blocking the Squamish River and breaking loose, only to be followed by successive waves of mud, which again blocked the river. A portion of the road was engulfed in the mud from the creek."

This report needs to be clarified. The event was not on the previous Thursday, but on June 28. Mud Creek is a local name for Turbid Creek. The road mentioned in the report is the logging road along the Squamish River. The bridge was across Turbid Creek near its mouth. Charlie Deminger and John Thompson of Empire Logging confirmed this information, and emphasized that many ice blocks were deposited in the stream bed of the creek near the logging road.

In summary, the debris flow on June 28, 1984, moved in waves, crossed the Squamish River and travelled up the west bank, partially blocking the river. Debris surges lasted at least 2 hours, because a wall of mud and debris came down at 16:30 and Jaugelis arrived about 18:00 and watched for over 30 minutes.

2.3 THE ROCK SLIDE

Stratigraphy

The bedrock has been divided into six units by Souther (1980) (Fig. 2.4). Unit 1 is basement rock, granodiorite, quartz diorite, and gneiss. Unit 2 consists of porphyritic hornblende dacite flows and rhyodacite pyroclastics. Unit 3 comprises pyroclastic rocks and

subordinate discontinuous flows, all of rhyodacitic composition. Unit 4 consists of porphyritic biotite rhyodacite flows. Unit 5 consists of porphyritic dacite tuff breccia and tuff. Unit 6 consists of porphyritic dacite flows, domes, and cupolas.

Only Units 4 and 5 are present in the depleted zone of the 1984 rock slide. We have divided these two units into 4 members (Lu 1988 and Fig. 2.5). Member 6, 60 m thick, consists of yellow hard tuff and breccia, and brown dacite. Member 7, 120 m thick, consists of purple lapilli, breccia and breccia tuff with white-grey tuff at the base. Member 8 is a white tuff layer, 20 m thick. Member 9 consists of purple lapilli, breccia and breccia tuff, 40 m thick. The main scarp of the rock slide developed along planar, northeast and northwest striking, vertical joint sets. The rupture surface is a weak tuff layer.

Geotechnical Properties of the Tuff

The white-grey fine tuff between Members 6 and 7 contained the rupture surface of the 1984 rock slide and its slaking made an important contribution of fines to the viscous debris flow. To understand the behaviour of the fine tuff, a laboratory programme (following Franklin and Chandra 1972; Bieniawski 1974, 1979, 1989; International Society of Rock Mechanics 1979; and Kirkaldie 1988) was carried out on the specimens prepared from four block samples of the fine tuff collected from the scarp of the 1984 rock slide (Fig. 2.5). The white-grey fine tuff has lithic fragments (5-10%) up to 4 mm in length in a submicroscopic matrix.

Laboratory testing showed that the tuff has a low dry density

(range of 1.28-1.47 g/cm³, and average of 1.39 g/cm³) and a high porosity (range of 30%-43%). Dry density was established by the water displacement method (ISRM, 1979), and porosity determined by the water absorption method (ISRM 1979) and the dry porosity determination method following Morgenstern and Phukan (1968). The tuff has a very low Slake Durability Index (25%) and a low uniaxial compressive strength, 1.5-2.4 MPa, when dry. Slake durability was determined by the standard apparatus and method recommended by Franklin and Chandra (1972) and ISRM (1979). Uniaxial compressive strength was determined by triaxial compressive testing (Bishop and Henkel, 1962) and compared with point load testing (Broch and Franklin, 1972; Bieniawski, 1974). The tuff has a friction angle of 34⁰-37⁰ when dry and 30⁰ when saturated (over normal loads in the range of 50-400 kPa in 51 mm diameter specimens in a high capacity shear box).

As the joints in the volcanic rocks on Mount Cayley are open, the cohesion and friction along these joints are assumed to be zero.

To summarize this information, we can estimate RQD, the rock quality designation, by 115-3.3 Jv (Palmstrom 1982), where Jv represents the total number of joints per cubic metre. As Jv=30, the RQD is 16, very poor rock. Again, as the spacing of the discontinuities is 100 mm, the surfaces of the discontinuities are slightly rough and their separation is less than 1 mm, and generally speaking, the rock mass is damp, then following Bieniawski (1979, 1989) and Kirkaldie (1988), the rock mass rating

is 42. As the orientations of the discontinuities on the slopes are unfavourable, the rating adjustment is -50. The rock mass class determined from the total rating is again very poor rock.

Slope Movement Mechanism

The main scarp of the rock slide developed along planar, steep joints which allow snow melt and rainfall to penetrate the slope. Similar open cracks are seen on the north slope of Avalanche Creek, 50 m downstream of the 1984 rock slide scarp and on the slope opposite the rock slide scarp. Cracks may open before slope failure as the toe of the slope is eroded by the creek. So these steep, open cracks may indicate future slope movements.

The tuff layers are the weak zones in the volcanic pile compared to the columnar-jointed dacite and breccia. Groundwater seeps out along the top of the tuff layer in Unit 4 indicating that the tuff layer is relatively impermeable compared to other rock layers in the volcanic pile (Fig. 2.5). So, at times, sufficient water may accumulate on the tuff layer to fully saturate it, causing strength reduction and build up of pore pressure. In addition, the top of the tuff layer may break and disintegrate into small particles resulting in further reduction of its strength.

The tuff layer in the depletion zone of the 1984 rock slide dips at 33° towards 168° , while the reconstructed slope face of the 1984 rock slide dips at 61° towards 152° . As shown in Figure 2.8, the joints of set 1 form a wedge with the bedding which is free to slide along the weak tuff layer when that layer is saturated. Notice that the dip direction of the tuff layer falls between the

dip direction of the slope face and the line of intersection, I_{j1-b} , of bedding and joint set 1, indicating by Hocking's criterion (Cruden 1984) that sliding can occur down the dip of the bedding.

Jordan (1987) and Evans and Gardner (1989, Table 12.1 P. 711) estimated the volume of the 1984 rock slide as $5 \times 10^6 \text{ m}^3$. Based on the thickness of the volcanic pile involved in the rock slide and field investigation, we made an estimate of the volume of the rock slide. The rock mass detached from the northwest slope involved Members 7 and 8, and 20 m of Member 9 as shown in Fig. 2.9-a. As it can be treated as a pyramid, the volume of the rock mass can be estimated as

$$V_a = \pi W_a L_a h_a / 12$$

Where W_a is the width of the detached rock mass, L_a is the length of the detached rock mass and h_a is the height of the detached rock mass.

As $h_a = 160 \text{ m}$ and $W_a = 200 \text{ m}$, so $L_a = 335 \text{ m}$ then $V_a = 2.8 \times 10^6 \text{ m}^3$.

The rock mass eroded from the southeast slope has dimensions shown in Fig. 2.9-b as $W_b = 400 \text{ m}$, $L_b = 90 \text{ m}$ and $h_b = 20 \text{ m}$. The volume of the rock mass is estimated as

$$V_b = \pi W_b L_b h_b / 6 = 0.4 \times 10^6 \text{ m}^3$$

Where W_b is the maximum width of eroded rock mass, L_b is the maximum length of eroded rock mass and h_b is the maximum height of eroded rock mass.

So, the total rock mass of volcanic rocks, V_a , V_b , detached from the head of Avalanche Creek was $3.2 \times 10^6 \text{ m}^3$. Swell due to breakage of the rock may have increased this volume by about 20%.

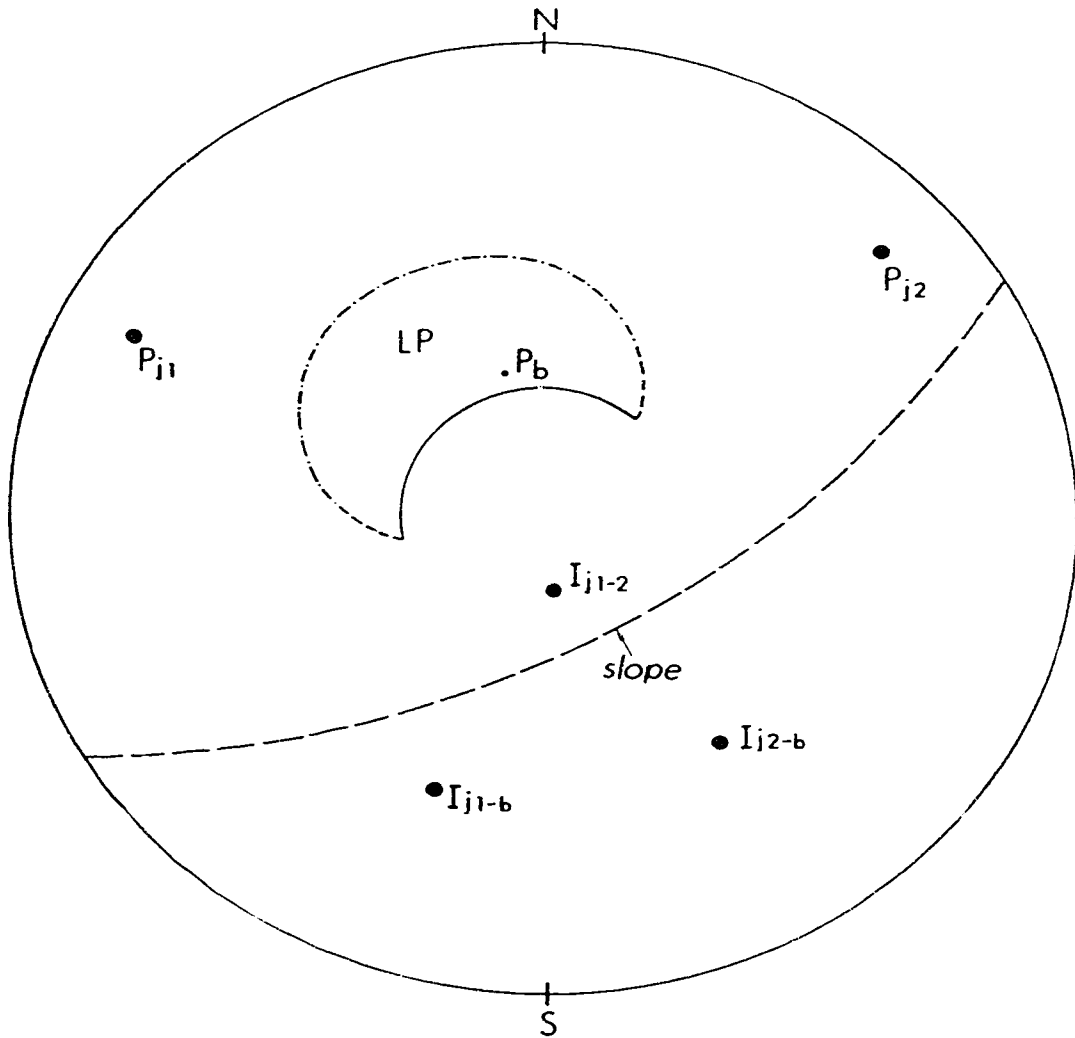


Figure 2.8 Projection on a Wulff net of the mean poles to bedding in the tuff (P_b) and to the joint sets (P_{j1} and P_{j2}). Averages are based on 50 measurements. The intersections of the three discontinuities are I_{j1-b} , I_{j2-b} and I_{j1-2} . LP is the locus of poles to discontinuities that can daylight on the slope; its solid margin is the 30° friction circle.

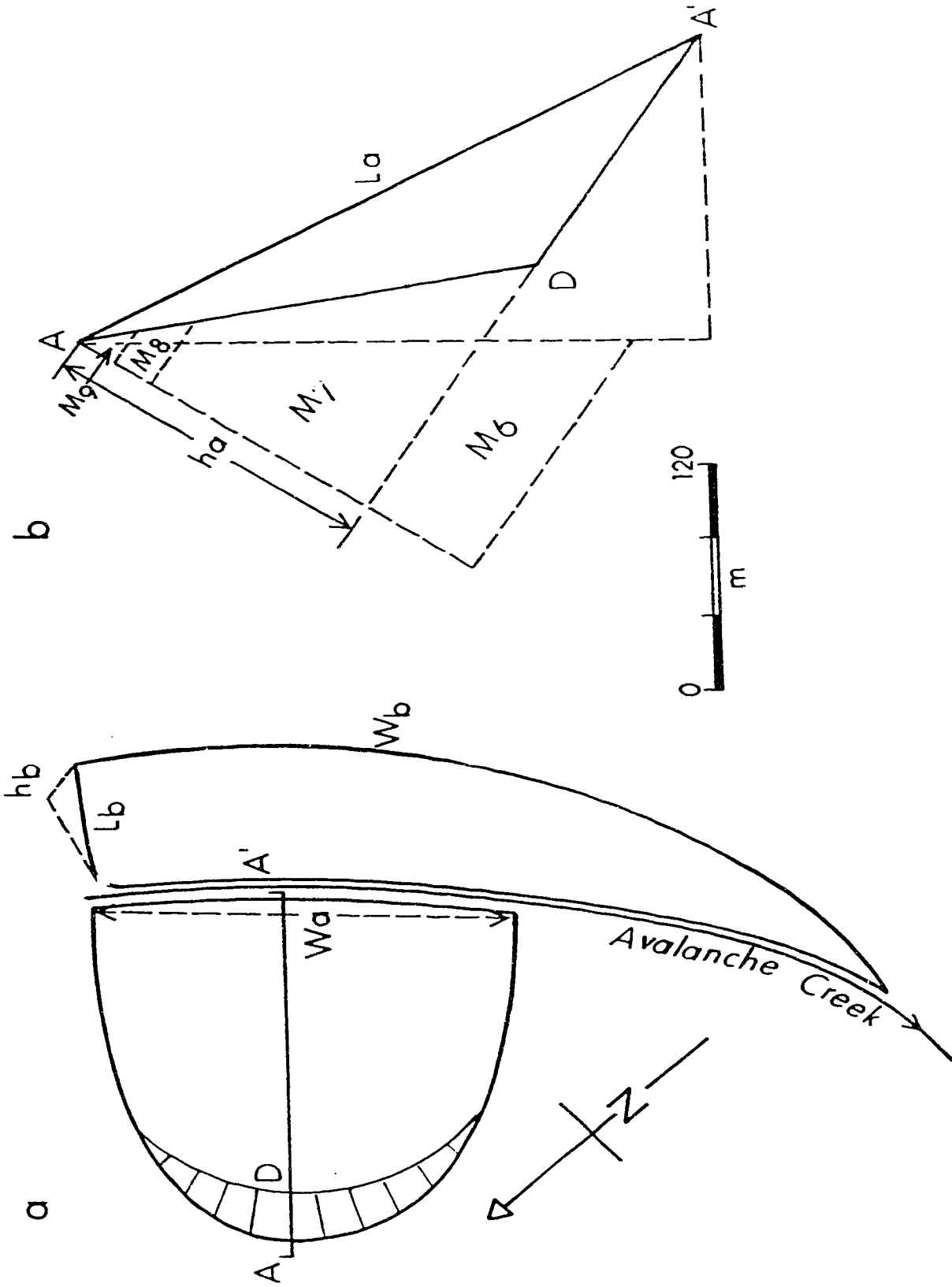


Figure 2.9 The geometries of the depletion zones of the 1984 rock slide. (a) The depletion zone on the northwest slope. (b) The depletion zone on the southeast slope.

Sliding occurred down the dip of the bedding, the section in Figure 2.9 can be used to carry out a back analysis following Hoek and Bray (1981, pp. 152-154) and Cruden (1984, p. 678)

Assuming conservatively that there was no pore pressure in the slope and as there was no cohesion along the tuff bedding surface, so

$$F = \cos \psi_p \tan \Phi / \sin \psi_p$$

where F is the factor of safety, ψ_p is dip angle of the rupture surface and Φ is the friction angle along rupture surface.

As $\psi_p = 33^\circ$ and $\Phi = 30^\circ$ (when the tuff layer was saturated), so $F = 0.90$.

As the factor of safety of the slope was less than 1 without pore pressure, pore pressures on the rupture surface do not seem necessary to cause slope failure.

Ice blocks

Figure 2.10 shows the snow cover over Avalanche Creek. This picture was taken on Aug. 12, 1989 at site 1. All but the first 100 m from the mouth of Avalanche Creek is covered by snow and ice with an average thickness of 15 m. The average width of the creek bottom is 30 m. The snow and ice in the creek is interbedded with debris fallen from both sides of the creek. As Avalanche Creek is in the shadow of both the steep slopes of the creek, the wide bottom of the creek traps and preserves snow blown from the surrounding mountain ridges. When the displaced rock mass of the 1984 slide moved downstream at high velocity, the snow and ice would have been eroded and carried away by the moving debris. As the length of



Figure 2.10 Ice covering over Avalanche Creek looking NEE at site 1 (Fig. 2.12).

Avalanche Creek covered by snow and ice is 1 km, about $0.45 \times 10^6 \text{ m}^3$ snow and ice would join the rock slide debris and come to rest at the confluence of Avalanche and Turbid Creeks forming a landslide dam which consisted of about $3.2 \times 10^6 \text{ m}^3$ of rock debris and about 15% of this volume of snow and ice.

Run up

When the 1984 rock slide debris entered the confluence of Avalanche and Turbid Creeks, it ran up on the northwest side of Turbid Creek and reached 63 m higher than the deposits on the southeast side of Turbid Creek, destroyed many trees and left yellow hard tuff and breccia on the slope (Figs. 2.2 and 2.11-a). After impacting the northwest slope, the debris fell back into Turbid Creek and came to rest. Assume no friction losses along the bottom and the sides of the valley, and no oscillatory movements the velocity can be estimated by

$$V = (2gh)^{1/2} = 35 \text{ m/s}$$

where V is the initial velocity of the debris movement at the confluence, g is the acceleration due to gravity, and h is the difference in elevation of the deposits on the two sides of the creek. Neglecting friction losses along the bottom and the sides of the valley and oscillatory movements, which occur in a debris flow, gives a velocity estimate is probably a low value.

2.4 THE LANDSLIDE DAM

Rock Slide Deposits

After the rock slide overtopped and eroded the ridge between Avalanche and Turbid Creeks, ran up the opposite slope on the

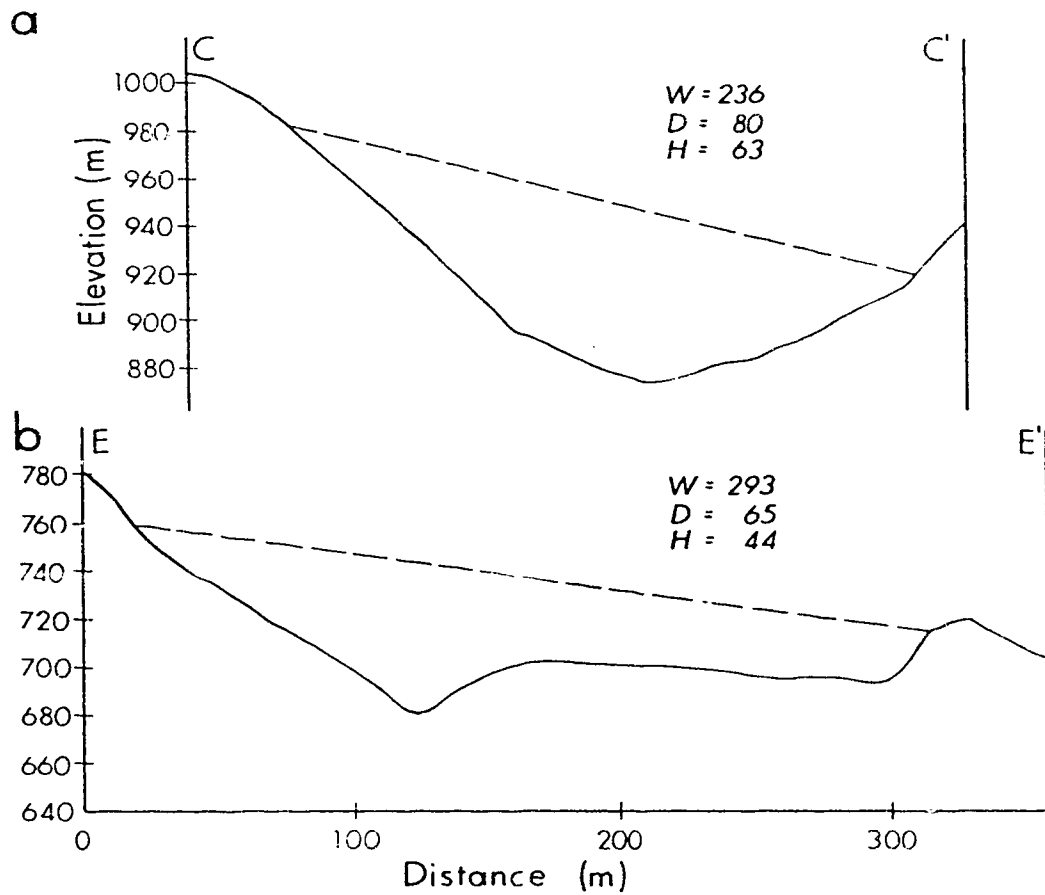


Figure 2.11 Cross-sections at bends C-C' and E-E' (Fig. 2.12) showing rock slide run up and debris flow super-elevation, respectively. Dashed lines represent the surfaces of the debris streams. W and D are the width and maximum depth, respectively, of the debris streams. H is the run up (a) or super-elevation (b).

northwest side of Turbid Creek and fell back into Turbid Creek at the confluence of Avalanche and Turbid Creeks, the main body of the rock slide came to rest in the Turbid Creek valley.

The junction angle between Avalanche Creek (the contributing channel) and Turbid Creek (the receiving channel) was in the range from 60° to 72° . It is close to debris flows 3 and 7 from Benda and Cundy (1990, Fig. 5). The rock slide debris collided with the valley wall opposite the channel junction and came to rest in the receiving channel within 500 m.

Other rock slides in the Garibaldi Belt have also deposited their displaced material when they entered larger channels at high angles to their path, the Devastation Glacier slide (Patton 1976, and Evans 1986), the Rubble Creek slide (Moore and Mathews 1978) and the 1986 rock avalanche from the peak of Mount Meager (Evans 1987) are examples.

We can explain these events by assuming with Benda and Cundy (1990) that when the junction angle between the contributing and the receiving channels approaches 70° , collision of the displaced material with the opposite valley wall causes significant energy losses. The return of this material back down into the valley after collision with the opposite wall impacts later material moving into the junction for the first time. This causes accumulation at the junction.

The rock slide deposits dammed Turbid Creek. Dam remnants can be seen on the 1986 air photos and at the site (Fig. 2.12). The remnants suggest the height of the debris dam was 70 m, its width

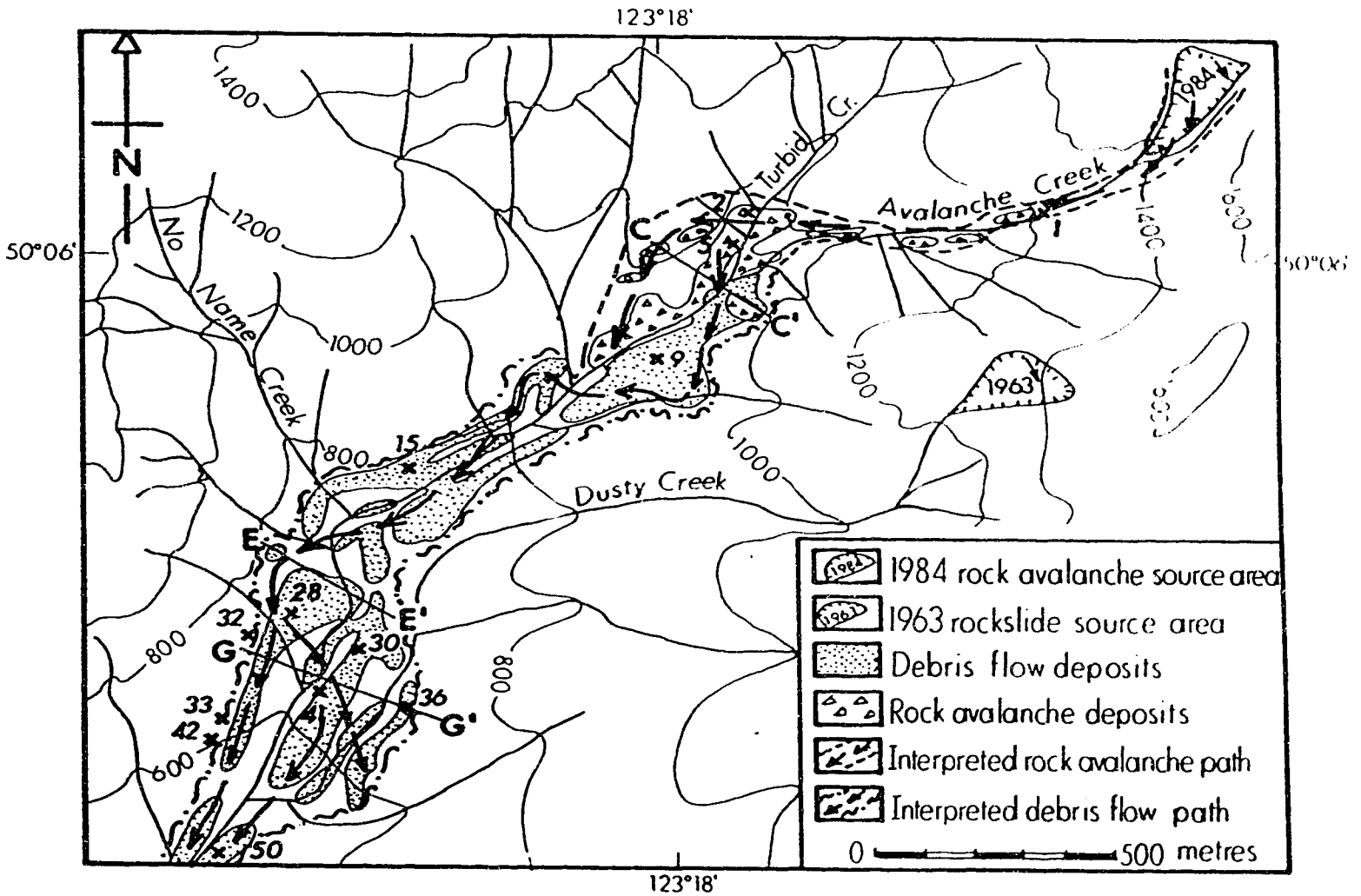


Figure 2.12 Distribution of 1984 rock slide and debris flow deposits, and locations of three cross sections (C-C', E-E' and G-G')

500 m, and the length of the debris dam along its crest was in the range of 100-120 m. The remnants consist of blocks of yellow breccia, hard tuff and purple lapilli up to 4 m across. These rock slide deposits show no apparent stratigraphic units or vertical gradation. The location of the dam and the reservoir is shown in Figure 2.6.

Following Costa and Schuster, this natural dam belongs to Type III dams, which "fill the valley from side to side, move considerable distances upvalley and downvalley from the failure, and typically involve the largest volume of landslide material" (Costa and Schuster 1988, p. 1057).

Filling of the Reservoir

As shown in Figure 2.6, if the height of the dam is 70 m, the length of the reservoir is 170 m and the average width of the reservoir is 40 m, the volume of the reservoir is estimated as $2.4 \times 10^5 \text{ m}^3$. As the watershed area above the dam in Turbid and Avalanche Creeks is approximately 3 km^2 and there was 50 mm of rain in the two days before the debris flow (Jordan 1987), this would supply about $1.5 \times 10^5 \text{ m}^3$ water to the reservoir. In addition, as $4.5 \times 10^5 \text{ m}^3$ of snow and ice was deposited in the dam with the rock slide debris, these ice blocks would contribute about $2 \times 10^5 \text{ m}^3$ water to the reservoir and saturate the debris. The normal channel flow in the summer, about $1 \text{ m}^3/\text{s}$, from ice melt and groundwater would contribute $1.7 \times 10^5 \text{ m}^3$ water for the reservoir to be filled up in two days.

Fines from samples from the 1984 rock slide and debris flow

Table 2.1

Atterberg limits of the fines in 1984 deposits

Sample	From	LL	PL	PI
1-1 (site 2)	Rock slide deposit	28.9	22.1	6.8
2-2 (site 5)	Rock slide deposit	33.1	25.1	8.0
3-1 (site 15)	Debris flow deposit	24.5	19.8	4.7
10-1 (site 28)	Debris flow deposit	24.3	20.5	3.8

LL-Liquid limit

PL-Plastic limit

PI-Plasticity index

Samples 3-1 and 10-1 are the fines from Curve No. 15 and samples 1-1 and 2-2 are the fines from Curve No. 10 (Fig. 13).

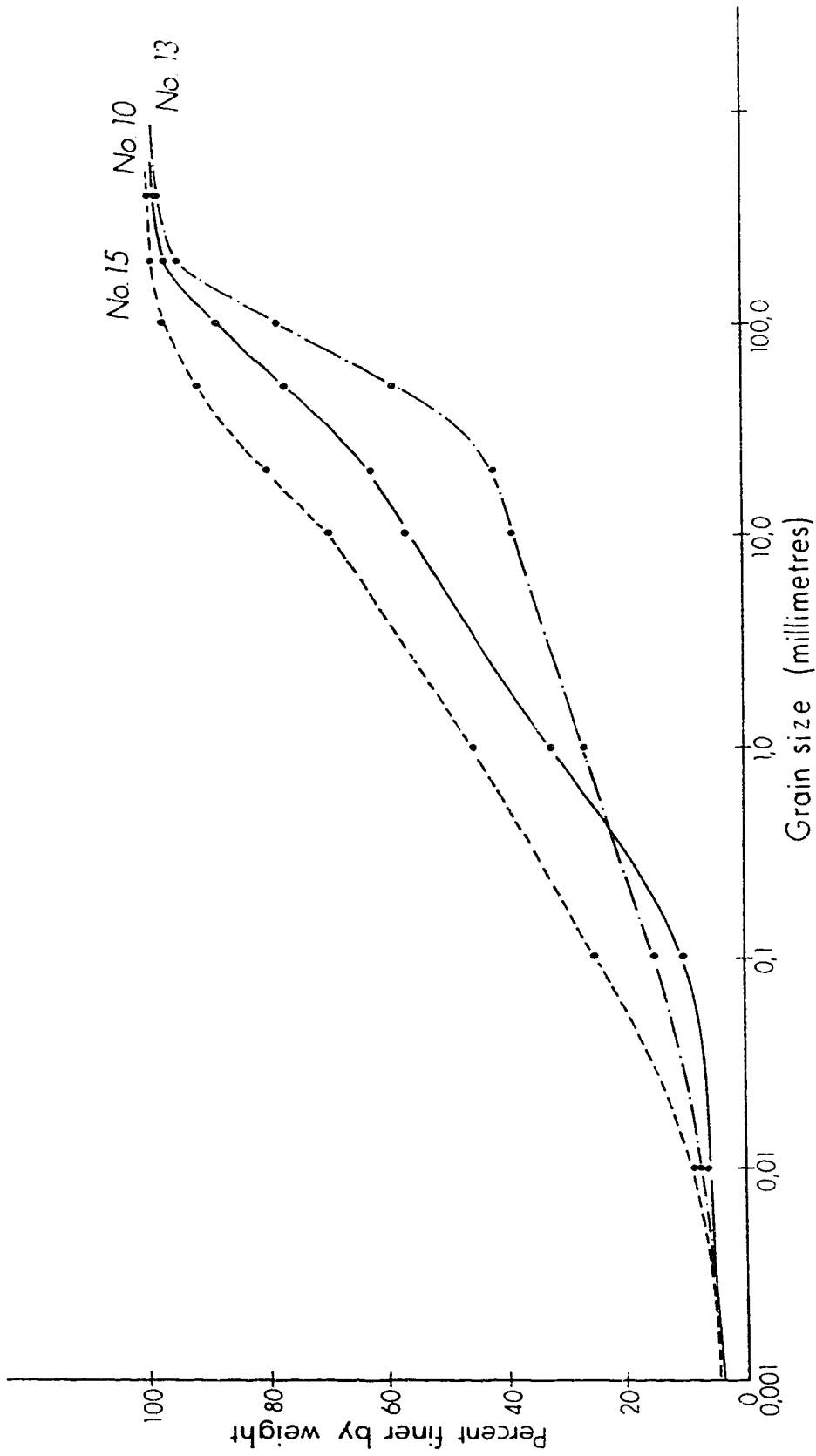


Figure 2.13 Cumulative grain size curves of rock slide deposits (No. 10), and subsurface (No. 15) and surface (No. 13) debris flow deposits.

deposits are plastic (Table 2.1 and Fig. 2.13). The plasticity index of the 1984 deposits is in the range of 4-8. Considering the large particles in the rock slide deposits, the blocks and boulders, have very limited ability to absorb water, the water stored in the reservoir should be enough to saturate the fines and form a debris flow when the debris dam collapsed.

We can also infer that the dam was short-lived because Empire Logging employees saw many ice blocks deposited by the debris flow in Turbid Creek near the logging road. As there was no ice in late June below the confluence of Turbid and Avalanche Creeks, these ice blocks would have come from the rock slide which picked up the ice from Avalanche Creek. The ice remained in the debris dam for one or two days. If the debris dam had lasted for a long time period, these ice blocks would have melted.

Transformation of the Landslide Dam into Debris Flow

"Our review of the literature on landslide dams, and our own experience, suggests that as a general class of landslide dams, dams formed from volcanoclastic sediments are especially susceptible to rapid failure." (Schuster and Costa 1986, P. 11)

The debris flow was caused by the bursting of the rock slide debris dam as water accumulated behind the dam. Tuff blocks played an important role in debris flow development, as the volcanic tuff blocks are easily slaked and disintegrate into fine particles. In slake durability tests, ten tuff specimens were subjected to two cycles of 6 hours drying and 10 minutes of tumbling and wetting. The slake durability testing indicated that more than 50% of the

dry tuff blocks disintegrated after they encountered water and were agitated for 10 minutes; 75% of the tuff blocks disintegrated after two cycles of drying and wetting. Tuff blocks may then have disintegrated into fine particles during the rock slide, within the landslide dam and after the debris dam burst. These fine particles were then entrained in the flow and transformed it into a slurry flow capable of carrying boulders in suspension. The 1984 deposits in Turbid Creek downstream are typical debris flow deposits, fine and coarse particles settled together without any interparticle movement (Pierson and Costa, 1987, p. 7).

The Velocity of the Debris Flow

The behaviour of the water retained by the landslide dam when the dam is breached can be compared to theoretical solutions of the dam break problem. An analytical solution exists for the case where the riverbed downstream of the dam is dry, rectangular in cross-section and with negligible slope and resistance to flow (Henderson, 1966, pp 304-307). If the dam break is instantaneous, the water surface profile downstream at any instant after the break is a parabola tangent to the riverbed. The leading edge of the water advances with speed, $2(gh)^{1/2}$ (Henderson, 1966, p 307), where h is the height of the dam. The water depth at the dam breach is $4h/9$ (Henderson, 1966, p 307), decreasing downstream.

Comparing the actual event to the theoretical model, the finite time for the dam break at Turbid Creek and the rough channel will slow actual wave in comparison to the theoretical wave. The channel slope will speed it. The water in the channel downstream from rain,

snow melt and other tributaries will reduce the channel roughness (Henderson, 1966, p.311). These balancing considerations suggest that the theoretical model of the dam breach is a useful approximation to the behaviour of the downstream flow. Water depth will be increased by the triangular cross section of the downstream channel and the roughness of the channel.

So, assuming a dam height of 70 m gives a theoretical wave velocity of 52 m/s ($2[gh]^{1/2}$) with a depth at the dam of 31 m ($4h/9$). These estimates are compatible with the observations we describe in the next section. More detailed analysis would require observations of the dam break and the rheology of the flow which are not available.

2.5 THE DEBRIS FLOW

Debris Flow Deposits

The debris flow deposits have mud films on the surfaces of the boulders, small particles stuck on the surfaces of the boulders and boulders deposited on the surface of the deposits. About 25% of the boulders in the debris flow were entrained from earlier deposits and the boulders of basement rocks, such as granodiorite, quartz diorite and gneiss are particularly noticeable.

Deposits of the debris flows on both sides of Turbid Creek downstream of the dam consists of up to 8 m of grey tuff, yellow hard tuff, breccia, purple lapilli and dacite fragments. The yellow hard tuff, breccia and purple lapilli in the deposits distinguish the 1984 debris flow deposits from the 1963 rock slide deposits (brown dacite and grey or green-grey tuff from Units 2 and 3).

The debris flow deposits thin downstream.

The debris flow deposits extend to 45 m above the thalweg of Turbid Creek. In Figure 2.14, deposits top the terrace formed by the 1963 rock slide deposits. Thin deposits (0.1-0.2 m) can be seen on the slopes between the creek bed and the top of the terrace. The blocks and the boulders in the debris flow deposits are supported by fragments of grey tuff. Huge boulders on the upper surface of the deposit are surrounded by small blocks and particles. Many small particles are still stuck on the boulders. Bedding is absent, and no sorting or preferred orientation could be seen in the deposits.

Below the confluence with Dusty Creek, the debris flow deposits are confined to the valley of the creek and up to 10 m above the bed of the stream.

The grain size distribution of the deposits of this event was determined by combining the "area-by-number" method (Hungry 1981) and mechanical analyses. Typical results are presented in Figure 2.13. Curve No.10 shows the grain size distribution of the rock slide deposits at the debris dam. Curve No. 15 shows the grain size distribution of subsurface debris flow deposits at site 15 (Fig. 2.12) and curve No. 13 shows the grain size distribution of the debris flow deposits on the ground surface at site 9 (Fig. 2.12). The D50 of the subsurface debris flow deposits is 1.6 mm, much less than those of the rock slide deposits, 5 mm, and that of the debris flow deposits on the surface, 35 mm. This suggests that the bulk of the debris flow is ungraded, indicating the active role of cohesive

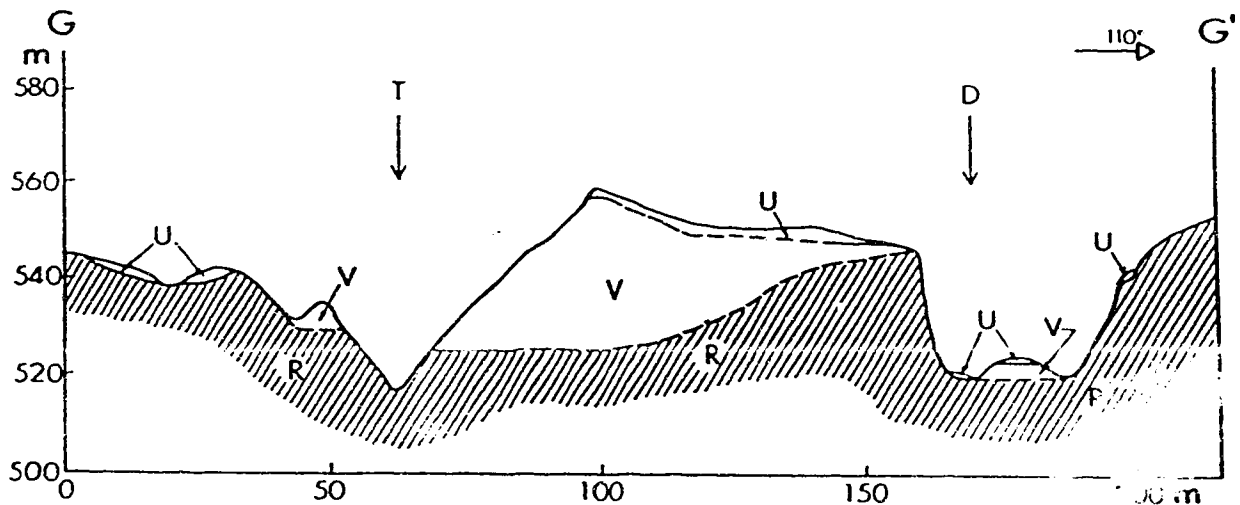


Figure 2.14 Cross-section G-G', showing basement rock (R) and 1963 rock slide deposits (V) blanketed by 1984 debris flow deposits (U) in the valleys of Turbid (T) and Dusty (T) Creeks.

forces in suspending boulders on the top of the flow.

A dacite boulder on the 1984 debris flow deposits covering the terrace of the 1963 rock slide deposits at site 41 (Fig. 2.12). The boulder was carried on the surface of the debris flow and was supported by fine particles and small blocks. Its dimensions, 3.2 x 1.6 x 1.5 m, give a volume of 7.7 m³ and a mass of 15 t. Some fine particles adhere to the surface of the boulder and blocks up to 0.3 m in size lie on the top of the boulder. The deposits beneath the boulder are just 2 m thick. At least eight similar dacite boulders sit on the top of the 1984 deposits.

According to Hampton (1975), the largest grain (D_{max}) that can be supported by a debris flow gives:

$$D_{max} = 8.8K/g(P_s - P_f)$$

If P_s , the density of the grain supported by the flow and P_f , the density of the fluid matrix are in kN/m³, and K , the yield strength of the matrix is in kPa, D_{max} is in metres.

We know the density of dacite is about 27 kN/m³, and field tests suggested the density of the fluid matrix is about 20 kN/m³. As the boulder gives $D_{max}=3.2$ m, the yield strength of the matrix is determined as 25 kPa, within the range of typical debris flow deposits (4-97 kPa) (Johnson and Rodine 1984 P. 294).

Superelevation of Debris Flow

A superelevation created by the debris flow is observed at the former confluence of Dusty and Turbid Creeks (Figs. 2.2 and 2.11-b). It can also be used to calculate the velocity of the debris flow. Following Henderson (1966, p. 250), $V^2 = Rg \tan P$, V is the

velocity of the debris flow, R is the radius of the curvature, and P is the tilt of flow surface at a bend. As $R=700$ m, and $\tan P=0.15$, the velocity of the debris flow is calculated as 32 m/s.

Mud Spatters on Trees

Mud spatters on trees at the edge of the valley occur up to 16 m above the ground. All mud spatters were found on the upstream sides of the trees (Fig. 2.15); the downstream side of these trees are mud free. The mud consists mainly of fine tuff and purple lapilli particles. The spattered trees are up to 20 m away from the 1984 deposits.

We can estimate a local minimum velocity from these mud spatters. Assume the debris flow velocity V can be resolved into two components, vertical, V_v , and horizontal, V_h . Assuming the velocity was zero when the mud spatter reached the highest point on the tree, V_v can be estimated as $(2gh)^{1/2}$, where h is the height of the mud spatter. As $h=16$ m, $V_v=17.7$ m/s. The duration, t , of the vertical mud spatter movement was determined by $t=V_v/g$, to be 1.8 sec. So the horizontal component was determined by $V_h=L/t$, to be 11.1 m/s. The velocity of the debris flow, $V=(V_v^2+V_h^2)^{1/2}$, is estimated as at least 20.9 m/s.

Uprooted Trees

Trees were uprooted on both sides of the creek at sites with thin or no debris deposits. The trees still have topsoil around their roots.

At site 33, on the northwest bank of Turbid Creek, 34-38 m above the stream bed and 80 m from the centre of the stream

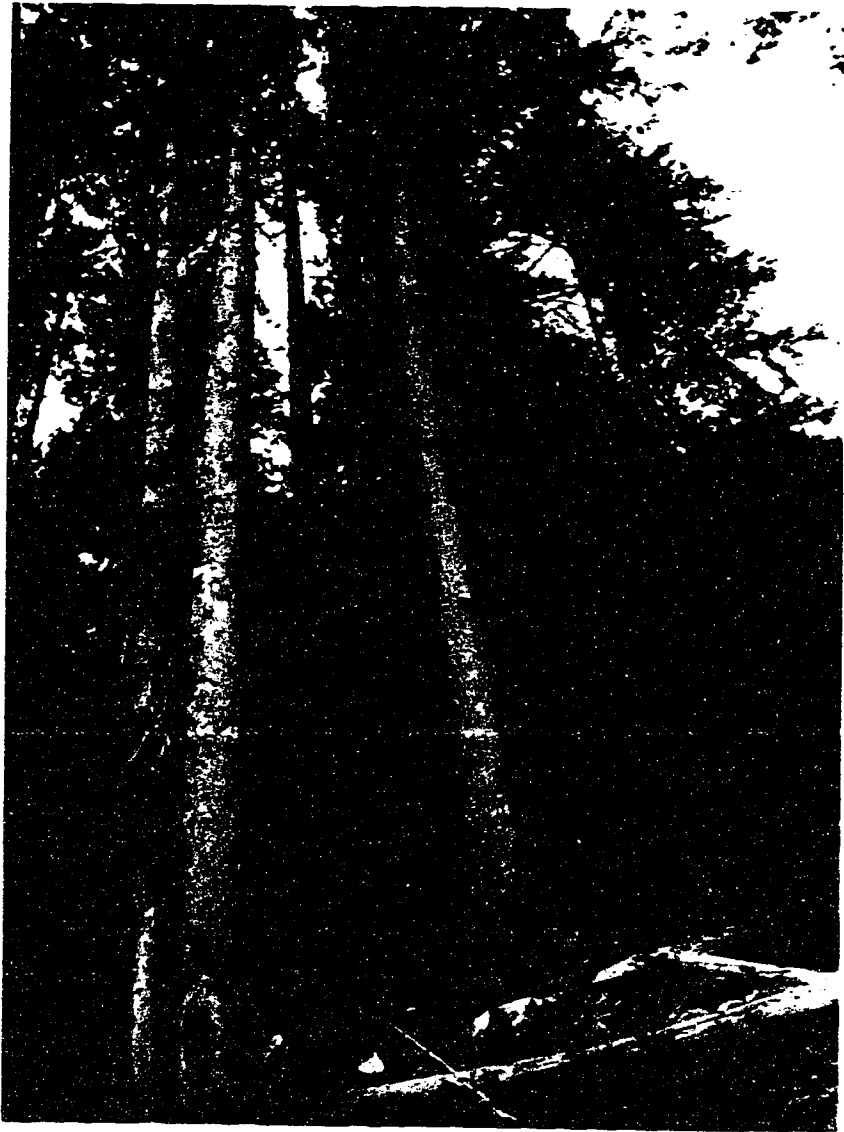


Figure 2.15 Mud splatters on the north (upstream) side of trees
(site 32, Fig. 2.12)

horizontally (Fig. 2.12), eleven mature cedars (0.5-1.5 m in trunk diameter) were uprooted and laid on the slope with their tops pointing downvalley (Fig. 2.16). Except for some mud spatters on the trunks and yellow breccia and purple lapilli particles lodged in the fallen trees, there is no evidence of contact between these trees and the debris flow. On the contrary, the topsoil with numerous small weathered rock fragments was dislodged along with the fallen trees. These trees were healthy, branches and leaves remain still green and alive on the trunks.

This circumstantial evidence suggests that the trees were uprooted by strong winds created by the debris flow. On Fujita's (1971) extension of the Beaufort scale to tornadoes, shallow rooted trees are pushed over at FO, the lowest division on the scale, wind velocities between 18-32 m/s. As the wind is unlikely to have a higher velocity than the debris flow which caused it, the scale gives a lower bound to the debris flow velocity estimates. The rough velocity estimate from these uprooted trees is in agreement with the velocity estimates made from superelevation, mud spatters on trees, airborne wood splinters and deposits on both sides of Dusty Creek. While a tornado or downburst may, of course, have occurred independently at this site, we have not found any similar wind damage elsewhere in the Squamish River valley.

Airborne Wood Splinters

In Figure 2.17, two pieces of wood stick in the trunk of a fallen tree. Their dimensions, 35 x 15 x 10 cm and 25 x 5 x 5 cm, give weights of 5 kg and 0.6 kg respectively. No huge boulders or



Figure 2.16 Uprooted trees up to 1.5 m across (site 33, Fig. 2.12). The height of trees, 16-20 m, gives scale.

thick deposits are found near this point, 200 m downstream from the uprooted trees on site 33 (Fig. 2.12). There are, however, impressions made on the trunk by small, flying stones. A reasonable interpretation would be that these pieces of wood were thrust by strong winds into the trunk. Keller and Vonnegut (1976) demonstrated that the minimum wind velocity driving splinters into pine was 30 m/s though substantial penetration into harder woods required higher wind velocities, at least in the F2 tornado range (50-69 m/s) in which Fujita (1971) noted "light-object missiles".

Windgusts or air-blast created by landslides have also been observed in other landslides: Elm landslide (Skermer 1989), Lower Gros Ventre slide (Voight 1978), Madison Canyon rockslide (Hadley 1978), Little Tahoka Peak rockfalls and avalanches (Fahnestock 1978), Hope rockslide (Mathews and McTaggart 1978) and Nevados Huascarán avalanches (Pflücker and Erickson 1978).

The most vivid descriptions of windgusts created by landslides are by Heim in his book "Landslides and Human Lives" (Skermer 1989, P. 125). "The rock rubble is preceded by windgusts. It lifts roofs off houses, breaks off trees and bowls them ahead of it. It rolls people along the ground or lifts them high in the air as the autumn wind whirls fallen leaves."

Deposits on Both Sides of Dusty Creek

The debris flow travelled over the terrace on the southeast side of the valley of Turbid Creek, and some debris reached the opposite, southeast slope of the valley of Dusty Creek. This allows an estimate of the velocity of the debris flow as it passed over



Figure 2.17 Airborne wood splinters (site 42, Fig. 2.12).

the ridge between the two creeks.

The horizontal distance, L , between the distal point of the debris deposit on the southeast side of Dusty Creek and the ridge crest is 40 m. The altitude difference, h , between these two points is 7 m, and the highest deposits on the southeast side are 30 m above the stream bed of Dusty Creek (Fig. 2.14). Assuming the debris flew over Dusty Creek, the transit time, t , can be determined by $t=(2h/g)^{1/2}$, as 1.19 sec. and the horizontal velocity, V_h , of the debris flow was determined by $V_h=L/t$ as 33.6 m/s.

These velocity estimates are summarized on Fig. 2.6.

2.6 CONCLUSIONS

In the first stage of the landslide, a rock mass with a volume of $2.8 \times 10^6 \text{ m}^3$, detached from the flank of the mountain at 1600 m elevation. Then the rock slide eroded $0.4 \times 10^6 \text{ m}^3$ of loose debris and fractured rocks from the opposite bank and swept it down Avalanche Creek, eroded $0.45 \times 10^6 \text{ m}^3$ of ice and some sediments from the bottom of Avalanche Creek, ran up the west bank of Turbid Creek and dammed these two creeks. The dam consisting of rock slide debris and many ice blocks (15% of the total volume) was 500 m wide, 70 m high and had a maximum crest length of 120 m.

In the third stage, a high velocity debris flow surged along Turbid Creek after the bursting of the debris dam. The valley of Turbid Creek was covered by up to 2 m of debris deposits comprising yellow hard tuff, breccia and purple lapilli. The debris flow overtopped the terrace of the 1963 rock slide deposits, rushed into Dusty Creek and left deposits on both sides of this creek. The

debris flow velocity reached 34 m/s, as determined from superelevations, rocks and wood hurled through the air and uprooted trees. Tornado-strength wind gusts also occurred.

Tuff layers dipping at 15° - 35° , daylight on the slope and form potential rupture surfaces. The uniaxial compressive strength of wet tuff specimens is about 2/3 of the strength of dry specimens. The friction angle of wet tuff specimens is 30° and 35° - 37° for dry tuff. So some parts of slopes in Avalanche Creek, 100-150 m high, separated by joints are free to slide along saturated tuff layers.

Slake durability tests show that volcanic tuff blocks easily disintegrate into fine particles in water. These fine particles may mix with water to form a slurry flow capable of suspending large boulders.

The coincidence of weak, slaking material, the tuffs, narrow steep creeks intersecting at high angles, high precipitation and ice accumulation in the bottom of Avalanche Creek has produced a particularly and peculiarly hazardous situation. It may occur elsewhere on Cordilleran volcanoes. It will reoccur on Mount Cayley. As logging and recreation bring more people into this area, the consequences of the rock slides and debris flows from Mount Cayley may need to be carefully estimated. It may also be necessary to set up warning systems at the mouth of Turbid Creek, on both sides of the logging road along the Squamish River.

3 THE KINEMATICS OF THE 1963 ROCK SLIDE ON MOUNT CAYLEY

3.1 INTRODUCTION

The rock slide on Mount Cayley in July, 1963 began at 1450 m, at the head of Dusty Creek, a small tributary of Turbid Creek, one of the main creeks draining Mount Cayley and a tributary of the Squamish River (Fig. 1.1). 5×10^6 m³ of columnar jointed dacite and poorly consolidated pyroclastic rocks slid 2.4 km to the new confluence of Dusty and Turbid Creeks.

Clague and Souther (1982) spent "several days ... examining the geology of the source area and the stratigraphy of the landslide deposits with the aim of determining the nature of the failure surface, the cause and sequence of failure and the mechanism of transport". Their reconnaissance is a basis for this more detailed study.

When on 28 June, 1984, a major debris flow roared down Turbid Creek, took the road bridge off its abutments and dumped millions of tons of sediment into the Squamish River (Jordan 1987), further study of mass movement on the southern slopes of Mount Cayley was indicated. To compare the 1963 and the 1984 events, we studied the 1963 rock slide, mapping the rock types in the depleted zone, the rupture surface, the profiles of the 1963 rock slide deposits exposed by erosion since 1984, and the drainage changes caused by the event. We also measured the evidence of the velocity of the rock slide. Comparing these two events leads to a new understanding of the 1963 rock slide. We have identified the kinematics of these

slope movements, they have implications for further slope movements from Mount Cayley.

Our nomenclature for these landslides follows the International Association for Engineering Geology's Commission on Landslides (1990) and the Working Party on World Landslide Inventory (1990).

3.2 AIR PHOTO INTERPRETATION

A fresh scarp at the head of Dusty Creek, rock mass movement path and distinct accumulation blocks are recognized from the air photos taken in 1964 (Fig. 3.1) comparing with the air photos taken in 1947 (Fig. 3.2). With a larger scale, the air photos taken in 1973 give the details of the 1963 rock slide (Fig. 3.3). Comparing these air photos shows a series of significant changes. Three stages of the event: rock slide, rock fragment flow and landslide dam, corresponding to the depletion, main track and accumulation zones, can be recognized.

Rock slide recognition

The rock slide can be identified from the air photos and the maps prepared from these air photos.

1. A depletion zone on the north slope of Dusty Creek is shown on the 1964 air photos (A in Fig. 3.1-b).
2. On the 1947 air photos, the rock mass to be displaced in 1963 forms two ridges with a small creek between the ridges (a in Fig. 3.2 indicating the creek).
3. The small creek between two ridges is clearly revealed by the pre-slide contours. The creek follows joint set j_{2d} (Fig. 3.7).
4. Three blocks, B_1 , B_2 and B_3 , in the depletion zone show on

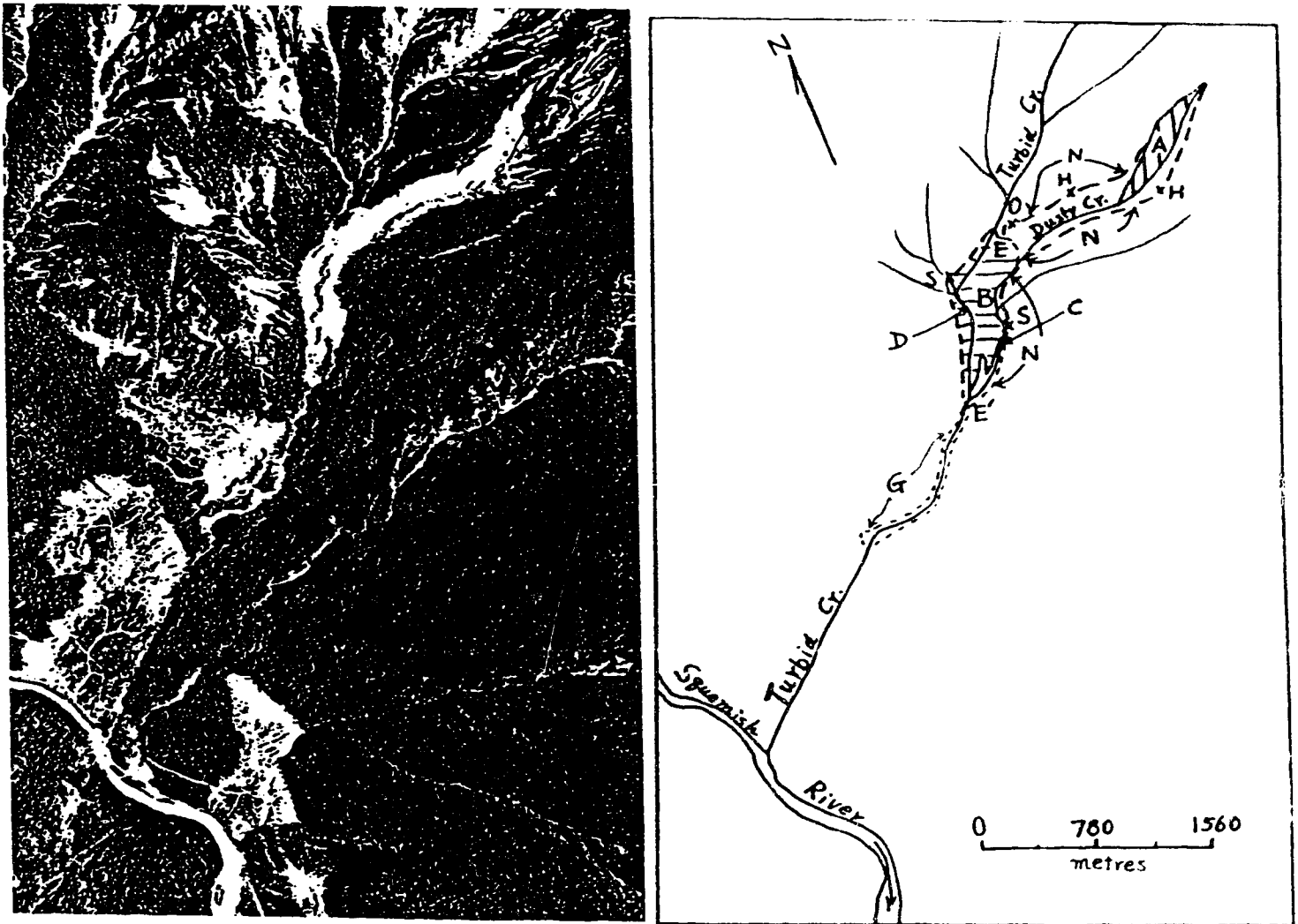


Figure 3.1 (a) Air photo showing the 1963 rock slide on July 26, 1964 (Province of British Columbia photo BC 5103-132). (b) An overlay on the air photo showing the landform change in Dusty Creek and Turbid Creek caused by the 1963 rock slide.

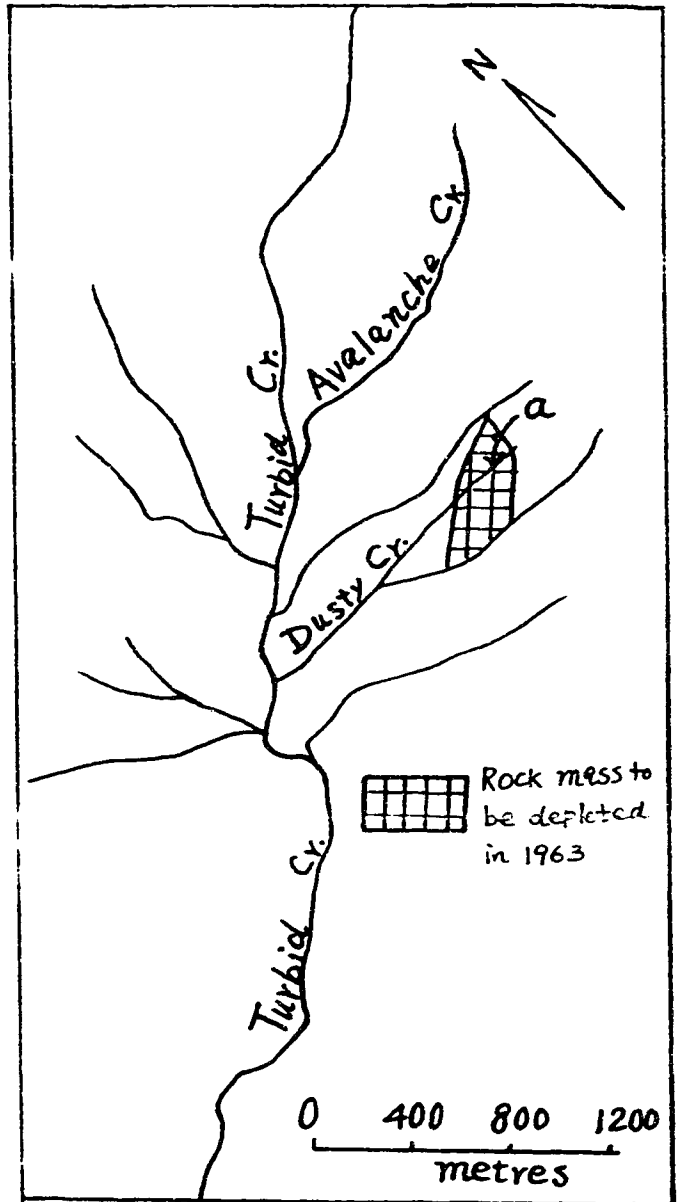


Figure 3.2 (a) Air photo taken on Aug. 2, 1947 (Province of British Columbia photo BC 424-31). (b) An overlay showing the location of the depletion zone.

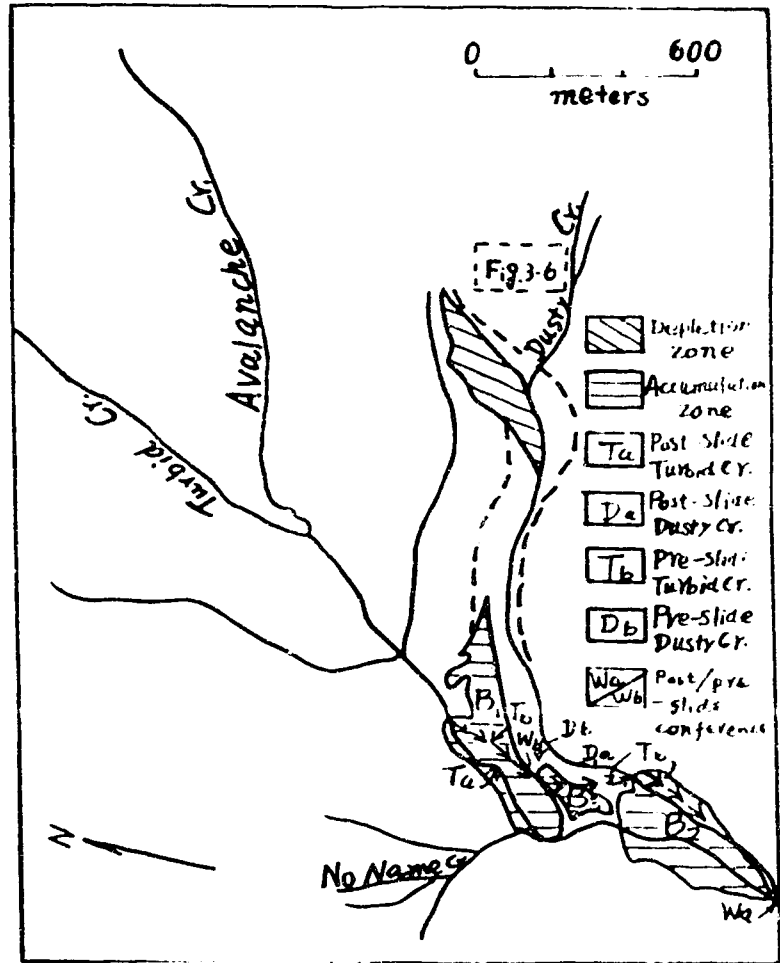


Figure 3.3 (a) Air photo giving the details of the landform changes on Aug. 8, 1973 (Province British Columbia photo BC7520-259). (b) An overlay showing the drainage change caused by 1963 rock slide. Note that the pre- and post-slide locations of Turbid Creek, Dusty Creek and their conference are indicated by T_b and T_a , D_b and D_a , and W_b and W_a respectively.

the isopleth map (Fig. 3.4) prepared from the topographic maps commissioned by the Geological Survey of Canada based on the air photos taken in 1947 and 1973 (Wong 1983). The boundary between blocks 1 and 2 was the small creek between two ridges. The boundary between blocks 2 and 3 follows joint set j_{1d} (Fig. 3.7).

The cross-sections, A-A' and C-D-A', in Figure 3.5 indicate the movement sequences of these blocks. The main body of the slide, block 1, slid first. Block 2 followed because of the loss of the lateral support. These two blocks moved in the same direction, southwards into Dusty Creek. Immediately after the movement of block 2, block 3 lost its lateral support and slid south-southwestwards until it entered Dusty Creek. The slide retrogressed from its toe in Dusty Creek.

These blocks have different isopleth patterns as shown in Figure 3.4. Block 1 has a maximum thickness of 110 m and an area of 80,000 m². Blocks 2 and 3 have maximum thicknesses of 60 and 80 m respectively and the areas of 20,000 m² and 15,000 m².

Rock fragment flow recognition

From the air photos and the isopleth map (Fig. 3.4), the main characteristics of the rock fragment flow can be recognized.

1. High forest trimlines are documented in the 1964 and 1973 air photos (N in Figs. 3.1 and 3.3).

2. A distinct main track is revealed on the isopleth map (Fig. 3.4). The air photos (Figs 3.1 and 3.3) and the isopleth map show that the rock slide left high forest trimlines on both sides of the creek in this zone without disturbing large volumes of material.

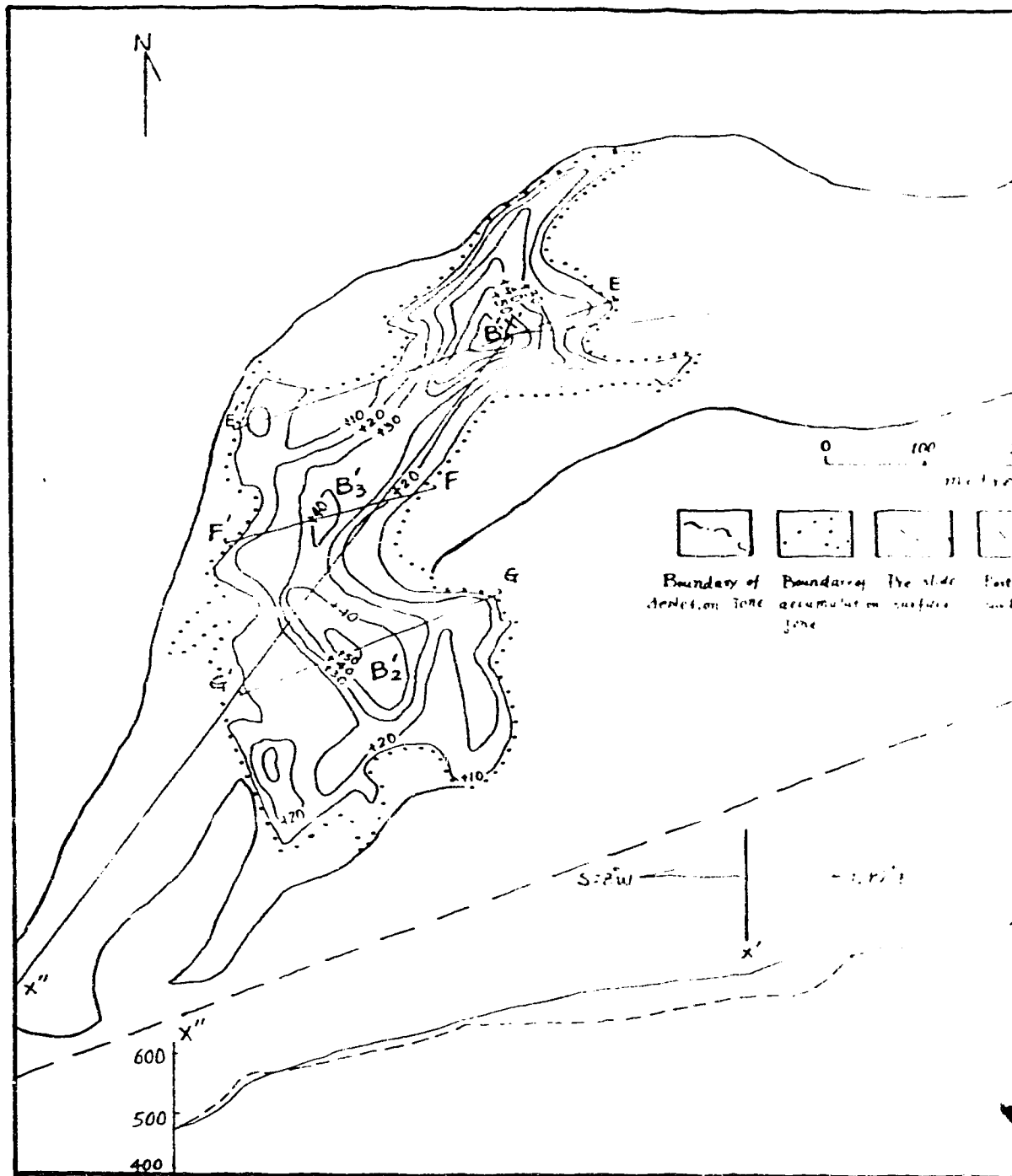
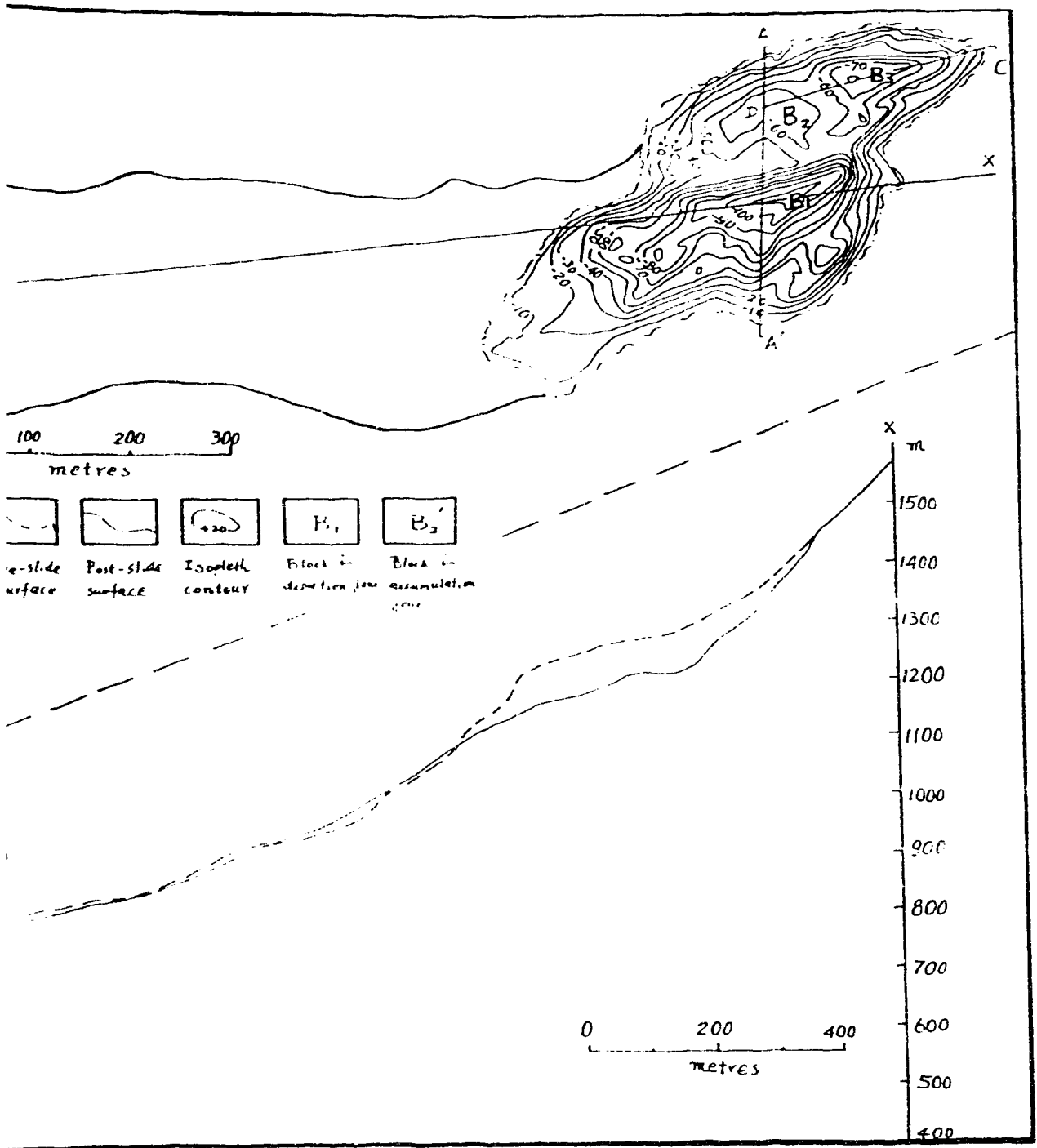


Figure 3.4 Isopleth map of the depletion, main track and accumulation. The cross-section X-X'' is determined from comparison of the contour maps based on air photos taken in 1947 and 1973 respectively.



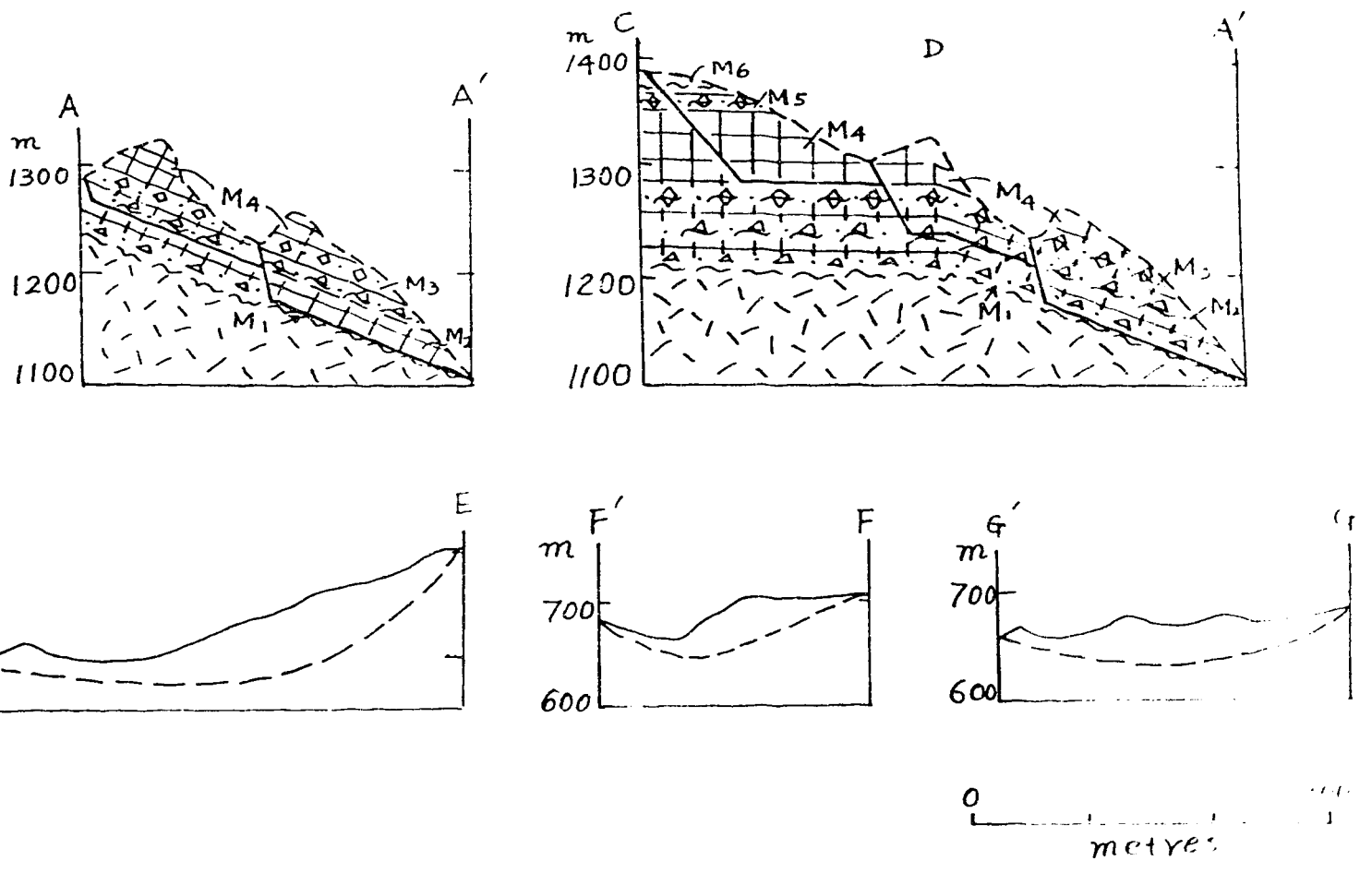


Figure 3.5 Cross-sections of the depletion and accumulation zones, lines of cross sections on Figure 3.4.

Both detachment and deposition in this zone are less than 10 m. This zone, 1 km long, is distinct from the depletion and accumulation zones.

The main track "... is the commonly scoured, original ground surface over which the debris flow/avalanche descends the slope, with gradually increasing velocity to a terminal velocity dependent on steepness, channel width, and effective viscosity of the flowing mass. Frictional contact between the flow and slope surface allows the debris flow/avalanche to scour vegetation and the upper few to tens of centimetres of colluvium from the slope. As the flow incorporates additional mass, the momentum of the flow increases along the main track." (Baldwin and others 1987, P. 225)

3. Run ups can be seen on both slopes of Dusty Creek (H in Figs. 3.1-b and 3.3-b).

4. A small ridge between Dusty and Turbid Creeks was overtopped by the rock fragment flow (O in Fig. 3.1-b). Some rock slide debris ran into Turbid Creek upstream of the confluence.

5. The main body of the rock fragment flow came into Turbid Creek and accumulated between the pre- and post-slide confluences of Dusty and Turbid Creeks for a length of 1 km along the Turbid Creek valley (B in Figs. 3.1-b and 3.3-b).

6. Two obvious superelevation sites can be clearly seen on the 1964 air photos (S in Fig. 3.1-b).

Landslide dam recognition

The landslide dam and its influence on the environment are identified from the air photos and the isopleth map also.

1. Three separated accumulation blocks can be recognized from the 1964 air photos, especially from the 1973 air photos and the isopleth map (B_1 , B_2 , and B_3 in Fig. 3.3 and B_1' , B_2' , and B_3' in Fig.3.4).

These accumulation blocks have different isopleth patterns and maximum thicknesses (Fig. 3.4)

2. The accumulation blocks dammed Turbid and Dusty Creeks for a short period of time. As a result of the rock slide dam, the new Dusty Creek took over a portion of the pre-slide stream of Turbid Creek (C in Fig. 3.1-b) and Turbid Creek was diverted 200 m westward (D in Fig. 3.1-b).

3. The confluence of Dusty and Turbid Creeks shifted about 1 km downstream from E to E' in Fig. 3.1-b.

4. Excepting the thin veneer of debris, 1-2 m thick, deposited downstream for 800 m (G in Fig. 3.1-b), no 1963 rock slide deposits can be found in Turbid Creek below the new Dusty Creek mouth. No significant topography changes took place below this point.

3.3 THE ROCK SLIDE

Geologic setting

Clague and Souther (1982) divided the bedrock in the Turbid Creek valley into six units. We subdivided the 5 units of the volcanic rocks into 9 members (Lu 1988). As shown in Figures 3.6 and 3.7, only Units 2 and 3 (Members 1-5) were involved in the 1963 rock slide.

Unit 2 consists up to 150 m of brown columnar-jointed dacite (Member 2) underlain by a bedded lapilli tuff (Member 1) about 5-15

m thick.

Unit 3 consists of three members; member 3 is a grey-white lapilli tuff, tuff breccia, and some dacite, 20 m thick; member 4 consists of dark brown columnar-jointed dacite, up to 150 m thick; member 5 consists of grey and white breccia tuff and breccia containing angular blocks about 1 m across, and lapilli, 30-50 m thick.

The average values of Schmidt hammer rebounds from the different rocks allow uniaxial compression strengths of the rocks to be estimated (Table 3.1) (PROCEQ 1977). Dacite, lapilli and breccia are medium strong rocks but they have different uniaxial compressive strengths, and tuff is very weak rock (Canadian Geotechnical Society 1985, p35). The differences in strength of these rocks cause the different performances of the 1963 and 1984 slope movements.

Figure 3.7 shows the rupture surface of the 1963 rock slide developed along tuff and lapilli tuff layers dipping southeastwards towards Dusty Creek at 30° - 35° , the surface is covered by up to 5 m of debris which has fallen from the landslide scarp.

Joint orientation measurements, 82 in dacites and 46 in tuffs were taken at site 62 (Fig. 3.11). The contoured pi diagrams (Fig. 3.8) shows three sets of joints in dacite j_{1d} , j_{2d} and j_{3d} with dip directions and dips of 221/80, 172/73, and 119/44; and three sets of joints in tuff j_{1t} , j_{2t} and j_{3t} with dip directions and dips of 231/78, 168/72 and 138/36. Probably, the sets j_{1d} , j_{1t} of steep-dipping joints are cooling joints. The joints j_{3d} and j_{3t}

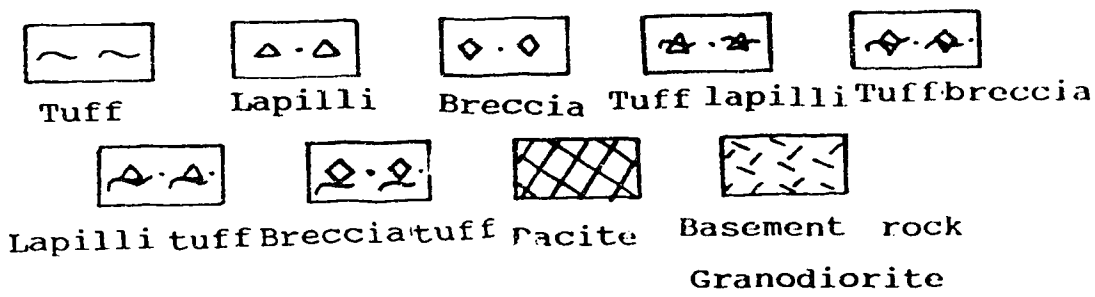
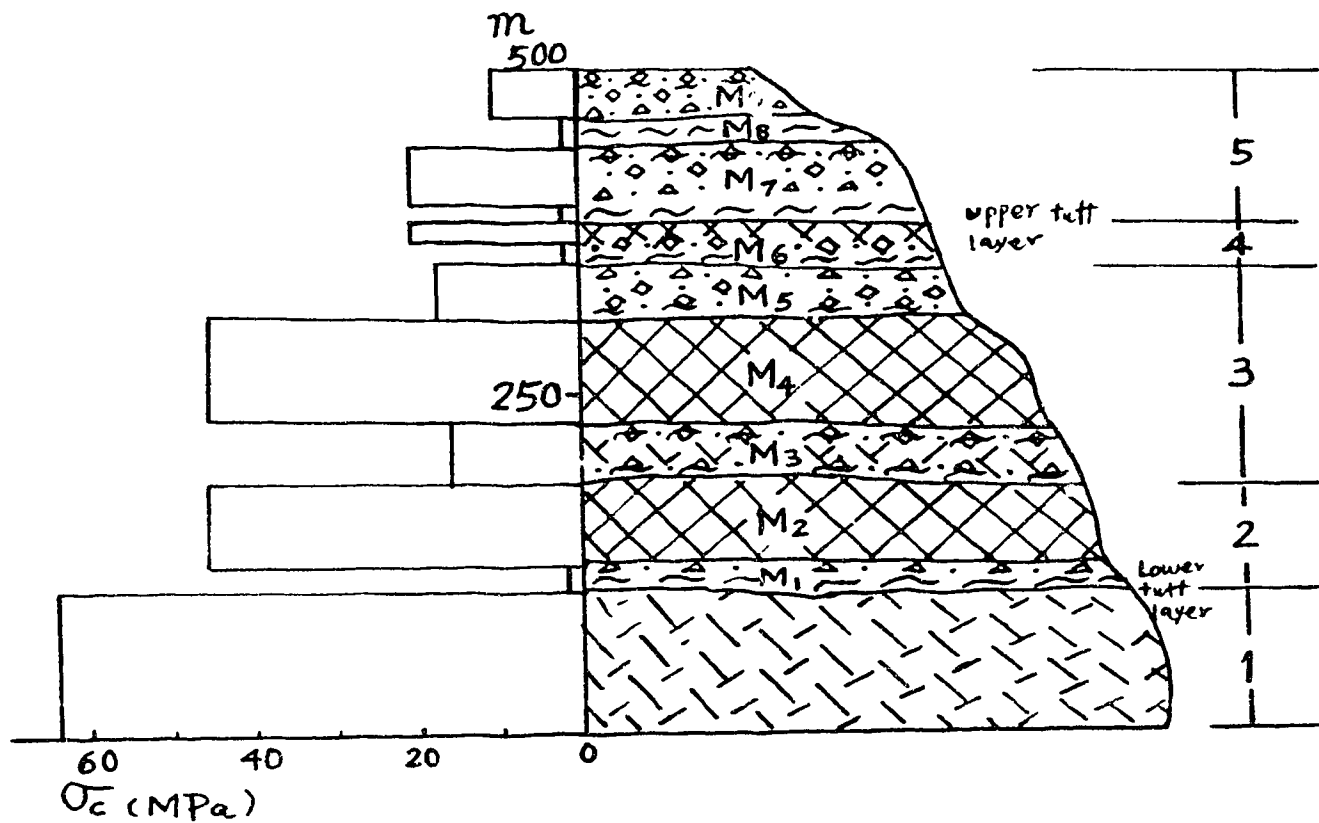


Figure 3.6 Rock Units 1-5 showing Members 1-9 (M₁)-(M₉).

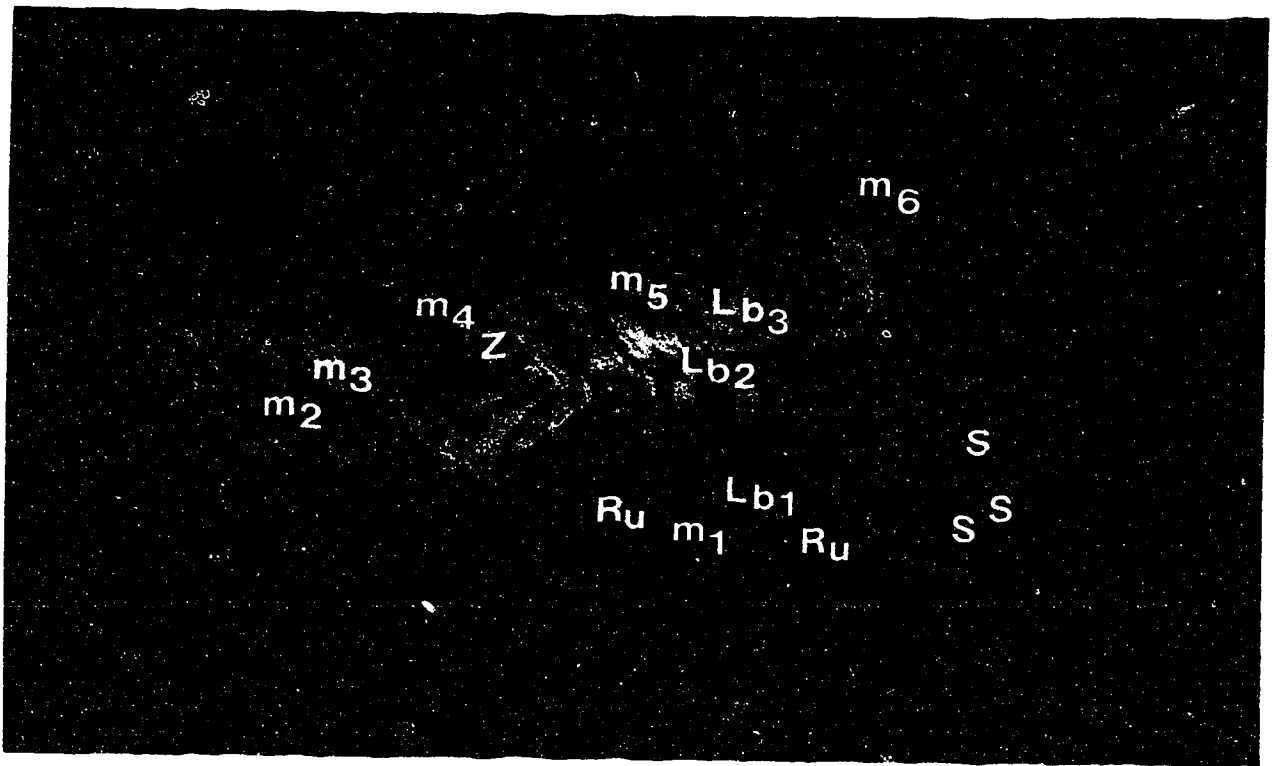


Figure 3.7 A view from the south-southeast of the rupture surface, R_u , developed along a tuff layer in Member 1, looking NE at site 63 (Fig. 3.11). Bushes in the foreground are about 0.5 m high. Note the seepages, S , along the tuff layer, the location, Z , of Figure 3.9, and the pre-slide locations of the blocks, L_{B1} , L_{B2} and L_{B3} , in the depletion zone. The eastern lateral margin followed joint set j_{1d} and the wedge formed on the lateral margin with joint set j_{2d} . M_1 - M_6 represent Members 1-6 respectively.

Table 3.1

Average Values of Schmidt Hammer Rebounds

Rock	From	Rebound	Strength (mPa)
Dacite	Units 2 & 3	44	48
Lapilli	Unit 5	36	31
Breccia	Unit 5	32	25
Tuff	Units 2 & 3	Less than 3	Less than 4
Tuff	Units 4 & 5	Less than 3	Less than 4

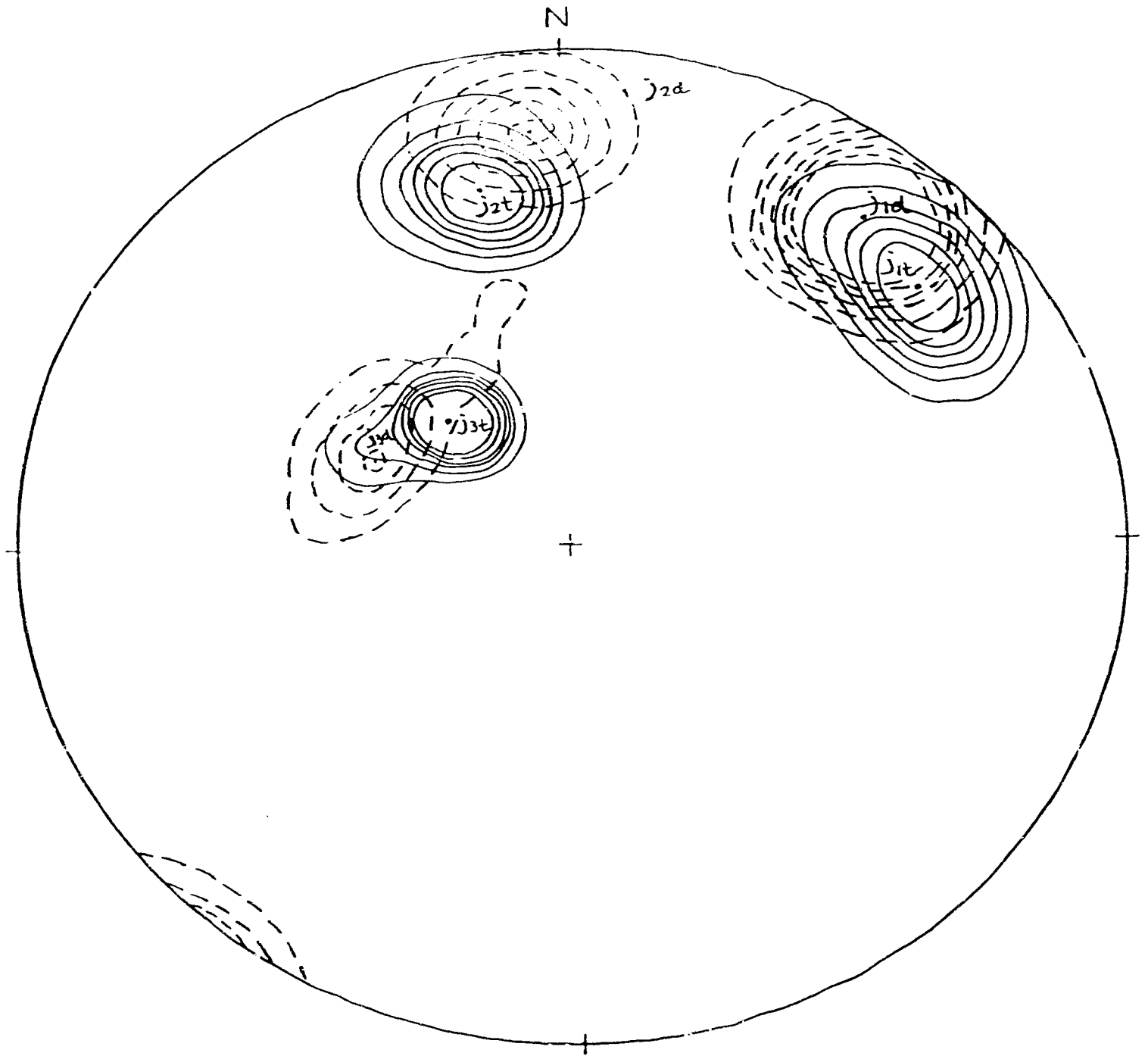


Figure 3.8 Contoured structural diagram of poles to joints in dacite (j_{1d} , j_{2d} and j_{3d}) and tuff (j_{1t} , j_{2t} and j_{3t}) on Schmidt net. Contours are multiples of uniform density. Contours at densities 2, 5, 8, 11, 14 and 17.

subparallel to bedding might be caused by slope movement immediately after deposition. The main scarp of the 1963 rock slide follows joint set j_{2d} and lateral margin follows joint set j_{1d} (Fig. 3.9).

Slope movement mechanism

As shown in Figures 3.5 and 3.7, the rupture surface of the main body of the rock slide, Block 1, follows bedding in the tuff of Member 1. The rupture surface of Block 2 follows the bedding of lapilli tuff on the bottom of Member 3. And the rupture surface of Block 3 follows the tuff breccia layer on the top of Member 3. The tuff layer of Member 1 in the depletion zone of the 1963 rock slide had a dip of 35° to 156° while the slope face of the 1963 rock slide can be reconstructed with an orientation of 161° , 65° (Fig. 3.9).

The tuff in Unit 2 is grey-white fine tuff, lithic fragments up to 4 mm in length make up the grain component while the matrix is submicroscopic. As the tuff layer in Unit 2 has the same Schmidt hammer rebounds as the tuff in Unit 5 (Table 3.1), it is reasonable to assume that the strength of the tuff in Unit 2 is similar to that of the tuff in Unit 5 (Cruden and Lu 1992). Laboratory tests on tuff collected from Unit 5 at the head scarp of the 1984 rock slide (Cruden and Lu 1992) give the friction angle of the saturated tuff bedding to be 30° .

As shown in Figure 3.10, the joints j_{1t} formed a wedge with the bedding which is kinematically free to slide along the weak tuff when the tuff is saturated. Notice that the dip direction of the tuff P_b falls between the dip direction of the slope face and the

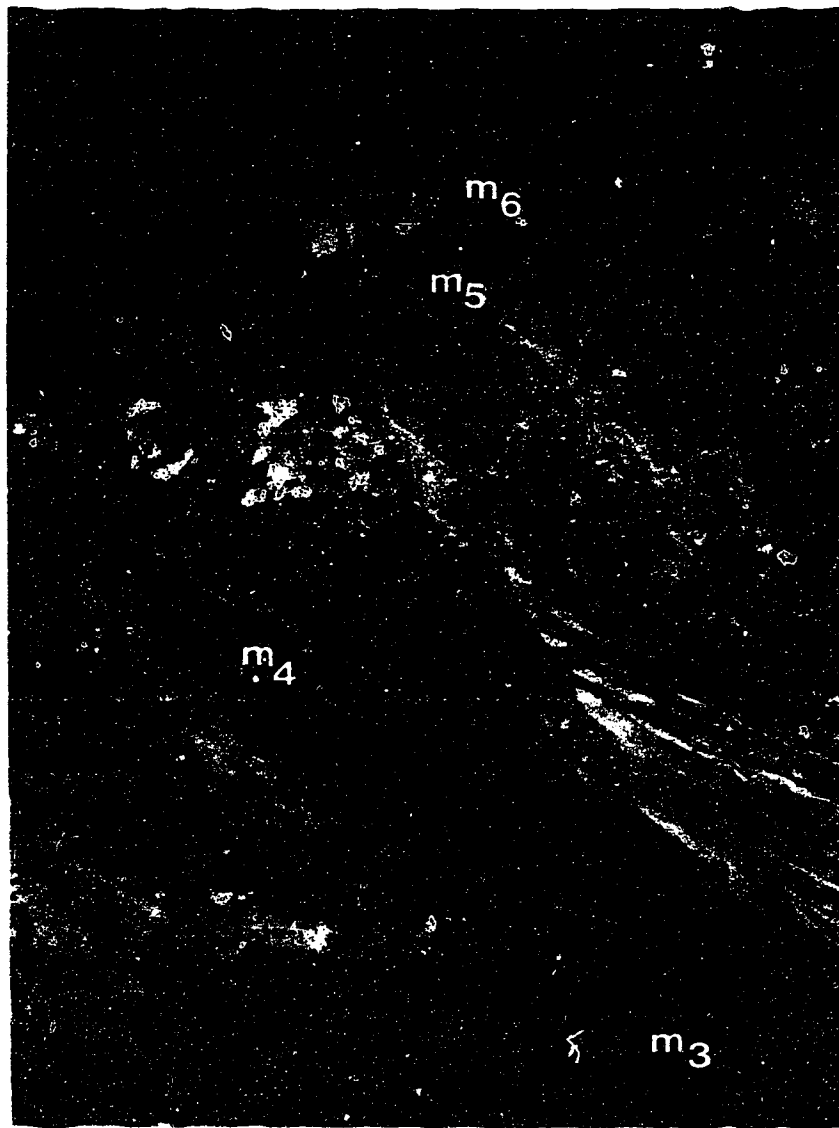


Figure 3.9 Lateral scarps and joints from the SSW. M_3 - M_6 represent Members 3-6 respectively, looking NNE at site 63 (Fig. 3.11). The height of trees, 16-20 m, gives scale.

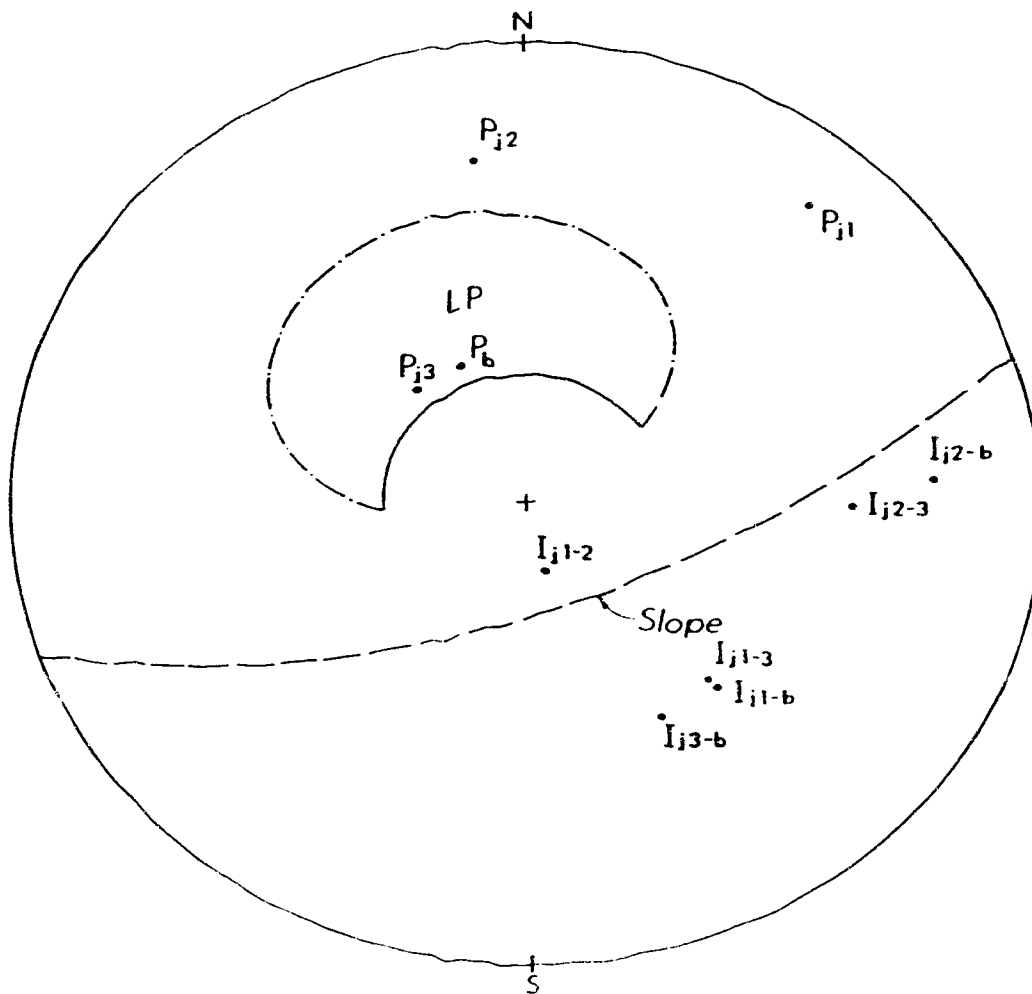


Figure 3.10 Slope stability analysis on a Wulff net based on the locus of poles to discontinuities daylighting on the slope, LP, on which sliding is possible, pole of bedding plane of tuff, P_b , poles of joint sets, P_{j1} , P_{j2} and P_{j3} , and their intersections, I_{j1-2} , I_{j1-3} , I_{j1-b} , I_{j2-3} , I_{j2-b} and I_{j3-b} .

line of intersection, I_{j_1-b} , of bedding and joint set j_{1r} , indicating by Hocking's criterion (Hocking 1976; Cruden 1984) that sliding can occur down the dip of the bedding.

3.4 THE ROCK FRAGMENT FLOW

General movement path

Air photo interpretation and field observations show that the 1963 rock slide began at the head of Dusty Creek where three blocks of tuff breccia and columnar jointed dacite detached from the north slope of Dusty Creek and slid to the south across Dusty Creek to impact against the south side of Dusty Creek valley. The impact partly broke up the displaced mass, and directed it towards the opposite side of the creek valley. There the mass curved along the north bank of Dusty Creek at site 61 (Fig. 3.11), and swung back to the opposite side of the valley. The mass impacted the south slope again and shifted movement direction. Finally the three blocks came to rest in Turbid Creek between the pre- and post-slide confluences of Dusty and Turbid Creeks one after another and at different locations.

Movement trajectory of blocks

It is believed that block 1 rushed into Turbid Creek and came to rest first in the Turbid Creek valley while a part of the debris overtopped the small ridge between Dusty and Turbid Creeks and travelled upstream in Turbid Creek. Then block 2 came to rest in Turbid Creek between the present confluence of Dusty and Turbid Creeks and 150 m downstream from the pre-slide confluence. Then block 3 filled in the space between blocks 1 and 2, leaving

unfilled depressions at its two ends. So the deposits formed an arc in plan.

The distances and travel angles (from the crown of the block pre-slide to the tip of the block post-slide) of the three blocks and the 1984 rock slide are listed in Table 3.2. The distance and travel angle of the 1963 rock slide is estimated as 2.4 km and 21° (Fig. 3.4).

Notice that the travel angles of the 1984 rock slide and block 1 of the 1963 rock slide are similar, the travel angle of block 2 is 3° less than that of block 1, and the travel angle of block 3 is 2° more. Block 1 overtopped the small ridge between Dusty and Turbid Creeks, entered Turbid Creek at 75° , impacted the opposite valley wall and came to rest in Turbid Creek immediately. Then, block 2 would have travelled on the creek valley smoothed by the deposition of fine debris from the movement of block 1 and entered Turbid Creek at an angle of 45° . So Block 2 made a turn at the pre-slide confluence of Dusty and Turbid Creeks and moved another 700 m downstream in Turbid Creek. Block 3 has a higher travel angle because when it moved into Turbid Creek, the rock fragment flow encountered substantial resistance from the deposits of blocks 1 and 2 and the opposite valley wall of Turbid Creek.

Velocity estimate

The obvious superelevation at site 61 showed a tilt, $\tan P$, of the debris flow surface of 0.1, and the radius, R , of the curvature of the bend is 700 m.

Following Henderson (1966, P251), the velocity of the debris

Table 3.2
Travel Distances and Junction Angles

Block	H (m)	L (m)	τ°	Q°	$V(10^6 \text{ m}^3)$
1	600	1600	60-75	20.6	2.7
2	750	2400	40-45	17.4	1.0
3	750	1800	50-60	22.6	1.2
1984	700	2000	60-72	19.3	2.7

*J-Junction angle between the contributing and the receiving channels.

can be estimated as

$$V^2 = (Rg \tan P)$$

Where V is the mean velocity of the debris movement,

g is the acceleration due to gravity.

So, the velocity of the 1963 rock slide may have reached 26 m/s.

3.5 THE LANDSLIDE DAM

Major characteristics of 1963 landslide deposits

The deposits of the 1963 rock slide accumulated in an elongate area between the pre-slide and present mouths of Dusty Creek (sites 16 and 35 in Fig. 3.11). The deposits extend 1000 m along the valley of Turbid Creek, and have a maximum width of 160 m and a maximum thickness of 60 m. The total accumulation is $5.0 \times 10^6 \text{ m}^3$ in three major blocks bounded by gullies (Figs. 3.11, 3.12 and 3.13).

These accumulation blocks can be seen on the air photos and the isopleth map (Figs. 3.3 and 3.4), and on photos taken from a helicopter and the ground as well (Figs. 3.14 and 3.15).

Block 1

The centre of block 1 is located at the pre-slide mouth of Dusty Creek. Block 1 extends from the right (north east) bank of Turbid Creek into Dusty Creek along its right (north) bank (Fig. 3.16). Block 1 looks like an arcuate platform as Turbid Creek has now cut through the block. Block 1 is 400 m long, with a maximum width of 220 m and a maximum thickness of 70 m resulting in a total volume of about $2.7 \times 10^6 \text{ m}^3$.

The boundary between blocks 1 and 3 is a gully-like depression.

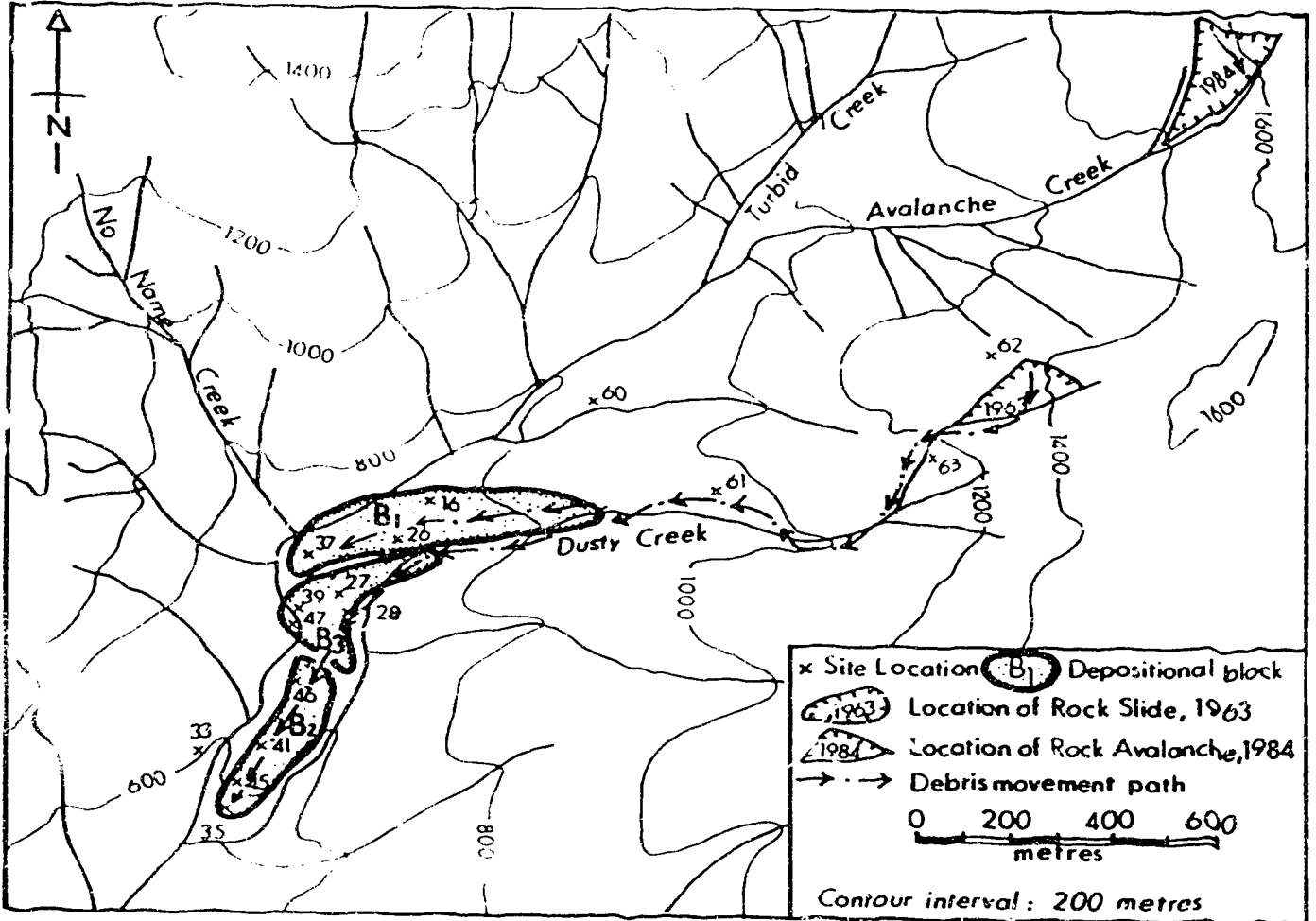


Figure 3.11 The accumulation zone of the 1963 rock slide.

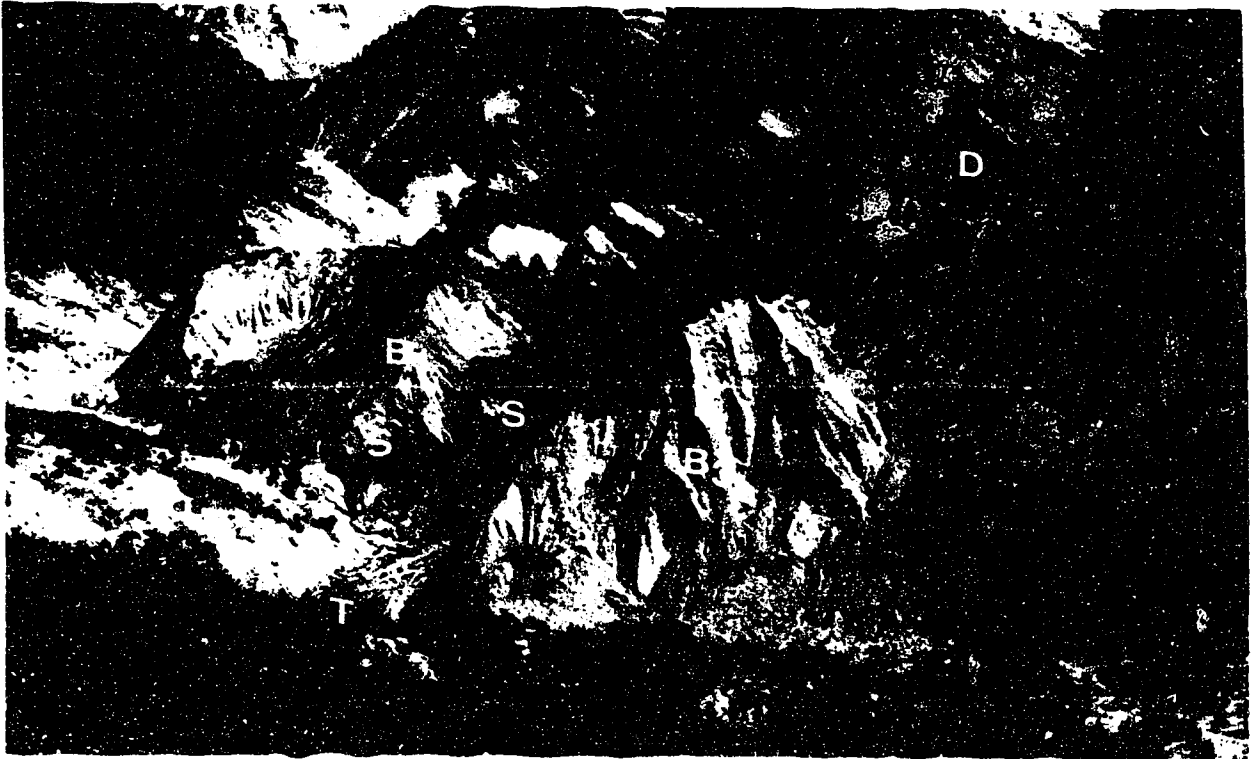


Figure 3.12 The boundary between block 1, B_1 , and block 3, B_3 , taken at site 39 (Fig. 3.11) looking E. Note the seepage, S, indicating the pre-slide confluence of Turbid Creek, T, and Dusty Creek, D. Bushes in the foreground are about 1.5 m high.

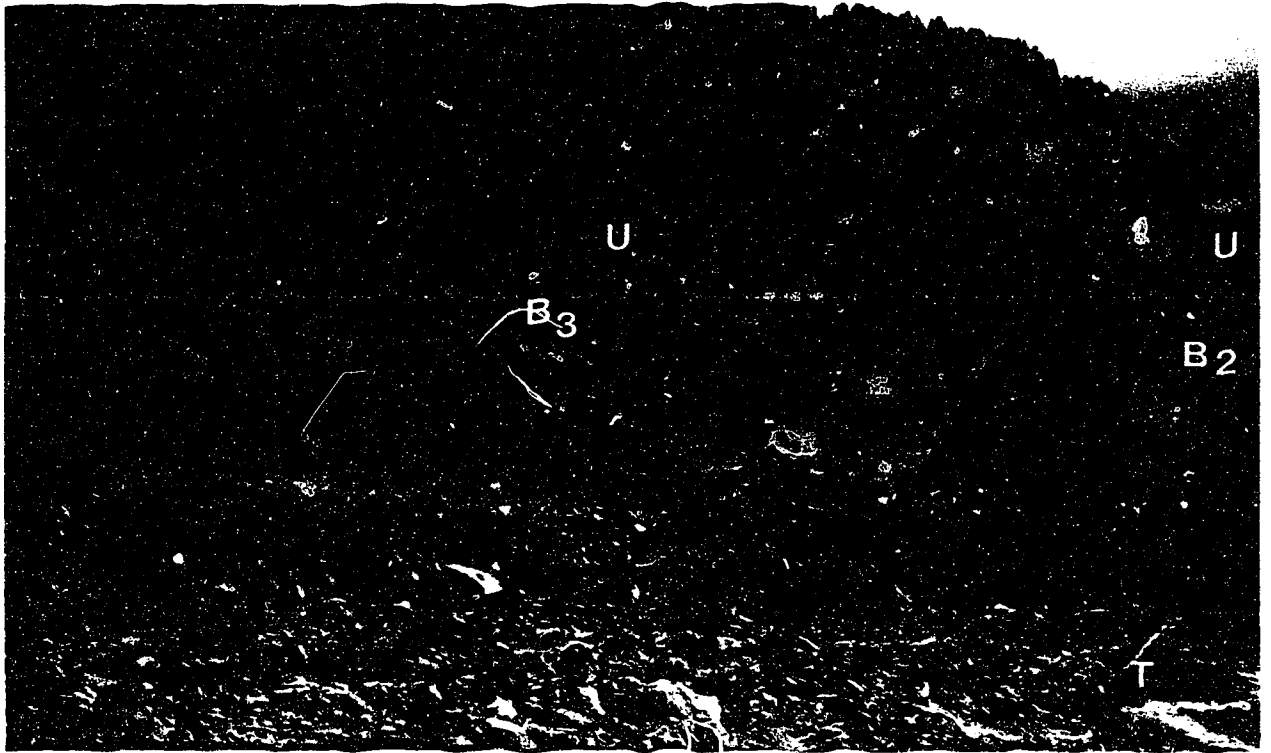


Figure 3.13 The boundary between block 2, B_2 , and block 3, B_3 , taken at site 47 (Fig. 3.11) looking SE. The dimensions of the boulder in the front, $2 \times 1.2 \times 0.7$ m, give scale. The 1984 debris flow deposits, U, blanketed block 2 and part of block 3. Turbid Creek, T, cut a new channel through the 1963 and 1984 deposits.

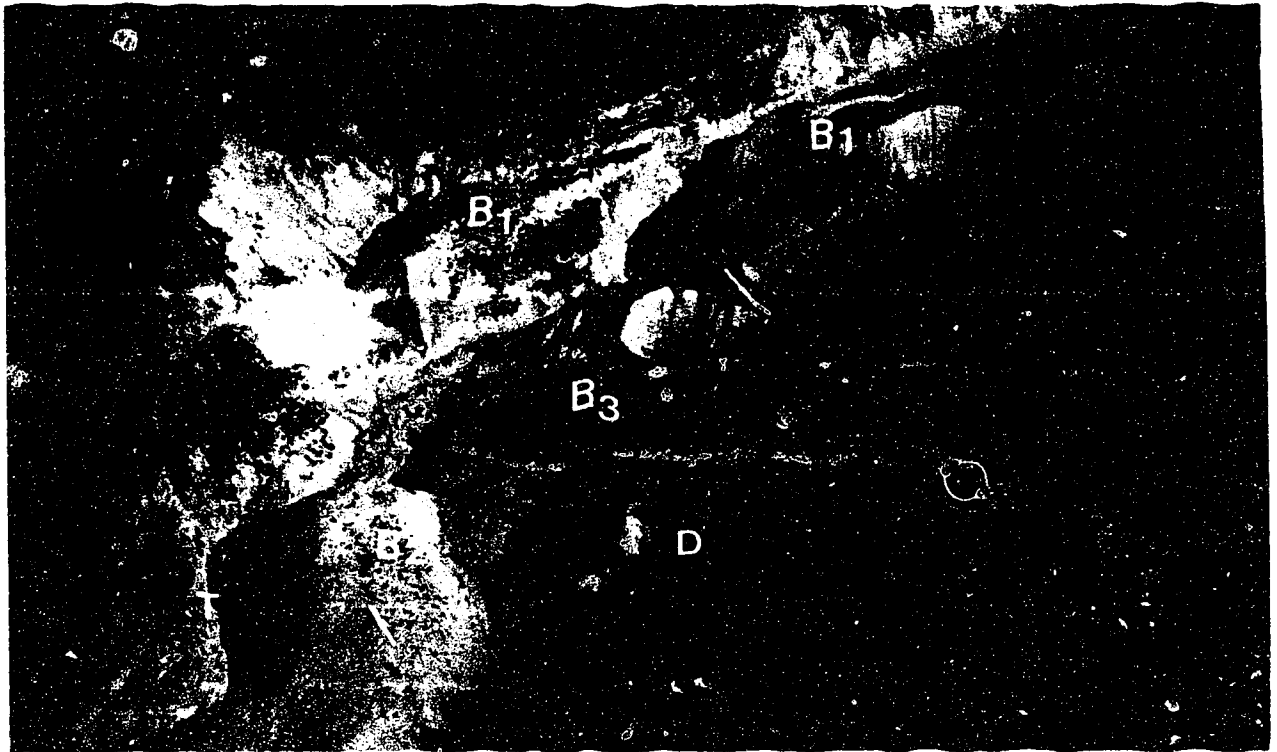


Figure 3.14 Three blocks, B_1 , B_2 , and B_3 viewed from a helicopter looking NNE at the intersection of Dusty Creek, D, Turbid Creek, T, and No Name Creek, C.

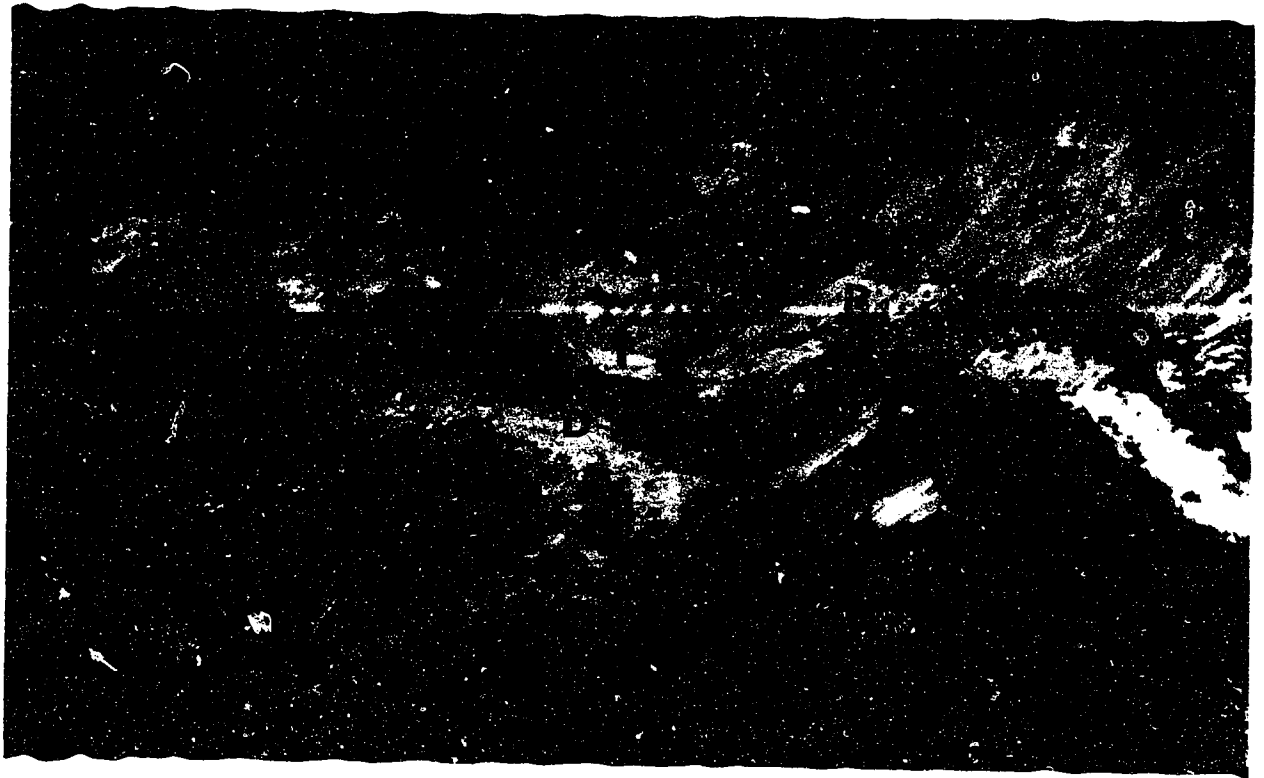


Figure 3.15 Three blocks, B_1 , B_2 and B_3 viewed from ground looking SSW at site 60 (Fig. 3.11). Bushes on block 3 are about 1.5 m high. Note their relationship with Rusty Creek and Turbid Creek, T.



Figure 3.16 Block 1 taken at site 47 (Fig. 3.11), looking NE. The thickness of the deposits in block 3, 40 m, gives a scale. Note block 1 was between Dusty Creek, D, and No Name Creek, C. Turbid Creek, T, cut a new channel through the 1963 deposits and separated block 1. Block 1 has three layers V_a , V_b and V_c .

Figure 3.12 shows that the top surface of block 1 is at least 5 m higher than that of block 3.

The deposits forming block 1 have three distinct layers (a, b and c). Their main characteristics are listed in Table 3.3. This sequence is now covered by 1-5 m of 1984 debris flow deposits. It seems likely that layer a came from Member 1 of the volcanic rock in the depletion zone, layer b came from Member 2, and layer c came from Member 3, with a little Member 2. This sequence of layers is seen only in block 1 (Figs. 3.6 and 3.16).

Block 2

Block 2 is between the confluence of Dusty and Turbid Creeks and Block 3. About 400 m in length, with a maximum width of 120 m and a maximum thickness of 50 m, its volume is approximately $1.0 \times 10^6 \text{ m}^3$. This block covered part of the pre-slide course of Turbid Creek and reached the far wall of Turbid Creek.

The deposits forming block 2 have distinct layers too. The bottom layer is similar to layer c in block 1. The main characteristics of the deposits in each layer in block 2 are listed in Table 3.4 and can be seen in Figure 3.17.

The 1963 rock slide deposits in block 2 lie on pre-1963 deposits or basement rock-granodiorite. There is a distinct contact, a buried wood layer, between the 1963 and pre-1963 deposits.

Pre-1963 deposits have two layers. A piece of wood from the lower layer yielded a radiocarbon date of 3720 ± 60 years BP (Clague and Souther 1982).

Table 3.3
Main Characteristics of Deposits in Block 1

Layer	a	b	c
Thickness (m)	6-8	14-18	5-15
Colour	Grey	Light brown	Grey-green
Consolidation	Poor	Poor	Poor
Sorting	None	None	None
Clasts	20-30%. Mainly small rock fragments, 0.02-0.05 m across; few dacite boulders, 0.6-0.8 m across.	60%. Mainly brown columnar jointed dacite blocks and boulders, 0.8-2.0 m across.	15%. Small dacite fragments, 0.1-0.2 m across.
Matrix	70-80%. Grey silt and sand.	40%. Brown and grey silt and sand.	85%. Mainly tuff and tuff breccia powder, silt and sand.

Table 3.4

Main Characteristics of Deposits in Block 2

Layer	c	d	e
Thickness (m)	6-17	3-13	2-6
Colour	Greenish-grey	Brown	Grey
Consolidation	Poor	Poor	Poor
Sorting	None	None	None
Clasts	Less than 20%. No boulders. Mostly angular tuff lapilli fragments, 5- 10 cm across	More than 70%. Large angular blocks and boulders, 0.1- 1.0 m across. Mostly brown columnar jointed dacite.	30%. Small angular rock fragments. Mostly grey breccia and some dacite, few boulders, 0.6-0.8 m across.
Matrix	More than 70%. Grey to green silt and sand.	Less than 30%. Green-grey silt and sand (disintegrated tuff mainly).	70%. Grey silt and sand.



Figure 3.17 Three layers, V_c , V_d and V_e , in block 2 and their relationship with the 1984 debris flow deposits, U, upper unit, P_u , lower unit of pre-1963 deposits, P_l , and basement rock, R, looking E at site 33 (Fig. 3.11). Bushes in the foreground are 1.5 m high.

1984 debris flow deposits unconformably overlies the 1963 rock slide deposits with, at some localities, a buried wood or root layer on the contact. They show signs of fluid transport such as mud spatters, mud film around boulders, mud and small particles stuck on the surfaces of the boulders, and tuff collapsed or disintegrated in the deposits. The main characteristics of the 1984 debris flow deposits compared with pre-1963 and 1963 deposits are listed in Table 3.6 showing the differences of these deposits.

It seems likely that layer d of the 1963 rock slide deposits is from Member 3, and layer e from Members 3 and 4, in the depletion zone (Figs. 3.6 and 3.17).

Block 3

Block 3 is located between blocks 1 and 2, and bounded by the two obvious depressions. Block 3 is a dome elongated downstream (Fig. 3.18), 260 m in length, with a maximum width of 150 m and a maximum thickness of 40 m. The volume of block 3 is $1.23 \times 10^6 \text{ m}^3$. The boundary between blocks 3 and 2 (Fig. 3.13) looks like a saddle.

The deposits in block 3 also have three distinct layers. (Fig. 3.19). The basal layer is similar to layer e in block 2. The main characteristics of the overlying layers, f and g, are listed in Table 3.5.

Layer f of the 1963 rock slide deposits (Fig. 3.19) has come from Member 4, and layer g from Member 5, and a little Member 6 of the volcanic rock in the depletion zone (Figs. 3.6 and 3.19).

The stratigraphy of blocks and the correlation between them are illustrated in Figure 3.19. The layers are continuous through

Table 3.5

Main Characteristics of Deposits in Block 3

Layer	f	g
Thickness (m)	20	15
Colour	Dark brown	Light purple to grey
Consolidation	Poor	Poor
Sorting	None	None
Clasts	Over 80%. Large angular blocks and boulders, 1.0-1.8 m across, consisting of dark columnar jointed dacite, keeping the original texture of Member r.	20-30%. Small rock fragments of tuff breccia and lapilli. Blocks only seen on the top of the layer, 0.2-0.4 m across.
Matrix	Less than 20%. Brown to grey silt and sand.	70-80%. Purple silt and sand from disintegrated tuff and tuff breccia.

individual blocks. For example, in block 2, a continuous 400 m long profile is exposed on the left (south-east) bank of Turbid Creek (Fig. 3.17). Layers c, d and e can be traced throughout it. The same succession was observed on the other side of the block, on the right (north-west) bank of Dusty Creek.

The same characteristics were also observed in blocks 1 and 3.

Figure 3.20 shows the profile exposed on the right bank of Dusty Creek, at site 29 on Figure 3.11. Three distinct layers can be easily recognized and compared with those in block 3 on the left bank of Turbid Creek (Fig. 3.19).

For different blocks, the sequences of layers are different, because they are derived from different rock units. Block 1 corresponds to Members 1, 2, and 3; Block 2, Members 3 and 4, and Block 3, Members 4 and 5 mainly and a little of Member 6.

Different layers have different grain size distributions. The grain size distribution curves of the different layers were determined by combining the "area-by-number" method (Hungr 1981) and mechanical analysis. Typical results are presented in Figure 3.21, in which b, c, d, e, f and g indicate the corresponding layers in the deposits. The values of D_{50} of these curves are 33, 3.6, 70, 1.56, 105 and 1.5 mm respectively. This suggests that the bulk of the 1963 rock slide deposits are ungraded, and each layer has its own grain size distribution characteristics resulting from its parent bedrock characteristics. Layers b, d and f form a group with a high D_{50} value, above 30 mm. Layers c, e and g form another group with a low D_{50} value, less than 5 mm. This shows the influence



Figure 3.18 Block 3 looking NEE at site 39 (Fig. 3.11). Bushes on the top of the block are about 1.5 m high. Note that block 3 containing three layers, V_e , V_f and V_g , is located downstream from block 1, B_1 , between Dusty Creek, D, and Turbid Creek, T. X gives the position of Figure 3.19.

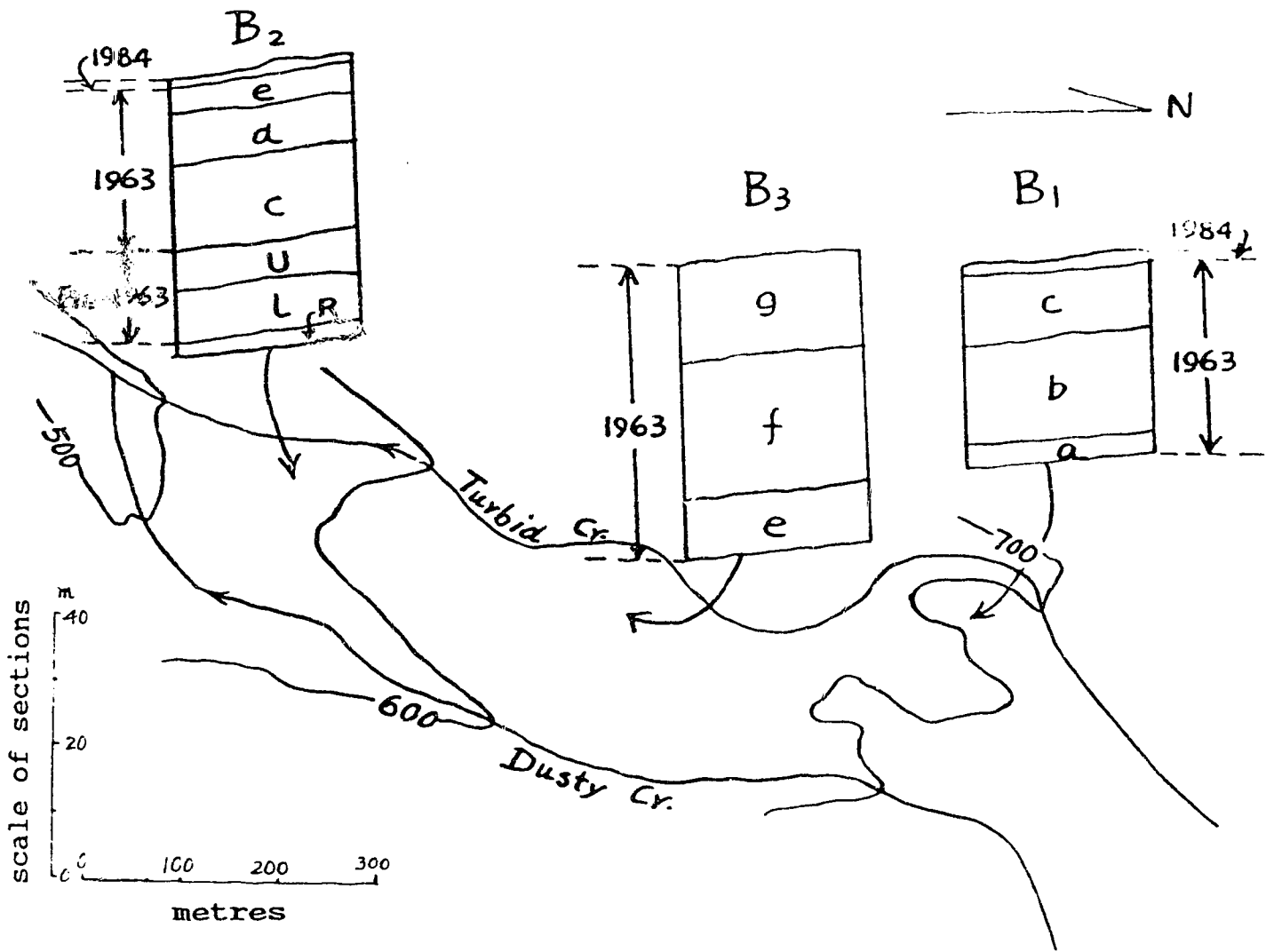


Figure 3.19 Stratigraphy of blocks, B₁, B₂, B₃, and their correlation. Note that R represents basement rock.

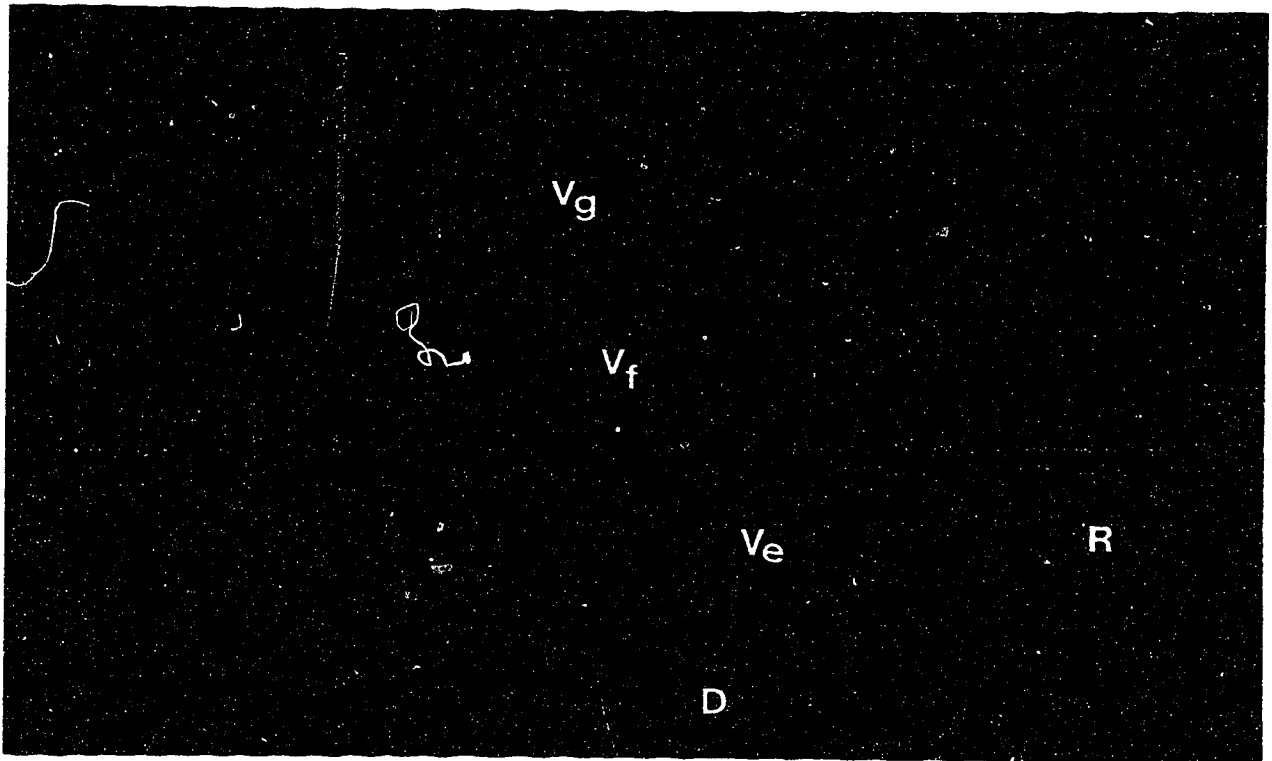


Figure 3.20 Three layers, V_e , V_f and V_g , on the other side of block 3 at site 29 (Fig. 3.11). Bushes are about 1.5 m high. D represents Dusty Creek, and R represents basement rock.

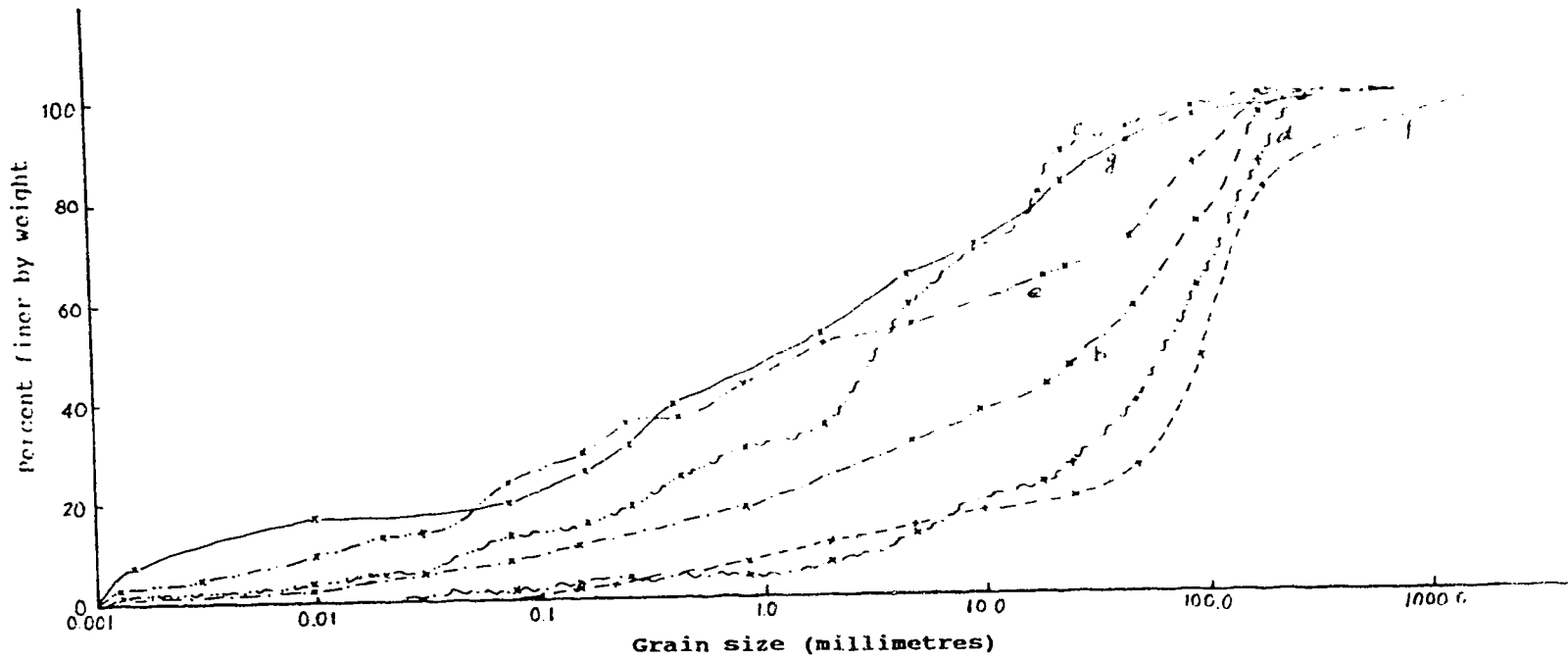


Figure 3.21 Cumulative grain size curves of the 1963 rock slide deposits. b, c, d, e, f and g indicate the corresponding layers in the deposits.

of the bedrock, because layers b, d and f came from dacite and layers c, e and g came from tuff, breccia tuff, lapilli tuff and tuff lapilli. The grain size curves clearly show that the deposits of the 1963 rock slide kept the order and sequence of the parent rocks.

All fines from these layers are non-plastic, differing clearly from the fines from the 1984 rock slide and debris flow deposits which are plastic.

From the distinct layers and topographic configurations of these major blocks, the different isopleth patterns of deposition blocks and the isopleth patterns of the blocks in the depletion zone, a reasonable inference is that the rock blocks in the 1963 rock slide moved as coherent units and the rock slide deposits kept the order of the rock sequences in the source area.

No sign of fluid transport can be seen in the 1963 deposits. For example, tuff blocks have not collapsed or disintegrated, they retain angular shapes. No mud films around boulders and mud and small particles stuck on the surfaces of boulders have been found. Evidently the 1963 event was a dry rock slide in contrast to the 1984 rock slide and wet debris flow.

Some thickness reductions of the original members of the volcanic sequence can be estimated. Layer f is a typical distinctive layer which came from Member 4, dark brown columnar jointed dacite. As the average thickness of layer f in block 3 is 20 m and the thickness of original Member 4 is 60 m, the thickness has been reduced to 1/3. Also layer g came from Member 5. The

Table 3.6
Comparison of pre-1963, 1963 and 1984 Deposits

Deposits	Pre-1963	1963	1984
Thickness (m)	12-15	10-40	0.5-5.0
Colour	Grey to red	Grey to dark brown	Light purple
Consolidation	Good	Poor	Very poor
Sorting	None	None	None
Layering	2 layers	7 layers	None
Clasts	20-50%. 0.2-2.0 m blocks and boulders of dacite.	Varying. Most of blocks and boulders are dacite.	60%. Blocks and boulders of basement rock, breccia, hard tuff and dacite, 0.2-4 m across.
Matrix	50-80%. Red to grey silt and sand.	Varying. Mainly grey silt and sand.	40%. Purple silt and sand.
Fluid Transport	None	None	Significant signs.

average thickness of the layer in block 3 is 15 m, and the thickness of the original Member 5 is 40 m. The reduction of the thickness is 0.38.

A comparison of the different characteristics of pre-1963, 1963 and 1984 deposits is made and the main results are listed in Table 3.6.

3.6 INFLUENCE OF 1963 ROCK SLIDE ON ENVIRONMENT

As the rock slide came to rest around the confluence of Turbid and Dusty Creeks, a series of topography changes took place. Dusty and Turbid Creeks were obstructed by the debris. Three blocks each dammed Turbid Creek separately. These dams formed a large dam separated by small unfilled spaces behind each of the small dams.

Block 1 overtopped the small ridge between Turbid and Dusty Creeks at the pre-slide confluence and dammed and occupied part of the pre-slide course of Turbid Creek. Turbid Creek flowed in the downstream course of No Name Creek until it cut through block 1 during the 1984 debris flow (Cruden and Lu 1992). So block 1 consists of a major part on the left bank of Turbid Creek extending upstream into Dusty Creek, and a minor part between the present course of Turbid Creek and No Name Creek (Fig. 3.16).

Block 2 overtopped the ridge between Turbid and Dusty Creeks 150 m below the pre-slide confluence, travelled downstream and reached the opposite bank of Turbid Creek, and totally blocked Turbid Creek. Later, Turbid Creek cut through the deposits near the west edge of block 1 and formed its present stream course.

Block 3 dammed Dusty and Turbid Creeks too.

These obstructions caused changes of the drainage. Turbid Creek cut through the west edge of block 2 and was diverted 200 m westwards in this section (Fig. 3.3). As block 1 blocked upper part of Turbid Creek, the new drainage course followed the downstream course of No Name Creek and Turbid Creek moved 150 m westwards (Fig. 3.3). As block 3 occupied the pre-slide confluence of Dusty and Turbid Creeks, Dusty Creek took over 700 m of the pre-slide stream course of Turbid Creek as its new stream course. The confluence of Dusty and Turbid Creeks shifted 1 km downstream. Figure 3.19 shows that the pre-slide confluence is at the boundary of blocks 1 and 3 where there is now significant seepage (Fig. 3.11).

The junction angle between Dusty Creek (the contributing channel) and Turbid Creek (the receiving channel) was in the range from 45° to 65° (Table 3.2). The rock slide debris collided with the valley wall opposite the channel junction and came to rest in the receiving channel within 1 km.

Other rock slides in the Garibaldi Belt have also deposited their displaced material when they entered larger channels at high angles to their path, the Devastation Glacier slide (Patton 1976, Evans 1986), the Rubble Creek slide (Moore and Mathews 1978), the Avalanche Creek slide (Cruden and Lu 1992) and the 1986 rock avalanche from the peak of Mount Meager (Evans 1987) are examples.

The 1963 rock slide shows that the larger the junction angle, the shorter the travel distance in the receiving channel. Following Costa and Schuster, the 1963 landslide dam is a Type 5

dam, which "form when the same landslide has multiple lobes of debris that extend across a valley floor and form two or more landslide dams in the same reach of river." (Costa and Schuster 1988, P.1057).

The records of the damage on the logging road bridge at the mouth of Turbid Creek indicate that there was no debris flow damage to the bridge from 1961 to 1966, it is inferred that no catastrophic burst happened in the first 3 years after the landslide dam formed. The narrow stream channel of Turbid Creek cut into the 1963 deposits suggests the dam was overtopped and eroded, but the major part of the dam remaining indicates that the process was not catastrophic.

The 1947 air photo (Fig. 3.2) shows clearly that large trees were growing on the banks along both sides of Dusty, Avalanche and Turbid Creeks indicating that the slopes of Mount Cayley in the Turbid Creek drainage were stable. Tree ring counting indicates that these trees are at least 100 years old. It is concluded that no large rock slides and debris flows had taken place for at least 100 years before 1947.

Another episode of active slope movement on Mount Cayley is going on now. In addition to the 1963 and 1984 events, several smaller, similar events are indicated by the records of the damage on the logging road bridge at the mouth of Turbid Creek. In 1967, 1981, 1984 and 1986, the bridge was removed by debris flow, and in 1972, the abutment of the bridge was eroded by a debris flow. So, the 1963 rock slide is the start of a new stage of active slope

movement on Mount Cayley.

3.7 DISCUSSION

The main conclusions of Clague and Souther (1982) were that the rock slide occurred in 1963 and a large block of volcanic rock formed the rock slide. The average velocity of debris movement was about 16 m/s.

From this study, some additional insights are obtained.

1. The depletion zone contained three separate blocks which detached and slid into the valley of Dusty Creek one after another. These separate blocks are clearly revealed by the isopleth map (Fig. 3.4). The cross-sections A-A' and C-A' in Figure 3.5 show the movement sequence of these blocks.

2. The accumulation zone is divided by two gullys into three blocks with different layers and different topographic characteristics. These accumulation blocks can be recognized from air photos (Figs. 3.1 and 3.3), the isopleth map (Fig. 3.4), and photos taken from a helicopter and the ground (Figs. 3.14 and 3.15).

3. The deposits of the rock slide have distinct layers (Figs. 3.16, 3.17, 3.19 and 3.20) which can be traced back to bedrock units in the depletion zone. Each accumulation block has its own deposit sequence differing from the other blocks.

4. As the three separate blocks in depletion zone, the three accumulation blocks in the accumulation zone and the distinct layers in the deposits are recognized, it is inferred that the rock slide moved in coherent blocks. It thus differed from the 1984 rock

slide (Cruden and Lu 1992).

5. The rock slide deposits formed a type 5 dam in Turbid Creek which caused significant channel changes.

3.8 CONCLUSIONS

The 1963 rock slide began at 1450 m and terminates at 500 m. About $5 \times 10^6 \text{ m}^3$ of columnar-jointed dacite and poorly consolidated pyroclastic rocks at the head of Dusty Creek slid 2.4 km along a slope of 21° . The movement velocity reached 26 m/s.

The depletion zone of the 1963 rock slide contained three separated blocks. Also the accumulation zone of the 1963 rock slide is divided into three blocks by two gullies. The deposits of the 1963 rock slide have distinct layers which can be traced to the bedrock in the zone of depletion. Each deposit block has its own deposit sequence which is different from the other blocks. The distinct layers are not only seen along the stream course of Turbid Creek, but also seen on the other side of the blocks along the present stream course of Dusty Creek, both sides of the blocks show the same distinct layers and structure. It is concluded that the 1963 rock slide slid in coherent units and came to rest at different localities, keeping the order of the rock sequences.

Dusty and Turbid Creeks were dammed by the 1963 rock slide deposits. Turbid Creek was diverted by the thick debris deposits shifting 200 m westwards, and the confluence of Dusty and Turbid Creeks shifted 1 Km downstream. Accompanying the deposition of rock debris, Dusty Creek took over a part of pre-slide stream course of Turbid Creek (700 m long), then joins Turbid Creek at the present

confluence again.

4 GEOTECHNICAL PROPERTIES OF VOLCANIC TUFF AND SLOPE MOVEMENT ON MOUNT CAYLEY

4.1 INTRODUCTION

Volcanic tuff constitutes the basal rupture zones of the 1963 rock slide and the 1984 rock slide on Mount Cayley, British Columbia (Fig. 1.1) and is one of the most important factors in the formation of the successive debris flow in the 1984 event. Many rock slides and debris flows have taken place in these volcanic rocks (Evans and Brooks 1991, Lu 1992), and in these events volcanic tuff also played an important role. It seems that to understand the mechanism of landslides in volcanic rocks on Mount Cayley, it is necessary to study the geotechnical properties of the volcanic tuff in detail. To understand the behaviour of the volcanic tuff in the slope movements on Mount Cayley, a laboratory programme was carried out on volcanic tuff collected in the summers of 1986 and 1989 from the layer that forms the crown of the 1984 rock slide. The sampling location, S, is indicated in Figure 2.5. As most of the tuff layers outcrop on very steep slopes which are inaccessible, six block samples were collected from the lower part, the white-grey tuff, of Unit 5 of the volcanic rock (Fig. 3.5) on Mount Cayley. As there was little exposure on the crown of the 1984 rock slide, these samples were collected from the same layer but at a different elevation (1550-1552 m).

These samples are grey-white fine tuff. Lithic fragments up to 4 mm in length make up the grain component. The matrix is submicroscopic. The matrix is surprisingly resistant to the point

of a steel needle and the lithic fragments could not be pried from the matrix with ease.

The grain size distribution was determined from the disintegrated specimens (Fig. 4.1).

The testing specimens were prepared from block samples 2 and 4 in the following order, as only these two blocks are large enough to do so.

1. Drilling columnar specimens. The diameters, D , of these specimens are almost the same (3.83-3.90 cm), but the lengths vary from 5.98 to 9.38 cm. Compressional wave velocity and dry porosity were measured from these specimens first. Then uniaxial and triaxial testing were conducted on these specimens whose lengths, L , were in the range of 7.5-8.1 cm. L/D ratios were about 2.

2. Drilling and cutting direct shear test specimens. The diameters of these specimens are the same, 5.1 cm, the heights vary from 1.27 to 2.56 cm. Before direct shear testing, some of the specimens were used for tilting table testing.

3. Finally, the remainder of the block samples were prepared for dry bulk density determination, point load testing, water absorption testing and slake durability testing.

The geotechnical behaviour of these tuff specimens was characterised by engineering classification tests, estimates of the uniaxial compressive strength of the intact rock material, q_u together with the ultimate shear strength. The objective of the laboratory programme was to investigate the relationship between the geotechnical behaviour of volcanic tuff and the rock slide and

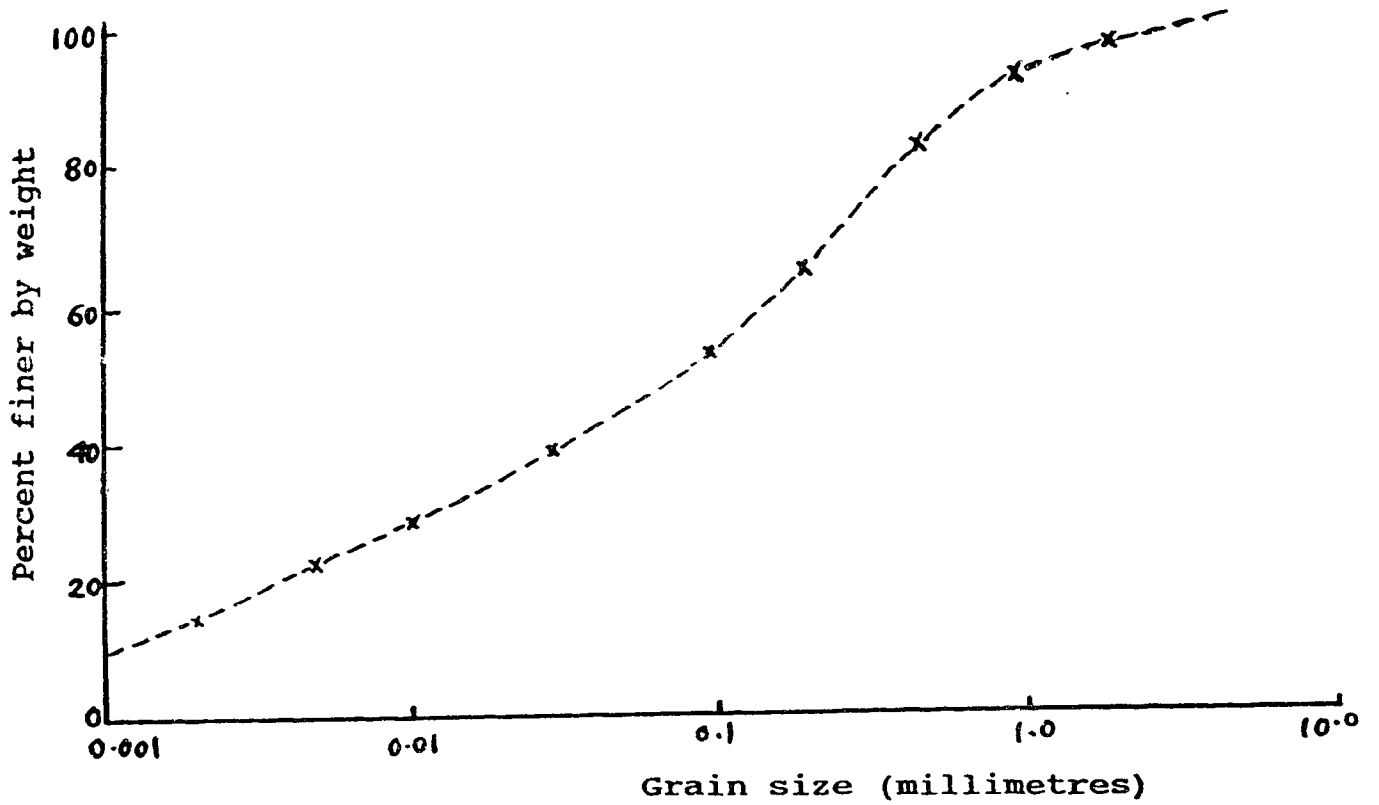


Figure 4.1 Cumulative grain size curve of Mount Cayley tuff

debris flow.

The laboratory work carried out is summarised in Table 4.1.

A laboratory programme had also been carried out in 1985 on the volcanic tuff collected from the Chasm Slides, Clinton, British Columbia. The results show that the geotechnical properties of the tuff from Chasm are different from those of the tuff from Mount Cayley. A comparison between them is made in this Chapter.

4.2 BASIC PROPERTIES OF VOLCANIC TUFF

Before doing uniaxial and triaxial testing, the basic characteristics of the tuff were determined. These include the homogeneity, isotropy, dry bulk density, porosity, slake durability, uniaxial strength determined by point load method, and shear strength determined by direct shear and tilting table tests.

Homogeneity and Isotropy

A large block, No. 4, with a length of 60 cm, a width of 40 cm and a thickness of 25 cm and the cores drilled from the block sample were checked for homogeneity and isotropy by measuring the compressional wave velocity in orthogonal directions using sonic velocity equipment. The locations of these specimens before drilling are shown in Figure 4.2. V_p values of the block sample with orthogonal directions and the specimens are listed in Table 4.2. No systematic differences can be figured out for any of the specimens and the large block sample investigated. We know that the tuff has layering. But as the block sample is comparatively small compared with the thickness, 0.7-2.5 m of the beds, it is difficult to obtain a block sample containing bedding. The samples collected

Table 4.1 Summary of Laboratory Work

Type of test	Material	Number of specimens
Elastic wave velocity	Tuff columns and block	15 (T4.1-T4.15) 1 (Block 4)
Dry density	Small tuff blocks	12 (from Blocks 2 and 4)
Wet porosity	Small tuff blocks	15 (from Blocks 2 and 4)
Dry porosity	Tuff columns	9 (T2.1-T2.9)
Slake durability	Small tuff blocks	4 sets (from Block 2)
Point load	Small tuff blocks	20 (from Blocks 2 and 4)
Direct shear	Tuff	4 sets (from Block 2)
Tilting table	Tuff	8 sets (from Block 2)
Uniaxial compression	Tuff columns	4 (T2.2, T2.5, T2.6 and T2.8)
Triaxial compression	Tuff columns	9 (T4.9, T4.8, T4.10, T4.6, T4.11, T4.2, T4.3, T4.1 and T4.5)

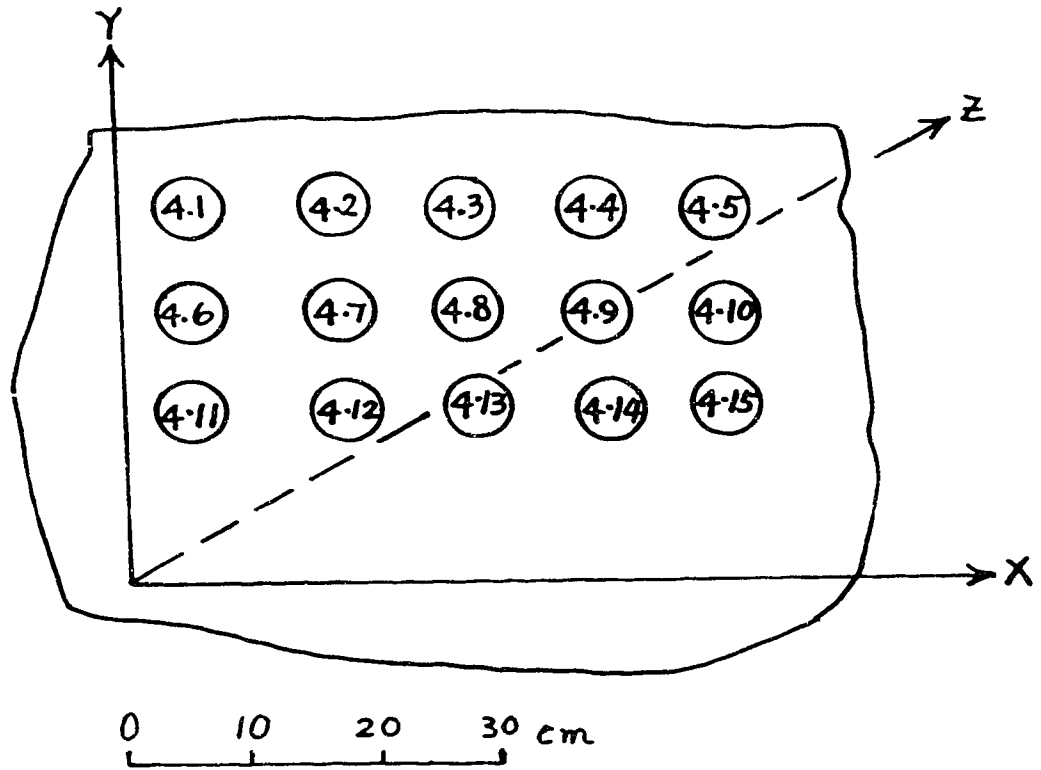


Figure 4.2 Locations of the specimens on the block sample before drilling.

Note that the diameters of the circles are not to scale.

Table 4.2 V_p Values of Tuff Block and Specimens

Specimen	V_p ($\times 10^3$ m/s)
4.1	1.416
4.2	1.627
4.3	1.478
4.4	1.607
4.5	1.578
4.6	1.739
4.7	1.593
4.8	1.412
4.9	1.611
4.10	1.329
4.11	1.481
4.12	1.579
4.13	1.445
4.14	1.516
4.15	1.418
B_x	1.442
B_y	1.612
B_z	1.525

B_x , B_y and B_z are the orthogonal directions on the large block sample. B_z is perpendicular to the bedding.

within a bed may be considered as homogeneous and isotropic.

Dry Bulk Density

The dry bulk density of the rock, r_d , was established by the water displacement method outlined in ISRM (1979).

The mean dry bulk density of the tuff was determined from 12 specimens as 13.6 KN/m^3 with a standard deviation of 0.49 KN/m^3 . The density is quite low.

Porosity

Porosity was measured by two different methods.

First, following the method suggested by ISRM (ISRM 1979), the porosity of the tuff was determined from 1 hour absorption and 48 hour absorption as 26.8% and 29.7% with standard deviations of 4.1% and 3.9% respectively.

Following Morgenstern and Phukan (1968), the porosity of dry specimens was also determined as 35.8% with a standard deviation of 4.2%.

Figure 4.3 shows a polarizing microscopic view of the composition of the tuff. It is estimated that the tuff contains a groundmass of 60% and phenocrysts of 40%. The phenocrysts consist of mainly plagioclase, 60%, and hornblende, 30%. There is 10% other minerals, including pyroxene, biotite and some undetermined minerals.

Following Goodman (1989, p. 31), as the dry bulk density, r_{dry} , of the tuff is determined as 13.6 KN/m^3 , the porosity, n , can be estimated by

$$n = 1 - r_{dry} / r_w \sum G_i V_i = 52\%$$

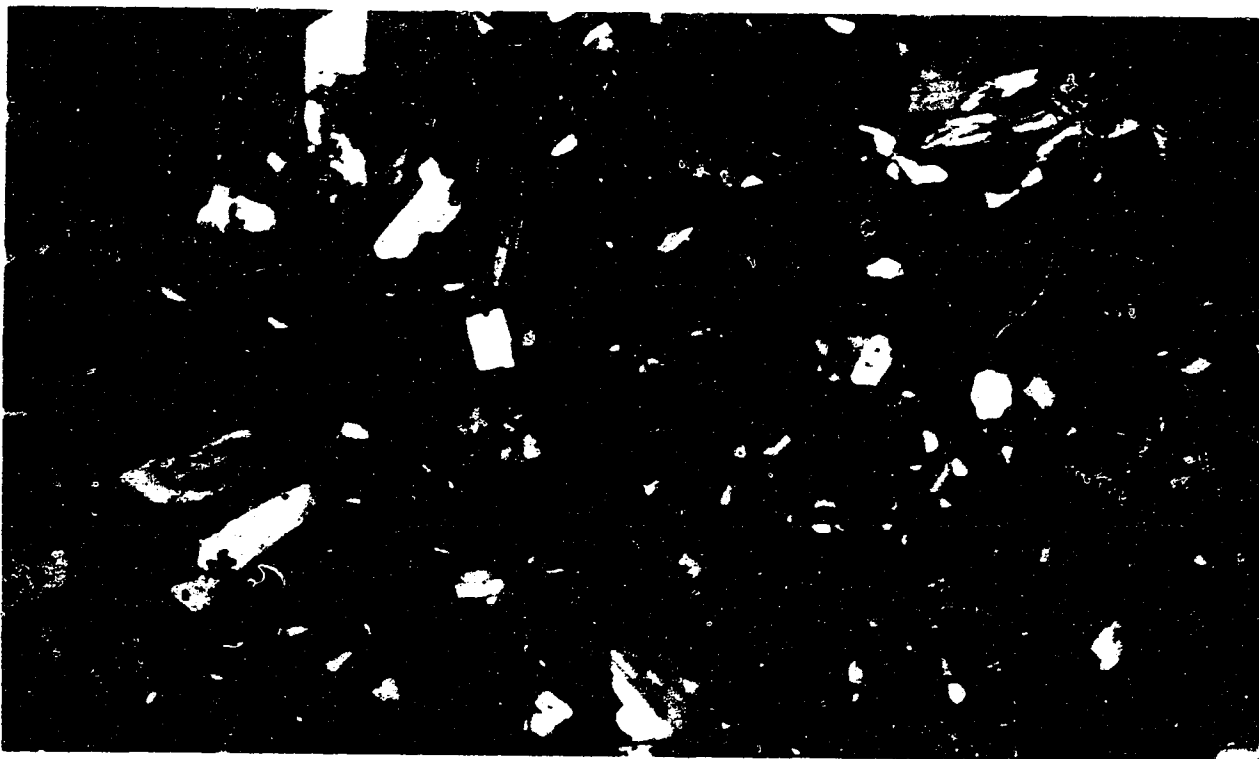


Figure 4.3 A microscopic view (100x) of the composition of Mount Cayley tuff.

Where G_i is the specific gravity of component i , V_i is its volume percentage in the solid part of the rock and r_w is unit weight of water.

Assuming the minerals are all plagioclase, density 2.7, the porosity will be 48.5%.

Comparing the porosity values determined from different methods, 52% from the composition of the minerals determined from polarizing microscope, 48.5% from the assumption of all plagioclase in the rock, and 35.8% from laboratory testing, it is suggested that the tuff contains substantial pores which are probably inaccessible by the laboratory test methods used. The actual porosity of the tuff should be higher than 35.8%.

Figure 4.4 shows the microstructure of the tuff examined by scanning electron micrographs.

Slake Durability

The Slake Durability test is a measure of the ease with which water can enter the rock, the reaction of the fabric to the ingress of water (e.g., solution of cement, hydration, destruction of interparticle bonds) and the resistance of the rock material to this reaction in the form of intergranular strength (i.e. water sensitive cohesion).

The water deterioration characteristics of 16 intact specimens from blocks 2 and 4 were established using the Slake Durability Test. Estimation of the water deterioration characteristics of the material is important in estimating the role of long term strength changes (softening) and changes of slope stability with time. The

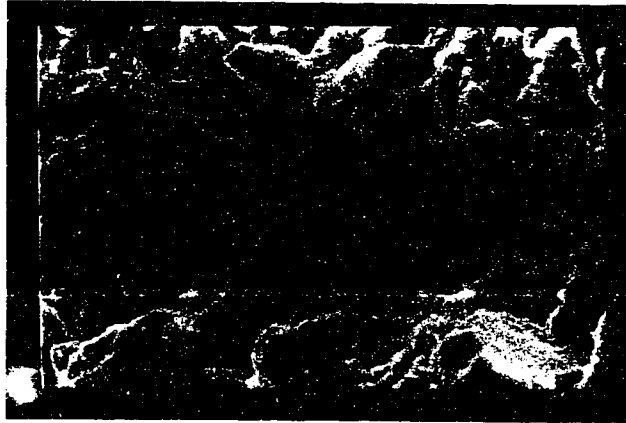


Figure 4.4 Scanning electron photomicrographs of Mount Cayley tuff.

standard apparatus and method, recommended by Franklin and Chandra (1972) and ISRM (1979) were used. In this test, ten lumps of material weighing approximately 500 g were subjected to two cycles of 6 hours drying and 10 minutes of tumbling and wetting. Distilled water was used in the test. The Slake Durability Index (SDI) is the ratio of the oven-dry weight of rock remaining in the drum after the 2 cycles of slaking to the initial oven-dry weight expressed as a percentage.

SDI after the first cycle is 41% with a standard deviation of 1.2%. SDI after the 2 cycles is determined as 25% with a standard deviation of 0.9%. It is important that the slake durability indexes of the tuff are very low following Gamble's (1971) scale and Franklin and Chandra's (1972) scale.

Point Load Strength

Point load tests were conducted on the volcanic tuff collected from Mount Cayley following Broch and Franklin (1972) and Bieniawski (1974). As discussed by these authors, an approximation to the uniaxial compressive strength (q_u) can be estimated for comparison with the results from uniaxial compressive test.

The Point Load Strength Index of the rock is determined as 0.224 MPa with a standard deviation of 0.011 MPa. The unconfined compressive strength (q_u) of the rock was estimated to be 5.37 MPa with a standard deviation of 0.26 MPa. Under the Geomechanics Classification Scheme of Bieniawski (1979) they are considered to be very low strength (1-5 MPa) or low strength (5-25 MPa).

As pointed out by Goodman (1989, p. 37) "The relationship

between q_u and I_s (Point Load Strength Index) can be severely inaccurate for weak rocks and it should be checked by special calibration studies wherever such a correlation is important in practice." As Mount Cayley tuff is very weakly bonded, its unconfined compressive strength estimated from Point Load Strength Index is strongly influenced by the effect of crushing of the weak bonds between the grains. The unconfined compressive strength estimated from Point Load Strength Index is inaccurate and should be checked by the uniaxial test results.

Direct Shear Test

Direct shear tests were carried out on the tuff specimens prepared from blocks 2 and 4 collected from Mount Cayley.

Four pairs of tuff specimens were tested in a D=5.1 cm high capacity shear box over normal loads in the range of 50-400 kPa at rate of 0.2-0.3 mm/s. Specimens were cut by saw and sanded to fit the box. Prior to placement an artificial shear surface was prepared by saw cut. The key point is to arrange the pre-cut surface to coincide with the real shear surface in testing.

Direct shear testing was carried out on dry specimens first. Then the shear box was flooded for 48 hours with distilled water, and the specimens were sheared again. In all of the tests on saturated tuff, a thin slickensided film of clay developed on the shear surfaces. This film probably accounts for the drop of the friction angle.

The results from direct shear tests show that the friction angle of dry tuff ranges 34° - 37° , with an average of 35° , and for

wet tuff ranges 29° - 31° , with an average of 30° .

Tilting Table Test

The friction angles of dry tuff specimens were also measured by the tilting table following Bruce et al. (1988). A pair of specimens with pre-cut surfaces were loaded on the tilting table. The friction angle was measured by a fixed protractor and LVDT respectively. The peak value of friction angle ranged from 36° - 39° .

The basic properties of the volcanic tuff determined from the laboratory programme are summarized in Table 4.5.

4.3 GEOTECHNICAL PROPERTIES DETERMINED FROM

UNIAXIAL AND TRIAXIAL TESTS

Introduction

To understand the geotechnical properties of the volcanic tuff collected from Mount Cayley and the relationship between the occurrence of landslides and the tuff in detail, a uniaxial and triaxial testing programme was carried out. The aim of these tests was to determine:

1. the general geotechnical behaviour of the tuff under uniaxial stress.
2. the uniaxial strength, peak and residual, of the tuff.
3. the general behaviour of the tuff under triaxial test.
4. the triaxial strength, peak and residual, of the tuff, and
5. pore water pressure influence.

Test results show that the behaviour of the tuff collected from Mount Cayley is not only different from other rocks, but also different from other volcanic tuffs, for example the tuff collected

from the Chasm slides, Clinton, British Columbia.

Two Yield Points and Collapse

Figures 4.5-4.8 show the results of four uniaxial tests on the naturally dried volcanic tuff specimens prepared from the tuff block 2 collected from Unit 5 at the crown of the 1984 rock slide on Mount Cayley. All these stress-strain curves show the same general features. Each stress-strain curve contains five portions. The change points between portions are denoted by A, B, C and D respectively.

The behaviour in the first portion, O-A, below a critical stress, σ_{c1} (point A on the stress-strain curves) is practically elastic and linear. The modulus of deformation is high, and deformation is very limited, less than 0.15% strain. When the first critical stress, σ_{c1} , between 0.75-1 MPa for these specimens, is reached, the stress-strain curve departs from the initial straight line, and the first abrupt change of deformation is produced by the start of destruction of the natural structure of the tuff. Point A can be considered as the first yield point corresponding to the start of destruction.

When the vertical stress is further increased, the behaviour is again linear up to another critical stress level, σ_{c2} (point B on the stress-strain curves). The modulus of deformation in portion A-B is lower than that in portion O-A and higher than those in the following portions. The deformation in portion A-B is a little larger than that in portion O-A, strain is about 0.3%, but substantially smaller than those in the following portions. When

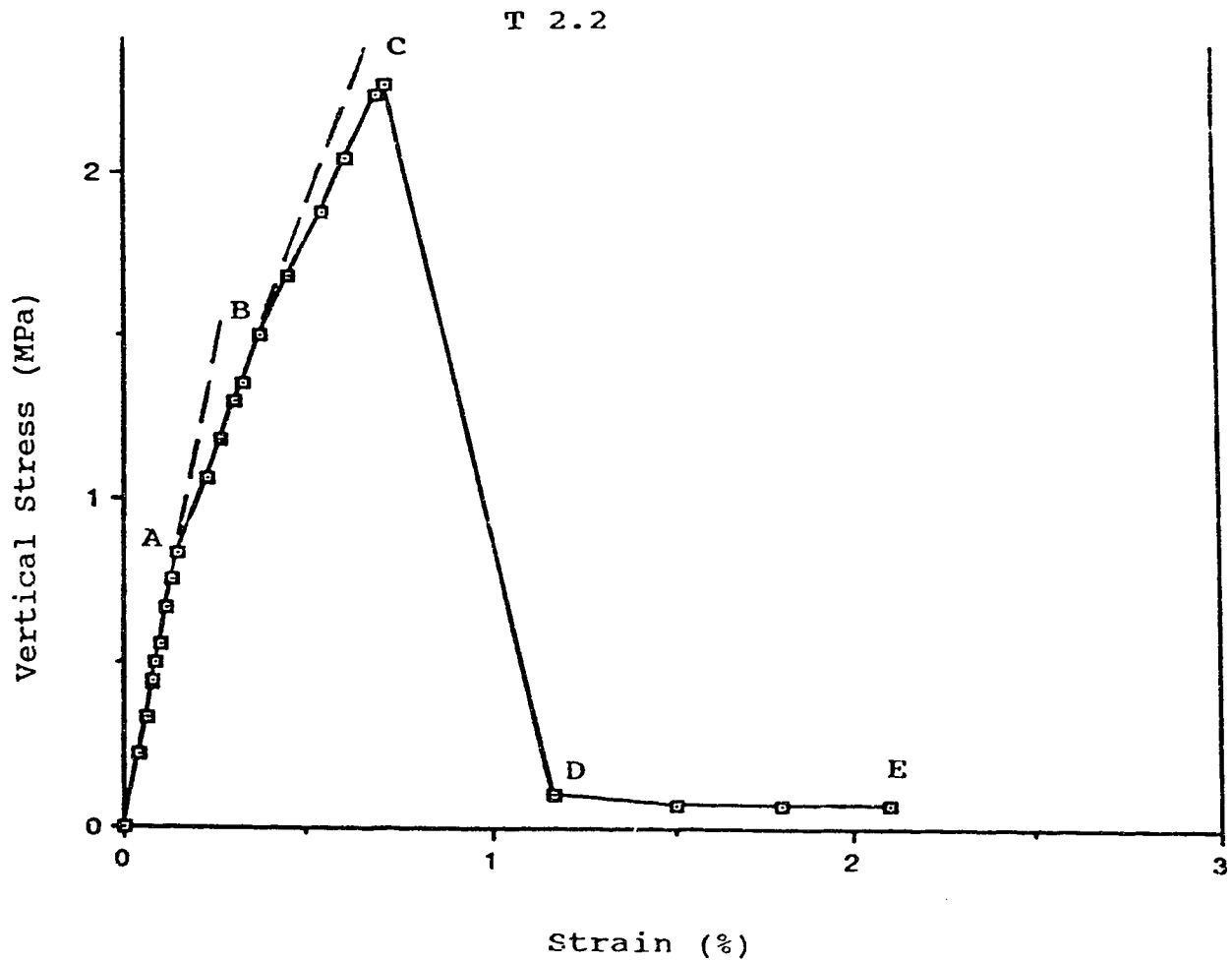


Figure 4.5 Stress-strain curve of dry tuff specimen, T 2.2, under uniaxial compression.

T 2.5

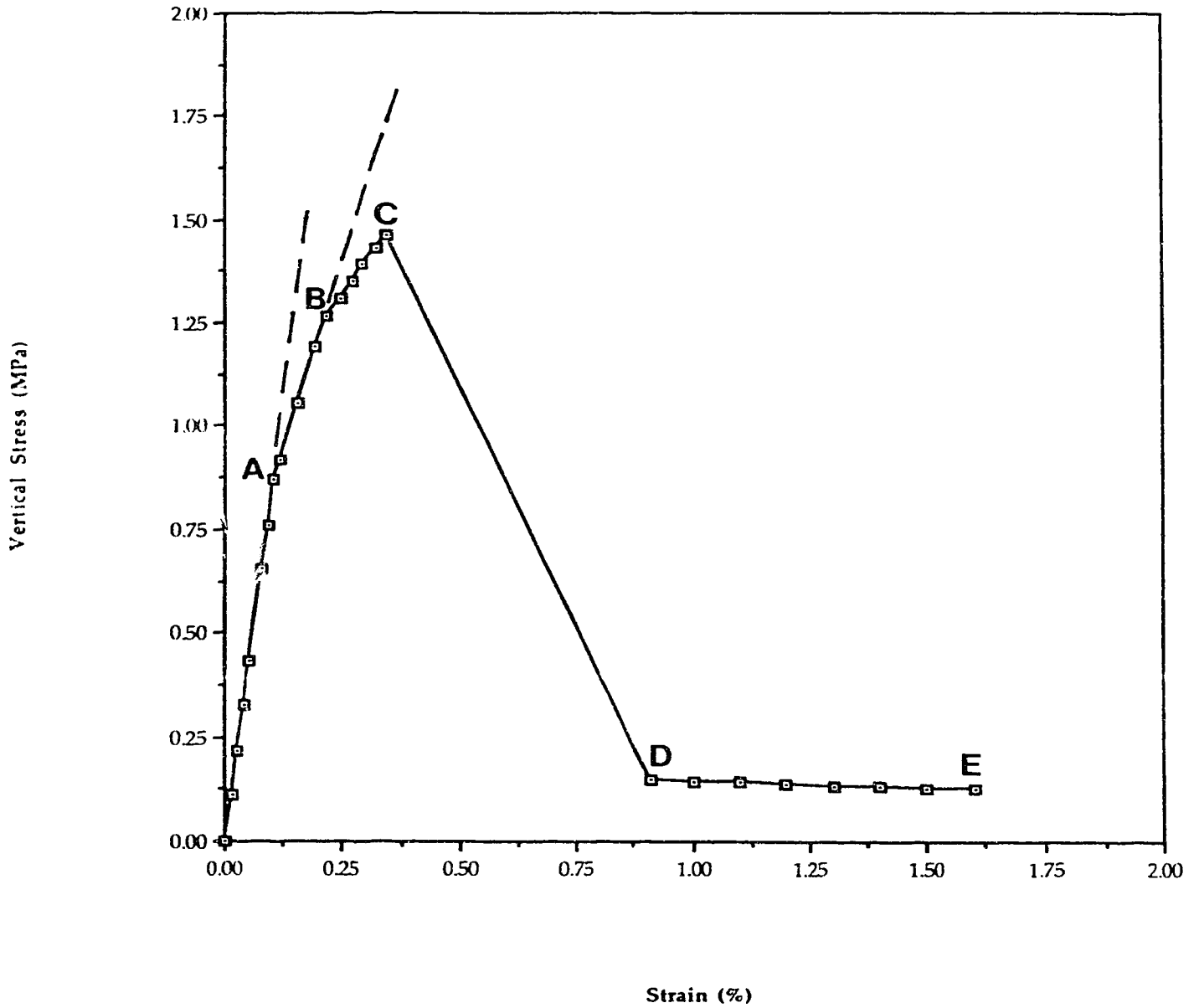


Figure 4.6 Stress-strain curve of dry tuff specimen, T 2.5, under uniaxial compression.

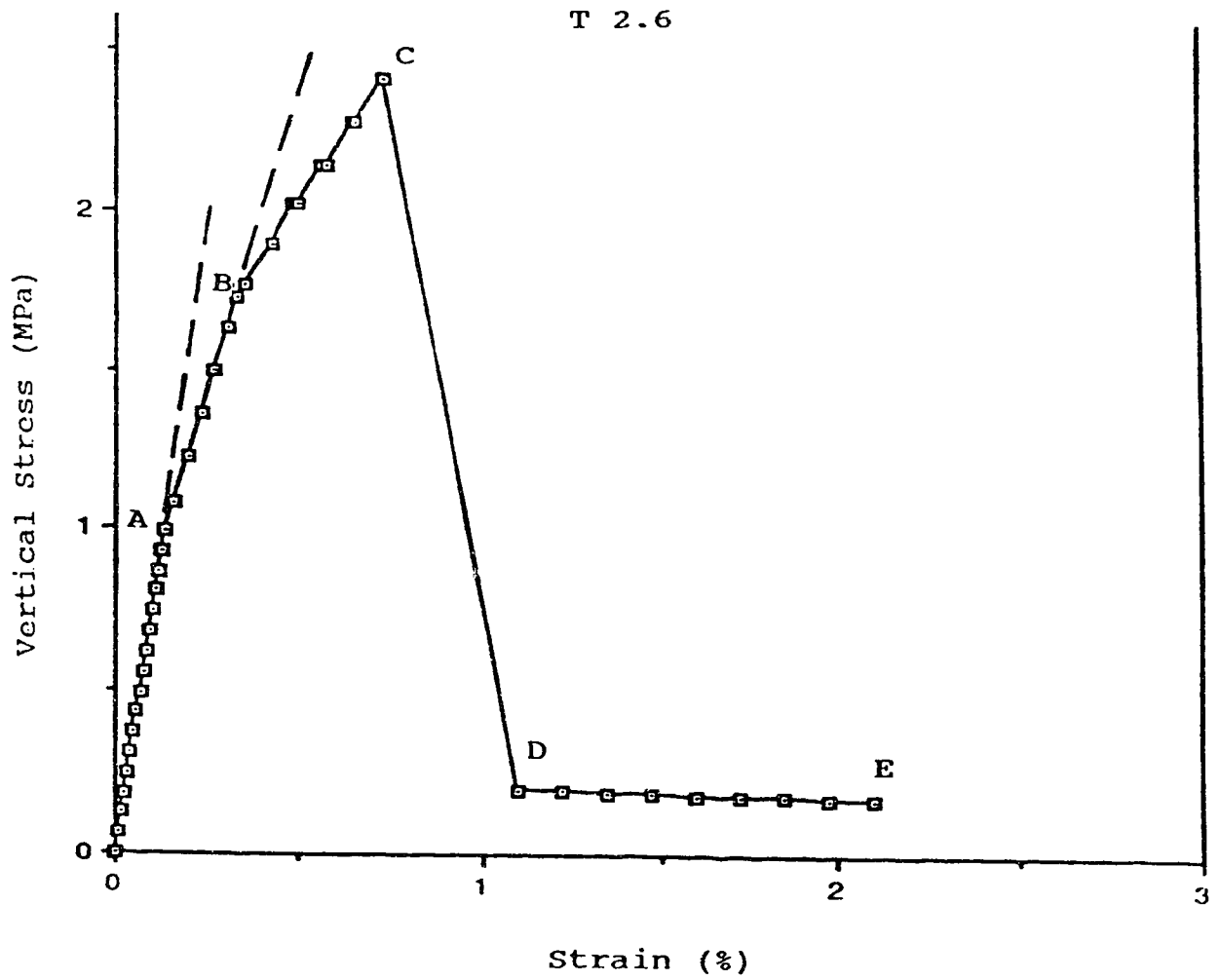


Figure 4.7 Stress-strain curve of dry tuff specimen, T 2.6, under uniaxial compression.

T 2.8

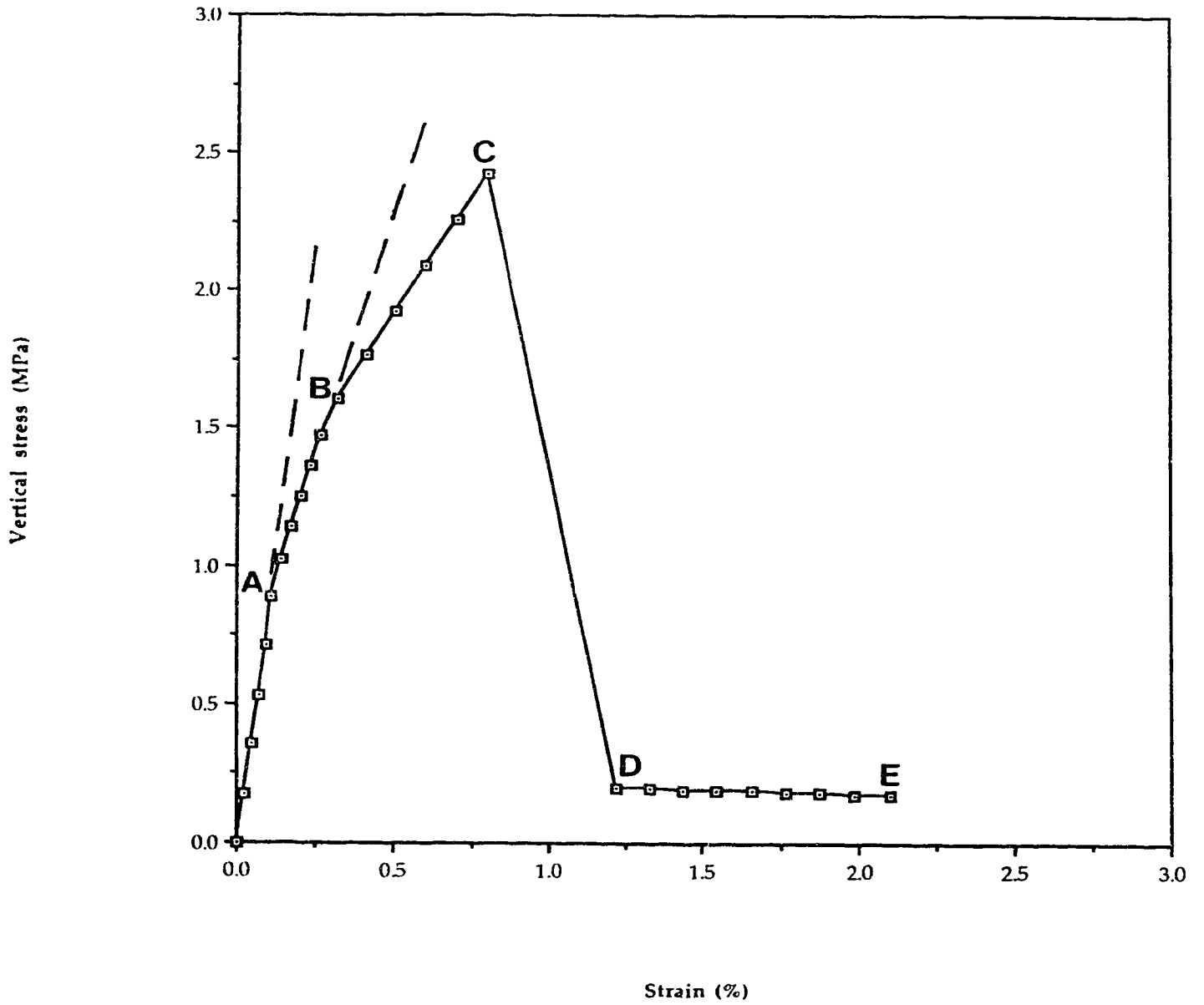


Figure 4.8 Stress-strain curve of dry tuff specimen, T 2.8, under uniaxial compression.

the second critical stress, σ_{c2} , is reached, the stress-strain curve once again departs from line A-B, and the second abrupt change of deformability is produced, probably by the start of shearing of the rock. B may be considered as the second yield point corresponding to the start of shearing. When the stress reaches this critical value, between 1.25-1.72 MPa for these specimens tested, shearing starts.

Past point B, when the vertical stress is further increased, the most abrupt change of deformability is produced. The modulus of deformation in portion B-C is low. The deformation is large. Very small cracks developed in the specimens and formed a shear surface. Point C is the peak strength of the specimen, after this critical stress is reached, the stress drops rapidly.

Past point C, stress decreases substantially, and strain increases in a small range. Between points C-D, the shear surface developed rapidly and completely. When the stress drops to a certain value, σ_r (point D on the stress-strain curves), another abrupt change of deformability is produced. After passing point D, the stress is constant, but the strain is still developing. Portion D-E shows the residual behaviour of the material.

Five main stages are distinguished from these test results. They are

1. Elastic phase, corresponding to point O-A in the stress-strain curves,
2. Crushing phase, corresponding to points A-B in stress-strain curves,

3. Crushing plus shearing phase, corresponding to points B-C,
4. Through going shearing phase, corresponding to points C-D in stress-strain curves, and
5. Macroscopic fracturing phase, corresponding to points D-E in stress-strain curves.

The evolution of the tuff structure during the five stages is clear. Between points A and B, the specimen crushes progressively. Shearing starts at point B. At that time the natural bonds between grains along the shear surface are almost totally destroyed. After point B, the behaviour of the specimen corresponds to a crushed soil. Between points D and E, the specimen shows the residual characteristics.

Critical Stresses in Collapse

Two yield points, the starts of crushing and shearing respectively, were found to coincide with the departures from the initial linear portions of the stress-strain curve. The critical stress values, σ_{c1} and σ_{c2} , for the starts of crushing and shearing are determined from Figure 4.5-4.8. σ_{c1} is in the range of 0.75-1 MPa, and σ_{c2} is in the range of 1.25-1.72 MPa.

Uniaxial Strength

From the stress-strain curves of the uniaxial tests, the peak uniaxial strength of the tuff can be determined as in the range of 1.5-2.4 MPa with an average of 2.1 MPa. The residual uniaxial strength may be in the range of 0.1-0.2 MPa with an average of 0.15 MPa. Comparing this with the uniaxial strength, 5.37 MPa, determined by Point Load Strength Index method shows that the Point

Load Strength Index method may be not suitable for the determination of uniaxial strength of the tuff on Mount Cayley, as it is too soft.

Behaviour of Tuff under Triaxial Stresses

Seven consolidated and drained triaxial tests were carried out on saturated tuff specimens prepared from block 4. The results are shown in Figures 4.9-4.15.

The shapes of the stress-strain curves under triaxial stress show five stages also. The two yield points indicating the starts of crushing and shearing respectively show up even more clearly. As the specimens were saturated and lateral stresses were applied, the deformations between the starts of collapse and shearing are larger than those observed in uniaxial tests carried out on dry specimens. The visible evidence of the development of small crackings and shear surface is also clear as observed in the uniaxial tests.

Except for specimen T 4.3 (Fig. 4.15), all specimens show very brittle behaviour.

Bishop (1973, p.339) pointed out "The most obvious soil parameter with which to relate post-rupture behaviour is the brittleness index which I proposed in 1967. This is defined in Fig. 2 and can be applied both to drained and to undrained conditions.

$$\text{Drained } I_B = (\tau_f - \tau_r) / \tau_f$$

Where τ is the resistance to shear on the sliding surface for a given value of effective normal stress, the suffixes f and r relating to the failure (peak) and residual states.

$$\text{Undrained } I_B = [(C_u)_f - (C_u)_r] / (C_u)_f$$

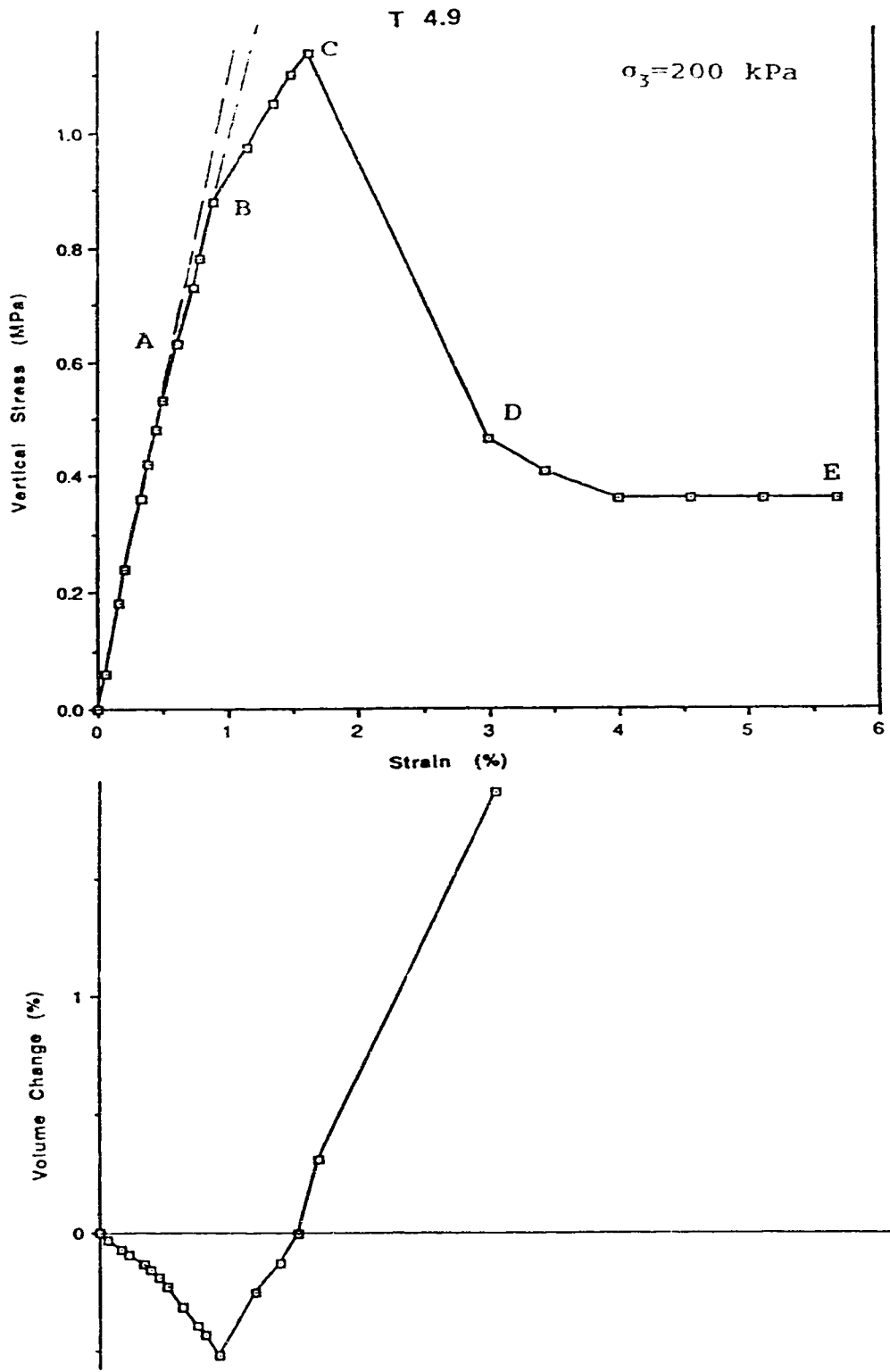


Figure 4.9 Stress-strain and strain-volume change curves of saturated tuff, T 4.9, under triaxial compression (consolidated and drained testing).

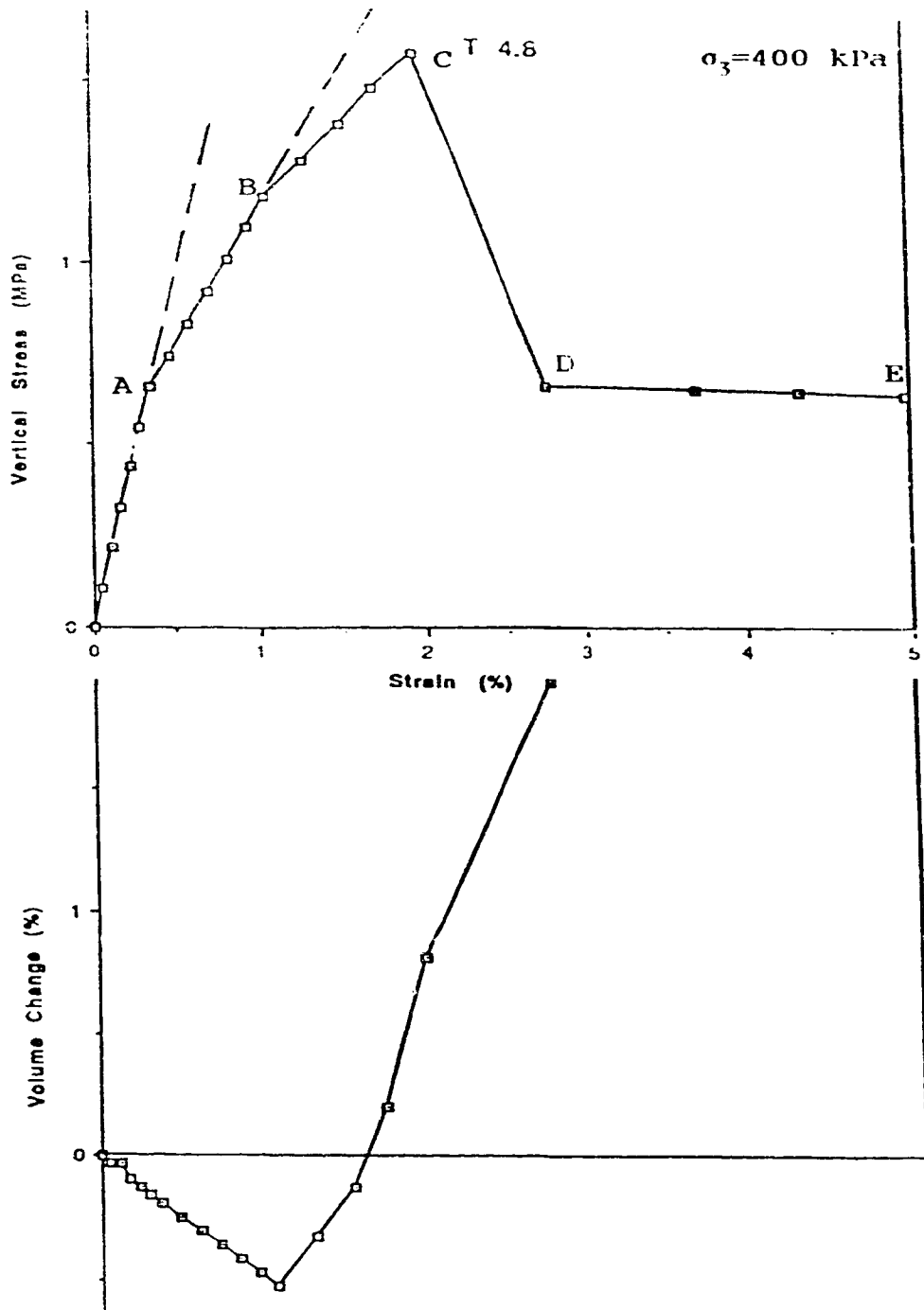


Figure 4.10 Stress-strain and strain-volume change curves of saturated tuff, T 4.8, under triaxial compression (consolidated and drained testing).

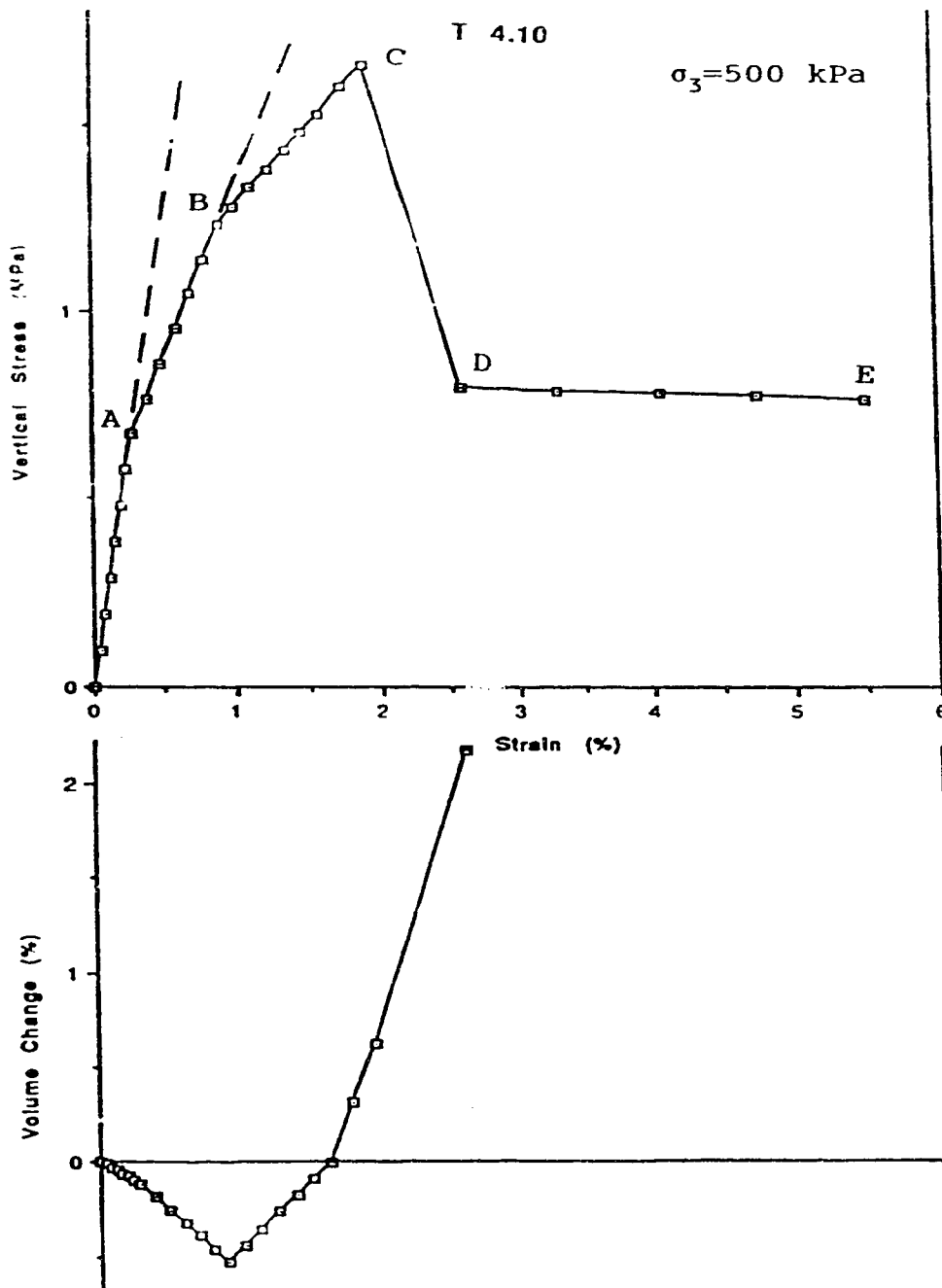


Figure 4.11 Stress-strain and strain-volume change curves of saturated tuff, T 4.10, under triaxial compression (consolidated and drained testing).

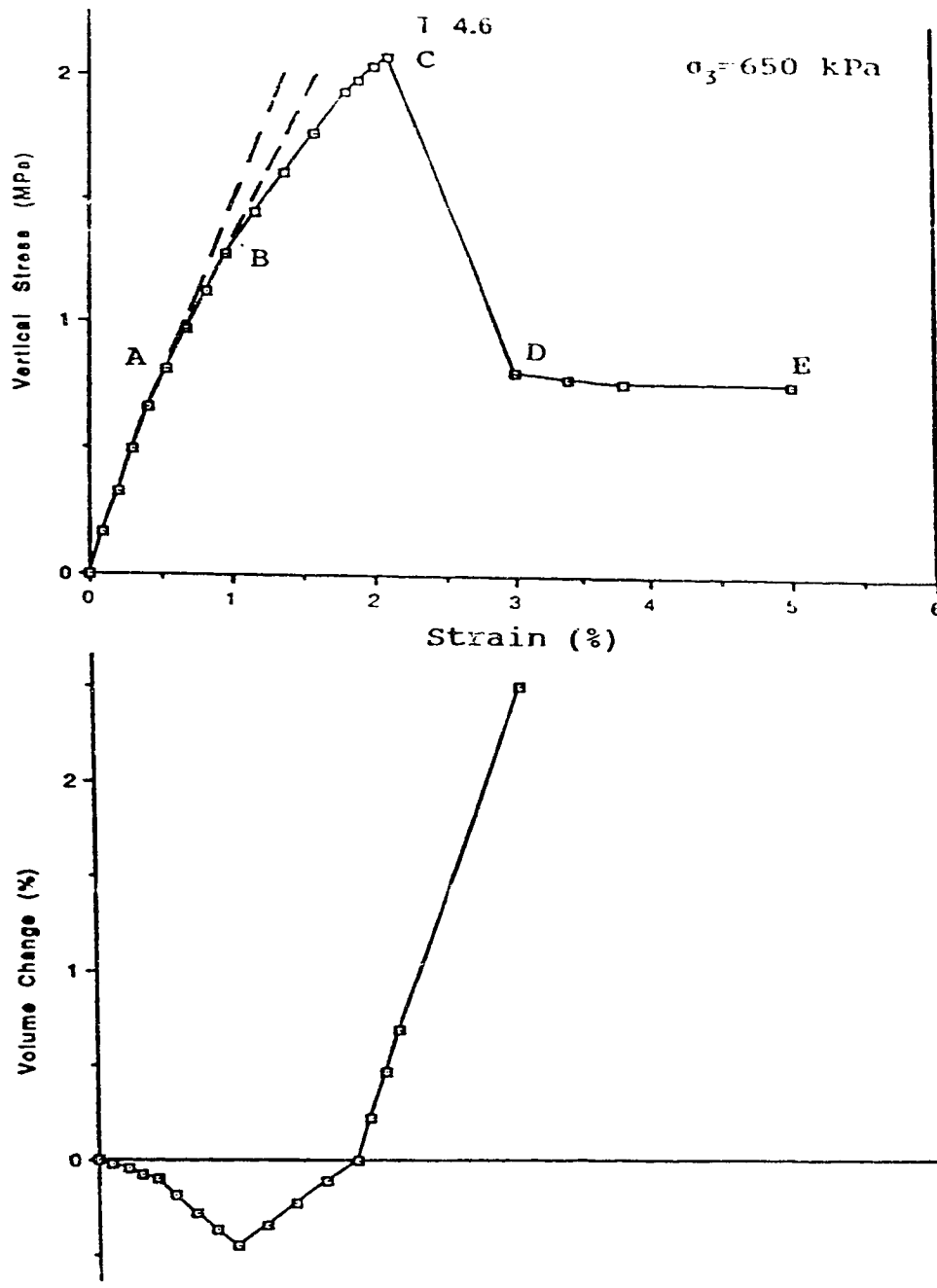


Figure 4.12 Stress-strain and strain-volume change curves of saturated tuff, T 4.11, under triaxial compression (consolidated and drained testing).

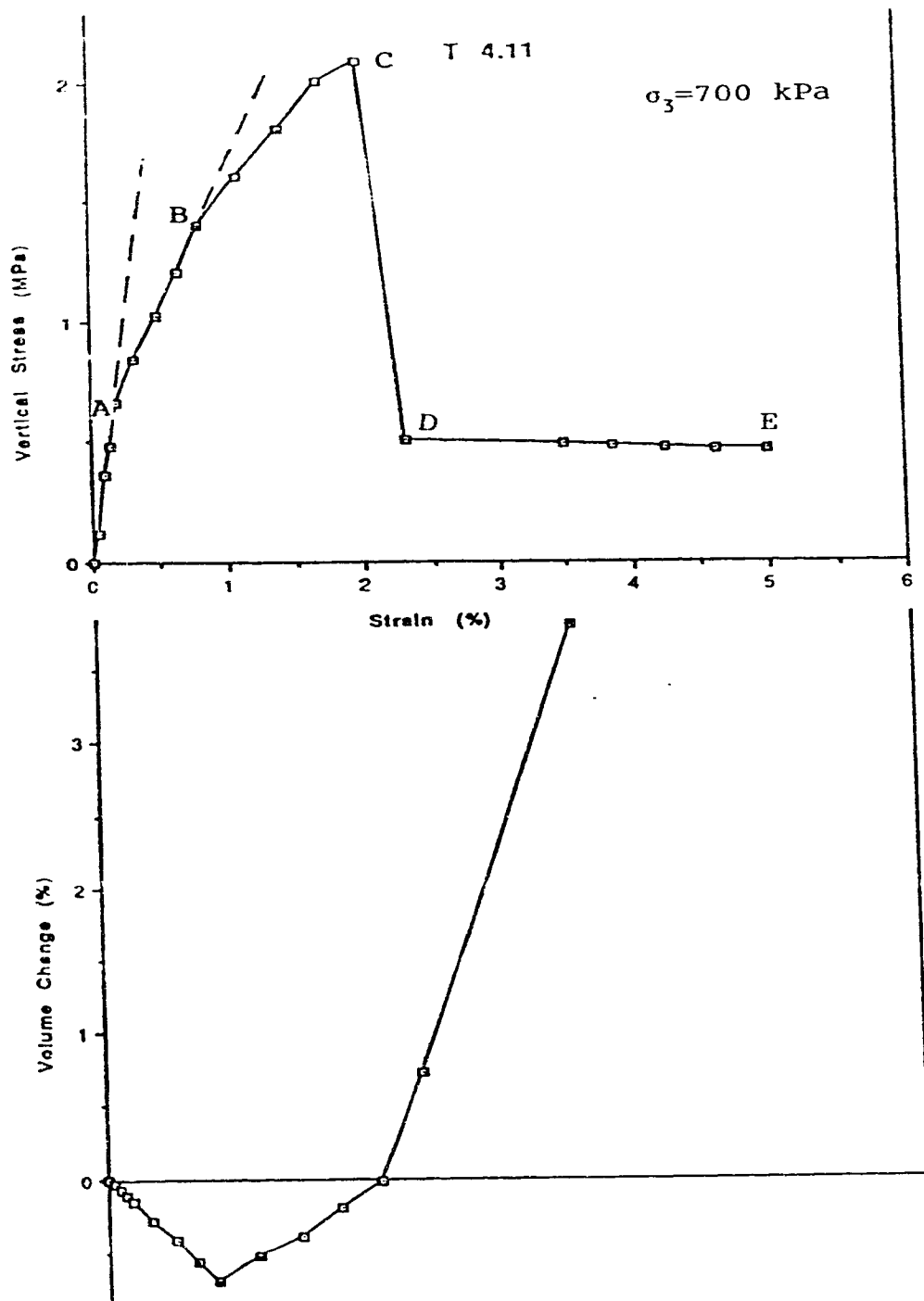


Figure 4.13 Stress-strain and strain-volume change curves of saturated tuff, T 4.6, under triaxial compression (consolidated and drained testing).

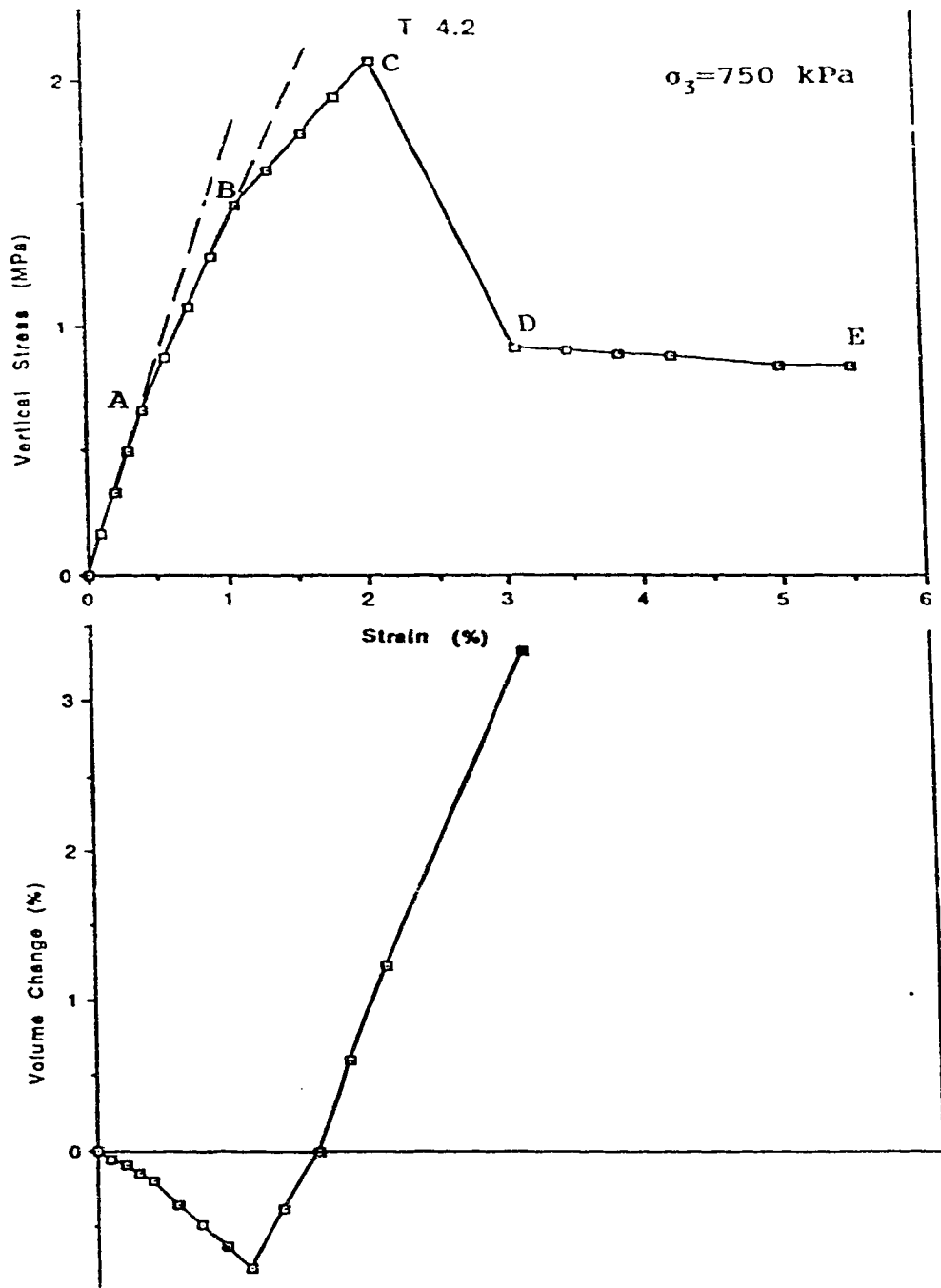


Figure 4.14 Stress-strain and strain-volume change curves of saturated tuff, T 4.2, under triaxial compression (consolidated and drained testing).

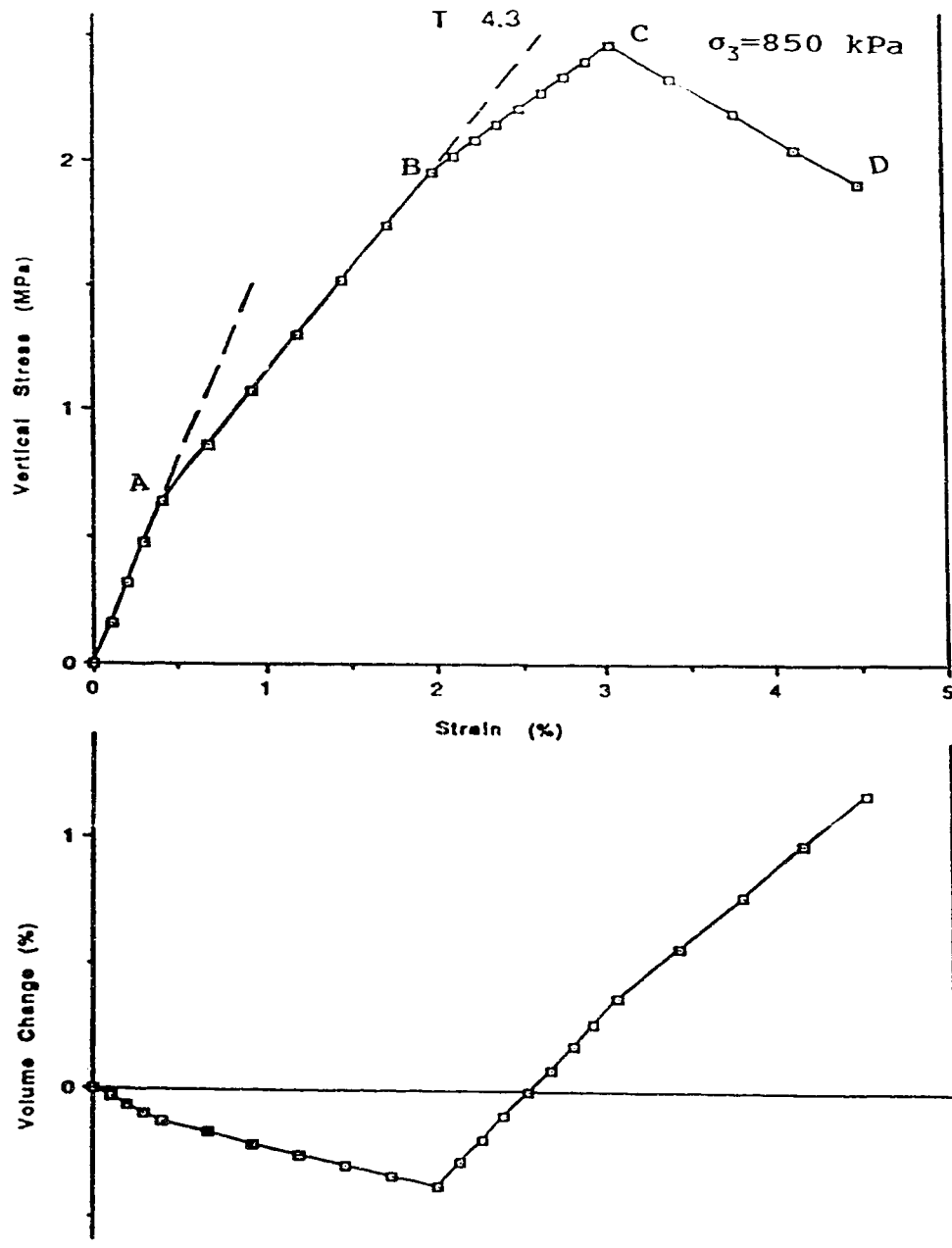


Figure 4.15 Stress-strain and strain-volume change curves of saturated tuff, T 4.3, under triaxial compression (consolidated and drained testing).

Where C_u denotes the apparent cohesion, the suffixes f and r relating to the peak and residual states, for the case when $\Phi_u=0$."

I_b values calculated from drained test results of Mount Cayley tuff are listed in Table 4.3. For comparison, the test results from uniaxial compression on dry Mount Cayley tuff were treated in the same way. These I_b values are also listed in Table 4.3.

The brittleness index of dry Mount Cayley tuff is in the range of 90-95% with the average of 92% and the brittleness index of wet Mount Cayley tuff is in the range of 54-78% with the average of 64%. From these data, two important conclusions can be reached.

1. The brittleness index of Mount Cayley tuff is high. Compare these values with the data listed in Bishop's Tables (1973, P.340, 349, Tables 3 and 5 respectively), the brittleness index of Mount Cayley tuff is very close to the index of Brown London Clay, 63%, and close to the index of Blue London Clay (intact), 77-93%.

2. The brittleness index of Mount Cayley tuff is strongly influenced by saturation. Saturation seems to reduce the brittleness index significantly from 92% dropping to 64%.

From Table 4.3, another interesting point can be recognized. τ_f values of dry tuff are in the range of 1.46-2.42 MPa with an average of 2.14 MPa. τ_f values of wet tuff are in the range of 1.14-2.09 MPa with an average of 1.77 MPa. Even though in the consolidated and drained testings, confining pressures were applied, τ_f values drop substantially from the τ_f values of dry tuff. It implies that the strength of dry tuff drops significantly when it becomes wet.

Table 4.3 Brittleness index

Specimen	Type of test	Condition	τ_f (MPa)	τ_r (MPa)	I_B (%)
T4.9	Triaxial	Wet	1.14	0.36	68
T4.8	Triaxial	Wet	1.58	0.63	60
T4.10	Triaxial	Wet	1.66	0.76	54
T4.6	Triaxial	Wet	2.07	0.76	63
T4.11	Triaxial	Wet	2.09	0.46	78
T4.2	Triaxial	Wet	2.08	0.84	60
T2.2	Uniaxial	Dry	2.28	0.1	95
T2.5	Uniaxial	Dry	1.46	0.15	90
T2.6	Uniaxial	Dry	2.41	0.20	92
T2.8	Uniaxial	Dry	2.42	0.2	92

The stress-strain curves contain five stages: elastic (portion O-A), crushing (portion A-B), crushing plus shearing (portion B-C), through going shearing (portion C-D) and macroscopic fracturing (portion D-E). Specimen T 4.3 is an exception. As the confining pressure for specimen T 4.3 was 850 kPa, about the critical pressure for yield, the specimen did not exhibit brittle fracture characteristics. The stress-strain curve shows typical transitional behaviour. Two yield points and peak were observed, but no sudden drop of stress took place after the peak strength.

It is inferred that confining pressure of 0.85 MPa is a critical value for saturated Mount Cayley tuff for the change of behaviour from brittle to ductile.

The volume change observations give interesting results and good indications of two yield points, and crushing of the specimens corresponding to the portions on the stress-strain curve.

In the first stage, corresponding to portion O-A on the stress-strain curve, the volume of the specimen decreases slowly and its change is small. The volume change-strain curve (Figs. 4.9-4.15) is almost linear. In the second stage, corresponding to portion A-B on the stress-strain curve, the volume of specimen decreases quickly, and its change is obvious, as the volume change-strain curve departs from the initial line substantially. Specimen T 4.3 is an exception because of its transitional behaviour under high confining pressure.

When the stress reaches point B, the start point of shearing, in most of specimens, volume decrease almost reaches the maximum

value, 0.5-0.8%. After that critical point, the volume of the specimen increases, while the volume change-strain curve departs from the previous portion. When passed the peak strength point (C on stress-strain curve), volume increases continuously.

These observations confirmed two yield points which represent the starts of the destruction of pores in the specimen and shearing respectively.

It is interesting to note that the significant volume decrease took place at the crushing stage, between the two yield points. It may be due to the significant destruction of the natural structure of the rock at the crushing stage. When shearing starts, the volume of the specimen increases.

These observations are in good agreement with definition of collapse by Uriel and Serrano (1973), and Uriel (1982). "It is normally said that a soil is collapsible when the modification of certain external conditions produce a change in its structure, accompanied by a more or less important reduction of volume of the soil mass" (Uriel and Serrano 1973, p. 257). "There is 'Collapse' of a soil or rock when the change of some external condition produces a substantial change in its structure with a more or less important reduction in volume." (Uriel 1982, p. 65).

It has become widely accepted that, in the brittle field, the stress-strain behaviour of a rock in compression can be divided into 4 stages prior to macroscopic fracture (Paterson 1978, p.157):

1. A "settle-down" phase.
2. Nearly perfect linear elasticity phase. It is thought to

involve predominantly the elastic deformation of the grains and pores.

3. Development of microfracturing and dilatancy involving stable microcrack propagation. Departures from perfect elastic behaviour are clearly in evidence from dilatancy.

4. Unstable developments in the pattern of microcracking, involving local weakening and leading to the growth of a macroscopic fracture. It begins with the onset of marked localization of the microcracking development and is here taken to include the complete progression from this point to macroscopic fracture.

Comparing with the general stress-strain behaviour of common rocks, the test results from this study show some noticeable characteristics.

As the "settle-down" phase depends on the placement of the specimen in the triaxial cell, it is omitted from the stress-strain curves in Figures 4.5-4.15 and 4.22-4.23.

The stress-strain curves show the typical elastic deformation phase (portion O-A), shearing phase (portion B-C)-the development of microfracturing and dilatancy, and the final phase-unstable development of microfracturing to macroscopic fracture (portions C-D and D-E) typical of the general behaviour of common rocks. Between the elastic and shearing phases, another distinctive phase (portion A-B) shows up in the stress-strain curves. As point A indicates the start of crushing and point B indicates the start of shearing, this phase can be called the pore collapse phase which is

a distinct deformation stage for these porous soft rocks.

Strength Determination

Figure 4.16 shows the Mohr Circles and the envelope plotted from the peak points of the triaxial test results. The peak strength was determined from the envelope: cohesion $c'=220$ kPa, and the friction angle $\Phi'=29^\circ$. Figure 4.17 gives the Mohr Circles and their envelope plotted from the residual points of the triaxial test results. The residual strength of tuff was: $c_r=65$ kPa, and $\Phi_r=17^\circ$.

p-q diagrams are prepared for both peak and residual behaviours respectively (Figs. 4.18 and 4.19). Linear regression method was used to treat these data. The linear regression equation of p-q at peak strength is determined as $q=189+0.492p$. The correlation coefficient is 0.995. From the k_f line in Figure 4.18 and the linear regression equation, α_f is determined as 26° and d as 189 kPa for peak strength. Φ' and c' are calculated from this diagram by

$$\Phi'=\sin^{-1}(\tan \alpha_f)=29^\circ \text{ and } c'=d/\cos\Phi'=216 \text{ kPa.}$$

Figure 4.19 shows the k_f line in the residual condition. The linear regression equation of p-q at residual strength is determined as $q=62+0.294p$. The correlation coefficient is 0.684. α_{fr} is determined as 16° and d_r as 62. So Φ_r and c_r are to be 17° and 65 kPa respectively.

The peak and residual cohesions of dry specimens determined from uniaxial tests, $q_u/2$, are 1 MPa and 75 kPa respectively. Comparing these values with the cohesions of wet specimens determined from triaxial tests, 220 kPa and 65 kPa respectively, it

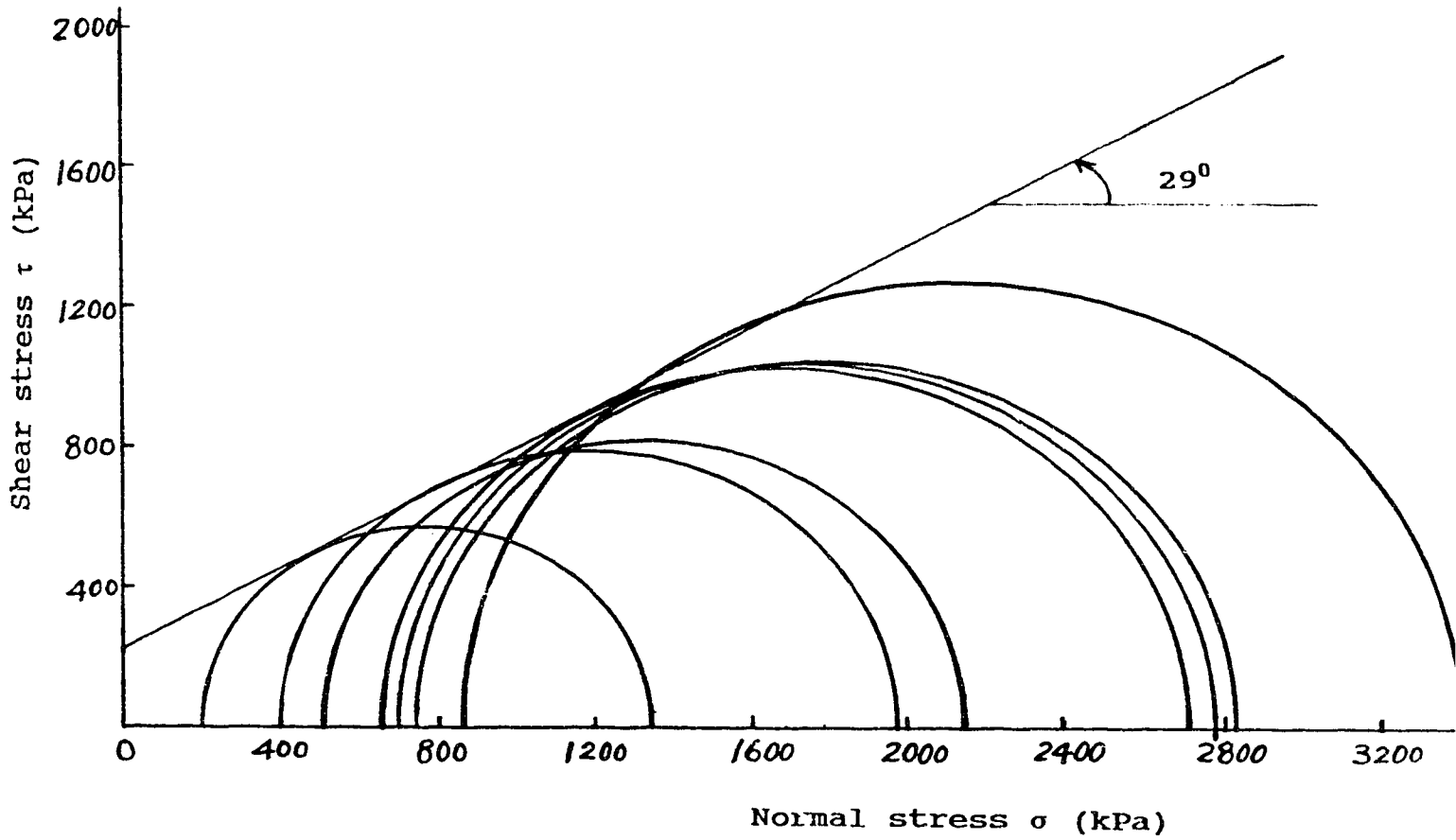


Figure 4.16 Mohr circles and envelope of wet tuff at peak strength.

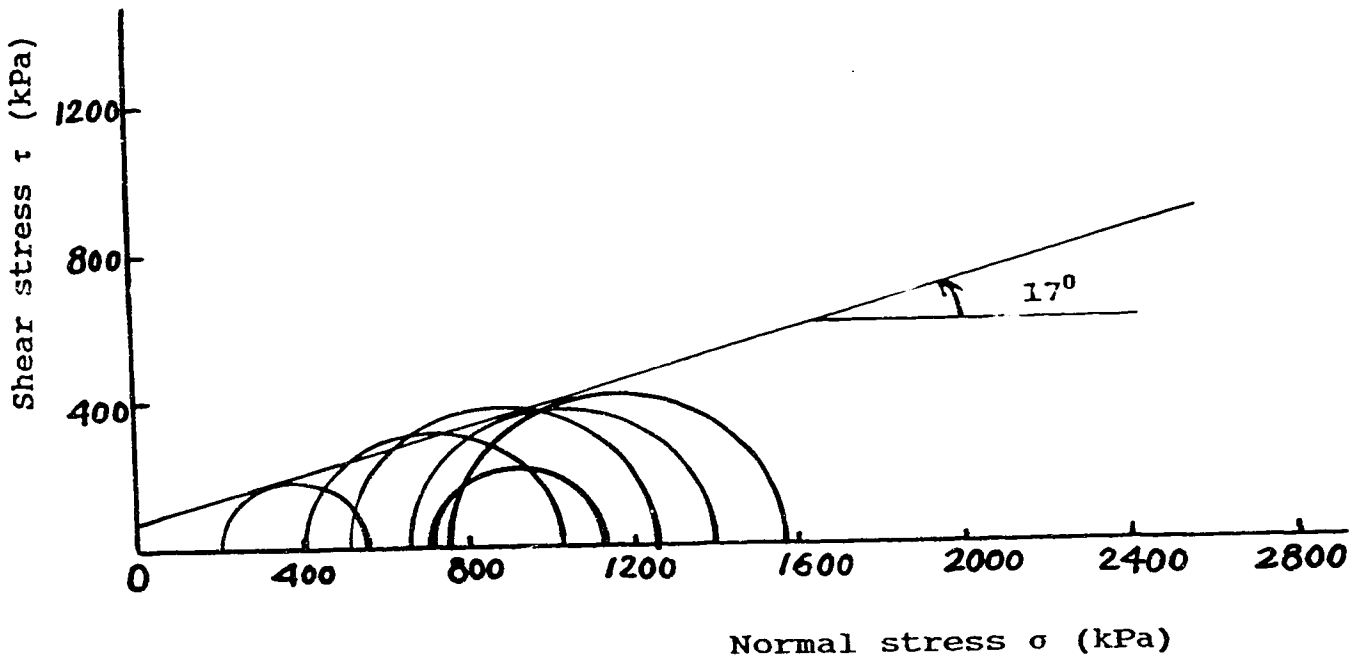


Figure 4.17 Mohr circles and envelope at residual strength.

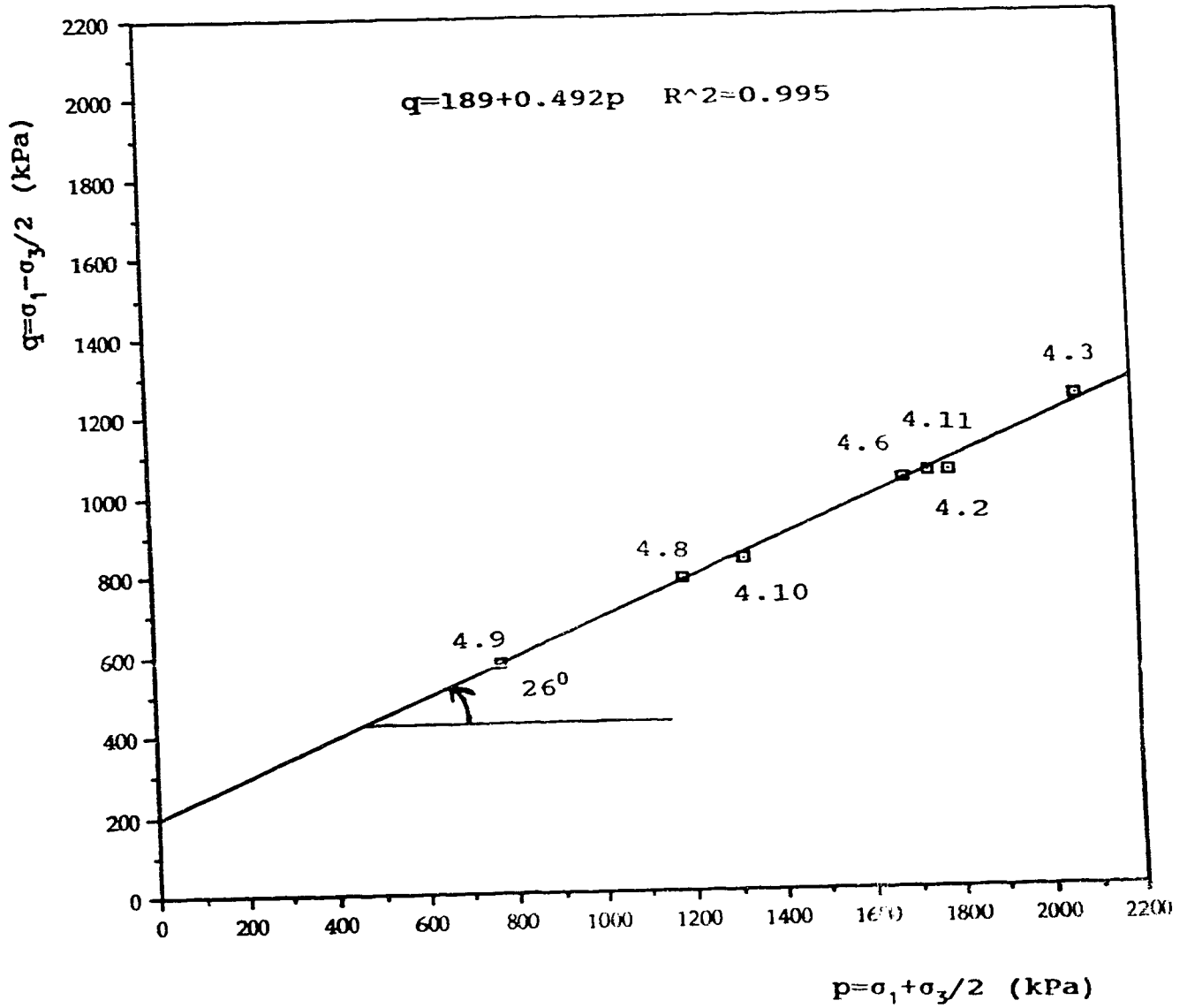


Figure 4.18 p-q diagram at peak strength.

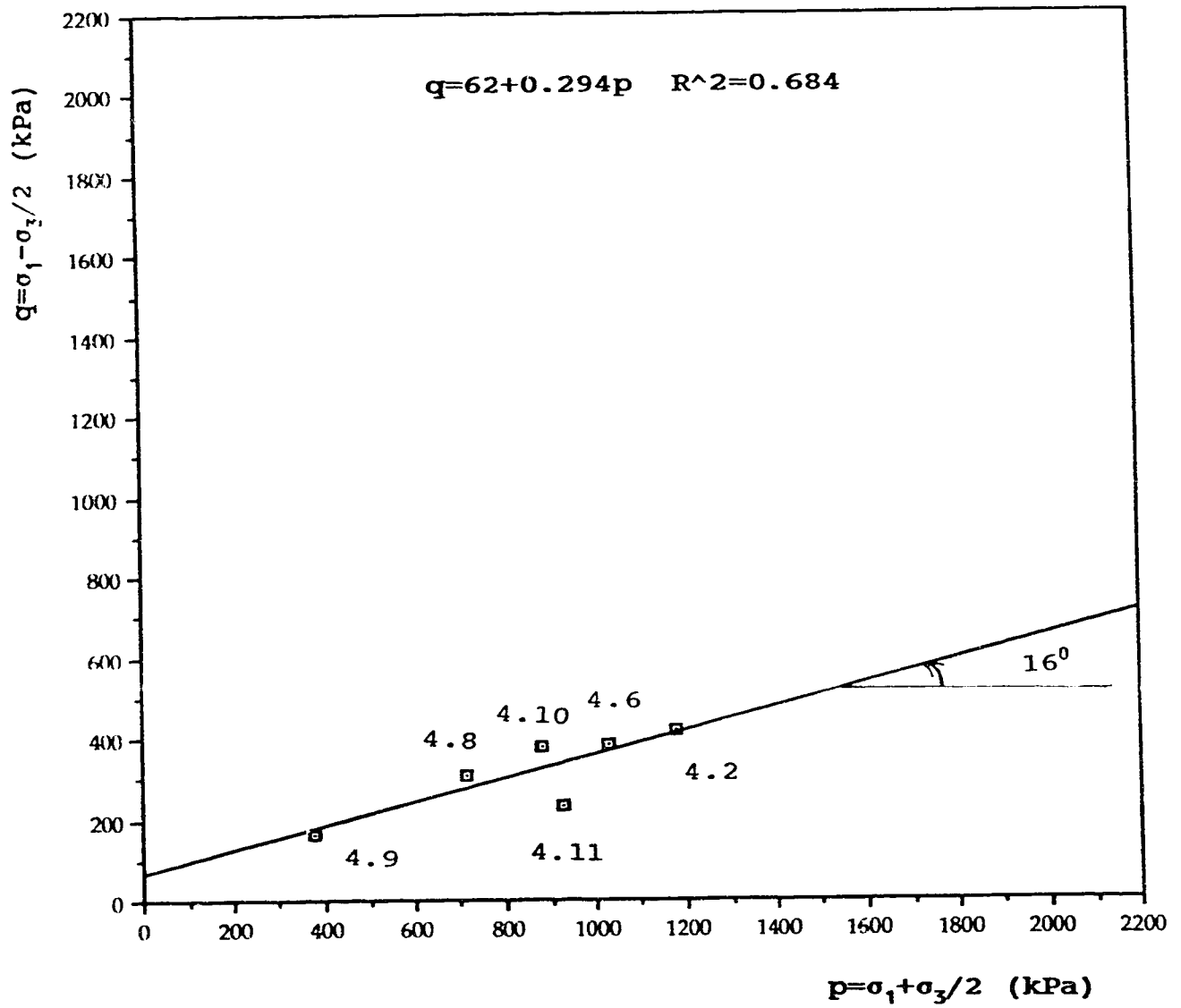


Figure 4.19 p-q diagram at residual strength.

It is clear that saturation causes a significant drop of peak cohesion, from 1 MPa to 0.22 MPa.

As direct shear tests gave the friction angle of wet tuff as 30° , it is concluded that the values determined from triaxial tests are in good agreement with the results from direct shear tests. It suggests that the peak friction angle of wet tuff can be chosen as $29-30^{\circ}$, the residual value may be chosen as 17° .

It is interesting to note that even though the confining pressures vary over quite a wide range, the critical vertical stresses at the first yield points are kept within a very limited range, almost constant (Fig. 4.20). But the critical vertical stresses at the second yield points increase with the increasing of confining pressures (Fig. 4.21).

Values of σ_3 and σ_1 at the first and the second yield points are recorded. Then p_c and q_c values corresponding to two yield points are obtained. The values of p_c and q_c are plotted in Figs. 4.20 and 4.21.

The first yield points show an obvious tendency, q_c values form a more gently sloping line. q_c values for the first yield points are around 0.3 MPa. It suggests that the first yield, corresponding to the start of crushing or collapse of the tuff takes place at certain critical stresses when the specimens are saturated and confining pressure is applied. It seems likely that the stress required by the start of collapse of pores is independent of the change of the confining pressure.

The second yield points show an obvious tendency, q_c values

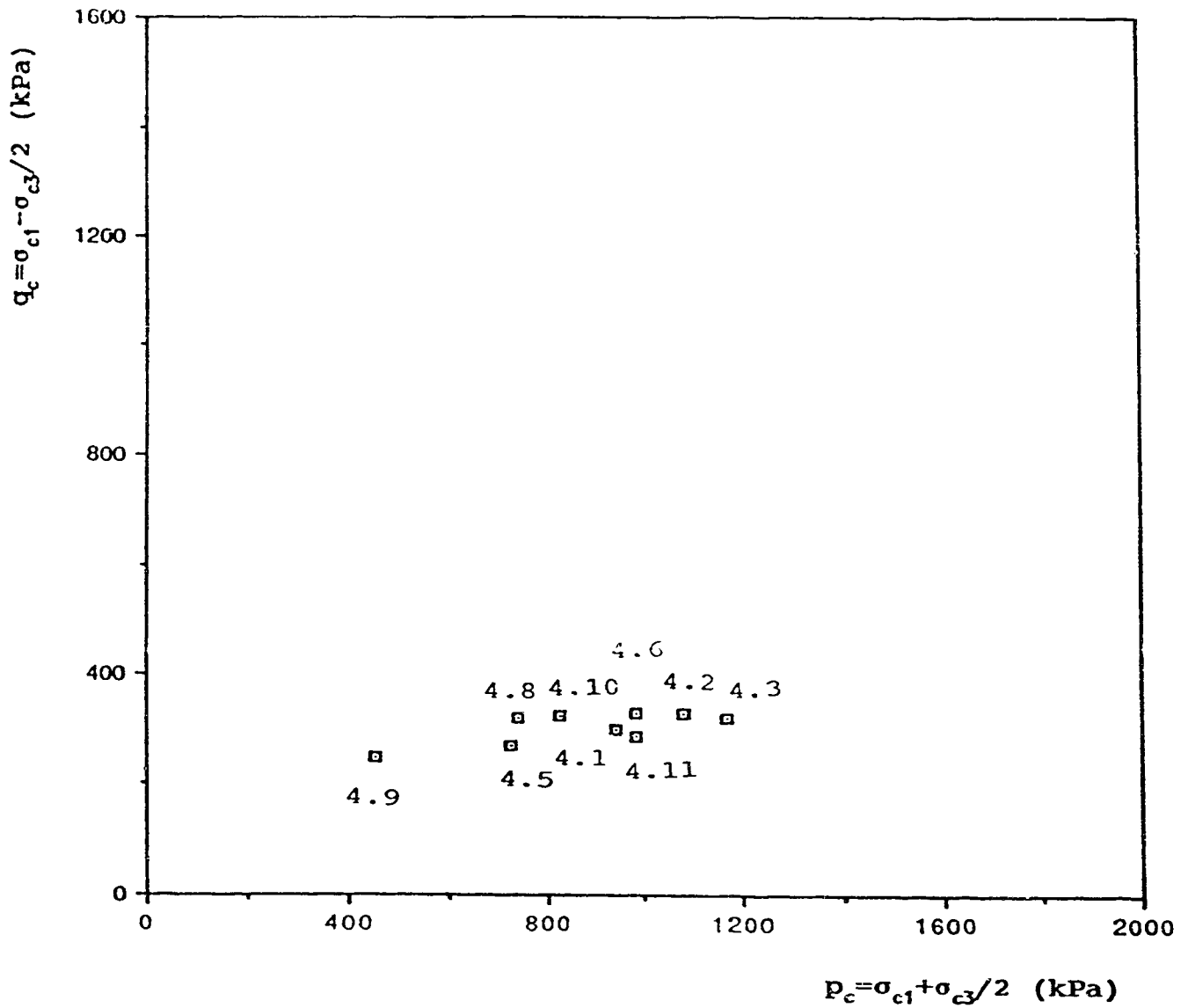


Figure 4.20 p_c - q_c diagram of critical stresses at the first yield points

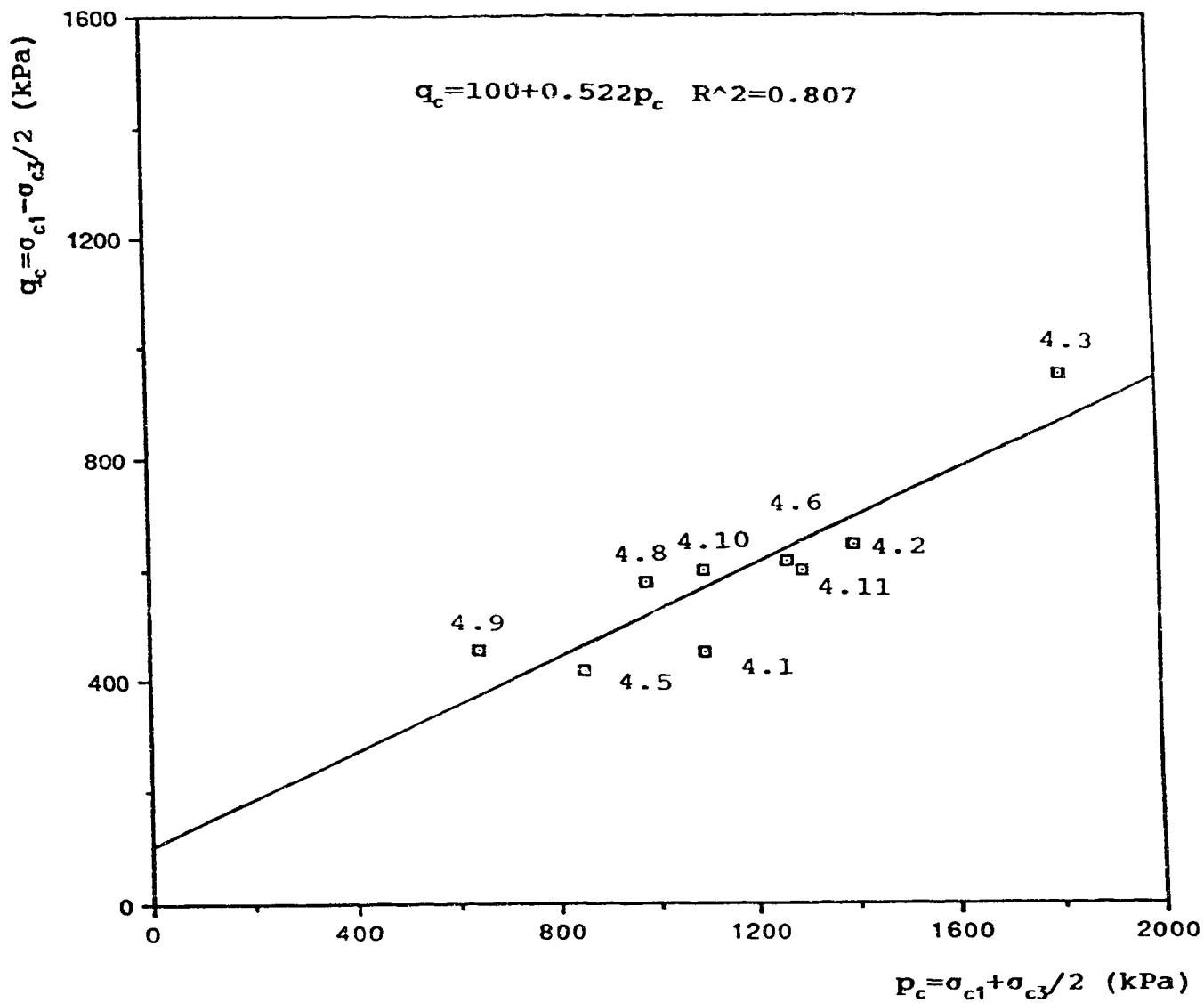


Figure 4.21 p_c - q_c diagram of critical stresses at the second yield points

form a line from 0.45 MPa to 0.95 MPa is dependent on p_c values.

The regression equation of p_c - q_c values of the critical stresses at second yield points was determined as $q_c=100+0.522p_c$, and the correlation coefficient was 0.807. The k_f line in Fig. 4.21 is very similar to the k_f line in Fig. 4.18. Compare these two k_f lines and the regression equations of the peak strength and the second yield points, it is found that they are almost the same except for some small difference in intercept (189 and 100 respectively) and correlation coefficient (0.995 and 0.807 respectively). It seems to confirm that the second yield point indicates the start of shearing. So the critical stresses at second yield points show the shearing characteristics, dependent on the confining pressures, but differing from the characteristics of the critical stresses at the first yield points.

It seems likely that the tuff has a critical stress level for the start of crushing or collapse, e.g. the destruction of the bonds between grains. The critical stresses at the first and second yield points are listed in Table 4.4. From Table 4.4, it is found that for the dry specimens σ_{c1} values are in the range of 0.75-1 MPa, for the saturated specimens, σ_{c1} values are in the range of 0.51-0.67 MPa, and independent of the confining pressures applied. It suggests that the bonds between grains have certain strength that we may call bond strength defined by the σ_{c1} values. Dry Mount Cayley tuff has a bond strength about 0.75-1 MPa and saturated Mount Cayley tuff has a bond strength about 0.5-0.7 MPa. The difference of the σ_{c1} values between dry and wet shows the influence

Table 4.4 Critical Stresses at Yield Points

Specimen	Type of test	Condition	σ_{c1} (kPa)	σ_{c2} (kPa)	σ_3 (kPa)
2.2	Uniaxial	Dry	750	1350	0
2.5	Uniaxial	Dry	875	1250	0
2.6	Uniaxial	Dry	1000	1725	0
2.8	Uniaxial	Dry	950	1575	0
4.9	C-D*	Wet	510	870	200
4.8	C-D	Wet	650	1170	400
4.10	C-D	Wet	650	1200	500
4.6	C-D	Wet	670	1280	650
4.11	C-D	Wet	530	1200	700
4.2	C-D	Wet	660	1530	750
4.3	C-D	Wet	640	1960	850
4.1	C-U*	Wet	600	900	645
4.5	C-U	Wet	540	820	450

σ_{c1} and σ_{c2} are the critical stresses at the first and second yield points respectively.

C-D*-Consolidated and drained triaxial test.

C-U*-Consolidated and undrained triaxial test.

of saturation on bond strength reduction.

Pore Pressure Behaviour

Consolidated and undrained tests were carried out on two saturated specimens prepared from block sample 4. Pore pressures were recorded. The typical results from these tests are shown in Figures 4.22 and 4.23. The stress-strain curves are similar to the stress-strain curves of consolidated and drained tests. The curves are gentle and smooth. Two yield points show up clearly. The interesting point is that pore pressure-strain curve also indicates two yield points obviously. Corresponding to the first portion, the elastic phase, of the stress-strain curves of the consolidated and undrained tests, the pore pressure increases a little. In the second portion, the crushing phase or the collapse stage, the line of pore pressure-strain departs from the initial line. Pore pressure decreases obviously. After passing point B on the stress-strain curve, the pore pressure-strain curve departs again from the previous line and behaves in two ways: still decreasing, but the drop of pore pressure is very small, or increasing a little. Passed peak strength, point C on the stress-strain curves, pore pressure increases gently, when the stress drops to the residual value, pore pressure recovered to the original value. Then pore pressure increases gently, but the value of increase is small.

The departures of the pore pressure-strain curve from previous portions distinctly define two yield points. Pore pressure drop between points A and B probably shows the destruction of the bonds and pores between the grains, the destruction of the natural

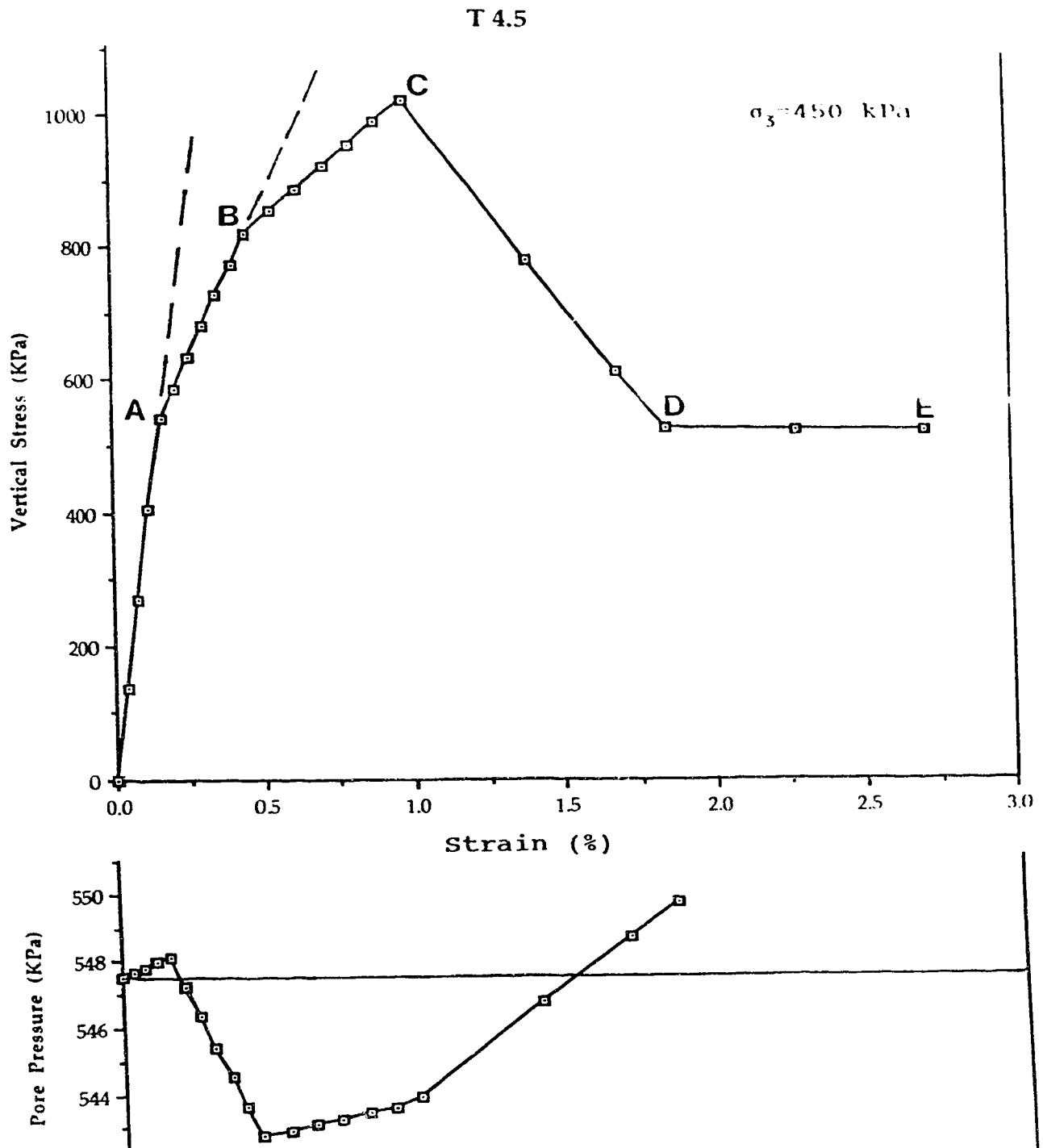


Figure 4.22 Stress-strain and strain-pore pressure curves of saturated tuff, T 4.5, under triaxial compression (consolidated and undrained testing).

T 4.1

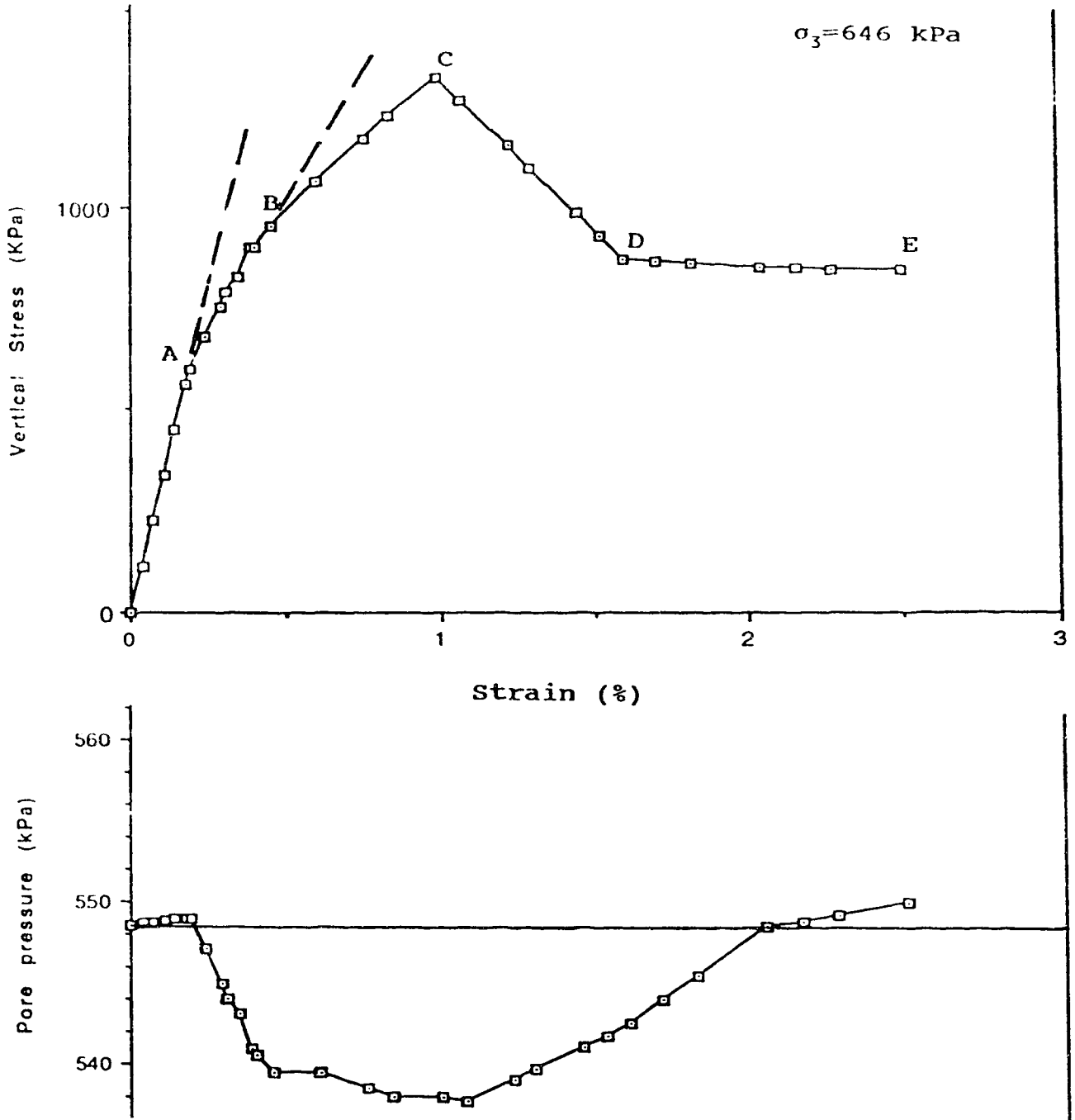


Figure 4.23 Stress-strain and strain-pore pressure curves of saturated tuff, T 4.1, under triaxial compression (consolidated and undrained testing).

structure of tuff.

It is found that the pore pressure behaviour in an undrained triaxial compression test on Mount Cayley tuff shows different characteristics from those of typical hard rocks. The obvious pore pressure drops in Mount Cayley tuff specimens take place at the crushing phase, between the two yield points, differing from the general behaviour of most rocks, the obvious pore pressure drop shows up in shearing phase. As the bonds between the grains are destroyed in the crushing phase, pores become connected in test specimens. So pore pressure drops off obviously. In the shearing phase, phase 3, as most pores in the sheared material have connected or crushed, pore pressure either continuously decreases in a very limited range or recovers a little.

From uniaxial and triaxial tests, the following characteristics of Mount Cayley tuff are recognized.

Mount Cayley tuff has two distinct yield points which indicate the starts of crushing and shearing respectively. The two yield points are defined by the departures from the initial linear elastic portion (for the first yield point) and the previous portion (for the second yield point) of all stress-strain, volume change-strain and pore pressure-strain curves.

The critical stresses, σ_{c1} and σ_{c2} , required for the start of crushing and shearing of dry Mount Cayley tuff are in the range of 0.75-1 MPa and 1.25-1.72 MPa respectively.

Saturation and lateral stress strongly influence the crushing of Mount Cayley tuff. When specimens are saturated and confining

pressure is applied, the stress-strain curves become more gentle and smooth. The first and the second yield points show more distinctly at critical shear stresses.

On p - q diagrams, q_c values at the first yield points are keeping in a certain level, around 0.3 MPa, forming a gently sloping line. It implies that the stress required for crushing is independent of confining pressure, but only depends on the strength of the bonds between the grains. q_c values at the second yield points vary with the change of confining pressure. It indicates that shearing starts at the second yield point and the stress required for shearing is obviously influenced by confining pressure.

Mount Cayley tuff specimens show a rapid drop of strength to the residual value after passing the peak, no matter whether they are d_w or saturated. The peak and residual strengths are determined from consolidated and drained triaxial compression tests. From the k_f line in p - q diagrams, α_f is determined as 26° and d as 189 kPa for peak strength, α_{fr} as 16° and d_r as 62 kPa for residual strength respectively. Φ and c values are determined from Mohr circles and checked by p - q diagrams. $\Phi' = 29^\circ$ and $c' = 216$ kPa for peak, and $\Phi_r = 17^\circ$ and $c_r = 65$ kPa for residual.

The result of consolidated and undrained tests confirm the two yield points. These tests show that pore pressure increases in the elastic deformation stage, decreases in crushing stage and picks up after peak strength. No significant pore pressure was built up during the whole test procedure. The destruction of the natural

structure and the connection of pores of Mount Cayley tuff in the crushing stage may account for the special behaviour of the pore pressure.

4.4 COMPARISON WITH OTHER ROCKS AND SOILS

As mentioned at the beginning of this Chapter, volcanic tuff has received limited attention. The geotechnical properties of volcanic tuff have been studied by Uriel and Serrano (1973), and Uriel (1982) at two dam sites in Spain. The results from this study are similar to the results of those studies. A laboratory programme had also been carried out on the volcanic tuff collected from Chasm Slides, Clinton, British Columbia before this study.

A comparison made in the following section shows interesting results.

Comparison with Chasm Tuff

Three landslide complexes were identified along Chasm Creek, northeast of Clinton, British Columbia (Fig. 4.24). The lower tuff layer contains the rupture surfaces of these landslides. To understand the geotechnical properties of Chasm tuff, block tuff samples were collected from the lower tuff layer in the summer of 1984. A laboratory programme was carried out in 1985. The results show that the geotechnical properties of Chasm tuff are obviously different from those of Mount Cayley tuff.

In the Chasm, Mio-Pliocene volcanic basalt and breccia overlie weakly bonded tuff of the Deadman River Formation. K-Ar ages of the Deadman River Formation reported by Bevier (1981) are in the range of 0.6-19.8 Ma with most dates being in the range of 6-10 Ma. The

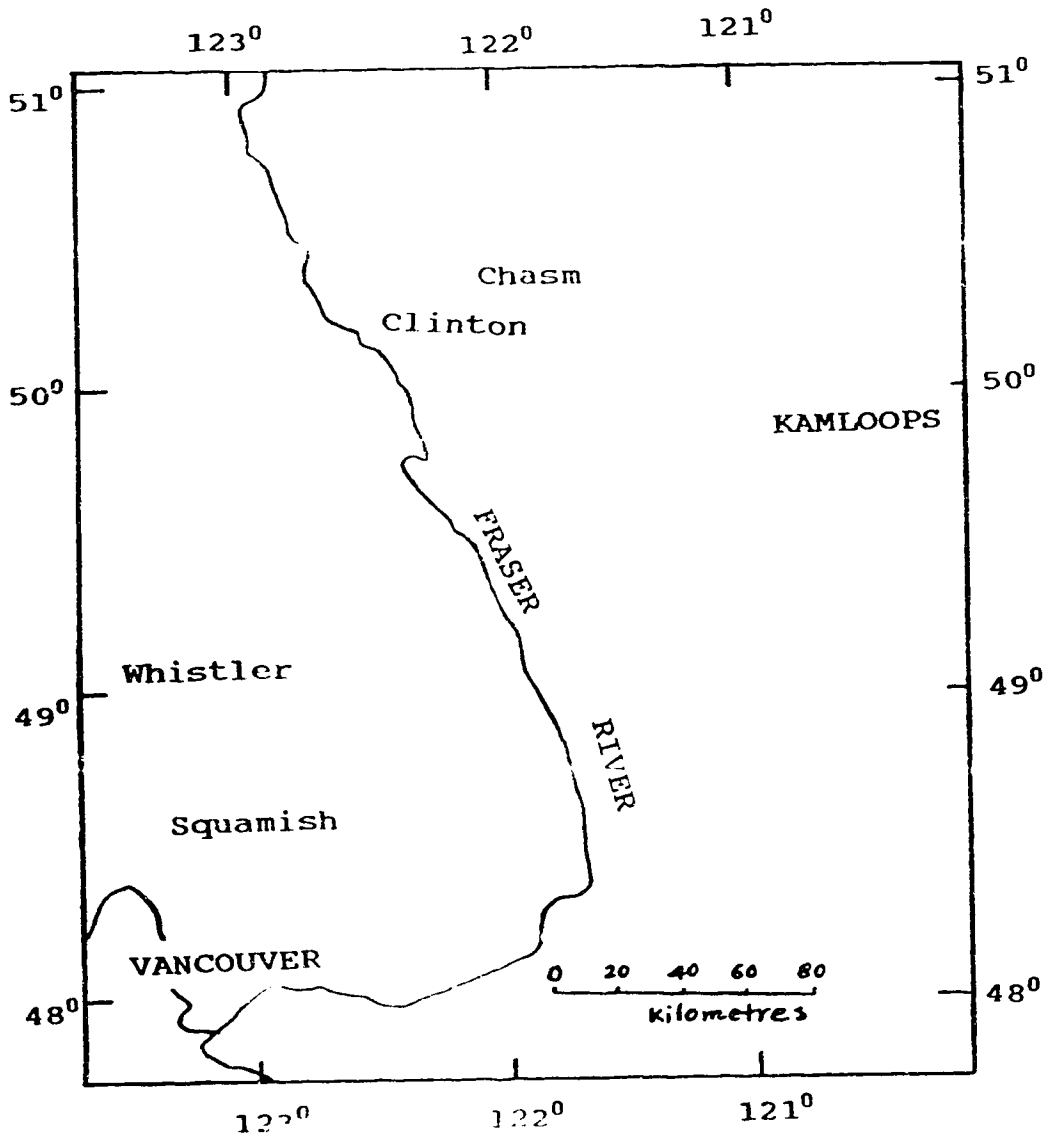


Figure 4.24 Location map of Chasm Slides.

Cenozoic Mount Cayley volcanic rocks have a much younger K-Ar age, in the range of 0.31-3.8 Ma with most dates being less than 2.7 Ma (Green et al 1988).

The basalt and breccia above the lower tuff layer in Chasm has a thickness of 290-350 m giving an approximate overburden pressure of 6 MPa. The breccia and lapilli above the tuff layer constituting the rupture surface of the 1984 rock slide on Mount Cayley have a thickness of 150-160 m giving an approximate overburden of 3 MPa.

The composition of Chasm tuff was estimated under a polarizing microscope. It has a groundmass of 60-70%, and phenocrysts of 30-40%. In the phenocrysts, vitric fragments are dominant, 50%. Other minerals include orthoclase, 20%, plagioclase, 15%, quartz, mica and carbonate, 5-10%, and oxides, 5-10% (Fig. 4.25).

Following Goodman (1989, p. 31), as the dry bulk density, r_{dry} , of Chasm tuff is determined as 15 KN/m^3 , the porosity, n , can be estimated by

$$n=1-r_{dry}/r_w \sum G_i V_i=47\%$$

Where G_i is the specific gravity of component i , V_i is its volume percentage in the solid part of the rock and r_w is unit weight of water.

Assuming the minerals are all orthoclase, the porosity will be 42.2%.

The porosity of Chasm tuff was determined by laboratory test as 37.7-39.4%, which is close to the value, 42.2%, calculated from the assumption of all orthoclase minerals in the rock, and the value, 47%, calculated from the mineral composition estimated from

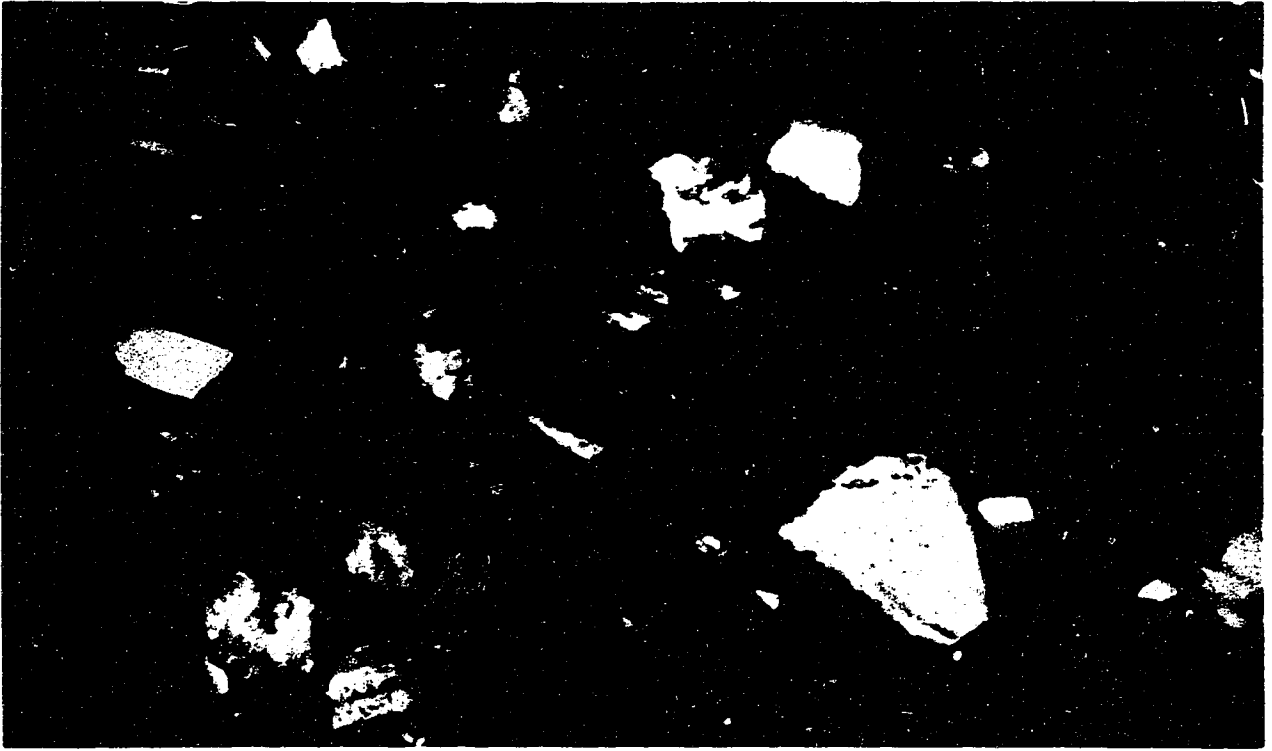


Figure 4.25 A microscopic view (100x) of the composition of Chasm tuff.

porarizing microscope.

It is interesting to note the differences in densities and porosities between Mount Cayley tuff and Chasm tuff. Generally speaking, the rock with a higher density has lower porosity. But Chasm tuff has a higher density, 14.9-15.3 KN/m³, than the Mount Cayley tuff, 13.6 KN/m³, and higher porosity, 37.7-39.4% determined from laboratory tests, than the porosity of Mount Cayley tuff, 35.8% determined from laboratory tests. It is inferred that Mount Cayley tuff has pores which are inaccessible to the porosity measuring methods used and the pores in Chasm tuff are accessible to the porosity measuring methods used. In fact the true porosity of Chasm tuff may be lower than the true porosity of Mount Cayley tuff.

There may be differences in the microstructures of these tuffs. The microstructures of these tuffs were examined by scanning electron micrographs (SEM). Figures 4.4 and 4.26 show typical views of the microstructures of these tuffs. Comparing these figures, it is found that Mount Cayley tuff has more pores, and Chasm tuff has some larger pores. As the overburden of Chasm tuff is much larger than that of Mount Cayley tuff, and the pores are still in good shape after probably 6 million years, it is probably correct to assume that the bonds between the grains in Chasm tuff are stronger than the bonds of Mount Cayley tuff.

Standard slake durability tests were also carried out on Chasm tuff. The Slake Durability Index (SDI) of Chasm tuff after the first cycle is 94% with a standard deviation of 0.6%, and the Slake

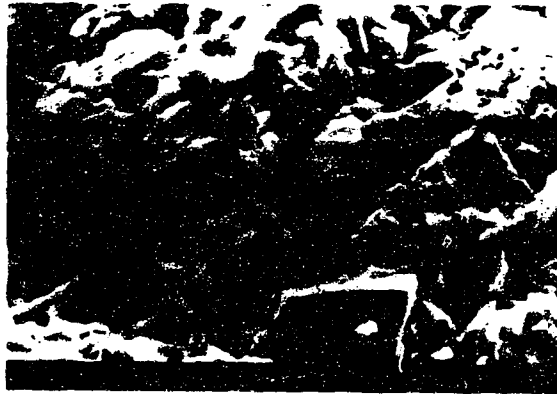


Figure 4.26 Scanning electron micrographs of Chasm tuff.

Durability Index (SDI) after two cycles is determined as 72% with a standard deviation of 0.8%. The Slake Durability Index of Chasm tuff is medium, following Franklin and Chandra (1972), and Gamble (1971), substantially differing from Mount Cayley tuff, very low (Section 4.2, p. 107).

Point load tests were also conducted on Chasm tuff, and unconfined compressive strength, q_u , was estimated from the point load index as in the range of 5.28-6.16 MPa. Following the Geomechanics Classification of Bieniawski (1979), Chasm tuff is between low strength to very low strength. Mount Cayley tuff has similar point load index, from which q_u values were also estimated. As discussed in the previous section, the q_u values of Mount Cayley tuff estimated from point load indexes are much higher than q_u values determined from uniaxial tests.

Figure 4.27 shows a typical stress-strain curve of dry Chasm tuff under uniaxial compression. The curve contains only one yield point (at point A). Comparison with the stress-strain curve of dry Mount Cayley tuff under uniaxial compression shows three major differences. First, Mount Cayley tuff shows two yield points and Chasm tuff, behaving like most rocks has just one yield point. Secondly, Mount Cayley tuff has a much lower uniaxial strength, 1.5-2.4 MPa, Chasm tuff has a higher uniaxial strength, 4.35 MPa. Finally when past the peak strength, Mount Cayley tuff has a very rapid stress drop, Chasm tuff has a relatively gentle stress drop.

Compare the q_u value, 4.25-4.65 MPa, determined from uniaxial tests with the q_u values, 5.28-6.16 MPa, estimated from point load

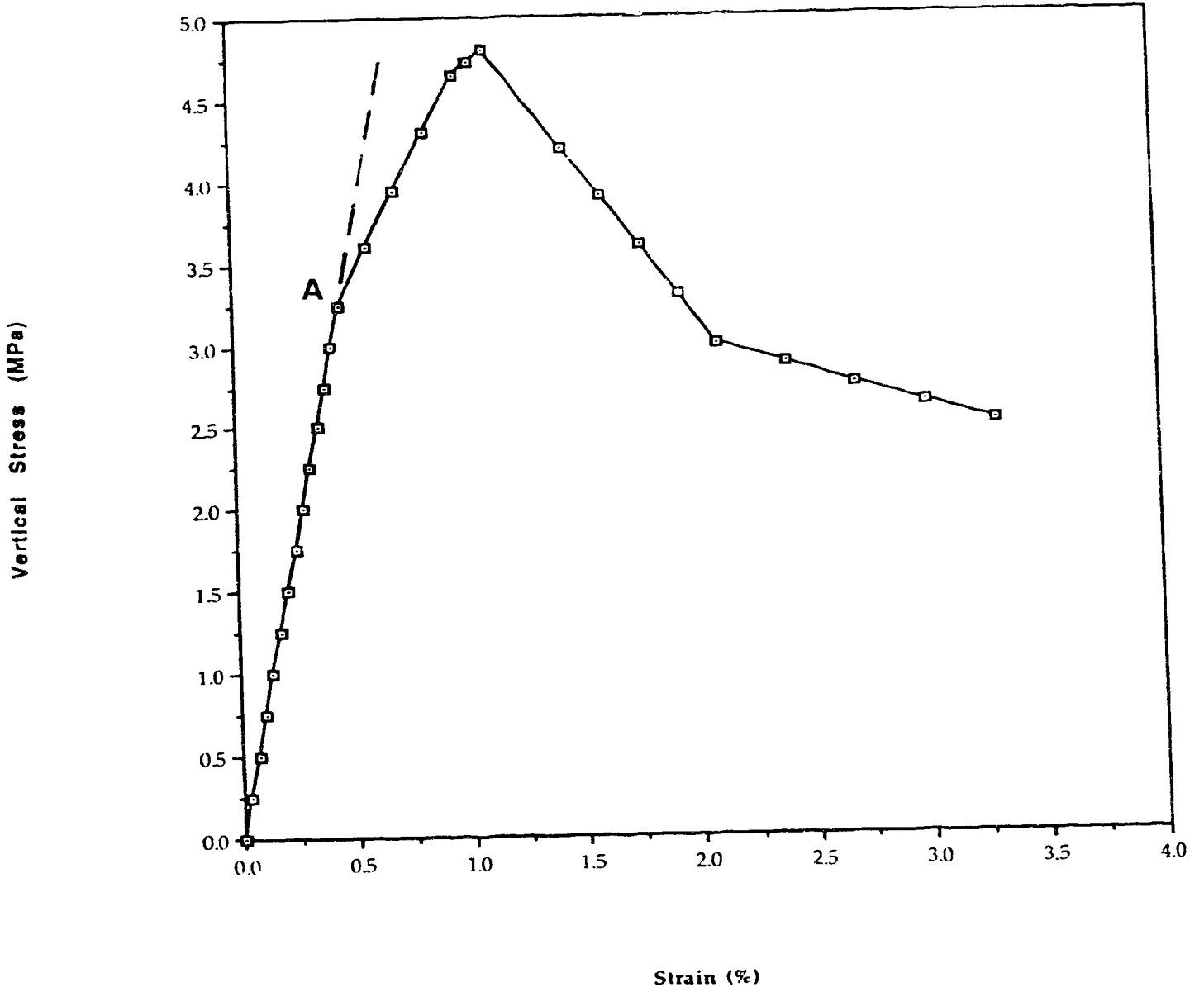


Figure 4.27 Stress-strain curve of dry Chasm tuff under uniaxial compression.

strength index, it is found that for Chasm tuff, these q_u values are close. The difference between them is in the range of 1 MPa. For Mount Cayley tuff, the difference between them, 1.5-2.4 MPa determined from uniaxial tests and 5.37 MPa estimated from point load strength index, are very high. It may suggest that the weaker the rock is, the more inaccurate the q_u value estimated from point load strength index will be.

Figure 4.28 shows a typical stress-strain curve of saturated Chasm tuff under consolidated drained triaxial compression. The curve also contains one yield point. After the peak was passed, the curve drops gently. As mentioned before, two yield points show up more clearly, and the curve becomes more gentle and smooth, but the stress drops rapidly after peak in tests on saturated Mount Cayley tuff under triaxial compression.

The shear strength of Chasm tuff was determined from direct shear tests, tilting table tests and triaxial tests. The friction angle of dry Chasm tuff was determined to be in the range of 30° - 35° . The peak and residual friction angles of wet Chasm tuff were determined to be 28° - 30° and 15° - 17° respectively.

Basic geotechnical properties of Chasm tuff and Mount Cayley tuff are compared in Table 4.5.

Chasm tuff has a higher density and porosity, and much higher uniaxial strength, but little lower friction angle in all aspects (dry peak, wet peak and wet residual) than those Mount Cayley tuff has.

From Fig. 4.28, I_g value of Chasm tuff can be determined as 46%

Z 2.1

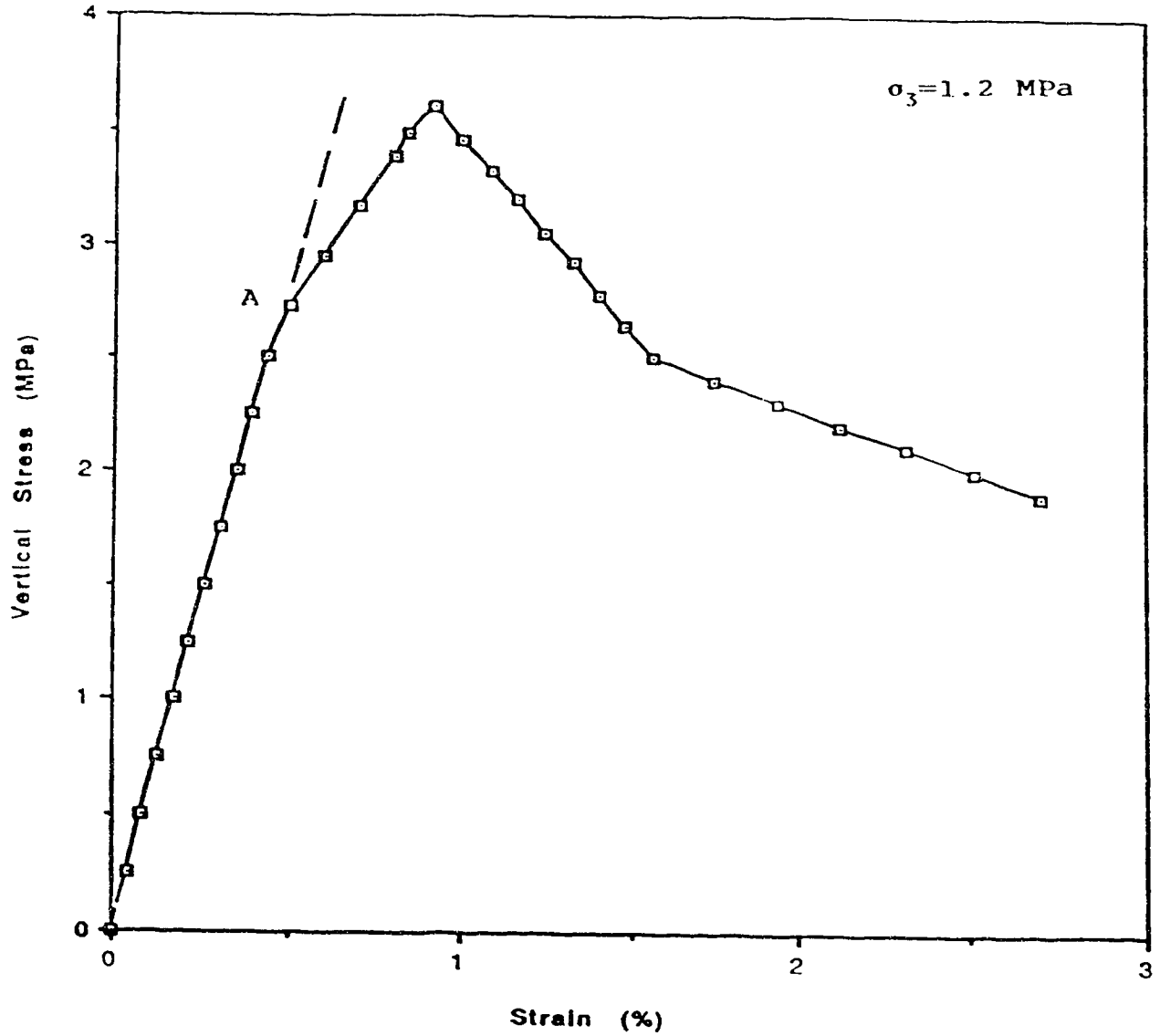


Figure 4.28 Stress-strain curve of saturated Chasm tuff under triaxial compression (consolidated and drained testing).

Table 4.5
Comparison of Geotechnical Properties of
Mount Cayley tuff and Chasm tuff

Sample	r_d (KN/m ³)	n (%)	q_u (MPa)	Φ_{dry} (^o)	Φ_{wet} (^o)	Φ_{wr} (^o)
Chasm tuff	14.9- 15.3	37.7- 39.4	4.25- 4.65	30-35	28-30	15-17
Mount Cayley tuff	14.6- 14.4	31.2- 41.5	1.5-2.4	34-37	29-30	17-20

r_d -Dry bulk density

n-Porosity

q_u -Uniaxial strength

Φ_{dry} -Friction angle of dry specimen

Φ_{wet} -Friction angle of saturated specimen

Φ_{wr} -Ultimate friction angle of saturated specimen

which is much lower than the brittleness index of Mount Cayley tuff. For the dry specimen under uniaxial test, I_{Bdry} is 48%, also much lower than the index of dry Mount Cayley tuff. It is clear that Mount Cayley tuff is much more brittle than Chasm tuff.

Also Chasm tuff has only one yield point. So the bond strength can not be determined. It may be correct to assume that the bond strength of Chasm tuff is not less than the critical stress at the start of shearing, the only yield point shown up. So the value is around 3.3 MPa for dry Chasm tuff and 2.5 MPa for wet tuff. These values are higher than the corresponding bond strengths of Mount Cayley tuff. As the uniaxial strengths of these tuffs are also quite different, it is reasonable to assume that Chasm tuff has stronger bonds between grains and stronger strength because of its heavy overburden over a long period of time, which may cause the volcanic clasts to consolidate. Mount Cayley tuff has a lighter overburden for a short period of time. It may cause the volcanic clasts to be less consolidated. As the bonds between grains of Mount Cayley tuff are extremely weak, Mount Cayley tuff is distinguished from most other tuffs, including Chasm tuff.

Comparison with Canary Islands Volcanic Rocks

Uriel and Serrano (1973), and Uriel (1982) reported the geotechnical properties of volcanic rocks on two dam sites, Arinez dam and Los Campitos dam, in the Canary Islands, Spain. The density of the volcanic rock on Arinez dam is 11.7-14.3 KN/m³, and the density of the volcanic rock on Los Campitos dam is 7.5-10.1 KN/m³. Two yield points were found from triaxial tests. The yielding

pressure of Arinez volcanic rock is 2.6-3.4 MPa, and the yielding pressure of Los Campitos volcanic rock is 1.4-1.8 MPa. From p-q diagrams in their 1973 paper, α_f and d values are determined. For Arinez volcanic rock, $\alpha_f=34^{\circ}$ and $d=110$ kPa. For Los Campitos volcanic rock, $\alpha_f=30^{\circ}$ and $d=20$ kPa. And ϕ and c values were determined from p-q diagrams (Uriel and Serrano 1973, Figs. 9 and 10, p. 4-42, and Uriel 1982, Figs. 18 and 19, p. 72). For the volcanic rock on Arinez dam site, $\phi=42^{\circ}$ and $c=147$ kPa, and for the volcanic rock on Los Campitos dam site, $\phi=35^{\circ}$ and $c=24$ kPa.

Comparing the stress-strain curves of the volcanic rocks on the two dam sites to the stress-strain curves of Mount Cayley tuff, it is recognized that even though both of them have two yield points, Mount Cayley tuff shows two yield points more clearly and the bond strength shown up at the first yield point is much lower than those of the volcanic rocks at these two dam sites. On the other hand, Mount Cayley tuff shows a clear sudden drop of the strength after peak strength. The volcanic rocks on Arinez and Los Campitos dam sites did not show these characteristics. It is also true that the peak shear strength of Mount Cayley tuff is much weaker than those of the volcanic rocks on the two dam sites in Spain. Relatively speaking, the geotechnical properties of Mount Cayley tuff approach those of the volcanic rock on Los Campitos. And the geotechnical properties of Chasm tuff approach those of the volcanic rock on Arinez dam.

It is interesting that Uriel and Serrano also noticed the tendency that within the range of tested consolidation pressure, q_c

values have small variations (1973, p. 262, Fig. 9). It is similar to what we have discussed in the previous section.

Uriel and Serrano (1973) mentioned that on the Arinez dam site the volcanic conglomerate is composed of altered hybrid tuffs of lapilli and cinderite with a sandy and clayey matrix, and on the Los Campitos dam site the volcanic soil is composed of vitric fragments embedded in a great mass of microcrystals of pyroxenes, plagioclases and feldspars with a cement of metahalloysite and montmorillonite and other clayey minerals.

Comparison with Volcanic Tuffs in Italy

Pellegrino (1989) reported the geotechnical properties of the volcanic tuffs in Italy. "The most important features of this rock are the high porosity, 40-60%, and the particular stress-strain behaviour. ... The uniaxial strength of volcanic tuffs of central and southern Italy generally ranges between 2 and 10 MPa. the Mohr envelope is almost linear, with a cohesion of about 0.5-1.5 MPa and a friction angle between 25⁰ and 30⁰."

Comparison of these data with the geotechnical properties of Mount Cayley tuff, shows that Mount Cayley tuff has similar characteristics to the volcanic tuffs in Italy, Mount Cayley tuff has strength at or beyond the lower margin of the strength range of Italian tuffs.

Comparison with Loess

Zur and Wiseman (1973) conducted a laboratory study of collapse phenomena of undisturbed Negev loess and concluded that the loess maintained a quasi-rigid structure even after saturation and the

collapse behaviour depends not only on the increase of the degree of saturation and the mean stress level but on the shear stress level as well. These conclusions are in a good agreement with the results we obtained from the laboratory tests on Mount Cayley tuff.

Comparison with Residual Soils

Vaughan et. al. (1988) conducted a series of laboratory testing on the geotechnical properties of residual soils using artificial material. They found that two yield points are often observed. At some point some of the bonds start to yield, and a first yield point is observed. Thereafter, the average contribution of the bonds to the strength of the soil (the bond strength) decreases with increasing strain. At some point the decreasing bond strength becomes equal to the increasing bond stress, and a second yield occurs. Typically, this is followed by large strains, the progressive loss of the remaining bond strength, and a matching reduction in bond stress, until the soil losses its bonding entirely and become de-structured. The behaviour of Mount Cayley tuff is very similar to the behaviour of residual soils as cited above.

After comparison with Chasm tuff, volcanic rocks on the Arinez and Los Campitos dam sites, volcanic tuffs in Italy, Negev loess and residual soils, it is believed that Mount Cayley tuff is a high porosity, very weakly bonded, soft rock. It shows crushing or collapse behaviour defined by two obvious yield points more clearly than all the materials used in the comparison. The crushing or collapse indicates the destruction of the natural structure of the

rock, destruction of the bonds between grains.

It is specially interesting that two yield points are observed from all three curves: stress-strain, volume change-strain and pore pressure-strain. In other rocks, the second yield point may be not observed, such as Chasm tuff, or may be observed only from stress-strain curves such as the volcanic rocks on two dam sites in the Canary Islands.

When the specimen is saturated and confining pressure is applied, Mount Cayley tuff shows two yield points much more clearly. The critical shear stress required for the start of collapse become more uniform. These behaviours are very similar to loess and most residual soils.

It is believed that Mount Cayley tuff shows geotechnical properties very close to residual soils and loess, but is more weakly bonded than Chasm tuff, and the volcanic rocks on Arinez and Los Campitos dam sites and most of volcanic tuffs in Italy. The geotechnical properties of Mount Cayley tuff have similarities to both soils and rocks, and Mount Cayley tuff is transitional between cemented soil and more common rock types.

4.5 GEOTECHNICAL PROPERTIES AND LANDSLIDES FROM MOUNT CAYLEY

Introduction

The 1963 and the 1984 events highlight the active landslide movements from Mount Cayley. The rock slide and debris flow deposits built up on the Turbid Creek fan tell the history of landslide movement from Mount Cayley after the deposition of the volcanic rocks (Evens and Brooks 1991, Lu 1992). It is believed

that the development of landslides from Mount Cayley depends substantially on the geotechnical properties of the tuff.

Tuffs and Rock Slides

As the studies of the 1963 and the 1984 rock slides pointed out tuff layers constitute the basal rupture zones, the geotechnical properties of tuff and the relationship between tuff properties and rock slides from Mount Cayley have received substantial attention here. The distinct characteristics of Mount Cayley tuff play an important role in the development of rock slides.

Because tuff is relatively impermeable in the volcanic pile, groundwater accumulates at the top of tuff layers, and saturates the tuff layer. The strength of the part of the layer that is saturated decreases substantially. Testing (Section 4.3) shows that especially the cohesion drops to 1/5 or less of its dry value. As creek erosion develops the deviator stress increases at the toe of the slope. These circumstances satisfy conditions required for tuff crushing or collapse: saturation, confining pressure and high shear stress. So the natural structure of tuff is destroyed and the tuff crushes or collapses. When it is fully saturated, tuff lost most of its cohesion, dropping from 1 MPa to 0.22 MPa or less. When the shear stress becomes large enough to overcome the peak strength of wet tuff, then the failure of the slope starts. As the tuff is saturated, its cohesion drops to 0.22 MPa and its friction angle drops to 29-30°. The bedding of the tuff dips at 30-35°. So the rupture surface of the rock slide develops following tuff bedding. A rock slide takes place. After moving a short distance, the

strength of the tuff drops rapidly to its residual value, friction angle of 17° and no cohesion. This process speeds up the rock slide and may contribute to the debris' excess travel.

It is interesting to note that the rock slides from Mount Cayley are naturally divided into two major groups: rock slides developed along the tuff layer at the bottom of unit 4 which may be called Tuff Type, and rock slides developed along the tuff layer at the bottom of unit 2 overlain by dacite mainly which may be called Dacite Type. A small creek erodes into units 4 and 5 first and exposes the tuff layer at the bottom of unit 4 on the creek bank. So a Tuff Type rock slide would occur first. When further erosion develops in the same valley, the tuff layer at the bottom of unit 2 is exposed at the bank. At that time a Dacite Type rock slide would take place.

Both types of rock slide follow the general sequence. Groundwater accumulates at the top of tuff layer. Creek erosion exposes the tuff layer and causes collapse of tuff. Shear stress develops, overcomes the peak strength of tuff and causes failure of the slope. And finally after a short movement the tuff strength drops to the residual value and it speeds up the movement of the rock slide.

Tuffs and Debris Flows

Tuff layers also play important roles in the development of debris flows on Mount Cayley. The Slake Durability Index of Mount Cayley tuff is only 25% (Cruden and Lu 1992, Chapter 2 and this Chapter). This means that after encountering water and agitating

for 20 minutes, 75% of tuff blocks would disintegrate into fine particles. These fine particles may easily mix with water to form a slurry capable of carrying boulders in suspension. So debris flows easily occur under these circumstances on Mount Cayley.

4.6 CONCLUSIONS

The volcanic tuff examined in this research constitutes the basal rupture zones of the 1963 and the 1984 rock slides, and is one of the most important factors in the development of the successive debris flow in the 1984 event. It seems likely that the volcanic tuff also played an important role in the history of landslides from Mount Cayley.

The geotechnical properties of the volcanic tuff on Mount Cayley are determined from laboratory tests. Test results show that the tuff has a low dry density, 13.6 KN/m^3 , high porosity, 35.8%, and very low Slake Durability Index, 25%. The uniaxial compressive strength of dry tuff is determined from uniaxial tests as 1.5-2.4 MPa with an average of 2.1 MPa. As the uniaxial strength determined by point load strength index method is 5.37 MPa, it is believed that the point load method may be not suitable for this kind of very soft rock.

The following distinct geotechnical behaviours of the tuff under uniaxial and triaxial compressive stress are also recognized. The tuff has two distinct yield points which define the starts of crushing and shearing at increasing stress levels. These yield points can be easily recognized from stress-strain, volume change-strain and pore pressure-strain curves. The critical stresses, σ_{c1}

and σ_{c2} , required for the starts of crushing and shearing of dry tuff are in the range of 0.75-1 MPa and 1.25-1.72 MPa respectively. When specimens are saturated and confining pressure is applied, the stress-strain curves become more gentle and smooth. Two yield points show up at certain shear stresses more distinctively. And q_c values on p-q diagram at the first yield point become steady as around 0.3 MPa. The tuff specimens show a rapid drop of the strength to the ultimate value after passing the peak, no matter they are dry or saturated. The peak and residual shear strengths of saturated tuff are $\phi'=29^0$ and $c'=216$ kPa, and $\phi_r=17^0$ and $c=65$ kPa respectively.

It is believed that after the initiation of shearing, the behaviour of the specimens is almost the same as dense sand except for the abnormal abrupt drop of stress after peak.

Comparing the geotechnical properties of Mount Cayley tuff with some other materials, such as Chasm tuff, volcanic rocks in the Canary Islands, volcanic tuffs in Italy, Negev loess and residual soils, it is found that Mount Cayley tuff is a highly porous, and weakly bonded soft rock. Its crushing is even more distinct than all materials used for comparison. The geotechnical properties of Mount Cayley tuff are quite close to those of loess and residual soils. It is believed that Mount Cayley tuff is transitional between soil and common rock types.

These geotechnical properties play an important role in the development of landslides on Mount Cayley. As the tuff is relatively impermeable in the volcanic pile, groundwater will

accumulate on the top of the tuff and saturate it. Creek erosion will induce the developing of shear stress on the slope. So when the tuff layer is exposed at the toe of the slope, tuff will start to collapse, and collapse will propagate deeply into the slope. After the tuff completely collapsed, and the tuff is fully saturated, the cohesion will drop from 1 MPa to 0.22 MPa or less and the friction angle will drop to $29-30^{\circ}$, less than the dip of tuff bedding. At that time the slope begins to fail and a rock slide occurs. After a short movement, the tuff strength drops to the residual value. This process may speed up the movement of the rock slide and partly cause the debris to travel an excess distance.

As after encountering water and agitating for 20 minutes 75% of the tuff disintegrates into fine particles, and these fine particles may easily mix with water to form a slurry capable of carrying boulders in suspension, debris flows occur on Mount Cayley often.

5 COMPARISON OF THE 1984 AND THE 1963 EVENTS

5.1 INTRODUCTION

Two major historic slope movement events, the 1963 rock slide, and the 1984 rock slide and debris flow, and prehistoric slope movements from Mount Cayley, British Columbia have attracted extensive attention (Clague and Souther 1982, Jordan 1987, Evans and Brooks 1991, Brooks and Hickin 1991, Cruden and Lu 1989, 1992, and Lu 1988). But no attempt has been made so far to distinguish the differences among them and to use their distinct characteristics to set up modes of landslides for further research on rock slides and debris flows from Mount Cayley. This Chapter makes an attempt to compare these events and define the major modes of slope movement from Mount Cayley and their main characteristics.

As the major characteristics of prehistoric slope movement deposits will be discussed in the following Chapter, and the characteristics of the 1963 and the 1984 events were studied in detail in Cruden and Lu (1992) and previous Chapters, the main aim of this Chapter is to compare these two major events and to set up types of slope movement from Mount Cayley for landslide prediction.

The depletion zones of two major historic slope movement events, the 1963 rock slide, and the 1984 rock slide and debris flow, from Mount Cayley are closely located in a small area. Figure 5.1 shows the depletion zones of these two events. The horizontal distance between these depletion zones is about 0.8 km. The 1963 rock slide, and the 1984 rock slide and debris flow started from the heads of two small tributaries, Dusty and Avalanche Creeks, of



Figure 5.1 Depletion zones of the 1963 and the 1984 events, taken from a helicopter in the summer of 1985 looking NE. Note that Avalanche Creek, Dusty Creek and Turbid Creek are represented by A, D and T respectively, and L₁ and L₂ indicate the depletion zones of the 1963 rock slide and the 1984 rock slide respectively.

Turbid Creek, one of the main creeks draining Mount Cayley and a tributary of the Squamish River.

The 1963 and the 1984 events are typical examples of two modes of slope movements on Mount Cayley. These two types informally called Tuff Type and Dacite Type, are useful modes of the prehistoric landslide deposits and interpretation of prehistoric events, and in landslide prediction in this area.

5.2 COMPARISON OF DEPLETION ZONE AND MAIN TRACK

The depletion zones of the 1963 rock slide and the 1984 rock slide are very close, but they have a major difference. The volcanic rocks exposed in the depletion zones are different. Only units 2 and 3 of the volcanic rocks on Mount Cayley were involved in the 1963 rock slide, and only units 4 and 5 were involved in the 1984 rock slide. Units 2 and 3 consist mainly of columnar-jointed dacite, and units 4 and 5 consist mainly of purple tuff breccia, tuff lapilli and soft tuff, and light yellow hard tuff. These rocks have different strengths (Table 3.1).

Thick dacite beds in Members 2 and 4 (Fig. 3.5) acted in the 1963 rock slide so that the displaced mass behaved as 3 cohesive units. There were three separate blocks in the depletion zone of the 1963 rock slide. The ridge which formed block 1 was divided from the ridge forming blocks 2 and 3 by a small creek (Fig. 3.4).

In units 4 and 5, there is one thick dacite layer in Member 6 (Fig. 3.5), so the displaced rock mass in the 1984 event behaved as a single block of weak and loose rocks.

The main track "... is the commonly scoured, original ground

surface over which the debris flow/avalanche descends the slope, with gradually increasing velocity to a terminal velocity dependent on steepness, channel width, and effective viscosity of the flowing mass. Frictional contact between the flow and slope surface allows the debris flow/avalanche to scour vegetation and the upper few to tens of centimetres of colluvium from the slope. As the flow incorporates additional mass, the momentum of the flow increases along the main track." (Baldwin and others 1987, p.225).

The main tracks of both the 1963 and the 1984 rock slides are distinct. The rock slides left high forest trimlines on the both sides of the creeks without disturbing large volumes of materials. In the main track of the 1963 event, there was no snow and ice accumulation on the bottom of Dusty Creek. In contrast, Avalanche Creek was covered by snow and ice with an average thickness of 15 m (Fig. 2.10) in July and August, 1986 and 1989, because the creek is in the shadow of both the steep slopes of the creek, and the wide bottom of the creek traps and preserves snow blown from the surrounding mountain ridges.

The 1984 rock slide travelled on the main track, the wide bottom of Avalanche Creek covered by a thick layer of snow and ice. The displaced rock mass dug out substantial ice blocks from the bottom of the creek and carried these ice blocks until coming to stop at the confluence of Turbid and Avalanche Creeks forming a debris dam containing 85% broken rock mass and 15% ice blocks.

These basic differences, different rock units with or without ice blocks in the displaced rock masses, lead to a series of

differences in the performances of the two events.

As the first result of these differences, the 1963 event was a rock slide. It contained three blocks which moved in coherent units resulting in distinct layers in the displaced mass which follow the bedrock sequences.

At the beginning, the 1984 event was a rock slide too. But the displaced mass was so broken that its deposits have no distinct layers and are very loose.

5.3 COMPARISON OF TRAVEL DISTANCE, ANGLE AND VELOCITY

As the 1963 rock slide slid in three blocks, one after another, the debris deposited around the confluence of Dusty and Turbid Creeks in three blocks also.

The 1984 rock slide moved as a single block but had three stages, rock slide, debris dam and debris flow. The rock slide debris deposited around the confluence of Avalanche and Turbid Creeks dammed Turbid Creek, and the successive debris flow deposited along the valley of Turbid Creek and entered the Squamish River.

The 1963 and the 1984 rock slides have different volumes, travel distances (from the crown of the block pre-slide to the tip of the block post-slide), and angles. These two rock slides also have different junction angles between the contributing and the receiving channels. These data are listed in Table 3.2.

Block 1 of the 1963 rock slide has a volume of $2.7 \times 10^6 \text{ m}^3$. It is almost the same as the volume of the 1984 rock slide. But the 1984 rock slide travelled 2000 m before it stopped, and Block 1 of

the 1963 rock slide travelled just 1600 m. Their junction angles between contributing and receiving channels are almost the same (60-75°). So the major cause for that difference may be the ice cover over Avalanche Creek. The 15 m thick ice cover would facilitate the rock mass mobility. And as no ice had accumulated in the open valley of Dusty Creek, Block 1 of the 1963 rock slide travelled less.

The travel distance of Block 2 is 400 m longer than that of the 1984 rock slide, probably a result of the different junction angles. Block 2 has a much lower junction angle than those of Block 1, Block 3 and the 1984 rock slide (Table 3.2). With a junction angle of 50-60°, Block 3 just travelled 1800 m, probably because the rock fragment flow encountered substantial resistance from the deposits of Blocks 1 and 2, and the opposite valley wall of Turbid Creek when it moved into Turbid Creek.

The velocity of the 1963 rock slide was determined from superelevation at site 61 to be 26 m/s (Chapter 3). The velocity of the 1984 rock slide was determined from run up at the confluence of Avalanche and Turbid Creeks to be 35 m/s (Cruden and Lu 1992). The velocity of the 1984 debris flow was determined from superelevation, mud spatters on trees, uprooted trees, airborne wood splinters and deposits on both sides of Dusty Creek in the range of 21-34 m/s (Cruden and Lu 1992).

The 1984 rock slide moved more quickly than the 1963 rock slide probably because of the ice cover in the movement path in Avalanche Creek and the higher elevation of the depletion zone, the 1984 rock

slide started from elevation 1600 m and the 1963 rock slide started from elevation 1450 m.

5.4 COMPARISON OF DEPOSITS

The deposits of the 1963 rock slide and the 1984 rock slide have a series of different characteristics, different geometry, different structures and different grain size distributions. Also the fines in these deposits show different plasticities.

Geometry

The deposits of the 1963 rock slide accumulated in an elongate area extending 1000 m along the valley of Turbid Creek between the pre-slide and present mouths of Dusty Creek. The deposits form a 1000 m long terrace which dammed Turbid Creek and Dusty Creek with a maximum width of 160 m and a maximum thickness of 60 m. The deposits of the 1963 rock slide form three major blocks and show distinct layers which kept the order of the rock sequences in the depletion zone.

The deposits of the 1984 rock slide accumulated around the confluence of Avalanche and Turbid Creeks forming a single block dam. The deposits extend 500 m along the valley of Turbid Creek with an average width of 110 m and a maximum thickness of 70 m. Most deposits of the 1984 rock slide were removed by the succeeding debris flow. The remnants formed terraces, but show no distinct layers.

The deposits of the 1984 debris flow blanketed the whole valley of Turbid Creek. So the 1984 debris flow deposits can be seen on the slopes, at the top of the terrace formed by the 1963 rock slide

deposits, and at the bottom of the creek. The maximum thickness of the 1984 debris flow deposits is only 20 m, but the deposits extend to 45 m above the thalweg of Turbid Creek. The debris flow deposits thin downstream. Below the confluence with Dusty Creek, the deposits are confined to the valley of Turbid Creek. The area blanketed by the debris flow deposits extended 4.8 km along Turbid Creek till it entered the Squamish River.

Structure

The deposits of the 1963 rock slide came from units 2 and 3 of the volcanic rocks on Mount Cayley. These deposits show distinct layers keeping the relative sequence of the parent rocks which can be traced back to the depletion zone. The deposits of the 1984 rock slide came from units 4 and 5 of the volcanic rocks on Mount Cayley, showing distinct colours-purple and light yellow. The 1984 deposits do not have any layers, and the rock mass was totally broken. The particles from the broken layers with different colours and lithologies were totally mixed. The 1984 debris flow deposits show distinct characteristics which are totally different from the 1984 rock slide and the 1963 rock slide deposits. In the 1984 debris flow deposits, about 25% of the boulders and blocks were entrained from earlier deposits, the boulders and blocks of the basement rocks, such as granodiorite, quartz diorite and gneiss are particularly noticeable (Fig. 5.2). The 1984 debris flow deposits do not have any layers, but have distinct mud films on the surface of the boulders, and small particles stuck on the surface of the boulders and blocks seated on the top surface of the deposits. The

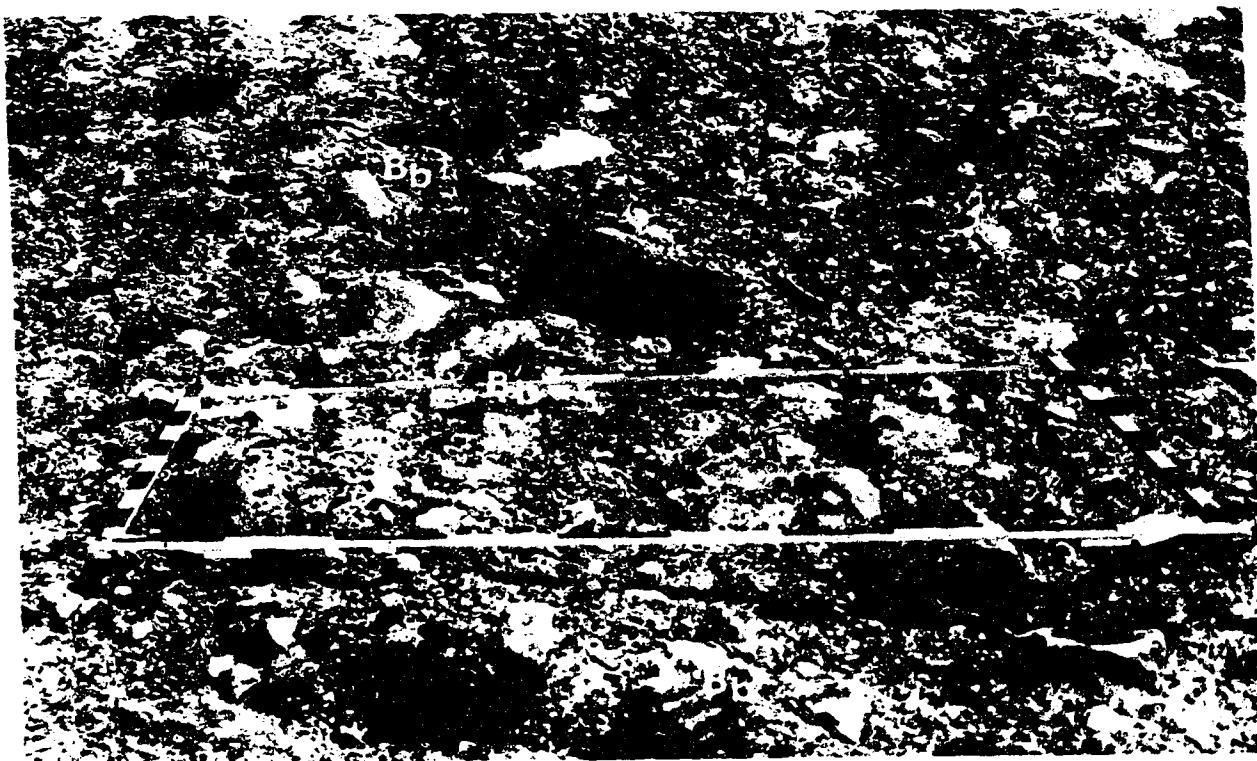


Figure 5.2 Components of the 1984 debris flow deposits. Note that it contains some blocks of basement rocks, B_p . The frame, 2x2 m, gives scale.

particles in the 1984 debris flow deposits from different sources were totally mixed.

Grain Size Distribution

Typical grain size distribution curves of the 1963 rock slide, the 1984 rock slide and the 1984 debris flow deposits can be found in previous Chapters (Chapter 3, Fig. 3.10 and Chapter 2, Fig. 2.3). D50 values of these deposits are listed in Table 5.1. All these deposits are ungraded.

The average value of D50 of the 1963 rock slide deposits, 36 mm, is much higher than that of the 1984 rock slide deposits. It is caused by the different movement patterns of the different rock types involved in these two events. First, a lot of columnar-jointed dacite was involved in the 1963 rock slide. And a lot of tuff breccia, tuff lapilli and hard tuff were involved in the 1984 rock slide. Tuff breccia, tuff lapilli and hard tuff are more easily broken than dacite. Secondly, the 1963 rock slide mainly moved in a laminar way, the deposits keeping the relative sequence of the parent bedrock, so that the sliding rock mass was just partly broken. The 1984 rock slide moved in a turbulent way, the deposits not keeping any layer features or the sequence of the parent bedrock, so that the sliding rock mass was totally broken.

Plasticity

It is interesting to note a special difference between the 1963 rock slide and the 1984 rock slide and debris flow deposits. The plasticity test results show the fines from the samples of the 1984 rock slide and the 1984 debris flow deposits are all plastic. The

Table 5.1
D50 Values

Item	b	c	d	e	f	g	A*	B*	C*
D50	33	3.6	70	1.56	105	1.5	5	1.6	35
Year	1963	1963	1963	1963	1963	1963	1984	1984	1984

b, c, d, e, f and g-Layers b, c, d, e, f and g in the deposits of the 1963 rock slide.

A*-The 1984 rock slide deposits.

B*-Subsurface deposits of the 1984 debris flow.

C*-Surface deposits of the 1984 debris flow.

plasticity index of the 1984 deposits is in the range of 4-8. All fines from the samples of the 1963 rock slide deposits are non-plastic (Chapter 3, p87 and Chapter 2, Table 2.1).

Water Involvement

It is clear that no water was involved in the 1963 rock slide. So soft tuff blocks in these deposits have not collapsed or disintegrated. They still retain angular shapes. Very little water was involved in the 1984 rock slide, as angular soft tuff blocks and clean breccia, lapilli and hard tuff blocks and boulders without any mud films or mud and small particles stuck on their surfaces can be seen everywhere at the landslide dam remnants. But a lot of water was involved in the 1984 debris flow, signs of fluid transport can be seen in the 1984 debris flow deposits; soft tuff blocks have totally collapsed or disintegrated, mud films around boulders and mud and small particles stuck on the surfaces of the boulders have also been found everywhere. The high mud spatters on trees give another clue of water involvement in the 1984 debris flow.

The major differences among the 1963 rock slide, the 1984 rock slide and the 1984 debris flow deposits are summarized in Table 5.2.

5.5 COMPARISON OF DAMS

The 1963 rock slide blocked Dusty and Turbid Creeks. The deposits formed a combined dam in Turbid Creek. This dam has a width of 1000 m along the valley of Turbid Creek, a maximum length of 160 m normal to the creek and a maximum height of 60 m. Also the

Table 5.2

Comparison of the Deposits of the 1963 and the 1984 Events

Deposits	1963 slide	1984 slide	1984 flow
Geometry	Three blocks	One block	A blanket
Material	Mainly dacite and some tuff from Units 2 & 3	Mainly tuff lapilli, tuff breccia and tuff from Units 4 and 5	Mainly tuff lapilli and tuff breccia 25% previous creek deposits and boulders of basement rock.
Structure	Partly broken. Layers keeping sequence of parent rock.	Totally broken and disturbed. No layers.	Totally stirred. No layers.
D50 value (mm)	1.5-105 mean=36	5	35 (surface) 1.6 (subsurface)
Plasticity	Non-plastic	Plastic	Plastic
Water involvement	No	No	Obvious

1963 rock slide has three lobes (three separate blocks) formed three dams bounded by gullies in the valley of Turbid Creek (Fig. 3.11).

The 1963 rock slide dam belongs to Type 5 dams, which "form when the same landslide has multiple lobes of debris that extend across the valley floor and form two or more landslide dams in the same reach of river." (Costa and Schuster 1988, p.1057)

The 1984 rock slide blocked Avalanche and Turbid Creeks. The deposits formed a dam in Turbid Creek. This dam has a width of 500 m along Turbid Creek, a length of 100-120 m and a height of 70 m. This natural dam belongs to Type 3 dams, which "fill the valley from side to side, move considerable distances upvalley and downvalley from the failure and typically involve the largest volume of landslide material." (Costa and Schuster 1988, p.1057)

The 1984 rock slide dam lasted for one or two days and burst rapidly. So debris flow surges formed. The main part of the dam consisting of loose debris and ice blocks was carried away by the debris flow. The debris flow damaged the logging road and the bridge at the mouth of Turbid Creek (Cruden and Lu 1992). The 1963 rock slide dam lasted for a long period of time, as the records of the damage on the logging road bridge at the mouth of Turbid Creek indicated that there was no debris flow damage to the bridge from 1961 to 1966. As the narrow stream channel that Turbid Creek cut into the 1963 deposits can still be seen, it is inferred that the dam was overtopped and eroded, but the main part of the dam is still standing which indicates that no catastrophic burst happened.

Several factors " that are relevant to natural stability (of landslide dams) are size, geometry, and material characteristics of the blockage; slow rates of inflow to the impoundment; and bedrock controls.... The most important characteristic of a dam in preventing failure is resistance to erosion, either at the surface of the dam as it overtops or internally due to seepage..... In general, materials consisting of large particles are more resistant than those made up of smaller sizes, and well-graded materials are more stable than those that are uniform or gap-graded. " (Schuster and Costa, 1986 p. 11).

For the 1963 and the 1984 events, the rates of inflow to the impoundments and the bedrock controls are almost the same (Table 5.3). Even though the dams have some differences in the size and the geometry (Table 5.3), the most important difference between these dams is the material characteristics. The 1984 rock slide deposits are very loose (Cruden and Lu 1992). The resistance of the 1984 rock slide deposits to erosion is very low. Also the ice blocks in the dam substantially weakened the dam resistance to the erosion. So the dam collapsed in a short period of time after it formed. The 1963 rock slide deposits are much denser and coarser, and kept the relative sequence of the volcanic rocks. Moreover, the 1963 rock slide deposits are mainly columnar jointed dacite which is just partly broken. These deposits have much stronger resistance to erosion than the 1984 rock slide deposits which consist of mainly tuff breccia, lapilli and tuff. So the 1963 dams did not burst after a long period of time.

The major characteristics of these two debris dams are summarized in Table 5.3.

5.6 COMPARISON OF IMPACT ON ENVIRONMENT

The 1963 and the 1984 events have significant impacts on the environment, but they show different characteristics.

The 1963 rock slide diverted Turbid Creek 200 m westwards, shifted the confluence of Dusty and Turbid Creeks 1 km downstream and brought millions of cubic metres of debris into the valley of Turbid Creek. As the rock slide stopped at the new confluence of Turbid and Dusty Creeks, about 3 km upstream from the mouth of Turbid Creek, there was no direct influence on the Squamish River.

The 1984 rock slide and debris flow introduced sufficient sediment into Turbid Creek and the Squamish River, to cause significant channel change in the Squamish River (Evans 1987, Jordan 1987, Hickin and Sichingabula 1988, Cruden and Lu 1989, Cruden and Lu 1992). The debris flow damaged the logging road and bridge at the mouth of Turbid Creek.

The main differences between the 1963 rock slide and the 1984 rock slide are summarized in Table 5.4.

The 1963 rock slide moved in coherent units resulting in some distinct layers in the displaced mass which retain the bedrock sequences. The displaced mass of the rock slide is only partly broken, and more or less shows laminar flow characteristics.

The 1984 rock slide moved in a turbulent way. The displaced mass is broken, the deposits show no distinct layers and the original rock sequences are totally disturbed.

Table 5.3

Comparison of the 1963 and the 1984 Dams

Dam	1963	1984
Dimension (m)	W=1000, L=120, H=60	W=500, L=100-120, H=70
Material	Partly broken, Units 2 and 3. Mainly cracked dacite and some tuff. No ice.	Totally broken, Units 4 and 5. Mainly soft tuff, hard tuff, breccia and lapilli. 25% of ice blocks.
Rate of inflow	1.2 m ³ /s	1 m ³ /s
Bedrock control	Basement rock	Basement rock
Type of dam	5	3
Last of dam	After a long period of time (at least for the first three years), no catastrophic burst. Overtopped and eroded. Main part of the dam remained.	In 1 or 2 days rapidly burst caused a debris flow downstream. Just very small parts of the dam remained.

L-Length measured perpendicular to the flow direction
W-Width measured parallel to the flow direction
H-Thickness

Table 5.4

Summary of the Comparison of the two events

Item	1963 rock slide	1984 rock slide
Rocks involved	Units 2 & 3, mainly dacite	Units 4 & 5, mainly tuff, breccia and lapilli
Ice in main track	No	Yes, 15 m thick
Stages	3, slide, fragment flow and landslide dam	3, slide, landslide dam and debris flow
Rock slide	3 blocks	1 block
Fragment flow	Laminar	Turbulent
Velocity	26 m/s	35 m/s
Travel distance	2.4 km	2 km
Landslide dam	Type 5. No catastrophic burst. Overtopped and eroded. Main part remained so far.	Type 3. Only lasted 1-2 days before burst. Very small part remained.
Deposits	Three separate blocks with distinct layers keeping parent bedrock sequence	One block. Totally broken. Without layers.
D50 (mm)	Larger than 10	Less than 5
Successive debris flow	No	Yes. Debris flowed downstream at a velocity of 21-34 m/s for 4.8 km. Its deposits blanket the valley of Turbid Creek.
Impact on environment	Turbid Creek diverted 200 m westwards, mouth of Dusty Creek shifted 1 km downstream	Introduced sufficient sediment into Squamish River and caused significant channel change
Type of slope movement	Dacite Type rock slide	Tuff Type rock slide

Hendersor. (1966, p14) pointed out "In laminar flow the exchange of material and momentum occurs on a microscopic scale through the random movement of molecules, ... In turbulent flow, momentum exchange alone is the basis of shear resistance; it occurs on a macroscopic scale, being caused by random fluctuations in velocity which are continually sending fluid particles back and forth between adjacent layers."

The structure of the 1963 rock slide deposits implies that the exchange of material and momentum occurred on a microscopic scale so that the original layers and the sequence of the parent rocks can be kept in the deposits. So it is inferred that the 1963 rock slide moved in a laminar way.

The structures of the 1984 rock slide deposits and the 1984 debris flow deposits imply that the exchange of material and momentum occurred on a macroscopic scale so that the particles are totally mixed. So it is inferred that the 1984 rock slide and the 1984 debris flow moved in a turbulent way.

Chow (1959, p7-8) pointed out "The flow is laminar if the viscous forces are so strong relative to the inertial forces that viscosity plays a significant part in determining flow behaviour. The flow is turbulent if the viscous forces are weak relative to the inertial forces. The effect of viscosity relative to inertial can be represented by the Reynolds number, R_e , defined as

$$R_e = \rho_w VR / \mu$$

Where ρ_w is the density of water,

V is the velocity of flow,

R is the hydraulic radius of the channel and
 μ is dynamic viscosity.

An open-channel flow is laminar if the Reynolds number R_e is small and turbulent if R_e is large, 500 or above."

We can estimate ρ_w , V and R values of the 1963 rock slide flow, the 1984 rock slide flow and the 1984 debris flow. Even though the dynamic viscosity of these flows cannot be determined, we know that in the 1984 rock slide flow there was some water, snow and ice involved and in the 1984 debris flow there was substantial water involved, but there was little or almost no water involved in the 1963 rock slide flow. So the dynamic viscosities of these flows are different: the 1984 debris flow's was the lowest, the 1963 rock slide flow's was the highest.

As $\rho_w=1 \times 9.81 \text{ KN/m}^3$, the velocities of the 1963 rock slide flow, V_{1963} , the 1984 rock slide flow, V_{1984R} , and the 1984 debris flow, V_{1984D} , are 26 m/s, 35 m/s and 34 m/s, and the hydraulic radii of the channels of the 1963 rock slide flow, the 1984 rock slide flow and the 1984 debris flow, R_{1963} , R_{1984R} , and R_{1984D} , are 20 m, 30 m and 20 m respectively, assume the dynamic viscosities of these flows are $\mu_{1963}=2 \times 9.81 \text{ KN/m.s}$, $\mu_{1984R}=(1.5-2) \times 9.81 \text{ KN/m.s}$ and $\mu_{1984D}=(1.2-1.3) \times 9.81 \text{ KN/m.s}$, based on the dynamic viscosities of water, $1.08 \times 9.81 \text{ KN/m.s}$, and dry flow, $(2-2.5) \times 9.81 \text{ KN/m.s}$, the following values can be obtained:

$R_{e1963}=260$, less than 500, so the 1963 rock slide flow is a laminar flow,

$R_{e1984R}=520-700$, larger than 500, so the 1984 rock slide flow is

a turbulent flow, and

$R_{e1984D} = 523-567$, larger than 500, so the 1984 debris flow is a turbulent flow.

Comparing the assumed dynamic viscosities of these flows to D50 values of their deposits listed in Table 5.1, it is found that the viscosity is in a reverse correlation with D50 values. For example, the average value of D50 of the 1963 rock slide deposits is 36 mm, much higher than that of the 1984 rock slide deposits, 5 mm, and much much higher than that of the 1984 debris flow deposits, 1.6 mm.

These events have such different behaviours because the rocks involved have very different properties. The 1963 rock slide involved units 2 and 3 of the volcanic rocks, which are mainly thick, columnar-jointed dacite. These rocks have higher strength than the rocks in units 4 and 5 (Table 3.1). So the sliding body could move in coherent layers which still kept the order of the rock sequences, when it deposited. The 1984 event involved units 4 and 5. They mainly consist of tuff lapilli, tuff breccia and tuff. As these rocks have very low slake durability (Cruden and Lu 1992), they are easily broken and disintegrated. They could not keep the order of rock sequences. So no distinct layers can be seen in the deposits. Also the debris dams consisting of totally broken debris were easily burst. So debris flows could form.

The difference in parent rocks also resulted in the different characteristics of their deposits. Among them, the difference in the grain size distribution, especially the D50 value, is

meaningful. The 1963 rock slide deposits have a D50 values above 10 mm in average. Both the 1984 rock slide and the debris flow deposits have D50 values below 5 mm.

The snow and ice accumulated in Avalanche Creek may have facilitated the movement of the rock slide and the later breaking of the landslide dam.

Two different modes of slope movement can be determined from this comparison. The 1984 and the 1963 events are two good examples leading to set up two modes of slope movement on Mount Cayley: Tuff Type and Dacite Type.

Tuff Type rock slides take place in units 4 and 5 of the volcanic rocks on Mount Cayley, mainly containing purple tuff breccia and tuff lapilli, white to grey soft tuff, and light yellow hard tuff. This type of rock slide has deposits without any layering features, and has low D50 value, less than 5 mm. As they are formed by totally broken loose and weak material, these landslide dams can just last for a short period time. And successive debris flows may probably form after the bursts of these dams.

Dacite Type rock slides take place in units 2 and 3 of the volcanic rocks, mainly containing brown dacite and some soft tuff. This type of rock slide has deposits just partly broken resulting in distinct layers which keep the bedrock sequences in the depletion zone, and has high D50 values, larger than 10 mm. As they are formed by partly broken rock mass and large dacite boulders, the landslide dams may last longer. Generally, no successive debris

flows occur in this type of events.

5.7 CONCLUSIONS

The 1963 rock slide, and the 1984 rock slide and its successive debris flow show a series of different characteristics. The depletion zone of the 1963 rock slide contained three separate blocks showing two ridges and a small creek between them. The depletion zone of the 1984 rock slide contained only one block. The rock mass displaced in the 1963 event consisted of units 2 and 3 of the volcanic rocks on Mount Cayley, mainly brown to dark brown columnar-jointed dacite and some grey tuff. The rock mass displaced in the 1984 rock slide consisted of units 4 and 5 of the volcanic rocks, mainly purple tuff breccia and tuff lapilli, white to grey soft tuff and light yellow hard tuff. The main track of the 1984 rock slide was covered by a thick layer of snow and ice. The main track of the 1963 rock slide had no ice cover. These essential differences resulted in the following differences in these two events.

The 1963 rock slide moved one block after another and deposited in the same way resulting in three separate depositional blocks and different layers which can be traced to the bedrock sequences in the depletion zone. The 1984 rock slide moved in a turbulent way so that the displaced mass was totally broken resulting in the deposits without layering features. These deposits formed different dams in Turbid Creek. The 1963 landslide dam belongs to Type 5 and the 1984 landslide dam belongs to Type 3. As the materials forming these dams have different characteristics, totally broken tuff,

breccia, lapilli and substantial ice blocks in the 1984 dam and partly broken large dacite blocks in the 1963 dam, the 1984 dam lasted just one to two days and burst rapidly caused serious debris flow with high velocity and the 1963 dam lasted much longer, then overtopped and eroded without causing debris flow.

Based on the comparison between the 1984 and the 1963 events, two basic modes of landslides from Mount Cayley are recognized, Tuff Type and Dacite Type. They are useful in the study of prehistoric landslide deposits and prediction of future landslides from Mount Cayley.

6 HISTORY OF SLOPE MOVEMENT FROM MOUNT CAYLEY

6.1 INTRODUCTION

The deposits in the valley of Turbid Creek and on the Turbid Creek fan reveal that rock slides and debris flows have taken place quite often after the deposition of the volcanic rocks on Mount Cayley. To figure out the history of slope movement from Mount Cayley, field investigation and mapping of the slope movement deposits in the Turbid Creek valley and on the Turbid Creek fan were carried out in 1986 and 1989. The results are presented in Section 6.2. Two major types of slope movement deposits are recognized: coming from units 2 and 3, and coming from units 4 and 5 of the volcanic rocks corresponding to the 1963 event and the 1984 event respectively, based on the different materials in the deposits and their grain size distribution curves (Section 6.3). Radiocarbon dates of buried wood from related deposits reported by Clague and Souther (1982), and Evans and Brooks (1991), were collected and re-interpreted carefully. The new interpretation is fully supported by field mapping. The new interpretation leads to a picture of the history of slope movement from Mount Cayley (Section 6.4). Furthermore, a new episode of slope movement is revealed by air photos taken at different times, annual ring counting of the trees buried by deposits and the records of logging road bridge. These form Section 6.5. Special attention was given to hazardous slopes on Mount Cayley, during field investigations in the summers of 1986 and 1989. Three major hazardous slopes on Mount Cayley are recognized. Based on the results of the comparison

between the 1963 and the 1984 events and the study of prehistoric deposits on the Turbid Creek fan and in the Turbid Creek valley, a prediction of the main characteristics of the slope movements from these three hazardous slopes is made in Section 6.6.

6.2 HISTORY ESTABLISHED FROM GEOLOGICAL MAPPING

Figures 6.1 and 6.2 show the deposits of slope movements from Mount Cayley in the downstream of Turbid Creek valley and on the Turbid Creek fan. Seven units deposited at different times and locations are distinguished. Their corresponding ages are 5030 ± 60 BP, 4540 ± 70 BP, 4130 ± 70 BP, 1250 ± 110 BP, 1060 ± 60 BP, 560 ± 65 BP and 350 ± 50 BP. There is an additional unit seen in the midstream of Turbid Creek. Its radiocarbon date reported by Clague and Souther (1982) is 3720 ± 60 BP.

These units are observed in several sections exposed in the Turbid Creek valley and on the Turbid Creek fan.

Section 51

Section 51 is located at site 51. This section contains six layers (Figure 6.3). The oldest layer is exposed at the bottom of the north bank of Turbid Creek. The base of this layer was not exposed. This layer has a thickness of 0.5-2.0 m above the stream bed. It is purple to grey, matrix-supported, and cemented hard. It can't be broken by a hammer with ease. This layer contains 5-10% of blocks less than 20 cm across, consisting of purple breccia, lapilli and soft tuff, light yellow hard tuff and basement rock-granodiorite. It is interesting that there are very few dacite blocks in this layer. So the deposits probably came from units 4

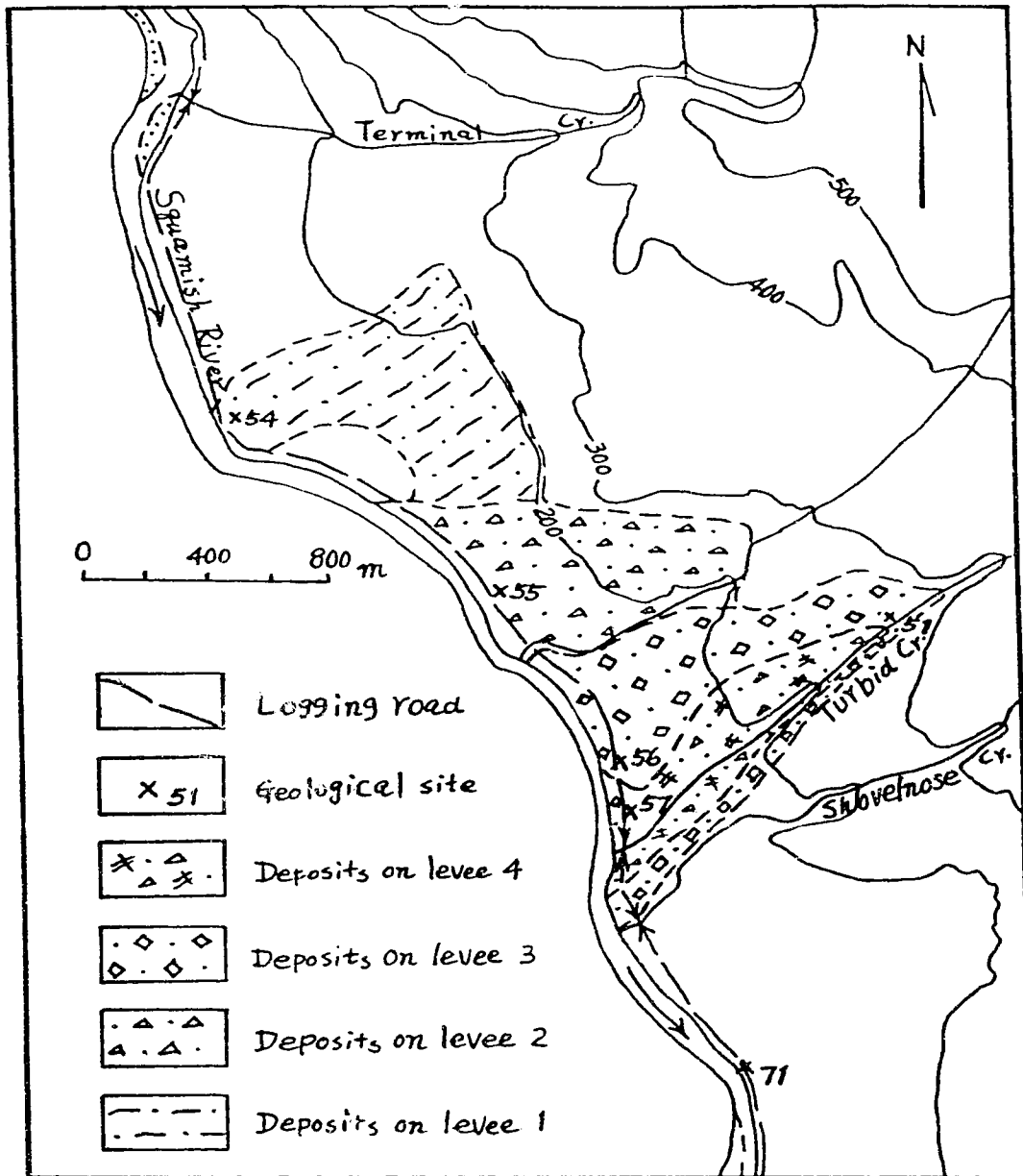
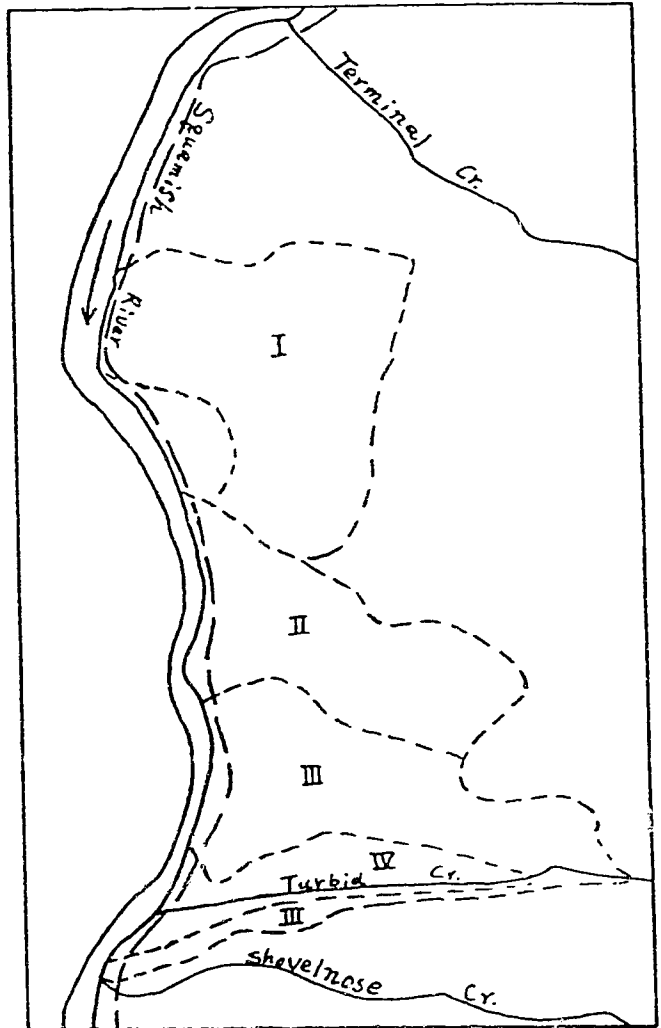


Figure 6.1 A map of slope movement deposits in downstream Turbid Creek valley and its fan. It is prepared from the topographic map commissioned by the Geological Survey of Canada based on the air photos taken in 1973.



IV Levee 4
 III Levee 3
 II Levee 2
 I Levee 1

Figure 6.2 (a) Air photo (Province of British Columbia photo BC 86061 No. 100) showing four levees between Turbid and Terminal Creeks. (b) An overlay of the air photo.

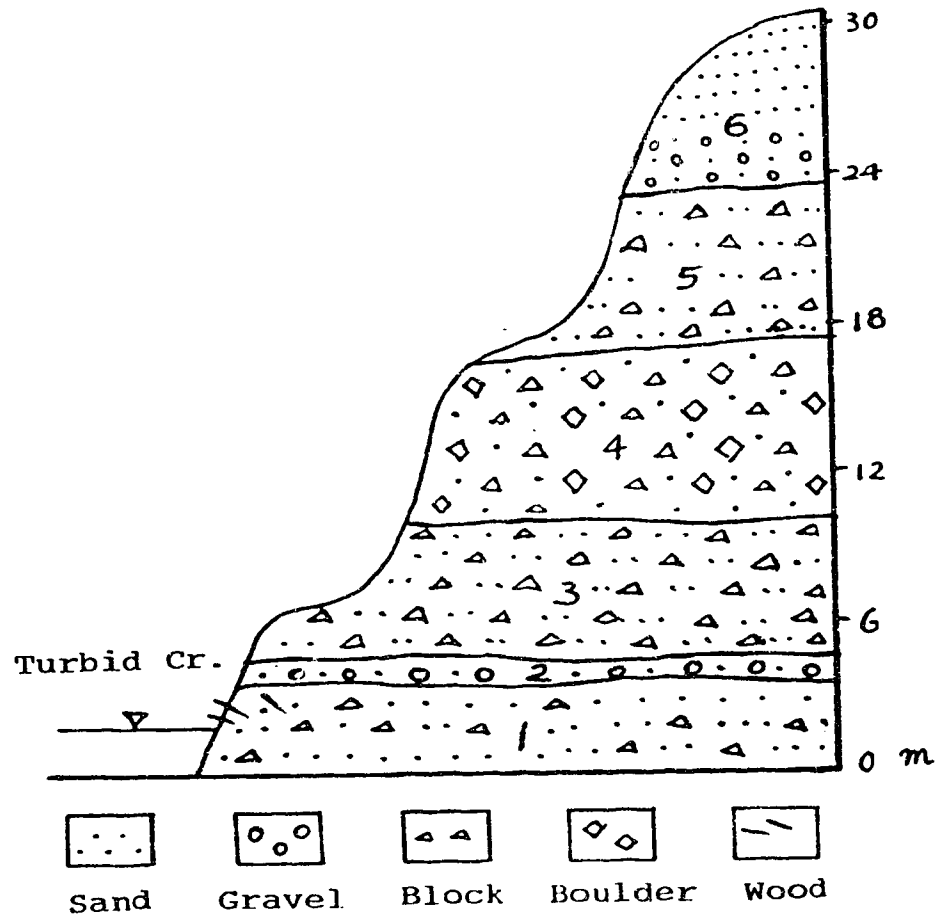


Figure 6.3 Section 51.

and 5 of the volcanic rocks on Mount Cayley. Some wood pieces were observed. One piece of wood from this layer was collected and dated. It yields a date of 5030 ± 60 years BP (GSC-4773).

Layer 2 in section 51 is a fluvial unit, grey, 0.5-1.0 m thick. Layer 2 has distinct layering, consisting of mainly rounded gravel and sand. Although no radiocarbon date is available for this layer, this layer may indicate a short lull in slope movement from Mount Cayley, subsequent to the deposition of layer 1 as discussed below.

Layer 3 in section 51 has similar characteristics to the bottom layer in section 71 (Figure 6.4). Layer 3 is purple to grey, matrix-supported, 5-6 m thick, and cemented hard. This layer has 10-15% small blocks, consisting of purple breccia, lapilli and tuff, and light yellow hard tuff. Very few dacite blocks showed up in this layer.

Layer 4 in section 51 is a brown, 5-8 m thick and clast supported diamicton. This layer consists of 60-70% large dacite blocks and boulders, 0.3-2.5 m across with clear columnar joints.

Layer 5 in section 51 is a grey, matrix-supported diamicton with a thickness of 5-7 m. It contains 20-30% small blocks mainly consisting of purple breccia and lapilli.

Layer 6, the top layer of section 51, consists of grey fluvial deposits, 6-9 m thick. It contains rounded gravels and sand with well developed layering.

Radiocarbon dates are available only from the bottom layer of the layers in section 51.

From section 51, it is established that layer 1 in the section

was deposited in 5030 ± 60 BP, and layer 3 in the section was probably deposited in 4130 ± 70 BP. Between these two layers there is a fluvial layer indicating a lull of slope movement from Mount Cayley. Although no radiocarbon dates for the three top layers in section 51 are available, it is clear that these three layers are younger than layer 3 and they have totally different characteristics from layer 3. It indicates that the six layers in section 51 were formed at different times and in different deposition environments. Layers 1, 3 and 5 are probably from units 4 and 5 of the volcanic rocks on Mount Cayley. Layer 4 is from units 2 and 3 of the volcanic rocks. Layers 2 and 6 are fluvial deposits.

Section 71

Section 71 is located at site 71 (Fig. 6.1) on the cliff of the Squamish River just downstream of Shovelnose Creek, corresponding to Evans and Brooks' (1991) section SQA. This section contains four layers (Figure 6.4).

The base of the layer 1, 3-5 m thick, of section 71 is exposed. This layer is purple to grey in colour, matrix-supported and cemented hard. It contains 15-25% blocks of purple lapilli, breccia and tuff, and light yellow hard tuff, 0.1-0.5 m across. There is a lot of pulverized wood, 1-3% in the deposits by volume. Wood pieces collected from this layer yield dates of 5080 ± 70 BP, 4960 ± 90 BP and 4130 ± 70 BP (GSC-4771, SFU-605 and SFU-609). So this layer probably deposited around 4130 ± 70 BP and contains previous slope movement deposits which were reworked by the 4130 BP event.

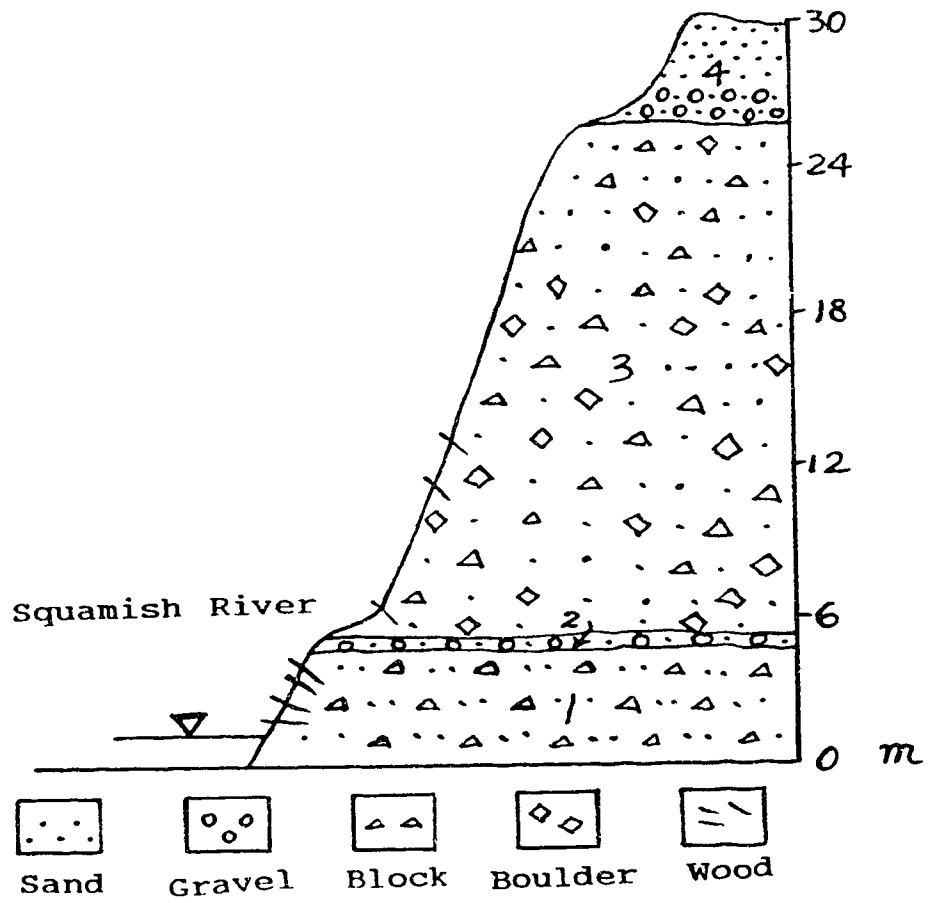


Figure 6.4 Section 71.

Layer 2 is a 20-50 cm thick fluvial unit. This layer contains laminated silt, sand and rounded gravels, indicating a distinct lull of slope movement from Mount Cayley.

Layer 3 is a grey diamicton, 20-25 m thick. This layer is matrix-supported, containing 20-40% of large blocks and boulders differing from layer 1 in lithology. This diamicton unit also contains much pulverized wood, but less than 2% by volume. Some of these wood pieces collected from this layer yield different radiocarbon dates: 5050±70 BP (GSC-4772), 4800±90 BP (SFU-584), 5180±80 BP (SFU-604), 4560±80 BP (SFU-681) and 5140±70 BP (GSC-4907). It is obvious that layer 3 formed in one single event. But it contains so many wood pieces dated with extensive scattering. Probably this layer formed with a lot of reworked slope movement deposits which contained differently dated broken trees.

The sequence of the layers in section 71 is normal. Layers are nearly horizontal. So layer 3 would be younger than layer 1. It would form later than 4130±70 BP.

Layer 4 is a fluvial unit consisting of two parts. The lower part mainly consists of coarse sand and rounded pebbles and gravels; the upper part mainly consists of fine sand and silt with laminations. Layer 4 is grey to brown, 2-4 m thick.

Comparing section 71 to the composite stratigraphy in Evans and Brooks' (1991, Figure 9), it should be mentioned while layer 2 was mentioned in Evans and Brooks' text, and shown in their Figure 9, it was not separately identified but classified with another unit.

From this section and the radiocarbon dates yielded by the

wood contained in the deposits, Evans and Brooks concluded that there was a 4800 BP event which formed the Turbid Creek fan. These conclusions prompted critical comments (Lu 1992).

Four levees subparallel to Turbid Creek were observed and mapped between Terminal and Turbid Creeks (Figs. 6.1 and 6.4). The logging road along the Squamish River provides slopes cutting through these four levees. Four typical sections 54, 55, 56 and 57 were studied in the field.

Section 54

Section 54 exposed at site 54 contains three layers (Figure 6.5).

Layer 1 is a brown to grey matrix-supported diamicton, 3-5 m thick above the ground. It contains 60-70% matrix, sand and silt, and 30-40% blocks and boulders, among which the largest boulder is a 3.4 m, columnar-jointed dacite.

Layer 2 is a brown clastic-supported diamicton, 5-10 m thick. It contains 60-80% of blocks and boulders of columnar-jointed dacite.

Both layers 1 and 2 mainly consist of brown columnar-jointed dacite and grey soft tuff. They probably came from units 2 and 3 of the volcanic rocks on Mount Cayley.

Layer 3 is a fluvial unit. At its base there is a rounded pebble and gravel layer, 0.5-1.5 m thick. The upper part of layer 3 is a grey sand and silt layer, 2-5 m thick.

A wood sample from layer 1 was collected by Evans and Brooks (Number 14 in Fig. 5 and Table 1, 1991). It yields a radiocarbon

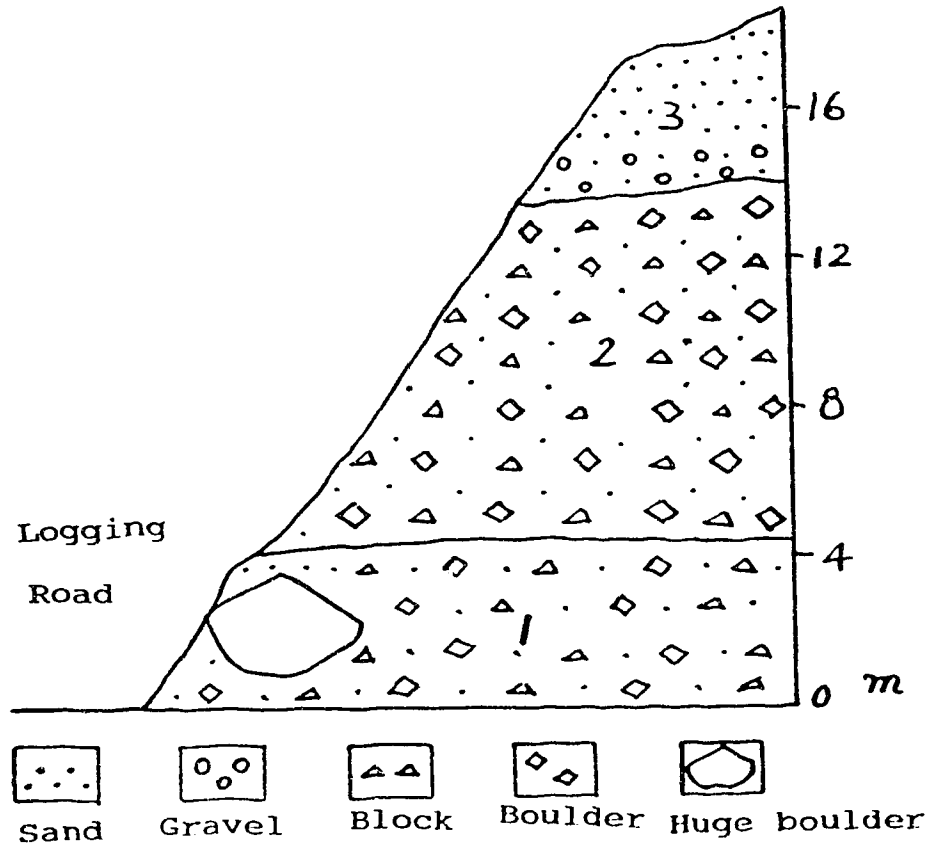


Figure 6.5 Section 54.

date of 1270 ± 50 BP (GSC-4770).

Section 55

Section 55 is exposed at site 55. It contains two layers. The base layer is a purple to grey diamicton, 12-15 m thick. It contains very few blocks, 0.2-0.3 m across and 80-90% matrix, fine sand and silt. The upper layer is a purple to brown matrix-supported diamicton, 4-5 m thick. It contains 90-95% matrix, fine sand and silt, and very few blocks, less than 0.1 m across. Both layers mainly consist of purple lapilli, breccia and soft tuff, and light yellow hard tuff. They probably came from units 4 and 5 of the volcanic rocks on Mount Cayley.

A wood sample was collected from this levee about 400 m upslope from site 55. It yields a radiocarbon date of 1010 ± 60 BP (GSC-4904).

Section 56

Section 56 is exposed at site 56. It contains a single layer. It is a red and dark brown diamicton, 20 m thick above the ground. It contains 50-60% of large blocks and boulders, 0.5-3 m across. Most of them are columnar-jointed dacite, probably from Units 2 and 3 of the volcanic rocks on Mount Cayley.

A wood sample from this layer yields a radiocarbon date of 500 ± 50 BP (GSC-4768).

Section 57

Section 57 is exposed at site 57 near the mouth of Turbid Creek. It contains a single layer which can be traced along Turbid Creek for about 0.8 km. This layer of deposits forms the main part

of present banks of Turbid Creek. It is a grey matrix-supported diamicton, 15-25 m thick. It contains 40-70% of grey to brown blocks and boulders, 0.2-3.5 m across, mainly columnar-jointed dacite. These deposits may probably come from Units 2 and 3 of the volcanic rocks on Mount Cayley. A wood sample from this layer yields a radiocarbon date of 350 ± 50 BP (GSC-4774).

It is obvious that the four levees formed in different times: 1270 ± 50 , 1010 ± 60 , 500 ± 50 and 350 ± 50 BP respectively and came from different source areas. While section 55 deposits came from units 4 and 5, the other three levee deposits came from units 2 and 3 of the volcanic rocks on Mount Cayley.

Seven Typical Deposition Units

From our mapping, seven typical units of the prehistoric slope movement deposits from Mount Cayley can be established.

Unit 1: the bottom layer of section 51 exposed at site 51 in Turbid Creek has a radiocarbon date of 5030 ± 70 BP. The deposits came from units 4 and 5 of the volcanic rocks as the deposits are mainly lapilli, breccia and hard tuff, and very few dacite blocks showed up.

Unit 2: the bottom layer of section 71 exposed at site 71 on the cliff of the Squamish River has a radiocarbon date of 4130 ± 70 BP. Layer 3 in section 51 has almost the same characteristics as the bottom layer of section 71. They probably formed by one event. It seems that they also came from units 4 and 5 of the volcanic rocks because the deposits are mainly lapilli, breccia and hard tuff, but very few dacite blocks.

Unit 3: the bottom layer of section 41 exposed at site 41 (Chapter 3) in Turbid Creek (Fig. 6.6) has a radiocarbon date of 3720 ± 60 BP (Clague and Souther 1982). It comes from units 4 and 5 of the volcanic rocks as the deposits mainly consist of purple lapilli, breccia blocks and lack brown columnar-jointed dacite.

Unit 4: the layers 1 and 2 of section 54 exposed at site 54 on the Squamish River have a radiocarbon date of 1270 ± 50 BP. They come from units 2 and 3 of the volcanic rocks as the deposits of this unit are mainly columnar-jointed dacite. This unit forms the oldest levee of Turbid Creek observed at present.

Unit 5: the layers of section 55 exposed at site 55 on a roadcut along the Squamish River have no radiocarbon date from this exposure, but the deposits about 400 m upslope on the same levee has a radiocarbon date of 1010 ± 60 BP (Evans and Brooks 1991, GSC-4904). They come from units 4 and 5, because the deposits mainly consist of breccia, lapilli and hard tuff. This unit forms the second oldest levee of Turbid Creek observed at present.

Unit 6: the layer of section 56 exposed at site 56 on a roadcut along the Squamish River has a radiocarbon date of 500 ± 50 BP (Evans and Brooks 1991, GSC-4768). It comes from units 2 and 3 of the volcanic rocks, because the deposits mainly consist of columnar-jointed dacite. This unit forms the second youngest levee of Turbid Creek.

Unit 7: the layer in section 57 exposed at site 57 on a roadcut beside the mouth of Turbid Creek has a radiocarbon date of 350 ± 50 BP (Evans and Brooks 1991, GSC-4774). It comes from units 2

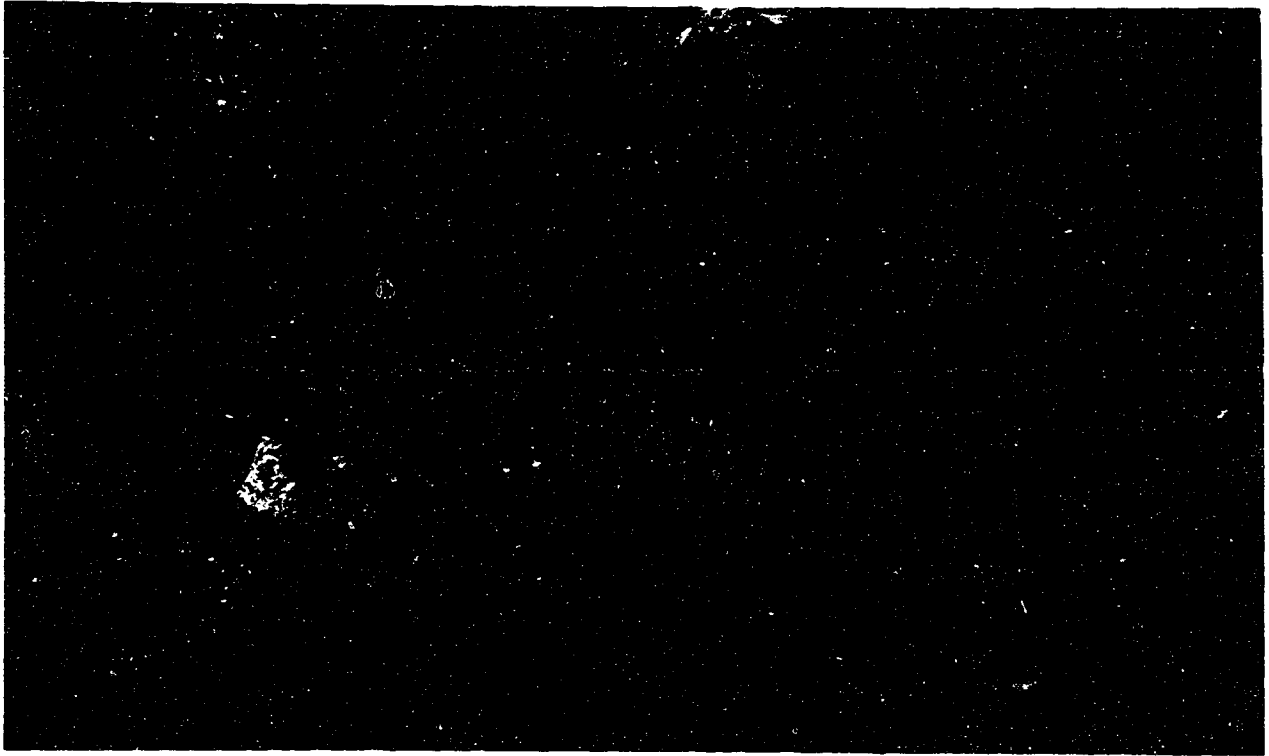


Figure 6.6 Section 41 (site 41, Fig. 2.12) showing two layers of old deposits, P_1 and P_u , and the 1963, V, and the 1984, U, deposits, looking E at site 33 (Fig. 3.11). The section is 45 m high.

and 3 of the volcanic rocks, because the deposits mainly consist of columnar-jointed dacite. This unit forms the youngest levee of Turbid Creek.

Two additional points may need to be discussed. From Section 71, it is obvious that during the period 4710-5380 BP, extensive rock slides and debris flows took place on Mount Cayley which destroyed forest at different times. These older deposits were later reworked and deposited farther downstream. Beside the bottom layer in section 51, which is an example of these older deposits, some more spots where these older deposits have been preserved in place may probably be found in the Turbid Creek valley someday.

Secondly, SFU-607 and SFU-681 yield radiocarbon dates of 4540 ± 70 BP and 4560 ± 80 BP respectively. These two radiocarbon dates may probably establish another unit of slope movement deposits from Mount Cayley. As SFU-607 was collected beyond the scope of our geological mapping, this unit was not included in the above description, but will be used as another slope movement indicator and discussed in the following section.

These units of slope movement deposits represent seven prehistoric active stages of slope movement from Mount Cayley. They are at 4800-5310, 4130, 3720, 1250-1270, 1010-1060, 500-560, and 350 years BP. As mentioned before the first active stage (4800-5310 years BP) probably includes several separate substages or events. As a lot of wood pieces in old deposits have been reworked and not enough exposures of the old deposits in place are found, except the 5030 ± 70 BP deposits observed at site 51, we have to combine these

events into a big, active stage of slope movement from Mount Cayley. During that period of time, extensive rock slides and debris flows took place on Mount Cayley and supplied a huge quantity of materials for the Turbid Creek fan to start building up its foundation.

From the depositional units and the corresponding active stages, a simple assumption can be made that slope movements from Mount Cayley were cyclic, active and inactive stages were alternating.

6.3 TWO MAJOR MODES OF SLOPE MOVEMENT

Two Major Types of Grain Size Distribution

Introduction

Different types of slope movement deposits have different grain size distributions. Grain size distribution is influenced by three major factors: the parent bedrock composition, the mode of slope movement and the weathering process after deposition.

The study of grain size distributions of the 1963 and the 1984 deposits reached some interesting results (Cruden and Lu 1992, and Chapters 2 and 3). Comparing the grain size distributions of prehistoric deposits with those of the 1963 and the 1984 deposits may provide more clues for identifying the source rocks of these deposits.

The grain size distribution was determined by combining the "area-by-number" method (Hunggr 1981) and mechanical analyses. The bottom layer in section 51 (unit 1), the bottom layer in section 71 (unit 2), two bottom layers in section 54 (unit 4), the bottom

layer in section 55 (unit 5), the layer in section 56 (unit 6) and the layer in section 57 (unit 7) were chosen for the study of grain size distribution.

These results are compared with the grain size distribution of the 1963 rock slide and the 1984 rock slide and debris flow deposits.

Basic Results

The typical grain size distribution curves of the prehistoric slope movement deposits are shown in Figure 6.7. The values of D50 for each unit are listed in Table 6.1.

Two types of deposits are indicated in the grain size distributions. Type 1 represented by units 1, 2 and 5, deposits have a D50 value less than 3 mm, and type 2, represented by units 4, 6 and 7, deposits have a D50 value larger than 10 mm. Plasticity tests show that all fines from type 1 (units 1, 2 and 5) deposits are plastic, and all fines from type 2 (units 4, 6 and 7) deposits are non-plastic.

It seems likely that in the same type of deposits, the older ones have lower D50 values especially in type 1. For example, the oldest deposit in type 1, unit 1, has a D50 value of 0.76 mm, and the oldest deposit in type 2, unit 4, has a D50 value of 13.5 mm.

Results from Comparison

The D50 values of prehistoric slope movement deposits, the 1963 rock slide deposits, and the 1984 rock slide and debris flow deposits are summarized in Table 6.2. The typical grain size distribution curves of the 1963 rock slide deposits, and the 1984

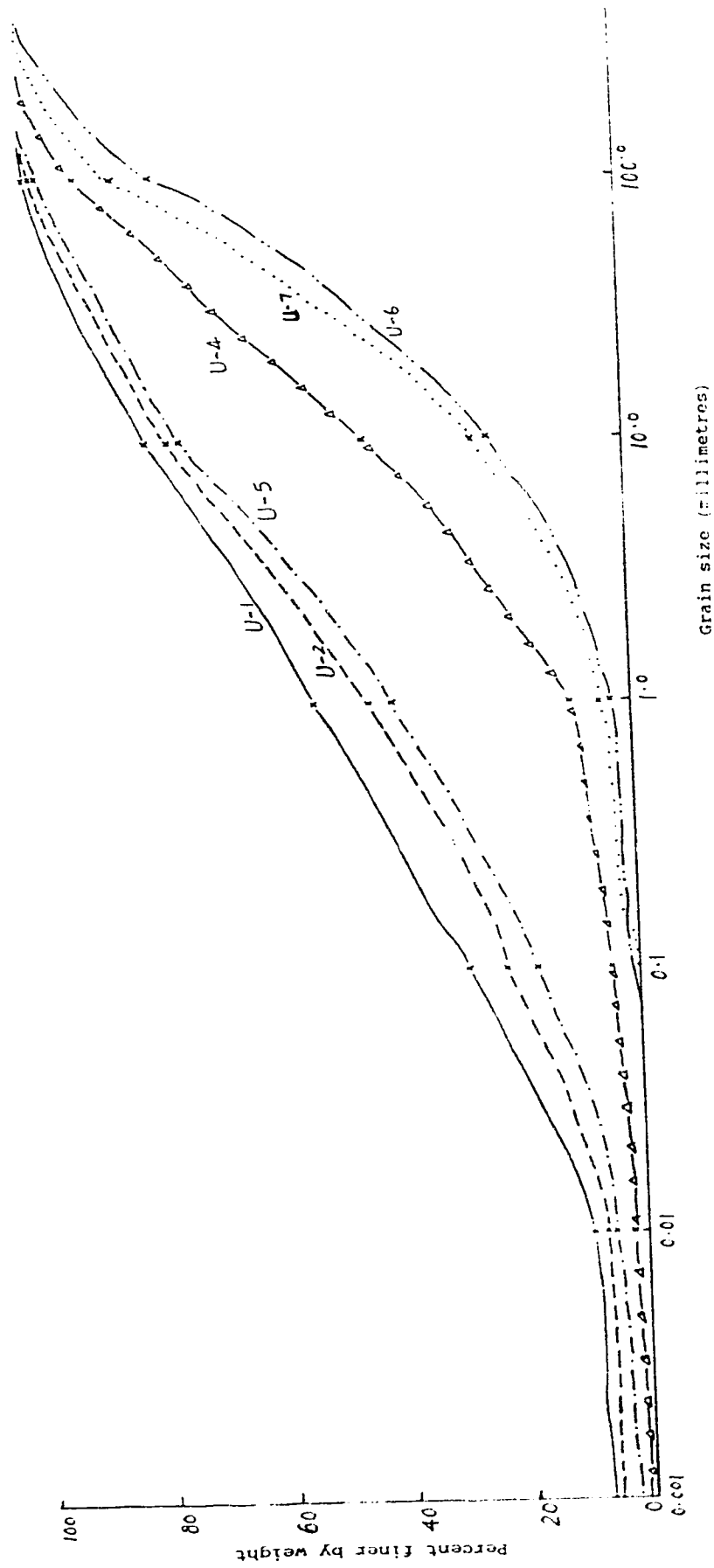


Figure 6.7 Cumulative grain size curves.

Table 6.1. D50 values of prehistoric slope movement deposits

Unit 1	Unit 2	Unit 4	Unit 5	Unit 6	Unit 7
0.76 mm	1.5 mm	13.5 mm	2.1 mm	40 mm	30 mm

Table 6.2 Comparison of D50 values

1984 A	1984 B	1963 A	1963 B	Pre- A	Pre- B
5 mm	1.6 mm	33-105 mm	1.5-3.6 mm	0.76-2.1 mm	13.5-40 mm

1984 A-the 1984 rock slide deposit.

1984 B-the subsurface of the 1984 debris flow deposits.

1963 A-layers b, d and f of the 1963 rock slide deposits.

1963 B-layers c, e and g of the 1963 rock slide deposits.

Pre- A-units 1, 2 and 5 of prehistoric slope movement deposits.

Pre- B-units 4, 6 and 7 of prehistoric slope movement deposits.

rock slide and debris flow deposits can be found in previous Chapters (Figs. 2.13 and 3.20).

The D50 values of the 1984 event deposits are interesting. As they came from units 4 and 5 of the volcanic rocks on Mount Cayley, the D50 values of No. 10 (rock slide deposits) and No. 15 (subsurface debris flow deposits) are 5 mm and 1.6 mm respectively. The ground surface deposits of the debris flow have a much higher D50 value, 35 mm indicating that in debris flow, fine particles mixed with water, have the ability to suspend coarse materials and lift the larger particles to the top surface.

The 1963 rock slide deposits contain two different kinds of layers: layers b, d and f came from dacite layers in units 2 and 3 of the volcanic rocks, and layers c, e and g came from tuff, lapilli tuff and breccia tuff layers in units 2 and 3 of the volcanic rocks. These layers have different grain size distributions. D50 values of layers b, d and f are 33 mm, 70 mm and 105 mm respectively. All of them are larger than 10 mm. Layers c, e and g have different D50 values, 3.6 mm, 1.56 mm and 1.5 mm respectively. All of them are less than 5 mm.

The prehistoric slope movement deposits from Mount Cayley have different D50 values forming two basic types. Prehistoric depositional units 1, 2 and 5 have D50 values as 0.76 mm, 1.5 mm and 2.1 mm respectively. All of them are less than 5 mm. Prehistoric depositional units 4, 6 and 7 have D50 values as 13.5 mm, 40 mm and 30 mm respectively. All of them are larger than 10 mm.

Based on these grain size distribution data, the following understandings are reached.

1. Two different types of bedrock occur in slope movements on Mount Cayley. Mode 1 slope movements involve only units 4 and 5 of the volcanic rocks, i. e. mainly purple lapilli, breccia and soft tuff, and light yellow hard tuff. This mode of slope movement can be called Tuff Type. All deposits from Tuff Type slope movements have D50 values less than 5 mm. Mode 2 slope movement involves only units 2 and 3 of the volcanic rocks, i. e. mainly brown or dark brown dacite. This mode of slope movement can be called Dacite Type. The deposits of Dacite Type of slope movement have D50 values larger than 10 mm.

2. If the rock sequence is little disturbed, as the 1963 rock slide deposits, the grain size distribution of each layer shows the characteristics of its parent bedrock layer. Layers c, e and g have D50 values of 3.6 mm, 1.56 mm and 1.5 mm respectively, all less than 5 mm. Layers b, d and f have D50 values of 33 mm, 70 mm and 105 mm respectively, all larger than 10 mm. If the rock sequence is seriously disturbed, as prehistoric depositional units 4, 6 and 7, the grain size distributions have D50 values larger than 10 mm. The average D50 value of the 1963 rock slide deposits is 35.8 mm, still larger than 10 mm and very close to the D50 values of depositional units 6 and 7.

3. D50 values vary with the distance of the deposits from the source. For example, all Tuff Type deposits, the 1984 rock slide deposits, the 1984 debris flow deposits and the prehistoric Tuff

Type deposits, 4800-5310 BP, 4130 BP and 1010-1060 BP deposits have different D50 values. The 1984 rock slide deposits with a short distance from the source have a D50 value of 5 mm (Chapter 2 and Table 6.2), and the prehistoric Tuff Type deposits with a long distance from their sources have D 50 values in the range of 0.76-2.1 mm (Table 6.2). All Dacite Type deposits, the 1963 rock slide deposits and the prehistoric Dacite Type deposits, 1250-1270 BP, 500-560 BP and 350 BP deposits have different D50 values. Layers b,d and f of the 1963 rock slide deposits with a short distance from the source have D50 values in the range of 33-105 mm (Table 6.2), and the prehistoric Dacite Type deposits with longer distances from their sources have D50 values in the range of 13.5-40 mm (Table 6.2).

D50 values also vary with the mode of slope movements. For example, the 1984 rock slide deposits have a D50 value of 5mm, and the 1984 debris flow deposits have a D50 value of 1.6 mm.

Two Modes of Slope Movement

Two types of different slope movement deposits have been recognized.

Tuff Type rock slide deposits mainly consist of purple lapilli, breccia and soft tuff, and light yellow hard tuff with very limited dacite blocks. They are matrix-supported. Rarely are boulders larger than 3 m across observed. In most cases, the matrix is about 60-70% and the fines from the matrix are plastic. These materials probably come from units 4 and 5 of the volcanic rocks. The depositional units 1, 2, 3 and 5 above-mentioned belong to this

type. This type of deposits is very similar to the 1984 rock slide or debris flow deposits.

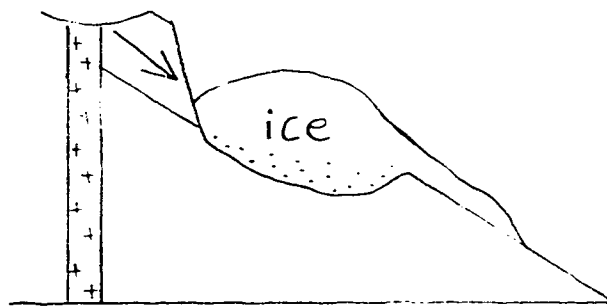
Dacite Type rock slide deposits are mainly consist of brown or dark brown dacite and grey soft tuff. They may be matrix-supported or clast-supported. The large blocks and boulders may reach 50-80%. The largest boulders may be 3-5 m across and contain columnar-joints. The fines from this type of deposits are non-plastic. These deposits might come from Units 2 and 3 of the volcanic rocks. The depositional units 4, 6 and 7 belong to this type. This type of deposit is similar to the 1963 rock slide deposits.

Obviously, there are two major different modes of slope movement resulting in two major different types of deposits in Mount Cayley. Tuff Type slope movement involves only units 4 and 5 of the volcanic rocks. Their rupture surfaces develop along the soft tuff layer at the bottom of unit 4 of the volcanic rock (Fig. 3.5). This tuff layer is very weak and its fines are plastic. Dacite Type slope movement involves only units 2 and 3 of the volcanic rocks. Their rupture surfaces develop along the soft tuff layer at the bottom of the volcanic pile, the base of Unit 2. This layer is weak and its fines are non-plastic.

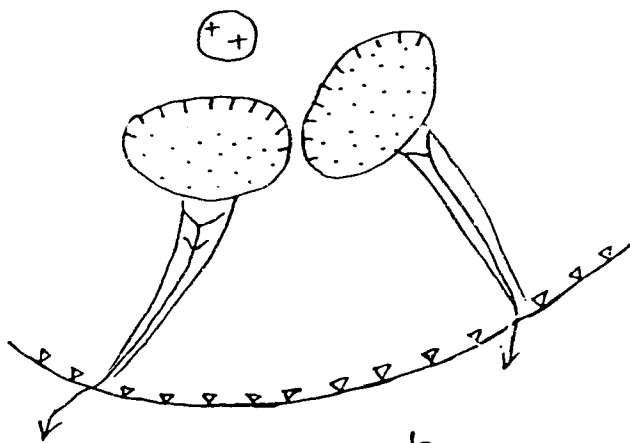
As shown in Figure 3.5, there are at least two major weak tuff layers at different levels in the volcanic pile. The upper weak tuff layer is located at the bottom of Unit 4 and the lower tuff layer is located at the bottom of Unit 2. The rupture surfaces of most large rock slides on Mount Cayley develop following these two weak tuff layers. As the rock mass above the rupture surface are

different, mainly breccia, lapilli and hard tuff above the upper weak tuff layer and mainly dacite above the lower weak tuff layer, so the two modes of slope movement show very different characteristics. Their deposits, of course, also differ from each other.

Interpretation of air photos (Figs. 2.3, 3.1, 3.2 and 3.3) shows that after the deposition of the volcanic rocks, Mount Cayley was probably extensively glaciated. Cirques developed on the volcanic slopes. Cirque glaciers eroded steep, straight, U-shaped valleys (Fig. 6.8). This process might cause the upper weak tuff layer at the bottom of unit 4 of the volcanic rocks to daylight on the steep slopes. As the rock block's lateral connection with the slope was not totally destroyed, the rock mass above the upper weak tuff layer would not fail. As the ice decayed, tributary drainage would develop presumably at high angle to the radial drainage (Fig. 6.8). So prehistoric inactive episodes of slope movement are correspond to glaciations and active episodes of slope movement are correspond to glacier recessions. In some cases, rock slopes would be cut into isolated blocks. At that time the rock block would fail and slide downstream along the upper weak tuff layer rapidly forming a rock slide similar to the 1984 rock slide, a Tuff Type rock slide. Sometimes even when the upper weak tuff layer at the bottom of unit 4 is daylighting on the slope resulting from erosion, if the lateral connections still exist, the slope won't fail immediately. On the other hand, if erosion is still developing after some slopes consisting of units 4 and 5 failed, and reaches



a



b

Figure 6.8 Slope movement and drainage development
a. A section, b. A plan.

the lower weak tuff layer at the bottom of unit 2, if the rock mass above the tuff layer is already isolated, a Dacite Type rock slide will take place.

This model may explain why the oldest deposits are Tuff Type, and more and more young deposits belong to Dacite Type. But it is also important to notice that as the lateral connections may be destroyed later, so substantial Tuff Type rock slides and debris flows have taken place lately.

6.4 INTERPRETATION OF RADIOCARBON DATES

Evans and Brooks (1991) suggested that debris avalanches nearly an order of magnitude larger than any historic avalanche (Evans and Gardner 1989; Evans 1990) are responsible for building the Turbid Creek fan 4800 years ago. This hypothesis has significant implications for public safety in the Squamish River drainage. The discussion below shows that the fan could have been built by numerous smaller events over a longer time period. The rate of construction is similar to present day rates of sedimentation on the fan.

Radiocarbon dates from the wood collected from the Turbid Creek valley and Turbid Creek fan are found in Clague and Souther (1982), and Evans and Brooks (1991). Clague and Souther (1982) reported a radiocarbon date of 3720 ± 60 years BP (GSC-3193) from a piece of wood from the lower unit, unit 3 in the previous section, of the two older units underneath the 1963 rock slide deposits in Turbid Creek. Evans and Brooks (1991, Table 1) reported 20 radiocarbon dates from wood pieces collected from the fan and the Turbid Creek

valley.

Based on these radiocarbon dates, Evans and Brooks (1991, pp 1366-68, 1372) reached the following conclusions:

1. "Three groups of radiocarbon dates are evident centered at approximately 4800, 1100, and 500 BP (Table 1), suggesting at least three prehistoric debris avalanche episodes. The scattering of dates within the date groups probably reflects the mixture of wood (different-sized trees of different ages; dead trees) incorporated within the deposits, although the 4130 ± 70 BP (SFU-609) date is anomalously younger than other samples from the same stratigraphic unit."

2. "The 4800 BP deposit is the product of two major, closely spaced, debris avalanche events. The lack of buried organic and (or) paleosol horizons along the unit 1- unit 2 boundary supports this interpretation. The thin interbed may represent a short lull between debris avalanche events. Fluvial deposits near the top of the section (unit 3) suggest a waning of debris avalanche activity. The overlaying diamicton unit (unit 4) may record continued debris avalanche activity from the source area or a secondary debris flow."

3. "Based on the thickness of the deposits at section SQA and the areal extent of the fan surface (about 8.0 km^2), the 4800 BP debris avalanches were very large. Using an approximate mean height of the fan surface of 30 m above the Squamish River, it is estimated that in the order of $2-3 \times 10^8 \text{ m}^3$ was deposited by these debris avalanches."

These conclusions prompt the following comments.

The avalanche deposits are not continuously exposed. Evans and Brooks retrieved datable wood samples from most of the few exposures on the fan, but there remains the problem of correlating these isolated exposures.

In the list of radiocarbon dates provided by Evans and Brooks, at least seven groups, not three, are evident: 4710-5380, 4470-4640, 4060-4200, 1140-1360, 950-1120, 450-625 and 300-400 BP (Fig. 6.1). There is an additional group if the radiocarbon date reported by Clague and Souther (1982) is included (Fig. 6.9). Fig. 6.9 suggests that during the period 4710-5380 BP, extensive rock slides and debris flows took place on Mount Cayley which destroyed forest at different times. These older deposits were later reworked and deposited farther downstream and closer to the Squamish River.

It is also evident from Fig. 6.9 that the radiocarbon date of 4130 ± 70 BP (sample no. 12) represents a distinct landslide event.

As the younger wood which yielded a date of 4130 ± 70 BP is from the lower part of section SQA, and older wood which dated from 4540 ± 70 BP to 5310 ± 70 BP is from the upper part of the section, a reasonable interpretation is that rock slide and debris flow deposits containing this older wood were reworked from their original deposition sites by a later rock slide and debris flow which probably occurred 4130 ± 70 BP (if the wood with this date was itself not reworked) or later. A good example of these older rock slide and debris flow deposits is seen at Number 7 (Fig. 5 in Evans and Brooks 1991). As Evans and Brooks themselves suggested,

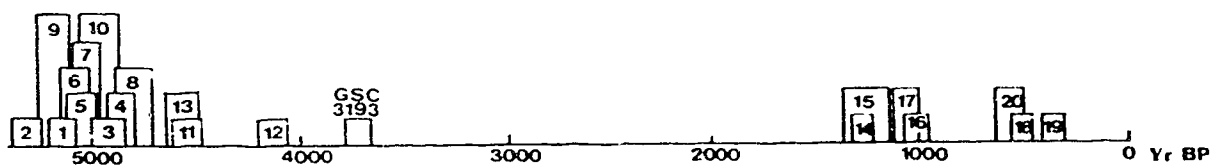


Figure 6.9 Radiocarbon dates on the time scale. Number represents the sample number in Table 1 of Evans and Brooks (1991); \lrcorner indicates the possible time span.

reworking may explain the extensive scattering of dates and the anomalous location of older wood they documented.

Unit 1 (see Evans and Brooks' Figure 9) would date 4060-4200 BP (or even later if the wood which yielded the date of 4130 ± 70 BP was reworked also), and unit 2 is younger than unit 1. Unit 3, a typical fluvial deposit, indicates a long lull in slope movements on Mount Cayley. It is clear that unit 4 has characteristics, such as very few boulders and blocks, that substantially differ from units 1 and 2, and thus there may also be a long lull between the deposition of unit 4 and units 1 and 2.

A single 4800 BP event can't be established from the radiocarbon dates or the stratigraphy of section SQA. Because section SQA can't be considered to be the deposit of one event, the estimate of the volume of the 4800 BP event is open to doubt.

In summary, at least eight groups of radiocarbon dates can be recognized. Each of these groups is represented by deposits in Turbid Creek valley and on its fan. So the Turbid Creek fan was probably formed by numerous major rock slides and debris flows from Mount Cayley. Mapping (Figure 6.1) has shown that, besides the materials displaced in the major landslides of 1963 and 1984, substantial other masses on Mount Cayley are unstable. Fifty landslides of the volume of the 1963 and 1984 events at 20 year intervals would build the Turbid Creek fan within the time constraints, 5380-4130 BP or less, indicated by Evans and Brooks' dates. So the fan is the site, not of a prehistoric catastrophe, but of a continuing hazard.

It is interesting to discuss further the relationship between Neoglaciation and slope movement on Mount Cayley.

Ryder and Thomson (1986) studied Neoglaciation in the southern Coast Mountains of British Columbia and pointed out three major glacier advances: the Garibaldi phase of glacier expansion, 6000-5000 ¹⁴C years BP, the mid-Neoglacial Tiedemann advance, 3300-1900 ¹⁴C years BP, and late Neoglacial expansion commenced before 900 ¹⁴C years BP (Ryder and Thomson, 1986, p. 273).

These three major glacier advances are in good agreement with the three major inactive episodes of slope movement on Mount Cayley. The Garibaldi glacier advance took place before the first prehistoric active episode of slope movement on Mount Cayley, 4710-5380 years BP. The mid-Neoglacial Tiedemann advance took place before the fifth prehistoric active episode of slope movement on Mount Cayley, 1140-1360 years BP. This glacial advance, 3300-1900 years BP, fills the distinctive inactive episode of slope movement on Mount Cayley between 3700-1300 years BP (Fig. 6.9). The late Neoglacial expansion took place before the last two prehistoric episodes of slope movement on Mount Cayley, 450-625 and 300-400 years BP. It is possible that during the late Neoglacial expansion some small and local glacier recessions may have taken place on Mount Cayley as two prehistoric episodes of slope movement are recognized. A local glacier advance might have taken place on Mount Cayley area between 300 years BP and 100 years BP. Finally it is probable that glacier recession is going on at present on Mount Cayley.

6.5 A NEW EPISODE OF SLOPE MOVEMENT

There are at least eight prehistoric stages of slope movement on Mount Cayley. Evidence indicates that a new episode of slope movement on Mount Cayley has started and is going on at the present time.

Evidence from Air Photos

It seems likely that the 350±50 BP stage is the last prehistoric distinct slope movement stage. This idea has been supported by counting the annual rings of the trees buried by the 1963 and the 1984 deposits and by the study of the air photos available.

The air photo taken in 1947 (BC 424-31, Fig. 3.2) clearly shows that large trees were growing on the banks along both sides of Turbid, Dusty and Avalanche Creeks, indicating that Mount Cayley above the Turbid Creek valley had not generated large rock slides and debris flows during the growth of the trees up to 1947.

On the air photos taken in July 1964 (photos BC 5103-132, Fig. 3.1), there is an evident change in vegetation, high trimlines show up along Dusty Creek and downstream of Turbid Creek between the pre- and post-1963 rock slide confluences of Dusty and Turbid Creek. But there is no change in vegetation along Avalanche Creek and Turbid Creek between the mouths of Avalanche Creek and Dusty Creek. On the air photos taken in 1986 (photos BC86061-097, Fig. 2.2), there is a big change in vegetation, clear high trimlines show up along Avalanche Creek and Turbid Creek downstream from the mouth of Avalanche Creek. Comparing these air photos taken in

different times gives a clue that large slope movements like 1963 and 1984 destroy the vegetation in the creek valley.

Clue from Annual Ring Counting

Two trees were found in the field at sites 37 (Fig. 3.10) and 15 (Fig. 2.12). They were cut down and buried by the 1963 rock slide and the 1984 debris flow respectively. The buried stems of these trees were sawn. The annual rings of these trees were counted to be 107 and 94 respectively. As these trees were not the largest nor oldest trees in the present valley, and counting the time for the growing of the pioneer vegetation, it can be suggested that the period of 200-300 years before 1963 was an inactive stage of slope movement on Mount Cayley. It may match the dating, 350 BP, of the last active stage.

Information from Records of Logging Road Bridge

In addition to the 1963 and the 1984 events, several small or similar events can be suspected from the records of the damage on the logging road bridge at the mouth of Turbid Creek. In 1967, 1981, 1984 and 1986, the bridge was removed by debris flows, and in 1972, the bridge was undermined by debris flow.

It seems likely that the 1963 rock slide is a starting sign of the new episode. And the other similar events including the 1984 rock slide and debris flow belong to that active stage.

The present episode is also indicated by the potential slope failures on Mount Cayley. Three special hazardous slopes were recognized during the field investigations conducted in the summers of 1986 and 1989. These hazardous slopes will be discussed in

detail in the following section.

It is clear that the present episode of slope movement on Mount Cayley probably contains several events and lasts hundreds of years.

6.6 HAZARDOUS SLOPES ON MOUNT CAYLEY

Introduction

One of the main aims of the study of the characteristics of historic slope movements is to find hazardous slopes in the research area and assess the size, path, velocity and impact of the slope movements which may occur in the future to diminish that impact of the slope movement on human lives and the environment.

Three major hazardous slopes were located in the field investigation, and examined from air photo interpretation. The possible size of the rock masses, the movement paths of the displaced rock masses, the velocities of these possible landslides and the impacts they may have on the environment are studied, essentially based on analogies with the geological and geomorphological conditions to the 1963 and the 1984 events. Also suggestions such as to set up warning systems on the logging road at the mouth of Turbid Creek and to do some more research in this area are made.

The locations of these three hazardous slopes are shown in Figure 6.10. They are the slope 200 m downstream from the 1984 rock slide head scarp, the slope east of Peak 2251 and the slope east of Peak Mount Cayley named hazardous slopes 1, 2 and 3 respectively.

Hazardous Slope 200 m Downstream from the 1984 Head Scarp

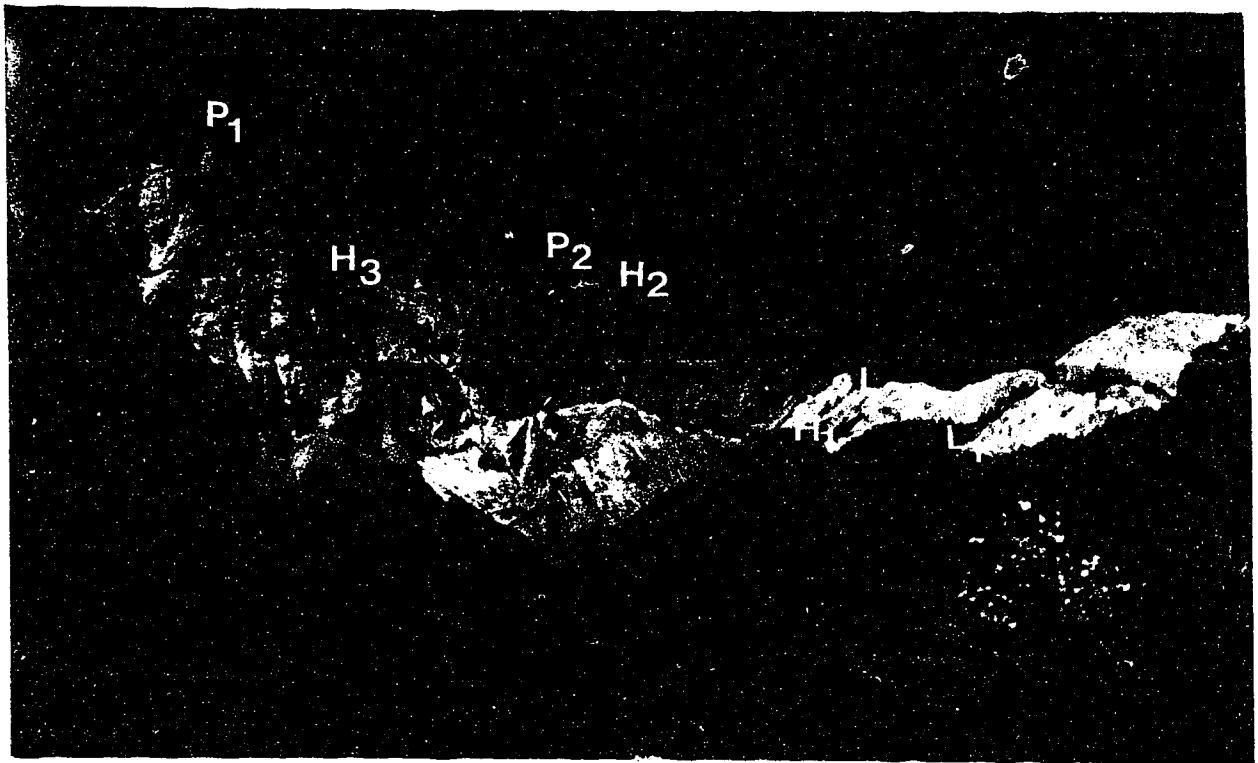


Figure 6.10 Location of three major hazardous slopes looking NNE at site 71 (Fig. 6.1). H_1 , H_2 and H_3 represent hazardous slopes 1, 2 and 3 respectively. L_1 and L_2 indicate the depletion zones of the 1963 and the 1984 events respectively. P_1 and P_2 represent the Peak of Mount Cayley and Peak 2251 respectively.

Figure 6.11 shows the location of the hazardous slope 1, 200 m downstream from the 1984 rock slide head scarp on the northwest side of Avalanche Creek. Figure 6.12 shows the front of the hazardous slope.

Hazardous slope 1 mainly consists of units 4 and 5 of the volcanic rocks on Mount Cayley. Units 4 and 5 are mainly purple tuff breccia and tuff lapilli, white and grey soft tuff, and light yellow hard tuff. These rocks are exposed on the opposite slope too.

Figure 6.13 shows ground tension cracks on hazardous slope 1. The maximum width of these cracks observed in the summer of 1989 was 20 cm. The vertical movement along these cracks was 15 cm. The maximum length of these cracks observed was 60 m. These cracks had not connected to form a continuous crack yet at that time. There was no vegetation covering these cracks suggesting that these cracks are new and active.

The crown of the slope is at the elevation of 1550 m and the toe is at 1300 m. The length of the slope is 260 m, with a width of 200 m and the height of 150 m. The estimated volume of the rock mass which may detach from the slope is about $5 \times 10^6 \text{ m}^3$. Considering the 1984 event, a large part of the rock mass on the opposite slope was knocked down and carried away, it is possible that a part of the loose rock on the opposite slope may also be knocked down and carried away joining into the fragment flow, especially the part of the opposite slope, O in Fig. 6.11, when this hazardous slope moves. So the total volume of the rock mass moving downstream

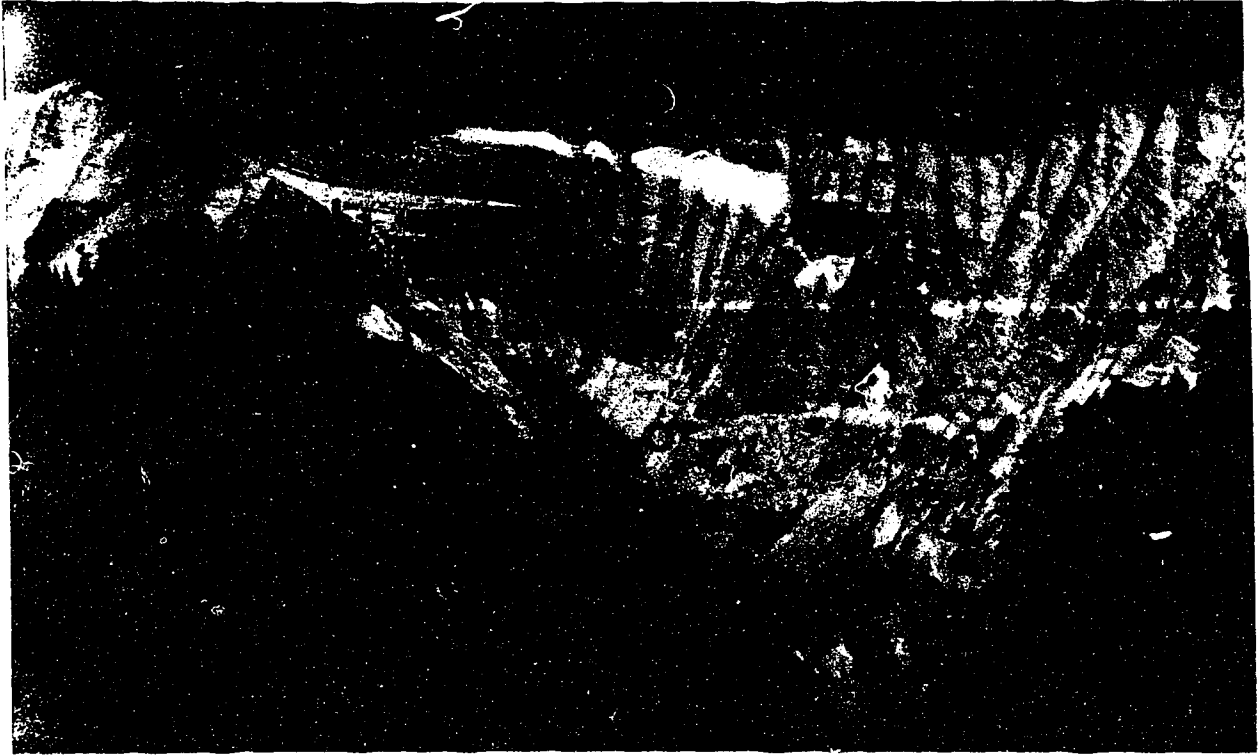


Figure 6.11 Hazardous slope 1, H_1 , 200 m downstream from the 1984 rock slide head scarp (L_2 , Fig. 5.1), looking NE at site 1 (Fig. 2.12). Large trees on the slope, 15-20 m high, give scale. A and O represent Avalanche Creek and the opposite slope which may be carried away by the rock slide from hazardous slope 1 respectively.



Figure 6.12 The front of hazardous slope 1, looking SSW at the scarp of the 1984 rock slide. The height of trees, 16-20 m, gives scale.

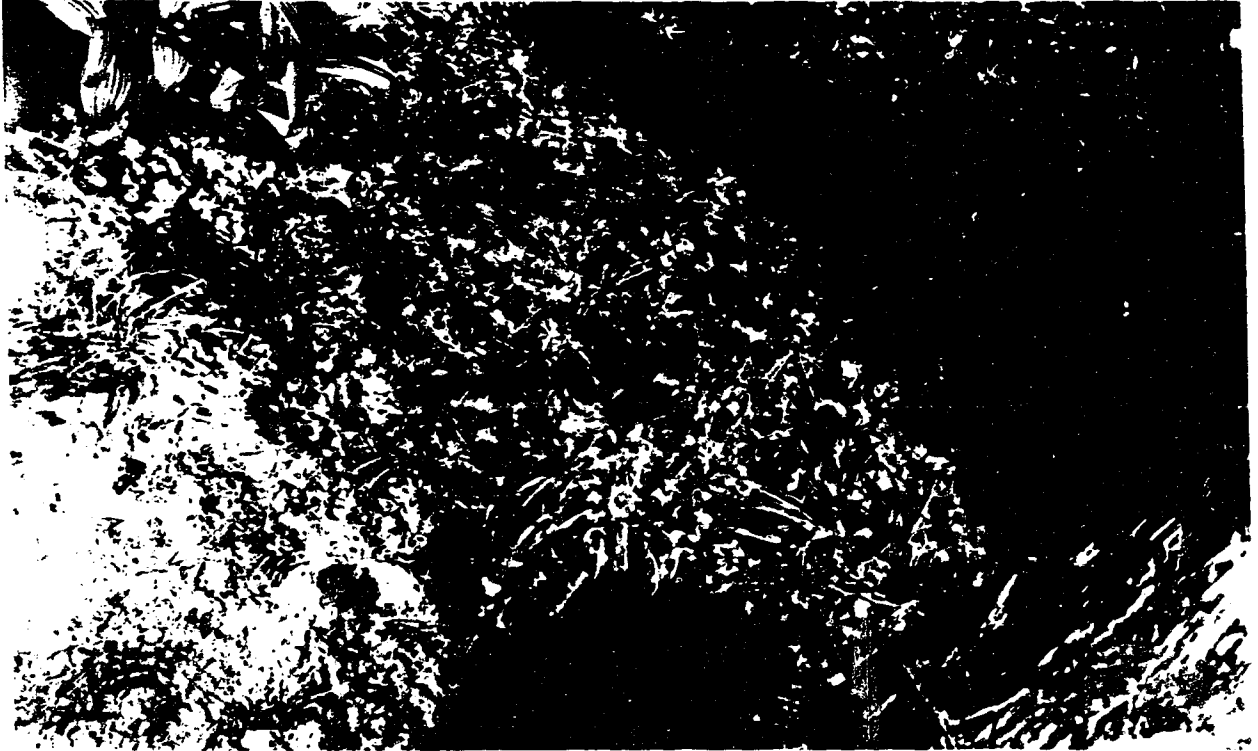


Figure 6.13 A tension crack observed on hazardous slope 1 on ground in the summer of 1989. The hammer across the crack gives scale.

may be up to $6 \times 10^6 \text{ m}^3$.

As the downstream of Avalanche Creek is covered by a snow and ice layer with debris imbedded in it with an average thickness of 15 m, the detached rock mass will travel on a smooth surface on the main track with a low friction, and will dig out substantial ice blocks from the creek bottom. These ice blocks will join the detached rock mass and move downstream with a high velocity until coming to a stop forming a dam. The dam will contain substantial ice blocks, probably 15% of the volume of the whole material. The probable dam site for this landslide will be the confluence of Avalanche and Turbid Creeks, the same situation as the 1984 event. As almost all conditions of this hazardous slope are the same as the 1984 rock slide, this event will be very similar to the 1984 event. The main elements of the 1984 rock slide and this hazardous slope are compared in Table 6.3.

As the 1984 rock slide, especially the 1984 debris flow left millions of cubic metres of debris in the channel of Turbid Creek, and the channel was significantly straightened by the 1984 debris flow, if the dam formed by the future rock slide bursts, the successive debris flow will have more energy than the 1984 debris flow and will travel with a higher velocity. Its impact and damage to the environment will be more serious. The bridge and the road approach may be removed completely, and the Squamish River will be blocked for a longer time.

The rock slide from hazardous slope 1 will belong to Tuff Type, similar to the 1984 event.

Table 6.3

Main Element Comparison between the 1984 Rock Slide
and hazardous Slope 1

Item	1984 rock slide	Hazardous slope 1
Location	At the head of Avalanche Creek	200 m downstream from the 1984 scarp
Elevation of crown	1600 m	1550 m
Rocks involved	Units 4 and 5	Units 4 and 5
Main track	Ice covered	Ice covered
Volume ($\times 10^6$ m ³)	3.2	5.5-6
Stop site	Mouth of Avalanche Creek	Probably mouth of Avalanche Creek
Junction angle	60-72 ⁰	60-72 ⁰ too
Dam	Type 3	Type 3
Ice block in dam	Yes, 1/4 of volume	Yes, 1/6-1/4
Dam burst	After 1-2 days	Probably the same
debris flow	Yes. Following dam burst	Yes. Following dam burst
Velocity of rock slide	35 m/s	30-35 m/s
Velocity of debris flow	21-34 m/s	probably 20-25 m/s
Volume of material involved in debris flow	4-6 $\times 10^6$ m ³	10-15 $\times 10^6$ m ³ because of too much debris stored in the valley
Impact on environment	Introduced huge quantity sediment into the Squamish River and caused significant channel change. The river was temporarily blocked. Logging road bridge was removed.	Will introduce more sediments into the river and cause more significant channel change. The river will be blocked for longer time. Logging road bridge will be removed.

Hazardous Slope near Peak 2251

Hazardous slope 2 is located about 0.9 km north of the scarp of the 1984 rock slide, and 1.2 km southeast of the peak of Mount Cayley (Fig. 6.10). Figures 6.14 and 6.15 show the locations of hazardous slope 2 and Peak 2251. Figure 6.16 shows the profile of the unstable slope. From the profile, five potential slope blocks can be determined. The first block in the front has moved a substantial distance already, and the major part of the displaced rock mass in this block still remains on the profile. The second block has moved an obvious distance. Part of block 2 has moved into the creek already. Between the third and the fourth blocks, a distinct tension crack is observed. As the slope is inaccessible, the dimensions of the crack and the vertical movement along the crack cannot be measured. From Figure 6.17, the width of the crack may be estimated in the range of 1-2 m. The head scarp is probably located at the front of block 5. Between blocks 4 and 5, two obvious tension cracks were observed (Fig. 6.17). A graben seems to form between these two cracks. It is interesting to note that a substantial movement has taken place along the scarp (d_s) in Fig. 6.17. The isolated peak, the fifth block also looks unstable. Some cracks are developing behind the isolated peak and its lower part.

This unstable slope is mainly units 4 and 5 of the volcanic rocks too, mainly purple tuff lapilli and tuff breccia, and white to grey soft tuff.

The crown of the unstable slope is at elevation of 2050 m. The slope has a length of 550 m, width of 200 m. The suspected rupture



Figure 6.14 Hazardous slope 2, H_2 , near Peak 2251, P_2 , above the head of Slide Creek, S_{cr} , looking NNE at site 9 (Fig. 2.12). The height of trees on the slope, 18-20 m, gives scale. Note that T and A represent Turbid and Avalanche Creeks respectively.

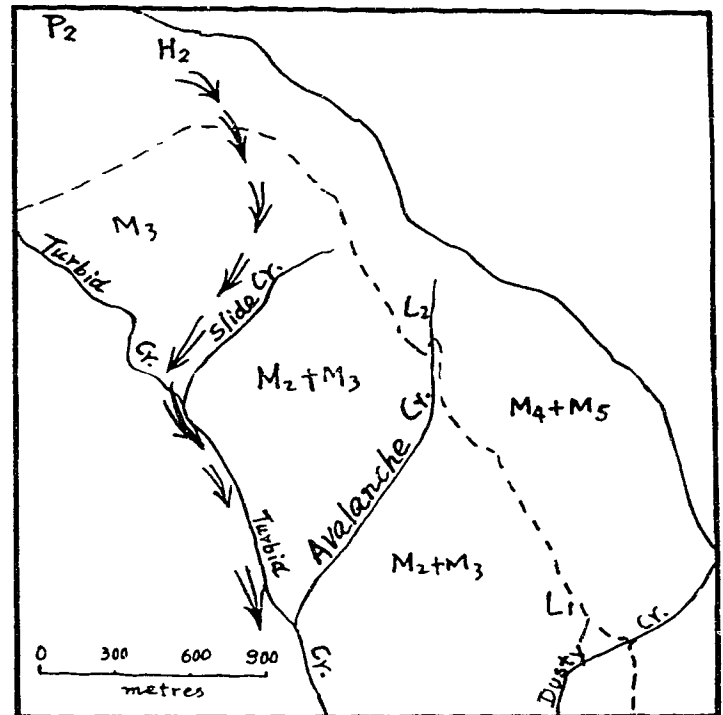


Figure 6.15 Air photo (BC86061 No. 096) and its overlay showing hazardous slope 2. L_1 and L_2 represent the depletion zones of the 1963 and the 1984 rock slides respectively. P_2 and H_2 point out the locations of hazardous slope 2 and Peak 2251. M_2 - M_5 represent Members 2-5 of volcanic rocks respectively.

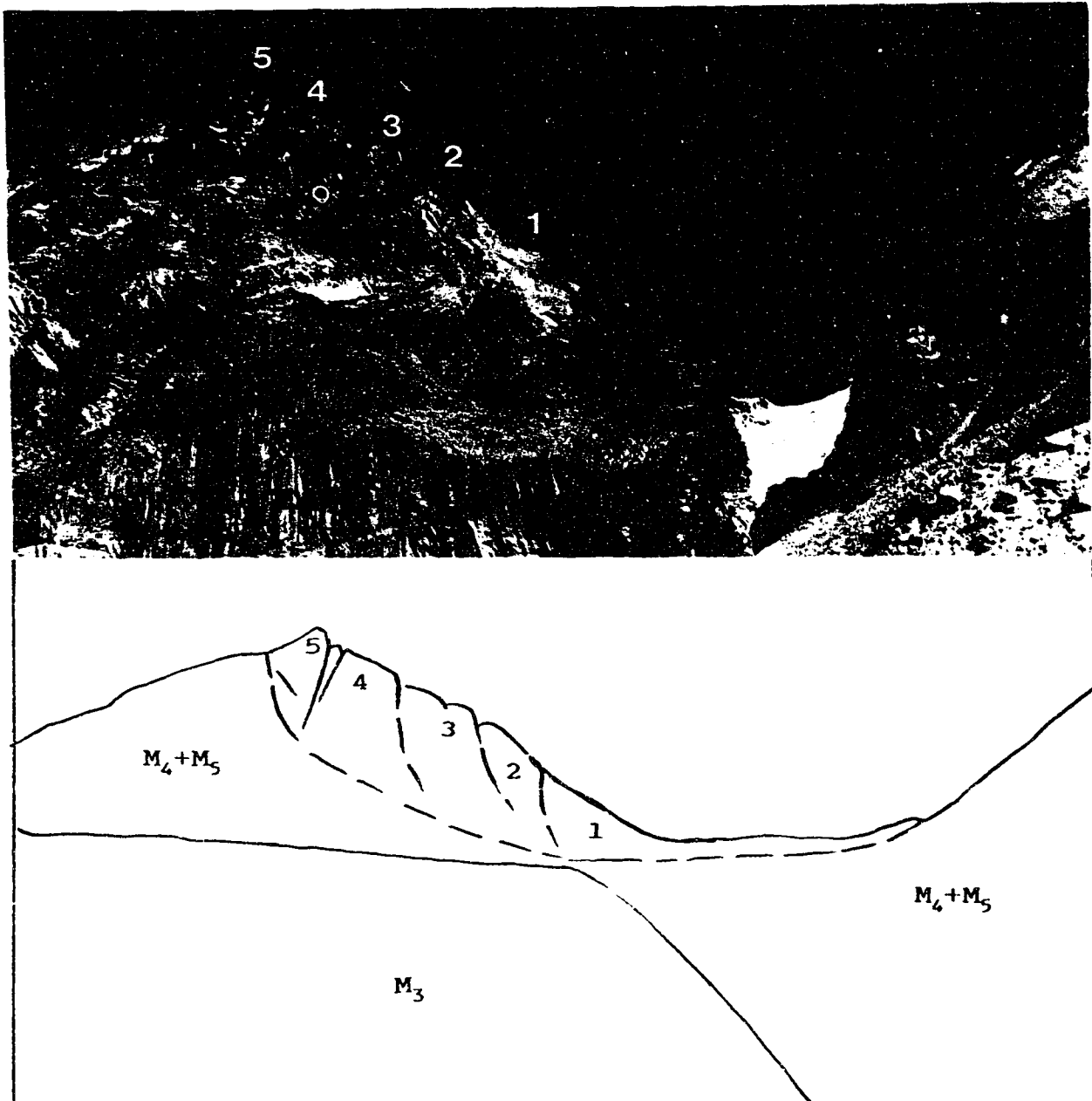


Figure 6.16 A profile of hazardous slope 2 and overlay, looking NNE at site 9 (Fig. 2.12). The thickness of the unstable slope figured out on the overlay, 200 m, gives scale. 1-5 represent blocks 1-5 and M_3 - M_5 represent Members 3-5 of volcanic rocks respectively. The dashed line represents the suspected rupture surface.

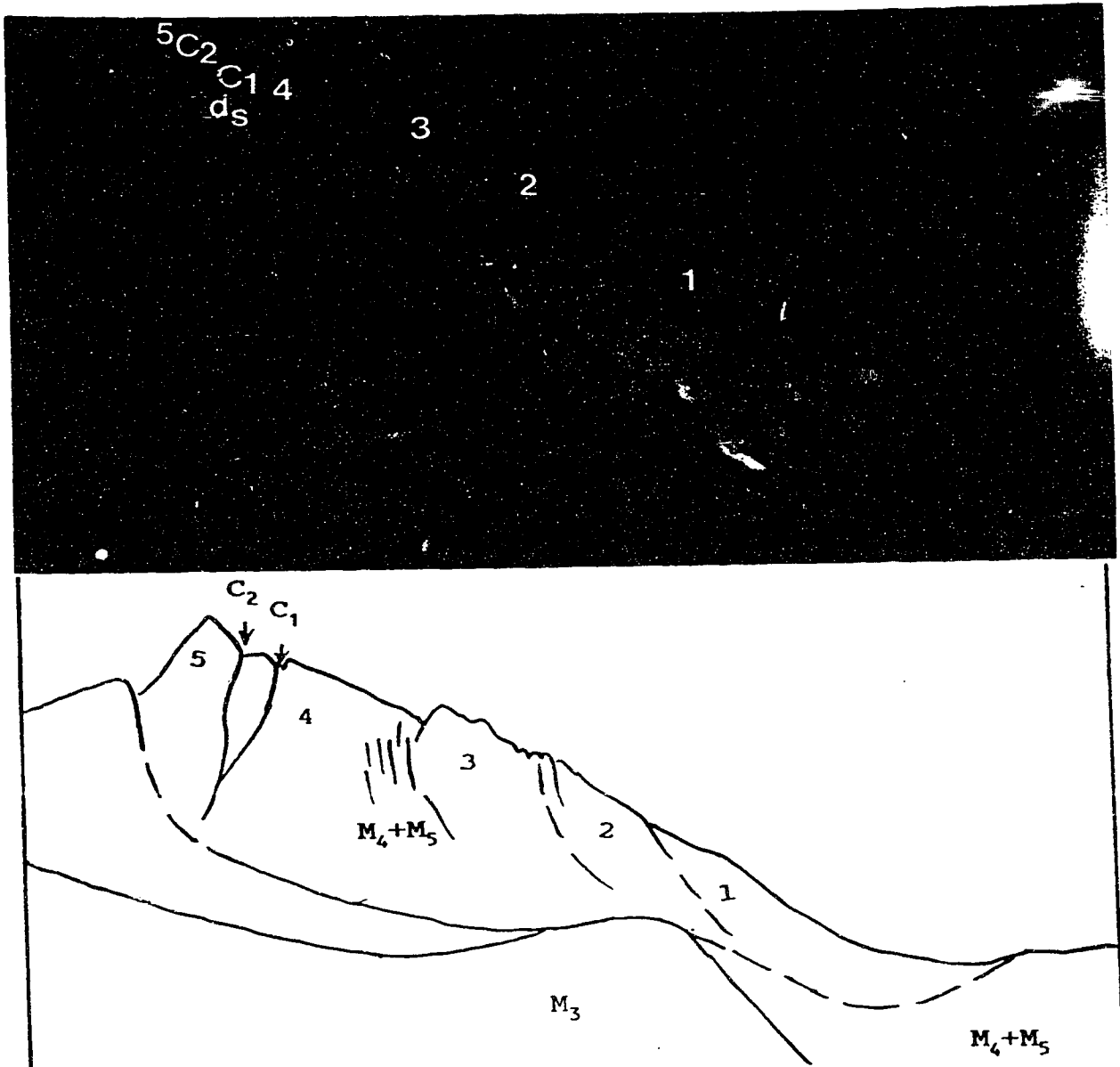


Figure 6.17 Cracking on hazardous slope 2 shown on photo and overlay, looking NW at the crown of the 1984 rock slide. The thickness of block 4, 200 m, gives scale. 1-5 represent blocks 1-5 and M_3 - M_5 represent Members 3-5 of the volcanic rocks. C_1 and C_2 point out the major cracks between blocks 4 and 5. d_s below C_2 points out the displacement along C_2 . Note some minor cracks appear on the back of block 3.

surface is figured on the profile (Fig. 6.16). The thickness of the rock mass to be displaced is 200 m. So the total volume of the unstable rock mass is approximately $10 \times 10^6 \text{ m}^3$. The rock slide will take place retrogressively. The velocity of the rock slide debris may reach 35-45 m/s, based on the velocity of the 1984 rock slide.

The path of the displaced rock mass can be predicted as follows.

The main direction of the rock slide at the first stage will be towards the southeast, almost in the same direction as the 1984 rock slide. After that, as the west side of the ridge is an open space, when the moving rock mass reaches the flat part of the ridge, at the second stage, the moving rock mass will probably rush into the source area of Slide Creek (Fig. 6.14). As the junction angle between Slide and Turbid Creeks is about 50° , so at the third stage the moving rock masses will enter the main course of Turbid Creek without stopping (Fig. 6.15). In the section between the mouths of Slide and Avalanche Creeks, the debris will travel on a snow and ice cover which accumulated in the valley of upstream of Turbid Creek (Fig. 6.15). In the summers of 1984 and 1989, we observed a snow and ice cover at the bottom of Turbid Creek about 100 m upstream from Avalanche Creek mouth. The rock slide debris may come to stop at the open space between pre- and post-1963 rock slide mouths of Dusty Creek and form a dam. This dam will consist of 10-15% ice blocks and totally broken rock masses. The dam may belong to Type 3 (Costa and Schuster 1988). After that, water from both upstream and the melt of snow and ice will accumulate behind

the dam. The dam may probably last for one to three days, and then burst catastrophically. A debris flow will form and travel downstream with a high velocity. The debris flow will enter and block the Squamish River. The velocity of the debris flow may reach the range of 30-40 m/s based on the results of the 1984 debris flow.

Another possibility is that the rock slide debris may not stop at the open space between the pre- and post-1963 rock slide mouths of Dusty Creek, but travel downstream directly until it enters the Squamish River. Considering that the crown of the rock slide is at 2050 m, and the mouth of Turbid Creek is at the elevation of 135 m, the elevation difference between these two points is 1915 m, the horizontal distance between them is 6.6 km. The travel angle will be 16.2° . This is very close to the travel angle of block 2 of the 1963 rock slide. As on the path of the rock slide from the unstable slope near Peak 2251 there is no special condition such as very high junction angle between the contributing and the receiving channels, but there is a thick snow and ice cover on the upstream of Turbid Creek, so it is not impossible that the rock slide debris may travel downstream continuously till it enters the Squamish River. If it happens, this rock slide will cause a serious blockage of the river and a dam-break flood downstream when the blockage collapses.

The event from hazardous slope 2 will belong to Tuff Type too, similar to the 1984 event.

Hazardous Slope near the Peak of Mount Cayley

Hazardous slope 3 is located near the main peak of Mount Cayley. Though the site is inaccessible, some cracks were observed from the opposite slope during the field investigation.

Figure 6.18 shows a slope, 400 m southeast of the peak of Mount Cayley. Figure 6.19 gives the location of the slope. Several parallel, nearly-vertical cracks developing along joints are seen. The slope is mainly units 4 and 3. The base of the slope is a thick white soft tuff layer between units 3 and 2. If creek erosion develops, the slope will become isolated. It will fail and move into the main branch of Turbid Creek. As the main body of the slope is dacite, the rock slide will belong to Dacite Type. The displaced rock mass will probably come to stop at the confluence of Turbid and Avalanche Creeks and dam Turbid Creek because this site will be the first relative open space on the movement path.

The dimension of the rock slide is estimated to be 300 m long, 120 m wide and 150 m thick resulting a volume of $2.7 \times 10^6 \text{ m}^3$.

After the failure of this part of slope, the steeper slope behind it will lose lateral support. The rock slide will develop retrogressively.

Figure 6.20 shows a tension crack developing in dacite below Peak 2356, 800 m south of Peak Mount Cayley. It is a sign indicating the possibility of the development of Dacite Type rock slide around the Peak of Mount Cayley.

6.7 SUMMARY AND DISCUSSION

The study of the radiocarbon dates and the geological mapping provide a clear picture of the sequence of prehistoric slope

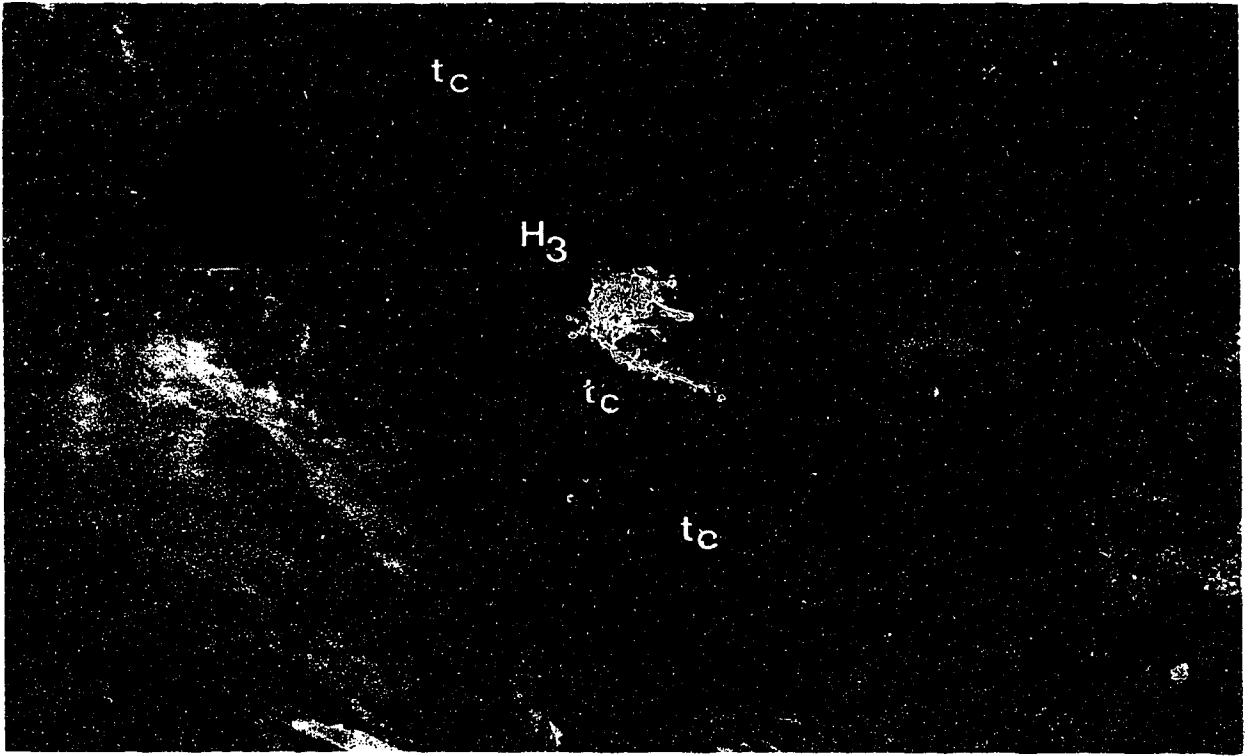


Figure 6.18 Hazardous slope 3, H_3 , looking W at the crown of the 1984 rock slide . The height of the slope, 150 m, gives scale. Note the nearly vertical cracks, t_c .

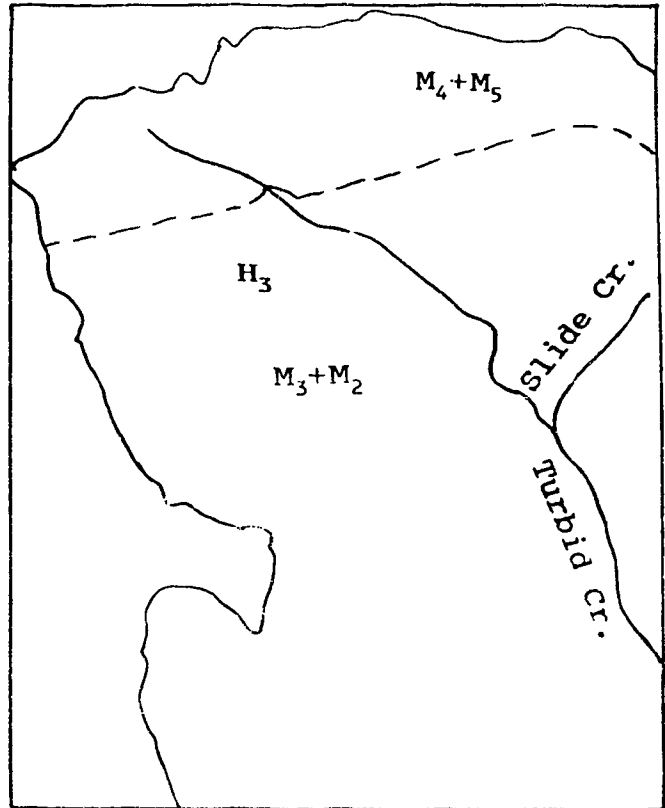


Figure 6.19 Air photo (Province of British Columbia photo BC 86061 No. 096) and its overlay showing hazardous slope 3. H_3 points out the location of hazardous slope 3. M_2 and M_3 represent Members 2 and 3 of the volcanic rocks respectively.

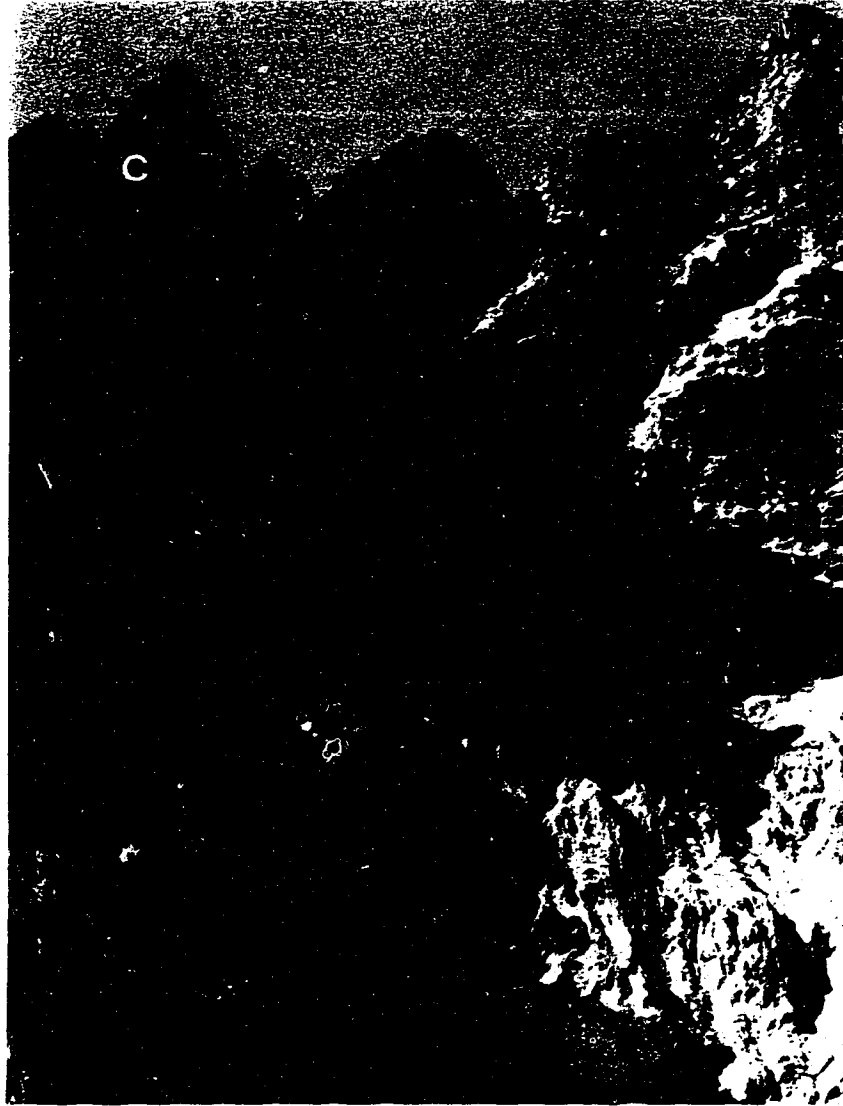


Figure 6.20 A tension crack, C, near the peak of Mount Cayley, looking SWW at the crown of the 1984 rock slide.

movements on Mount Cayley. At least eight prehistoric active stages of slope movement from Mount Cayley are established. While the 4540-4560 BP stage is without a field exposure of the original deposits, all other seven stages have both original deposits and radiocarbon dates. These prehistoric active episodes of slope movement on Mount Cayley are probably related with glacier recessions.

The study of air photos taken at different times, the annual rings of the debris buried trees, the records of the damage on the logging road bridge at the mouth of Turbid Creek, and the 1963 and 1984 events indicate a new episode of slope movement from Mount Cayley which started in 1963 and is going on at present.

From the study of the annual rings of trees buried by the landslide deposits and the air photos taken in 1947, it is believed that between 1963 to 200-300 BP, there was little slope movement on Mount Cayley. When erosion reaches one of the two weak tuff layers and the rock mass is isolated, the inactive stage ends and another active stage begins and is going on at the present time.

So it may be concluded that the Turbid Creek fan has been built by numerous major rock slides and debris flows from Mount Cayley over a long time period. The rate of construction is similar to present day rates of sedimentation on the fan. Fifty landslides of the volume of the 1963 and 1984 events at 20 year intervals would build the Turbid Creek fan within the time constrains, 5380-4130 BP or less, indicated by Evans and Brooks' dates. The fan is the site, not of a prehistoric catastrophe, but of a continuing hazard.

Two major types of deposits are found which result from two major modes of slope movement, Tuff Type and Dacite Type. Tuff Type rock slide deposits contain mainly purple breccia, lapilli and soft tuff, and light yellow hard tuff coming from Units 4 and 5 of the volcanic rocks on Mount Cayley, there are few dacite blocks and boulders. Dacite Type rock slide deposits contain mainly brown to dark brown columnar-jointed dacite and grey soft tuff coming from Units 2 and 3 of the volcanic rocks; there are very few blocks of purple breccia, lapilli and light yellow hard tuff.

Three hazardous slopes on Mount Cayley were mapped and their dimensions, possible movement paths, velocities and impacts on environment are discussed. In the near future, the hazardous slope near Peak 2251 may fail as a Tuff Type rock slide followed by successive debris flow and may cause a series of problems on the logging road and downstream on the Squamish River. A Tuff Type rock slide and successive debris flow may also start from another hazardous slope, 200 m downstream from the 1984 rock slide head scarp. That event would be very similar to the 1984 event. Slope instability is also developing near the peak of Mount Cayley. A Dacite Type rock slide may occur in future in this area.

To minimize the impact of future landslides from Mount Cayley on human lives and the environment, I suggest a warning system on both sides of the logging road at the mouth of Turbid Creek. The warning system will give signals to stop the traffic before debris flow reaches the road. It may also be necessary to consider emergency strategies to prevent abnormal floods caused by the burst

of a landslide dam in the Squamish River. As Mount Cayley is in a remote area, and the hazardous slopes are inaccessible it is recommended to monitor the hazardous slopes by careful comparison of air photos taken at regular intervals and by subsequent investigation from helicopters.

7 CONCLUSIONS AND SUGGESTIONS

7.1 CONCLUSIONS

The 1984 event includes three stages: rock slide, landslide dam and debris flow after the burst of the landslide dam. The velocity of the rock slide was estimated as 35 m/s from the run up at the confluence of Avalanche and Turbid Creeks. The velocity of the successive debris flow and associated wind gusts was estimated as up to 34 m/s, caused superelevations, hurled rocks and wood through the air, uprooted trees and spattered mud 16 m up trees. The debris flow removed the logging road bridge and road approaches at the mouth of Turbid Creek completely, blocked the Squamish River during surges and introduced huge quantities of sediments to the Squamish River.

The tuff layer at the bottom of Unit 4 dipping at 15° - 35° , daylighting on the slope forming the rupture surface of the 1984 rock slide. As the tuff has a very low slake durability index, tuff blocks in the rock slide debris easily disintegrate into fine particles in water. These fine particles would mix with water to form a slurry flow capable of suspending large boulders.

The coincidence of weak, highly slaking material, the tuff, narrow steep creeks intersecting at high angles, high precipitation and snow and ice accumulation in the bottom of Avalanche Creek has produced a particularly and peculiarly hazardous situation which caused the 1984 event.

The 1963 rock slide contained three separated blocks in its depletion zone. These blocks moved one after another and deposited

at the confluence of Dusty and Turbid Creeks in the same way. The velocity of the 1963 rock slide was estimated from superelevation as 26 m/s. 1963 rock slide deposits have distinct layers which can be traced back to the bedrock units in the depletion zone. The accumulation zone is divided by two gullies into three separated blocks with different layers and different topographic features. The 1963 rock slide caused significant creek channel changes. Turbid Creek was shifted 200 m westwards, Dusty Creek took over a part of the pre-slide stream course of Turbid Creek and the confluence of these creeks shifted 1 km downstream.

As the 1963 and the 1984 rock slides involve different units of volcanic rocks, so they have different characteristics. The 1984 event just involved Units 4 and 5, mainly purple tuff lapilli, tuff breccia, light yellow hard tuff, and white to grey soft tuff. The 1963 rock slide just involved Units 2 and 3, mainly brown to dark brown columnar-jointed dacite and some soft tuff. As these rocks have different strengths, they performed differently in the slope movement. The 1963 rock slide flow moved in a laminar way resulting in three separate depositional blocks with distinct layers which kept the main characteristics of the parent rock sequence. Both the 1984 rock slide and the 1984 debris flow moved in a turbulent way. The rock mass was totally broken and the particles in the moving body and in the deposits were totally mixed resulting in deposits without layering features.

Both the 1963 rock slide and the 1984 rock slide formed dams in Turbid Creek. The 1963 landslide dam belongs to Type 5 and the 1984

landslide dam belongs to Type 3. As the materials forming these dams have different characteristics, totally broken tuff breccia, tuff lapilli, tuff and substantial ice blocks in the 1984 dam and partly broken large dacite blocks in the 1963 dam, the 1984 dam lasted just one or two days and burst rapidly caused serious debris flow with high velocity, and the 1963 dam lasted much longer, then overtopped and eroded without causing debris flow.

Two major modes of slope movement related to the different source rocks in the depletion zones on Mount Cayley are recognized from the comparison of the 1963 and the 1984 events, Dacite Type and Tuff Type. These two modes of slope movement are also identified from the study of the history of slope movement on Mount Cayley. Tuff Type slope movements transport deposits with a grain size distribution with D_{50} value less than 5 mm. Dacite Type slope movements transport deposits with D_{50} value larger than 10 mm. In most cases, Tuff Type slope movements move in a turbulent way and its rupture surfaces develop along the upper weak tuff layer at the base of unit 4 in the volcanic pile. Dacite Type slope movements move in a laminar way and rupture surfaces develop along the lower weak tuff layer at the base of Unit 2 in the volcanic pile.

The geotechnical properties of Mount Cayley tuff were determined by a laboratory testing programme. Mount Cayley tuff has a low dry density, 13.6 KN/m^3 , high porosity, 36%, and very low slake durability, 25%.

Mount Cayley tuff specimens show a rapid drop of the strength to the residual value after passing the peak within a very limited

strain, no matter whether they are dry or saturated. The brittleness index of Mount Cayley tuff is high, very close to Brown London Clay, and close to Blue London Clay (intact). Also it is obvious when Mount Cayley tuff is getting wet that its average peak strength decreases, from 2.14 MPa when dry to 1.77 MPa when wet, and its brittleness index, 92% when dry, drops substantially to 64% when wet.

Mount Cayley tuff has distinct two yield points recognized from uniaxial tests, consolidated and drained tests, and consolidated and undrained tests. All the stress-strain, volume change-strain, and pore pressure-strain curves show these two yield points by the departures from the initial linear elastic portion (first yield), and the previous portion (second yield). The yield points define the starts of crushing and shearing respectively, the destruction of the natural structure and the development of microfracturing. The first yield point indicates the start of destruction of the bonds between grains. From the analysis of the critical stresses, σ_{c1} and σ_{c2} , corresponding to the first and the second yields at different confining pressures, it is found that even though the confining pressures vary over quite a wide range, the critical vertical stresses at first yield points are kept within a very limited range, almost constant. But the critical vertical stresses at the second yield points increase with the increasing confining pressures. It seems likely that Mount Cayley tuff has a certain critical stress level for the start of crushing or collapse, e.g. the destruction of the bonds between grains. For dry Mount Cayley

If the critical stresses, σ_{c1} , are in the range of 0.75-1 MPa. For saturated Mount Cayley tuff, the critical stresses are in the range of 0.51-0.67 MPa. It suggests that the bonds between grains have certain strength that we may call bond strength defined by the σ_{c1} values. As dry Mount Cayley tuff has a bond strength of 0.75-1 MPa and saturated Mount Cayley tuff has a bond strength of 0.5-0.7 MPa, the decrease, about 1/3, of the bond strength shows the strong influence of saturation on bond strength.

A special deformation phase is figured out from the stress-strain curves of Mount Cayley tuff between the first and the second yield points, differing from common rocks. It may be called the crushing phase indicating the destruction of the weak bonds between grains. In this phase, in the consolidated and drained tests, the volumes of the specimens decreased by 0.6-0.8%; in the consolidated and undrained tests, pore pressures drop obviously, though in a small range (1-2 kPa) which may indicate the connection of the pores. All the volume changes and the pore pressure changes combining with the stress-strain curves define the crushing phase clearly.

Mount Cayley tuff has an uniaxial strength in the range of 1.5-2.4 MPa with an average of 2.1 MPa giving the peak cohesion of dry tuff as 1 MPa. The peak friction angle of dry Mount Cayley tuff is 35° . The peak and residual shear strengths of saturated tuff are $\phi'=29^{\circ}$ and $c'=220$ kPa, and $\phi_r=17^{\circ}$ and $c_r=65$ kPa respectively. It is clear that saturation causes a substantial strength drop, cohesion dropping from 1 MPa (dry) to 0.22 MPa (wet) and friction angle

dropping from 35° to 29°.

Based on the geological mapping and the interpretation of radiocarbon dates from the wood buried by slope movement deposits, eight prehistoric active stages of slope movement from Mount Cayley are established. They are at 4800-5310, 4540-4560, 4130, 3720, 1250-1270, 1010-1060, 500-560, and 350 years BP. It is clear that the Turbid Creek fan has been built by numerous major rock slides and debris flows from Mount Cayley over a long time period.

The study of air photos taken at different times, the annual rings of debris buried trees, and the records of the damage on the logging road bridge at the mouth of Turbid Creek, especially the 1963 and the 1984 events indicates a new episode of slope movement from Mount Cayley, started in 1963 and is going on at present.

Three recognized unstable slopes, hazardous slope 200 m downstream from 1984 head scarp, hazardous slope near Peak 2251 and hazardous slope near the peak of Mount Cayley, on Mount Cayley also suggest the new episode of slope movement. The most hazardous slope is the slope near Peak 2251. When this slope fails, a rock mass with a volume of $10 \times 10^6 \text{ m}^3$ will travel at a high velocity, 35-45 m/s, rush into Turbid Creek. With a stop in Turbid Creek, the debris will form a Type 3 dam. Debris flow at a high velocity will occur. Without a stop in Turbid Creek, rock slide debris will travel downstream directly until it enters the Squamish River. In this case, the rock slide debris will cause a serious block of the river and a remarkable flood downstream when the blockage collapses.

7.2 SUGGESTIONS FOR FUTURE RESEARCH

In the field investigation, we have described special phenomena created by the 1984 rock slide and its successive debris flow, such as run ups, superelevations, uprooted trees, mud spatters, airborne wood splinters and hurled rocks in the air. They are useful in determining the velocities of the rock slide and the debris flow. Further considerations of these phenomena are required to use them for estimating the velocity of the landslides more precisely.

Grain size distribution curves of landslide deposits may be important evidence to distinguish modes of slope movement in a small area. It may be an interesting area to do more detailed study.

The geotechnical properties of Mount Cayley tuff are interesting. Especially the two yield points, high brittleness index, and the concept of bond strength may be found in other young tuffs, loess and residual soils. These characteristics may be important in the study of slope movement in these porous, weak transitional materials.

It needs to be emphasized that in the near future, the hazardous slopes on Mount Cayley may fail and form Tuff Type (hazardous slopes 1 and 2), and Dacite Type (hazardous slope 3) rock slides. They will cause a series of problems, especially on the logging road and downstream, in the Squamish River. To minimize the impact of future landslides from Mount Cayley on human lives and the environment, warning systems should be set up on both sides of the logging road at the mouth of Turbid Creek. The warning systems will give signals to stop the traffic before debris flows

reach the road. It may also be necessary to consider emergency strategies for abnormal floods caused by the burst of landslide dams in the Squamish River. As Mount Cayley is in a remote area, and the hazardous slopes are inaccessible, the hazardous slopes should be monitored by careful comparison of air photos taken at different times and by regular investigation from helicopters.

BIBLIOGRAPHY

- Baldwin, J.E., Donley, H.F., and Howard, T.R. 1987. On debris flow/avalanche mitigation and control, San Francisco Bay area, California. in Debris flows/avalanches: process, recognition, and mitigation. Edited by J.E. Costa and G.F. Wieczorek. Reviews in Engineering Geology, 7:223-236.
- Benda, L.E., and Cundy, T.W. 1990. Predicting deposition of debris flow in mountain channels. Canadian Geotechnical Journal, 27:409-417.
- Bevier, M. L., 1981. Stratigraphy and petrology of the Miocene plateau lavas of British Columbia. Geological Association of Canada Joint Meeting, Calgary, 1981, Abstracts, 6, p. A-4.
- Bieniawski, Z.T. 1974. Estimating the strength of rock materials. Journal of the South African Institute of Mining and Metallurgy, 88: 312-320.
- 1979. The geomechanics classification in rock engineering applications. Proceedings, 4th International Conference on Rock Mechanics, ISRM, Montreux, 2: 41-47.
- 1989. Engineering rock mass classification. Wiley, New York. 251p.
- Bishop, A.W., 1973. The stability of tips and spoil heaps. Quarterly Journal of Engineering Geology, 6:335-376.
- Bishop, A.W., and Henkel, D.J. 1962. The measurement of soil properties in the triaxial test. Edward Arnold, London. 227p.
- Broch, E., and Franklin, J.A. 1972. The point load strength test. International Journal of Rock Mechanics and Mining Science, 9:

669-697.

- Brooks, G.R., and Hickin, E.J. 1991. Debris avalanche impoundments of Squamish River, Mount Cayley area, southwestern British Columbia. *Canadian Journal of Earth Sciences*, 28:1375-1385.
- Canadian Geotechnical Society, 1985. *Canadian Foundation Engineering Manual*. Canadian Geotechnical Society, Toronto.
- Chow, V.T., 1959. *Open-channel hydraulics*. McGraw-Hill. New York.
- Clague, J.J., and Souther, J.G. 1982. The Dusty Creek Landslide on Mount Cayley, British Columbia. *Canadian Journal of Earth Sciences*, 19: 539-542.
- Costa, J.E., and Schuster, R.L. 1988. The formation and failure of natural dams. *Geological Society of America Bulletin*, 100:1054-1068.
- Cruden, D.M. 1984. More rapid analysis of rock slopes. *Canadian Geotechnical Journal*, 21: 678-683.
- Cruden, D.M., and Lu, Z-Y 1989. The geomorphic impact of the catastrophic October, 1984, flood on the planform of Squamish River, southwestern British Columbia: Discussion. *Canadian Journal of Earth Sciences*, 26:336.
- Cruden, D.M., and Lu, Z-Y. 1992. The rock slide and debris flow from Mount Cayley, British Columbia in June, 1984, *Canadian Geotechnical Journal*, 29: 614-626.
- Evans, S.G. 1984. The landslide response of tectonic assemblages in the southern Canadian Cordillera, *Proceedings, 4th International Symposium on Landslides*, Toronto, pp. 495-501.
- 1986. *Landslide damming in the Cordillera of western Canada*.

- in Landslide dams: process, risk and mitigation. Edited by R.L. Schuster. American Society of Civil Engineering, Special Publication 3, pp. 111-130.
- 1987. A rock avalanche from the peak of Mount Meager, British Columbia. Geological Survey of Canada, Paper 87-1A, pp. 929-934
- 1990. The Canadian landslide inventory: a national data base for landslides. Paper presented at 43e Canadian Geotechnical Conference, Quebec City.
- Evans, S.G. and Brooks, G.R. 1991. Prehistoric debris avalanches from Mount Cayley volcano, British Columbia. Canadian Journal of Earth Sciences, 28:1365-1374.
- Evans, S.G., Clague, J.J., Woodsworth, G.J., and Hungr, O. 1989. The Pandemonium Creek rock avalanche, British Columbia. Canadian Geotechnical Journal, 26:427-446.
- 929-934.
- Evans, S.G., and Gardner, J.S. 1989. Geological hazards in the Canadian Cordillera. in Chapter 12 of Quaternary Geology of Canada and Greenland, edited by R.J. Fulton, Geological Survey of Canada, Geology of Canada. no. 1, PP. 702-713.
- Fahnestock, R.K. 1978. Little Tahoka Peak rockfalls and avalanches, Mount Rainier, Washington, U.S.A. in Rockslides and avalanches, vol. 1, pp.179-196. Edited by B. Voight. Elsevier. New York.
- Franklin, J.A., and Chandra, R. 1972. The slake-durability test. International Journal of Rock Mechanics and Mining Sciences, 9: 325-341.
- Fujita, T.T. 1971. Proposed characterization of tornadoes and

- hurricanes around the world by area and intensity. Unive
of Chicago, Satellite and Mesometeorology Research Project,
Research Paper 91.
- Gamble, J.C., 1971. Durability-plasticity classification of shales
and other argillaceous rocks, Ph. D. Thesis, Unversity of
Illinois.
- Green, N.L. 1977. Multistage andesite genesis in the Garibaldi
Lake area, southwestern British Columbia, Ph. D. thesis,
University of British Columbia, Vancouver, B.C., 246 p.
- Green, N.L., Armstrong, R.L., Harakal, J.E., Souther, J.G., and
Read, P.B. 1988. Eruptive history and K-Ar geochronology of the
late Cenozoic Garibaldi volcanic belt, southwestern British
Columbia. Geological Society of America Bulletin, 100: 563-579.
- Hadley, J.B. 1978. Madison Canyon rockslide, Montana, U.S.A. in
Rockslides and avalanches. vol. 1 pp. 165-180. Edited by B.
Voight. Elsevier. New York.
- Hampton, M.A. 1975. Competence of fine-grained debris flows.
Journal of Sedimentary Petrology, 45: 834-844.
- Henderson, F.M. 1966. Open channel flow. MacMillan, New York, 522p.
- Hickin, E.J., and Sichingabula, H.M. 1988. The geomorphic impact of
the catastrophic October, 1984, flood on the planform of the
Squamish River, southwestern British Columbia. Canadian Journal
of Earth Sciences, 25: 1078-1087.
- Hocking, G. 1976. A method for distinguishing between single
and double plane sliding of tetrahedral wedges.
International Journal Rock Mechanics and Mining Science, 13:

225-226.

Hoek, E., and Bray, J. 1981. Rock slope engineering. Institution of Mining and Metallurgy, London, 358p.

Hungr, O. 1981. Dynamics of rock avalanches and other types of slope movements, Ph.D. thesis, University of Alberta, Edmonton, Alta.

International Association of Engineering Geology Commission on Landslides, 1990. Suggested nomenclature for landslides. Bulletin of the International Association of Engineering Geology, 41:13-16

International Geotechnical Societies' UNESCO Working Party on World Landslide Inventory, 1990. A suggested method for reporting a landslide. Bulletin of the International Association of Engineering Geology, 41:5-12.

International Society for Rock Mechanics, Commission on Standardisation of Laboratory and Field Tests. 1979. Suggested methods for determining water content, porosity, density, absorption and related properties and swelling and slake durability index properties. International Journal of Rock Mechanics and Mining Sciences, 16: 141-156.

Johnson, A.M., and Rodine, J.R. 1984. Debris flow. in Slope instability, edited by D. Brunnsden and D.B. Prior. Wiley. New York. P. 257-360.

Jordan, P. 1987. Impacts of mass movement events on rivers in the southern Coast Mountains, British Columbia. Environment Canada, Water Resource Branch, Summary Report IWD-11Q-WRS-SS-83-3.

- Keller, D., and Vonnegut, B. 1976. Wind speeds required to drive straws and splinters into wood. *Journal of Applied Meteorology*, 15: 899-901.
- Kirkaldie, L. 1988. Rock classification systems for engineering purposes, American Society for Testing and Materials, Special Technical Publication, 167p.
- Lu, Z-Y. 1988. Rock avalanches on Mount Cayley, British Columbia. M.Sc. thesis, University of Alberta, Edmonton, Alberta.
- Lu, Z-Y. 1992. Prehistoric debris avalanches from Mount Cayley volcano, British Columbia: Discussion. *Canadian Journal of Earth Sciences*, 29: 1342-1343.
- Mathews, W.H., and McTaggart, K.C. 1978. Hope rockslides, British Columbia, Canada. in *Rockslides and avalanches*. vol. 1 pp. 259-275. Edited by B. Voight. Elsevier. New York.
- Moore, D.P., and Mathews, W.H. 1978. The Rubble Creek landslide, southwestern British Columbia. *Canadian Journal of Earth Sciences*, 15:1039-1052.
- Morgenstern, N.R., and Phukan, A.L.T. 1968. Non-linear deformation of a sandstone, *Proceedings of the First Congress of the International Society of Rock Mechanics*, pp. 543-548.
- Palmstrom, A. 1982. The volumetric joint count- a useful and simple measure of the degree of rock jointing. *Proceedings, 4th International Congress, International Association of Engineering Geology, Delhi, Vol. 5*, pp. 221-228.
- Paterson, M. S., 1978. *Experimental rock deformation-the brittle field*. Springer-Verlag, New York.

- Patton, F.D. 1976. The Devastation Glacier slide, Pemberton, B.C.. Geological Association of Canada, Cordilleran Section, Program and Abstracts, P. 26-27.
- Pellegrino, A., 1989. Soft rocks and indurated soil: a short overview on recent researches in Italy. in Recent advances in soft rock research, Report of ISSMFE Technical Committee on Soft Rocks and Indurated Soils and Proceedings of discussion session No. 5 XII ICSMFE, Rio De Janerio, 1989. pp. 92-95.
- Pierson, T.C., and Costa, J.E. 1987. A rheologic classification of subaerial sediment-water flows. in Debris flows/avalanches: Process, recognition, and mitigation. Edited by J.E. Costa and G.F. Wieczorek. Reviews in Engineering Geology, 7: 1-12.
- Plafker, G., and Erickson, G.E. 1973. Nevados Huascarán avalanches, Peru. in Rockslides and avalanches. vol. 1 pp. 277-314. Edited by B. Voight. Elsevier. New York.
- PROCEQ SA. 1977. Operating instructions: concrete test hammer. Zurrich, Switzerland. 16P.
- Ryder, J.M., and Thomson, B. 1986. Neoglaciation in the southern Coast Mountains of British Columbia: Chronology prior to the late Neoglacial maximum. Canadian Journal of Earth Sciences, 23:273-287.
- Skermer, N.A. 1989. Landslides and human lives. BiTech, Vancouver, B.C.
- Schuster, R.L., and Costa, J.E. 1986. A perspective on landslide dams. in Landslide dams: process, risk and mitigation. Edited by R.L. Schuster. American Society of Civil Engineering,

- Special publication 3, PP. 1-20.
- Souther, J.G. 1980. Geothermal reconnaissance in the central Garibaldi Belt, British Columbia. in Current research, part A. Geological Survey of Canada, Paper 80-1A, pp. 1-11.
- Uriel, S.R. 1982. Phenomene deffondrement dans les roches volcaniques a forte porosite. Revue Francaise de Geotechnique, 20:65-77. English translation by D.M. Cruden
- Uriel, S.R., and Serrano, A.A. 1973. Geotechnical properties of two collapsible volcanic soils of low bulk density at the site of two dams in Canary Islands (Spain). Proceedings of the Eighth International Conference on Soil Mechanics and Foundation Engineering, Moscow. vol.2.2. pp. 257-264.
- Varnes, D. J. 1978. Slope movement types and processes, In Landslides: Analysis and control. Edited by R.L. Schuster, and R.J. Krizek. Transportation Research Board, National Research Council. Special Report 176. pp.11-33.
- Vaughan, P.R., Maccarini, M. and Mokhtar, S.M. 1988. Indexing the engineering properties of residual soil. Quarterly Journal of Engineering Geology, 21:69-84. London.
- Voight, B. 1978. Lower Gros Ventre Slide, Wyoming, U.S.A. in Rockslides and avalanches. vol. 1 pp. 113-166 Edited by B. Voight. Elsevier. New York.
- Wong, W. W. 1983. An investigation and analysis of Dusty Creek landslide. M. Eng. Report, University of Alberta, Edmonton, Alta.
- Zur, A. and Wiseman, G. 1973. A study of collapse phenomena of an

undisturbed loess. Proceedings of the Eighth International Conference on Soil Mechanics and Foundation Engineering. vol. 2.2. pp. 265-269.